George J. Thaler

SELF-ADAPTIVE CONTROL SYSTEMS, PART II:
BLOCK DIAGRAM MODELS FOR THE AIRFRAME ...

UNITED STATES
NAVAL POSTGRADUATE SCHOOL

SELF-ADAPTIVE CONTROL SYSTEMS PART II

BLOCK DIAGRAM MODELS FOR THE AIRFRAME, AND SOME APPROACHES TO ACTIVE COMPENSATION

By

Geo. J. Thaler	Dr. Eng.
R. B. Borthwick	Lt., USN
R. E. McCamey	Capt., USMC

Technical Report
No. 20
Supported in Part by the Office of Naval Research

October 1961

SELF ADAPTIVE CONTROL SYSTEMS

PART II BLOCK DIAGRAM MODELS FOR THE AIRFRAME, AND SOME APPROACHES TO ACTIVE COMPENSATION

BY

GEORGE J. THALER	Dr. Eng.
R. B. BORTHWICK	Lt., USN
R. E. McCAMEY	Capt., USMC

TECHNICAL REPORT NO. 20

UNITED STATES NAVAL POSTGRADUATE SCHOOL
MONTEREY, CALIFORNIA

OCTOBER - 1961

TABLE OF CONTENTS

Section		Page
1.	Introduction	1
2.	Development of the Standard Block Diagram and the Standard Determinant	
	2.1 Purpose	3
	2.2 The Standard Block Diagram	4
	2.3 Mathematical Analysis Based on the Standard Block Diagram	12
3.	An Illustration of the Use of the Determinantal Approach	
	3.1 Introduction	20
	3.2 The Characteristic Determinant and Steady-State Error	20
	3.3 Summary of Compensation Schemes Which Appear Feasible and Restrictions to be Observed When Attempting Compensation	24
	3.4 Compensation Schemes Attempted in the Feedback Path Around the Mag Amp	24
	3.5 Ross-Warren Method Used for Compensation	30
	3.6 Compensator with Zero at the Origin	34
	3.7 Combining of Amplidyne Path with Tach Path	40
4.	Definition of Symbols used in Following Sections	59
5.	Derivation of the Standard Block Diagram for the Airframe	65
	5.1 Introduction	65

5.2 Consideration of External Forces and Moments on a Body in Motion 72

5.3 The Airframe Equations in a Standard Form 81

6. Expansion of the Standard Form for Greater Disturbances 107

7. Application of the Determinantal Approach to a Simplified Airframe Control Problems. 121

8. The Generation of Complex Zeros

8.1 Introduction 132

8.2 Investigation of Some Active Networks 138

8.3 Algebraic Equations for the Loci 156

9. Manipulations and Design

9.1 Introduction 159

9.2 Construction of the Locus of Complex Poles or Complex Zeros Producing a Constant Phase Angle at a Point in the S-plane 163

9.3 A Technique for Compensation Using Active Networks 168

9.4 Numerical Examples 173

9.5 Summary 186

10. Application to a Jet Airplane 188

References and Bibliography 202

Appendix I
Basic Equations of Motion 204

Appendix II
Roll, Yaw and Pitch 224

Appendix III
Notes on Determinant Manipulation 228

1. INTRODUCTION

This report represents the second phase of a long-range project to study self-adaptive control principles and apply them to the control of aircraft. The primary purpose of this phase is to develop a suitable mathematical model for the study of aircraft dynamics including all degrees of freedom, and the secondary purpose is to test the feasibility of using active compensators in the autopilot as a basis for self-adaptive schemes of control.

It was decided to restrict the model to that of a rigid airframe, and it was also decided to use a block diagram model because of well established correlations between the block diagram and a determinantal array on one hand, and between the block diagram and analog simulation on the other hand. The initial block diagram model is to a linear model for two reasons: first, it is necessary that the model be reducible to simpler, well-known linear block diagram models when the proper restrictions are imposed; second, analysis of a linear model is readily obtained and provides a basis for estimating the importance of nonlinear effects as they are introduced. It is anticipated that nonlinear effects can be introduced by the injection of properly derived signals, and it is expected that this modification of the model will lead to simulation studies since the complications caused by the nonlinearities may make an analytic treatment impossible.

Another reason for choosing a block diagram model for the airframe is the ease with which an autopilot configuration can be added to the model. It is expected that the self-adaptive compensation devices will be incorporated in the autopilot, though it is believed that the block diagram model may lead to profitable analysis of the aerodynamic characteristics of the airframe, with resultant indications of ways to improve its design.

2. DEVELOPMENT OF THE STANDARD BLOCK DIAGRAM AND THE STANDARD DETERMINANT.

2.1 Purpose

It is the purpose of this section to develop the mathematical background leading to the derivation of the block diagram model. It will be shown that there is a unique relationship between a properly arranged block diagram and a determinantal array such that either may be written down by inspection of others. The theoretical development starts with the block diagram and leads to the mathematical representation; when applied to the airframe one starts with the simultaneous equations and arrives at the block diagram.

2.2 The Standard Block Diagram

The theory of simple, single loop control systems is reasonably well developed, and the block diagrams of such systems are not complicated. On the other hand the theory of multiple-loop, multiple-input, multiple-output and multicoupled control systems is not well developed because of the complexity of the problems involved. The block diagrams of such systems are naturally complicated and sometimes difficult to interpret. The obvious approach to the analysis of such a system is the formulation and solution of a set of simultaneous differential equations for the system. Perhaps the easiest way to formulate the equations is from a block diagram of the system. In using this approach certain advantages accrue from standardizing the block diagram, and certain other advantages accrue from generalizing the diagram. By standardizing is meant specifying the arrangement of the summing points, blocks and pick-off points, and specifying a notation for the transfer functions. By generalizing is meant extending the standardization rules so that the maximum number of blocks is clearly specified and organizing the mathematical approach so that the presence or absence of any block is readily evident in the equations. It is clear that few systems will contain the maximum number of blocks, so that the ability to recognize the presence or absence of blocks from the equation is in itself an advantage. It

is also clear that block diagrams set up from physical analysis must be manipulated to get them into the standard form.

Any system contains a finite number of summation points, and some of these are in a main transmission path in the sense that the signal output from the summer is fed into a block which produces a signal output closer to a system output. If all other summing points are ignored these main summing points are lettered in sequence, a, b, c, d .....n, and the standard block diagram is drawn by arranging these summing points in a straight line from left to right, with intermediate blocks as required. It is obvious that the numbering sequence is not completely arbitrary. In general summer "a" feeds a block whose output feeds summer "b", etc., though there may be breaks in the signal flow as will be shown later. Also the output of the block following the nth summer, is normally a system output though additional system outputs may be derived at preceding points.

Each summer may receive a number of signals, but delivers only one output. At each summer there is the possibility that one of the signals received is an input command from an external source or a disturbance signal such as noise. No distinction is made here. It is convenient to designate such inputs (at their sources) by numbers in sequence 1, 2, 3, etc. It is also convenient to relate the input sequence with the summer sequence so

that input 1 feeds summer "a", input 2 feeds summer "b", etc. If any summer does not have an external input signal, the corresponding number for the input signal is not used. In writing the equations the signals from the input stations are designated by Roman numerals.

The transfer functions designated in the blocks shall, in general, be designated by double subscript notation. To implement this the signal at the output of a summer is designated by the same lower case letter which designates the summer, and the signal output of the block which receives this signal is designated by the same letter, but using the upper case form. This has the advantage of clearly indicating all important signal sources, and the disadvantage of permitting two symbols which represent the same transfer function, as will be shown. The double subscript notation shall consist of two letters or a combination of a number and a letter. The first subscript designates the input to the block and the second subscript designates the summer into which the output of the block is fed.

Thus,

G_{1a} = transfer function of a block between input 1 and summer "a"

G_{1b} = transfer function of a block between input 1 and summer "b"

$G_{aA} = G_{ab}$ = transfer function of a block between summer "a" and summer "b"

G_{Aa} = transfer function of a feedback block between signal A and summer "a"

G_{Ba} = transfer function of a feedback block between signal B and summer "a"

G_{Ca} = transfer function of a feedback block between signal C and summer "a"

Many other interconnections are obviously possible and are readily handled by the double subscript notation.

It is common terminology to speak of systems in terms of the numbers of loops involved. From the viewpoint of mathematical analysis the number of loops is not a convenient description of the complexity of the system. A better criterion is the number of summing points or "nodes," and this terminology will be used in this text.

The development or manipulation of the standard block diagram is most readily shown by a series of illustrations. Figure 2.1a shows the simplest case of a single node system. For many practical systems $G_{1a} = G_{Aa} = 1.0$. All other variations of the single node system may be reduced to this form if desired Figure 2.1b shows a single node system with additional blocks and summers representing the insertion of tachometer feedback and input velocity feedforward. Note that the simple rules for block diagram manipulation permit reduction of Figure 2.1b to

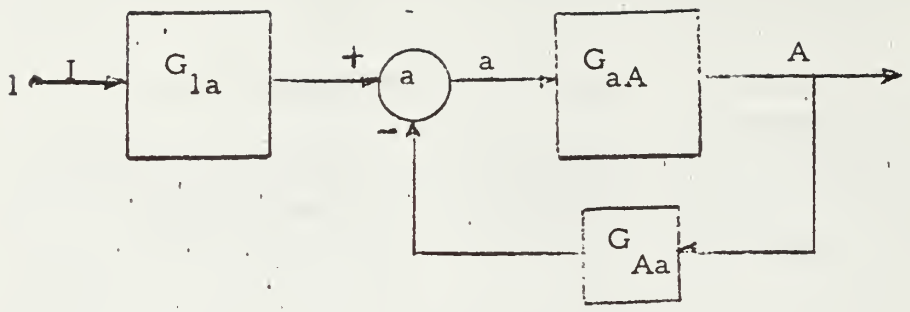

a) The Standard Diagram

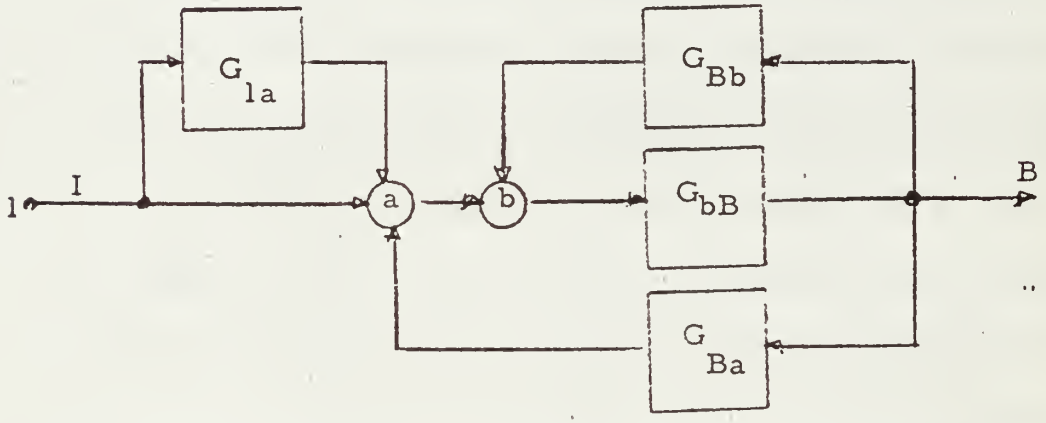

b) A block diagram which readily manipulates to the standard form.

Fig. 2-1 STANDARD BLOCK DIAGRAM FOR SINGLE NODE SYSTEMS

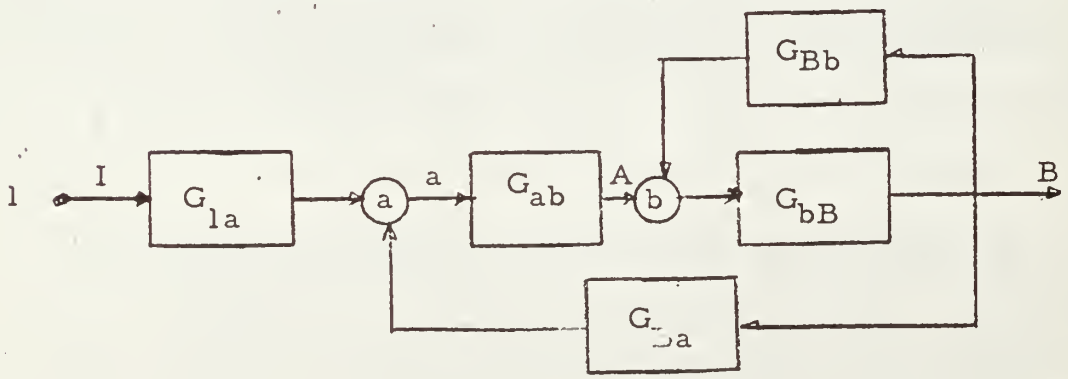

Fig. 2-2 A TWO NODE SYSTEM DERIVED FROM FIG. 2-1b.

the form of Figure 2.1a. Of course, it is not always desirable to carry out such a reduction. If the particular problem involves determination of suitable parameters for G_{Bb}, a slight manipulation results in the block diagram of Figure 2.2, which is a two node system. In this figure G_{1a} is a new transfer function obtained by manipulating Figure 2.1b, and $G_{ab} = 1.0$.

The block diagram of Figure 2.2 is in the standard form, but is a special case since it obviously does not contain all the signals and blocks possible for a two node system. A generalized block diagram for a two node system is shown in Figure 2.3. Note that each summer receives a number of signals, and it is necessary to designate whether the signal adds (+) or subtracts (-). The configuration of Figure 2.3 is easily expanded to the block diagram of a n-node system as shown in Figure 2.4.

The preceding figures have illustrated the multiple node block diagram for cases with only a single output but many inputs. In practice any number of outputs may exist in combination with one or many inputs. The basic procedure for putting the block diagram is standard form is unchanged, but the results of the manipulations sometimes take a peculiar configuration. A number of block diagrams are therefore presented to illustrate some of the possible configurations.

Figure 2.5 shows a system with one input and two outputs. The summers are lettered and arranged in sequence as usual.

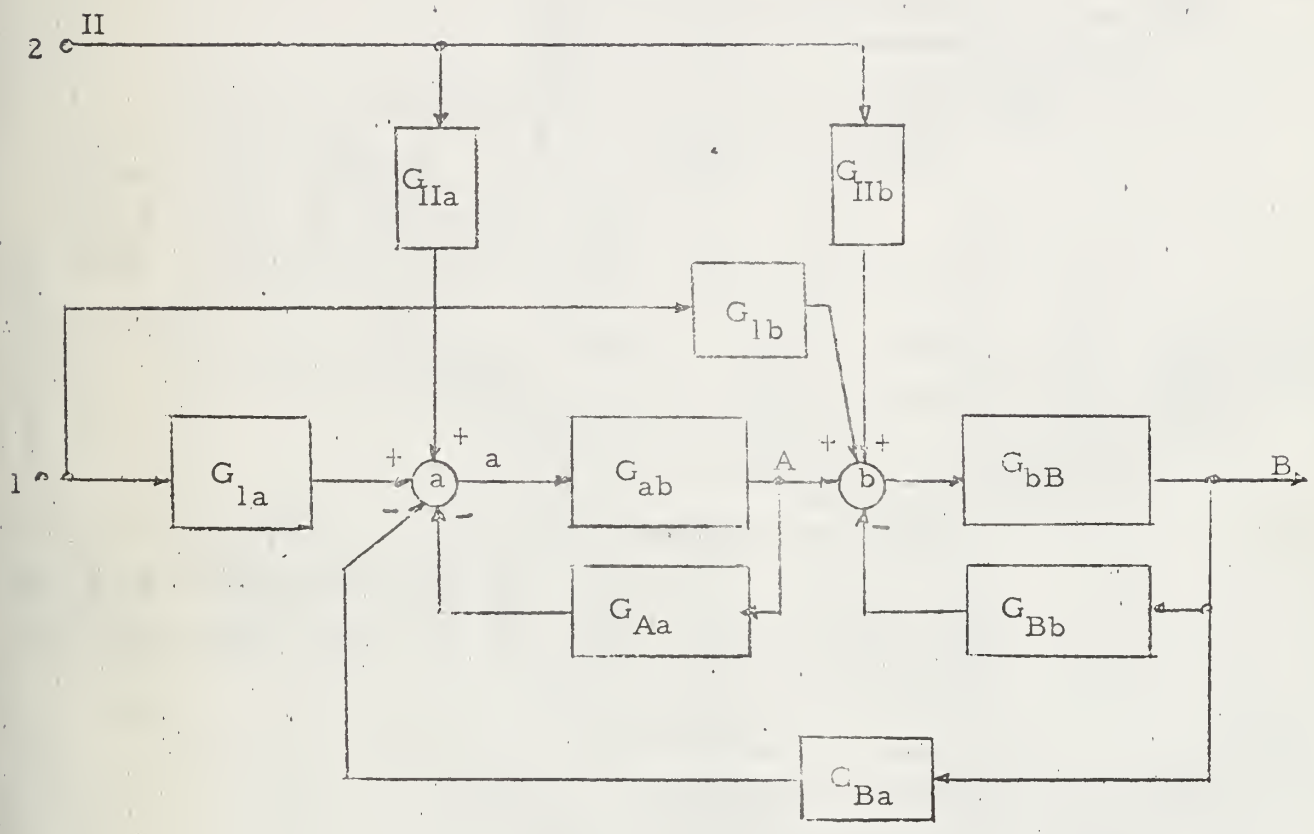

Fig. 2.3 GENERALIZED BLOCK DIAGRAM FOR A TWO NODE SYSTEM

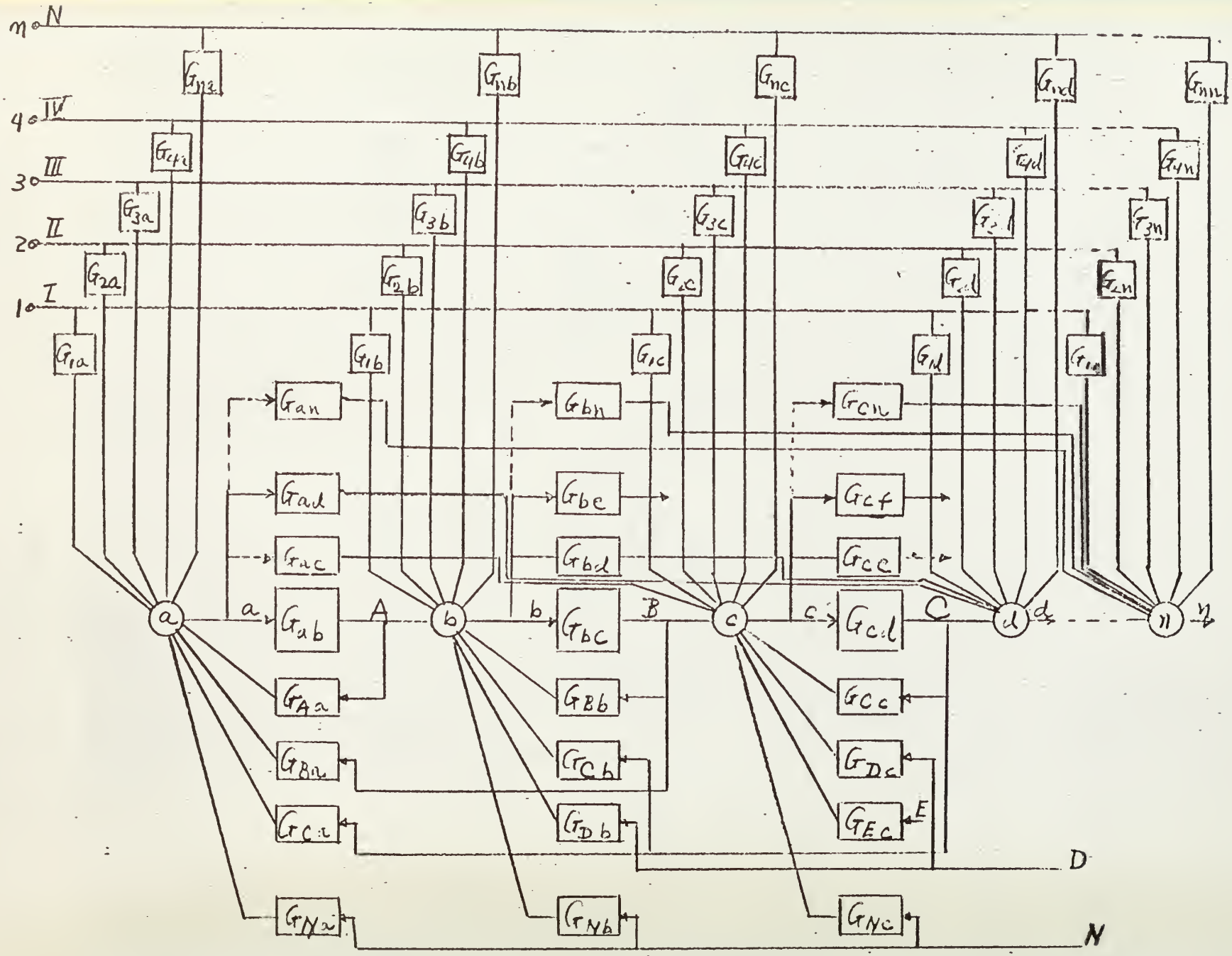

Fig. 2.4 STANDARD BLOCK DIAGRAM OF AN N-NODE SYSTEM

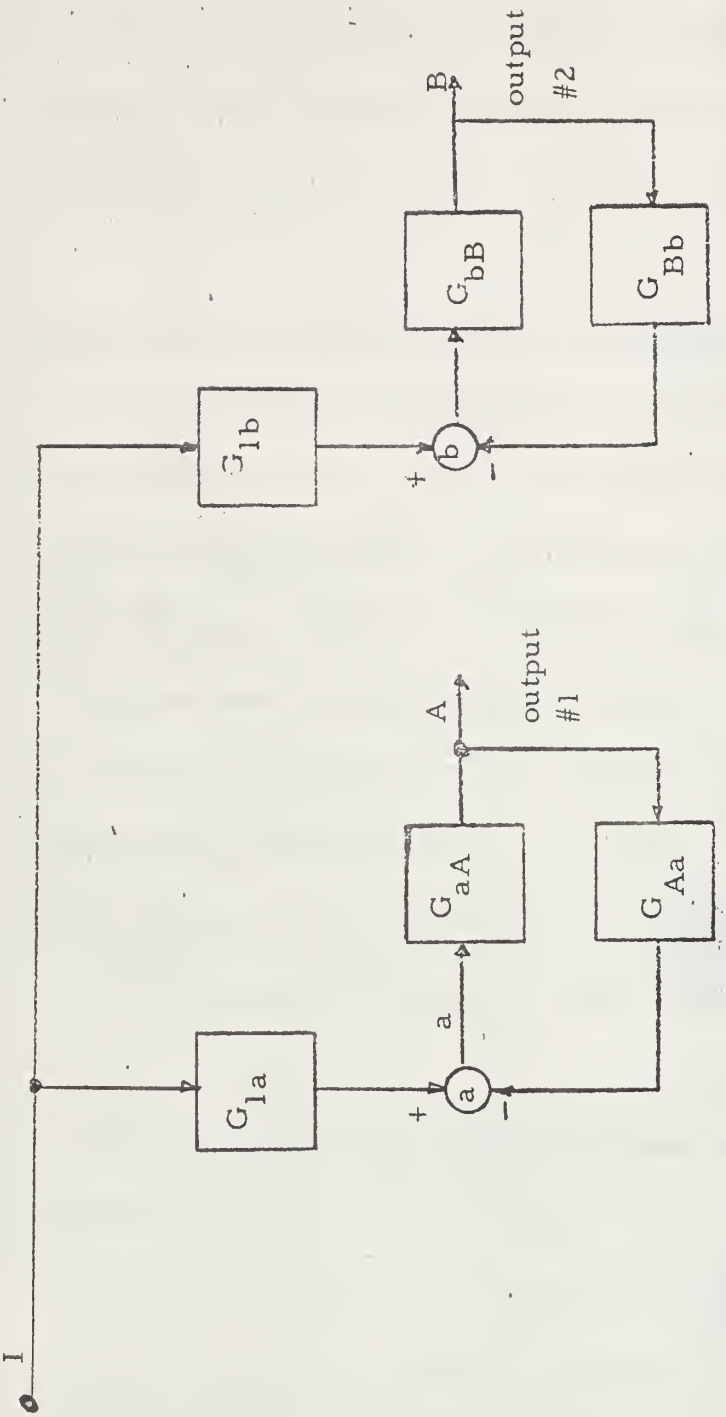

Fig. 2.5 ONE INPUT; TWO OUTPUTS

There is a break, or cut, in the main path since the output of G_{aA} is not fed into node b. Figure 2.6 shows a system with two inputs, two outputs, and a reduced number of paths coupling the nodes.

2.3 Mathematical Analysis Based on the Standard Block Diagram

The obvious approach to system analysis is to derive a set of simultaneous equations for the system. This is readily accomplished by writing an equation for the signal summation at each summer or node. If this is done for the n-node standard block diagram of Figure 2.4 (with proper attention to subscripts in arranging the terms) a determinant can be obtained which has a sort of symmetry. In addition, as will be shown, each term in the determinant has a specific relationship to a definite path in the system so that a reasonable amount of physical correlation exists.

Referring to the n-node block diagram, note that at each node there is only one output signal, but many signals being fed in. Of the signals being fed in some are from input stations, some are feedforward signals, and some are feedback signals. From the nature of a summing device it follows that at each node the output signal must be the algebraic sum of all input signals.

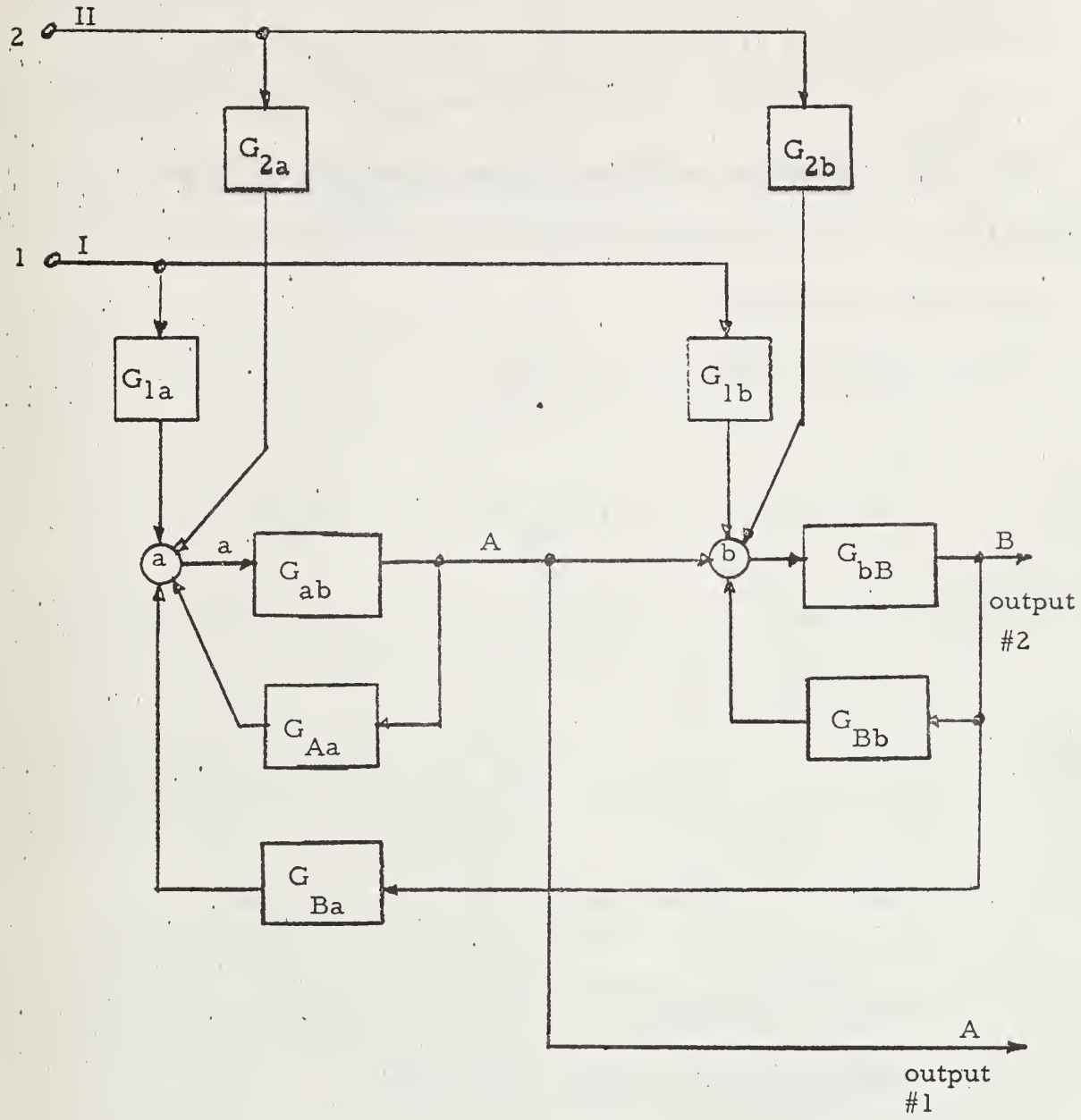

Fig. 2-6 TWO INPUTS; TWO OUTPUTS

In feedback control systems inverse or negative feedback is normally used, so it is convenient to treat feedback signals as subtractive. Input and feedforward signals may either add or subtract, so it is convenient to consider them additive in the generalized treatment.

At node "a" the output of the node is:

$$a = -(G_{ab}\,G_{Aa})\,a - (G_{bc}\,G_{Ba})\,b - (G_{cd}\,G_{Ca})\,c - (G_{de}\,G_{Da})\,d - \ldots - (G_{no}\,G_{Na})\,n + G_{1a}\,I + G_{2a}\,II + G_{3a}\,III + G_{4a}\,IV + \ldots G_{na}\,N \quad (2\text{-}1)$$

This rearranges to

$$(1 + G_{ab}\,G_{Aa})\,a + (G_{bc}\,G_{Ba})\,b + (G_{cd}\,G_{Ca})\,c + (G_{de}\,G_{Da})\,d + \ldots (G_{no}\,G_{Na})\,n = \sum_{m=1\,(I)}^{m=n\,(N)} (G_{ma})_m \quad (2\text{-}2)$$

At node "b" the arrangment of signals is similar to that at node "a", but the first feedforward signal appears. It is the signal fed forward from node "a" through G_{ab}. The equation at node "b" may be written as:

$$b = (G_{ab})\,a - (G_{bc}\,G_{Bb})\,b - (G_{Cb} - (G_{de}\,G_{Db})\,d - \ldots (G_{no}\,G_{Nb})\,n + G_{1b}\,I + G_{2b}\,II + G_{3b}\,III + \ldots + G_{nb}\,N \quad (2\text{-}3)$$

Keeping the signals in normal sequence this rearranges to:

$$-(G_{ab})a+(1+G_{bc}G_{Bb})\,b+(G_{cd}\,G_{Cb})\,c+G_{de}\,G_{Db})\;\;d+$$

$$\ldots+(G_{no}\,G_{Nb})\,n=\sum_{m=1\,(I)}^{m=m\,(N)}(G_{mb})\,m \qquad (2\text{-}4)$$

In like manner the equilibrium equation at node "c" is:

$$c=(G_{ac})\,a+(G_{bc})\,b-(G_{cd}\,G_{Cc})\,c-(G_{dc}\,G_{Dc})\,d$$

$$-\ldots-(G_{no}\,G_{Nc})\,n+G_{1c}\,I+G_{2c}\,II\,G_{3c}\,III+\ldots+G_{nc}\,N \qquad (2\text{-}5)$$

This rearranges to

$$-(G_{ac})\,a-(G_{bc})\,b+(1+G_{cd}\,G_{Cc})\,c+(G_{de}\,G_{Dc})\,d+\ldots$$

$$+(G_{no}\,G_{Nc})\,n=\sum_{m=1\,(I)}^{m=n\,(N)}(G_{mc})\,m \qquad (2\text{-}6)$$

By inspecting equations 2-2, 4, 6, the symmetry of arrangement of terms is easily determined, and the equation at any node may be written without the need to refer to the block diagram. It should also be noted from these equations that all of the input signals or forcing functions are located on the right hand side of each equation leaving on the left hand side the terms which refer to components and signals within the closed loops. Thus the left hand sides may be arranged to form the characteristic determinant of

the system. This determinant may be called Δ and is:

$$\Delta = \begin{vmatrix} 1 + G_{aA}G_{Aa} & + G_{bB}G_{Ba} & G_{cC}G_{Ca} & G_{dD}G_{Da} \text{ --- } G_{nN}G_{Na} \\ - G_{ab} & 1+G_{bB}G_{Bb} & G_{cC}G_{Cb} & G_{dD}G_{ab} \text{ --- } G_{nN}G_{Nb} \\ -G_{ac} & -G_{bc} & 1+G_{cC}G_{Cc} & G_{dD}G_{Dc} \text{ --- } G_{nN}G_{Nc} \\ -G_{ad} & -G_{bd} & -G_{cd} & 1+G_{dD}G_{Dd} \text{ --- } G_{nN}G_{Nd} \\ \cdot & \cdot & \cdot & \cdot \quad \cdot \\ \cdot & \cdot & \cdot & \cdot \quad \cdot \\ \cdot & \cdot & \cdot & \cdot \quad \cdot \\ -G_{an} & -G_{bn} & -G_{cn} & \text{-----} \quad 1+G_{nN}G_{Nn} \end{vmatrix} \qquad (2\text{-}7)$$

The arrangement of the characteristic determinant has certain features which can be useful:

a) Every term in the main diagonal is of the form $1 + G_{12}G_{21}$ and each of these terms is itself the characteristic equation of the basic loop at the designated node.

b) Every term above the main diagonal represents a feedback path consisting of forward transmission from a node through one block, then transmission from the output of that block through one feedback block to a prior node. The node at which this path starts is designated by the column, and the node to which the signal is fed is designated by the row.

c) Every term below the main diagonal represents a feedforward path through one block only. The starting point of each path is the output of the node designated by the column and the node to which the signal is fed is designated by the row.

In practical systems not all paths will exist. When a path does not exist the transfer function of the block which is omitted is zero. On the other hand if the path exists but there is a direct connection rather than transmission through a block, then that transfer function is unity. Thus the characteristic determinant of any specific system may be obtained easily by arranging its block diagram in the standard form, writing the determinant of the general system for the given number of nodes, and inserting the transfer functions of the specific system at the proper location in the determinant structure.

The characteristic determinant of any system is simply that portion of the N-node determinant which is specified by the number of nodes in the given system. For example, for a one node system:

$$\Delta \text{ (one node)} = 1 + G_{aA}G_{Aa} \qquad (2\text{-}8)$$

for a two node system:

$$\Delta \text{ (two nodes)} = \begin{vmatrix} 1 + G_{aA}G_{Aa} & G_{bB}G_{Ba} \\ -G_{ab} & 1 + G_{bB}G_{Bb} \end{vmatrix} \qquad (2\text{-}9)$$

for a three node system:

$$\Delta \text{ (three nodes)} = \begin{vmatrix} 1 + G_{aA}G_{Aa} & G_{bB}G_{Bb} & G_{cC}G_{Ca} \\ -G_{ab} & 1 + G_{bB}G_{Bb} & G_{cC}G_{Cb} \\ -G_{ac} & -G_{bB} & 1 + G_{cC}G_{Cc} \end{vmatrix} \qquad (2\text{-}10)$$

The solution of the system equations for system performance is obtained with the usual manipulations of the determinant. That is, the column representing the input functions replaces the column for the desired signal in the characteristic determinant, and the resulting determinant is the numerator determinant Δ is the denominator determinant, and expansion of these determinants provides the solution for the desired signals. If all inputs exist and are activated, then the column for the input functions is:

$$\sum_{m=1(I)}^{m=n(N)} (G_{ma})(m)$$

$$\sum_{m=1(I)}^{m=n(N)} (G_{mb})(m) \qquad (2\text{-}11)$$

$$\sum_{m=1(I)}^{m=n(N)} (G_{mc})(m)$$

$$\sum_{m=1(I)}^{m=n(N)} (G_{mn})(m)$$

This column replaces the nth column in the general determinant of equation 2-7 to form the numerator determinant. When any other

signal is to be computed Equation 2-11 replaces the corresponding column in the numerator determinant.

In most practical cases only one input is activated at a time, so that the terms in Equation 2-11 are relatively simple. In analysis and design computations the test functions likely to be used as inputs are the step and the ramp, and for these the terms in Equation 2-11 are extremely simple. It should be noted that this theory has been developed for linear systems, so the principle of superposition is valid. Thus even in the case of multiple inputs acting simultaneously the system may be analyzed for response to one input at a time and the results superimposed.

3. AN ILLUSTRATION OF THE USE OF THE DETERMINANTAL APPROACH.

3.1 Introduction

A high gain uncompensated positioning servo is shown in block diagram form on Fig. 3.1. It is the purpose of this section to study the effect of amplidyne voltage feedback, either positive or negative, to the mag amp input.

Values of K and K_1 have been determined as

$K = 57.5$ and $K_1 = .315$

3.2 The Characteristic Determinant and Steady-State Error

The characteristic determinant may be written down by inspection of the block diagram Fig. 3.1. This determinant is:

$$\Delta = \begin{vmatrix} 1 & 0 & \dfrac{315 \times 10^3}{s(s+100)^2(s^2+10s+100)} \\ -50 & 1 + \dfrac{11,500}{s+200} G_c & 0 \\ 0 & \dfrac{-11,500}{s+200} & 1 \end{vmatrix} \qquad (3\text{-}1)$$

Expansion yields:

$$\Delta = 1 + \frac{11,500}{s+200} G_c + \frac{18.1 \times 10^{10}}{s(s+200)(s+100)^2(s^2+10s+100)} \qquad (3\text{-}2)$$

The steady state error from a step input is:

$$E_{ss_{step}} = \lim_{s \to 0} \left[1 - \frac{G_{cd} \Delta_{ac}}{\Delta} \right] \qquad (3\text{-}3)$$

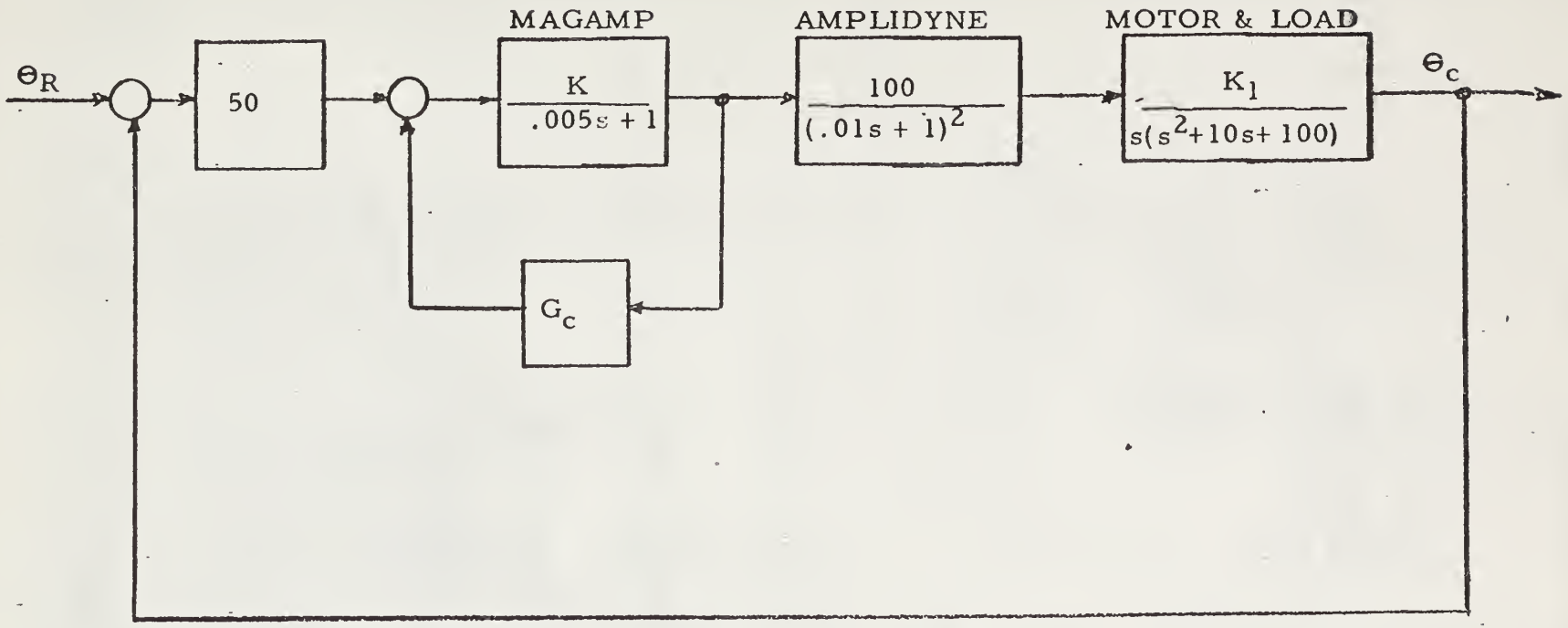

Fig. 3.1 BLOCK DIAGRAM OF A CONTROL SYSTEM

Evaluating each term independently before combining:

From Equation 3-2:

$$\lim_{s \to 0} \Delta = 1 + 57.5G_c + \frac{905}{s}$$

$$\lim_{s \to 0} \Delta_{ac} = \begin{vmatrix} -50 & 1 + 57.5G_c \\ 0 & -57.5 \end{vmatrix}$$

$$= 2876$$

$$\lim_{s \to 0} G_{cd} = \frac{.315}{s}$$

Substituting into Equation 3-3 yields

$$E_{ss_{step}} = \left[1 - \frac{\frac{.315}{s}(2876)}{1 + 57.5G_c + \frac{905}{s}}\right]_{s \to 0}$$

$$= \left[1 - \frac{905}{s + 57.5G_c s + 905}\right]_{s \to 0}$$

$$= \left[1 - \frac{905}{57.5\, G_c\, s + 905}\right]_{s \to 0}$$

$$= \left[1 - \frac{905}{905 + 57.5s\, \frac{K_c (z_1)(z_2) \cdots (z_n)}{(p_1)(p_2) \cdots (p_n)}}\right]_{s \to 0}$$

This error will be zero if there be no p = 0.

The steady state error for a ramp input is:

$$E_{ss_{ramp}} = \frac{1}{s}\left[1 - \frac{G_{cd}\,\Delta_{ac}}{\Delta}\right]_{s \to 0} \qquad (3\text{-}4)$$

Substituting values:

$$E_{ss_{ramp}} = \frac{1}{s}\left[1 - \frac{905/s}{1 + 57.5\,G_c + 905/s}\right]_{s \to 0}$$

$$= \frac{1}{s}\left[\frac{1 + 57\,G_c + 905/s - 905/s}{1 + 57.5\,G_c + 905/s}\right]_{s \to 0}$$

$$= \frac{1 + 57.5G_c}{s + 57.5\,G_c\,s + 905}\Bigg|_{s \to 0}$$

$$E_{ss_{ramp}} = \frac{1+57.5\,\dfrac{K_c\,(z_1)\,(z_2)\,---\,(z_n)}{(P1)\,(P2)\,(P3)\,---\,(P_n)}}{57.5\,G_c s + 905}\Bigg|_{s \to 0}$$

Compensators containing terms of the form $\frac{1}{s}$ are not allowed.

Therefore,

$$E_{ss_{ramp}} = \frac{1 + 57.5\,K_c\,\dfrac{(z_1)\,(z_2)\,---\,(z_n)}{(p_1)\,(p_2)\,---\,(p_n)}}{905}$$

In order that the steady state error be as small as possible, the term

$$\frac{57.5\,K_c\,(z_1)\,(z_2)\,---\,(z_n)}{(p_1)\,(p_2)\,---\,(p_n)} \ll 1 \qquad (3\text{-}5)$$

This may be best obtained by having one or more of the z's identically zero. Then the steady state error is the minimum obtainable.

3.3 Summary of Compensation Schemes Which Appear Feasible and Restrictions to be Observed When Attempting Compensation.

Compensators containing a term 1/s are prohibited because this essentially results in reducing the servo to a type zero system and producing a $K_v = 0$ and an infinite error to a ramp input,

In all other compensators,

$$\frac{57.5\, K_c\, (z_1)\, (z_2)\, ---\, (z_n)}{(p_1)\, (p_2)\, ---\, (p_n)} \qquad (3\text{-}6)$$

must be much less than 1. This is needed so that the steady state error to a ramp input will be as small as possible. The optimum case will be for one of z's = 0.

3.4 Compensation Schemes Attempted in the Feedback Path Around the Magamp.

A compensator having the transfer function

$$G(s) = \frac{K_c\, (s^2 + 2\zeta_z\, \omega_{nz}\, s + \omega_{nz}^2)}{(s + p_1)\, (s + p_2)} \qquad (3\text{-}7)$$

was investigated. It was determined that if $s = -10 \pm j\,10$ were points through which it was desired to pass a 180 degree locus and if $p_1 \cong p_2 \cong 230$ were selected that using a pair of complex conjugate zeros at $s = -16 \pm j\,10$ would force a 180° locus to pass through the desired points.

Since:

$$\frac{57.5\, K_c\, \omega_{n3}^2}{p_1\, p_2} \ll 1$$

$$\frac{57.5\, K_c\, (356)}{(230)^2} \ll 1$$

$$K_c \ll 2.585 \qquad (3\text{-}8)$$

Letting $K_c = 1$ does not satisfy specifications, but it is a convenient place to start. Using Equation 3-7 and Equation 3-2 yields:

$$\frac{K_c\,(s + 16 + j\,10)\,(s + 16 - j\,10)}{(s + 230)\,(s + 230)} \qquad (3\text{-}9)$$

$$\frac{11.5 \times 10^3\, s\,(s + 100)^2\,(s^2 + 10s + 100)}{(s + 197)\,(s+135)\,(s+60+j43)\,(s+60-j43)\,(s+21+j28.5)\,(s+21-j28.5)} = -1$$

An Esiac investigation performed on the root locus of Equation 3-9 to find the roots of the characteristic equation with this compensator resulted in the root locus of Fig. 3-2. For $K_c = 2$ the system was unstable. By making $K_c = 6.17 \times 10^3$ the system could be made stable, but this violates Equation 3-8. This compensator was therefore adjudged unsatisfactory.

A compensator having the transfer function

$$G(s) = \frac{K_c}{s^2 + 10s + 100} \quad \frac{(s + z)}{(s + p)} \qquad (3\text{-}10)$$

was investigated.

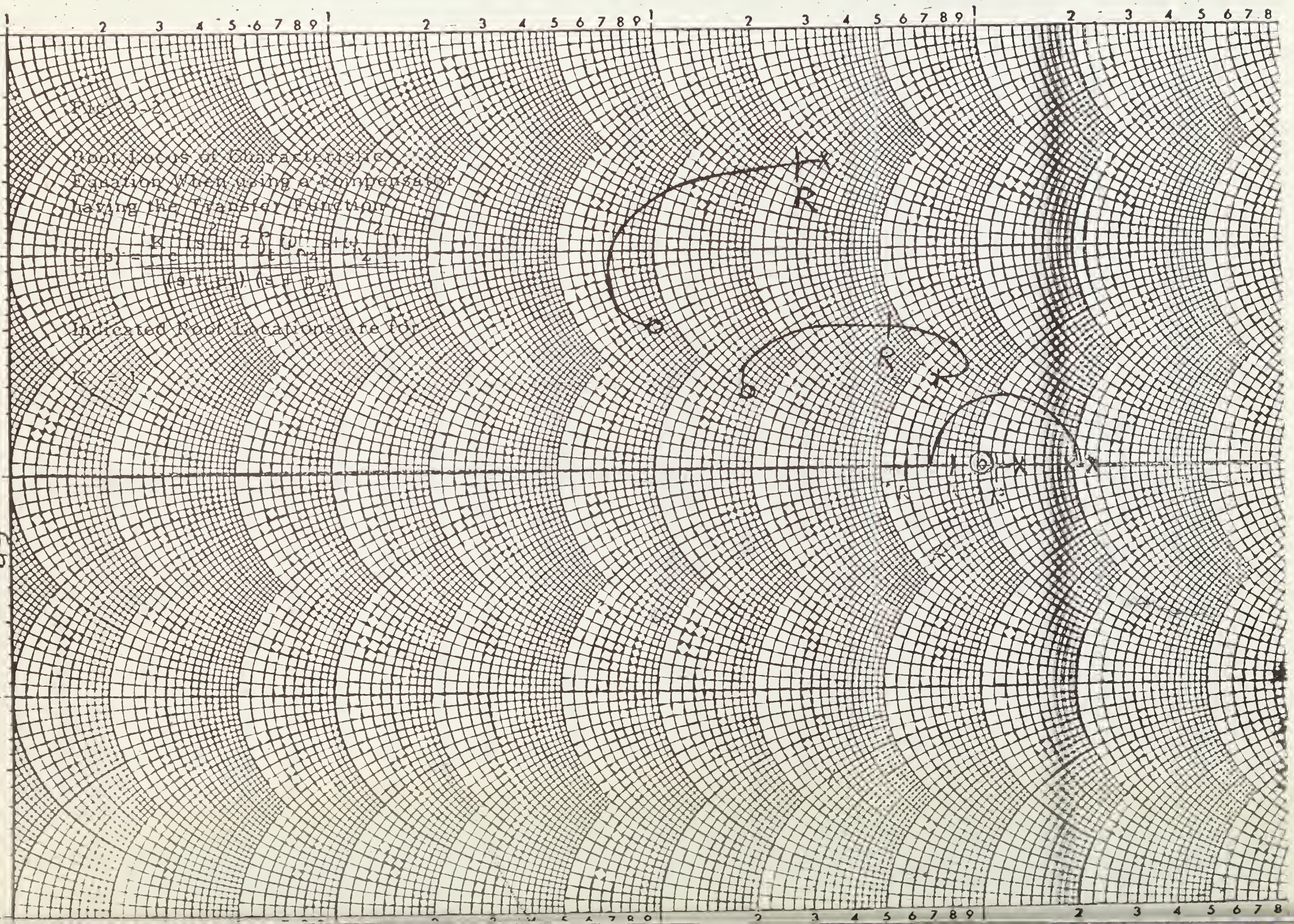

Fig. 3-2

Root Locus of Characteristic Equation When Using a Compensator Having the Transfer Function

$$G_c(s) = \frac{K_c(s^2 + 2\zeta_c\omega_c s + \omega_c^2)}{(s + p_1)(s + p_2)}$$

Indicated Root Locations are for

$K_c = 1$

Substituting Equation 3-10 into Equation 3-2 yields:

$$\frac{K_c (s + z)}{(s^2 + 10s + 100)(s+p)}$$

$$\left[\frac{11,500(s)(s+100)^2 (s^2+10s+100)}{(s+197)(s+135)(s+60+j43)(s+60-j43)(s+21+j28.5)(s+21-j28.5)}\right] = -1 \qquad (3\text{-}11)$$

$$\frac{K_c (s + z)}{(s + p)}$$

$$\left[\frac{11,500\, s\,(s+100)^2}{(s+197)(s+135)(s+60+j43)(s+60-j43)(s+21+j28.5)(s+21-j28.5)}\right] = -1$$

By examining the pole - zero array of Equation 3-11 it was determined that z = 20, p = 183 would cause a 180° locus to pass through $s = -10 \pm j\,10$. Substituting these values for z and p

$$\frac{57.3\,K_c}{100} \qquad \frac{(20)}{(183)} \ll 1$$

$$K_c \ll 16.1 \qquad (3\text{-}12)$$

Again $K_c = 1$ does not satisfy this criterion adequately, but it make a convenient starting point. An Esiac investigation (Fig. 3-3) was performed on the root locus of Equation 3-11 and was found to be unstable for $K_c = 1.0$. Stability could be achieved by setting

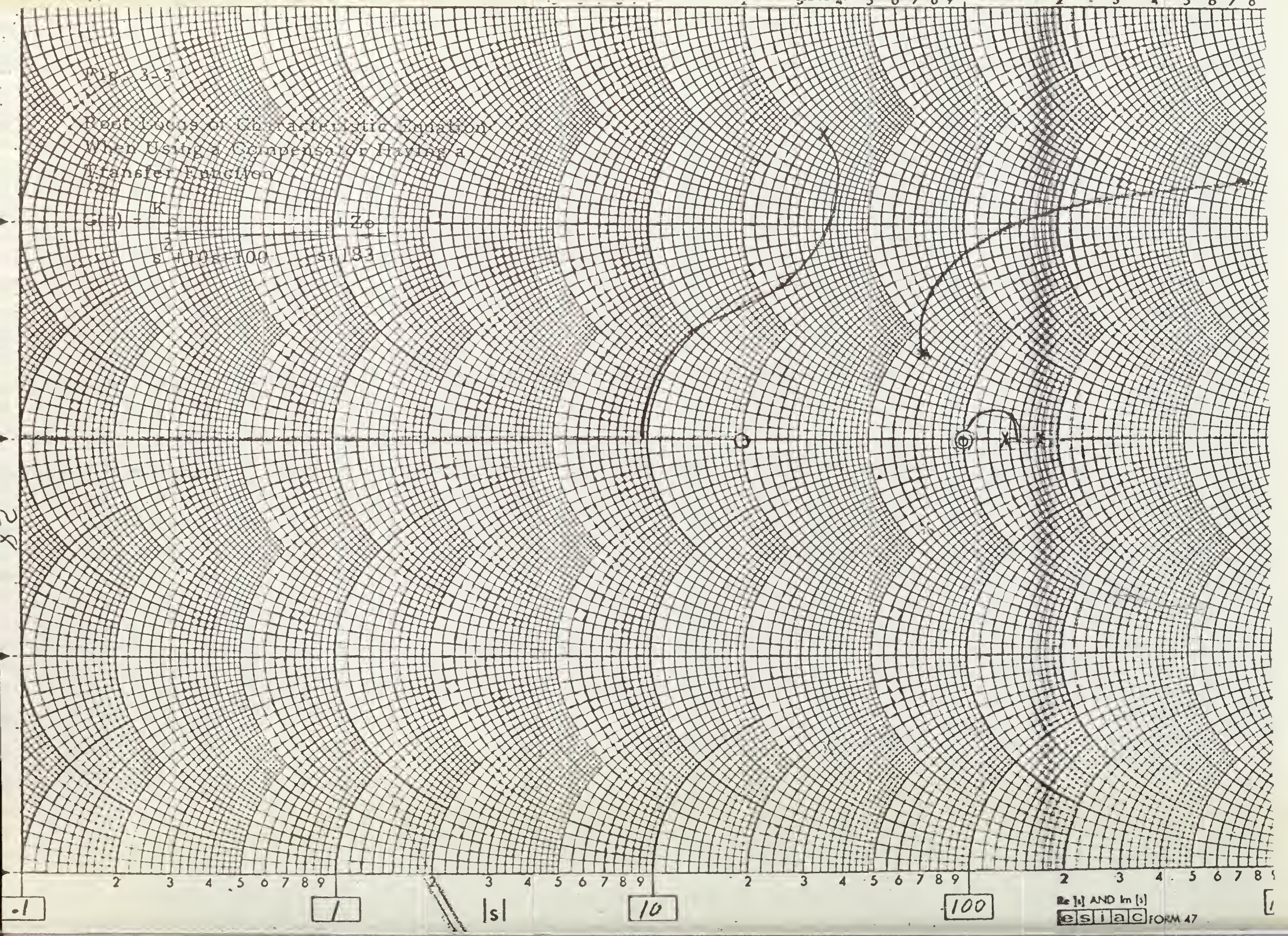

Fig. 3-3

Root Locus of Characteristic Equation When Using a Compensator Having a Transfer Function

$$G(s) = \frac{K}{s^2+10s+100} \cdot \frac{s+Z_o}{s+183}$$

$K_c \gtrsim 285$, but this violates Equation 3-8. Therefore this compensator was adjudged unsatisfactory.

A compensator having the transfer function

$$G(s) = \frac{K_c}{s^2 n + 10s + 100} \left(\frac{s + z}{s + p} \right)^2 \qquad (3\text{-}13)$$

was investigated.

Substituting Equation 3-13 into Equation 3-2 yields.

$$\frac{K_c (s + z)^2}{(s^2+10s+100)(s+1)^2}$$

$$\left[\frac{11.500 (s) (s^2 + 10s + 100) (s+100)^2}{(s+135)(s+197)(s+60+j43)(s+60-j43)(s+21+j28.5)(s+21-j28.5)} \right] = -1$$

$$\frac{K_c (s+z)^2}{(s+p)^2} \qquad (3\text{-}14)$$

$$\left[\frac{(11.500)(s+100)^2 s}{(s+135)(s+197)(s+60+j43)(s+60-j43)(s+21+j28.5)(s+21-j28.5)} \right] = -1$$

By examining the pole zero array of Equation 3-14, it was determined that $z = 43$, $p = 250$ would cause a 180° locus to pass through the points $s = 10 \pm j10$. Applying the criterion of Equation 3-8 yields:

$$\frac{57.5 K_c}{100} \left(\frac{43}{250} \right)^2 \ll 1 \qquad (3\text{-}15)$$

$$K_c \ll 58.7$$

Assume $K_c = 1$ satisfies this criterion. Performing an Esiac investigation (Fig. 3.4) on the root locus of Equation 3-14 showed that the system was unstable for $K_c = 1$. Stability could be achieved for $K_c \geq 452$, but this violates Equation 3-15. Therefore this compensator was adjudged unacceptable.

3.5 Ross-Warren Method Used for Compensation

From the root locus plot, it was desired to bring the unstable roots ($s = 21.66 \pm 28.6j$) over into the left hand plane at a desirable location of $s = -10 \pm 10j$. This location should give a damping ratio, ζ, within the specifications. This location should also give a good transient response. In order to obtain the original K_v of 905, a 4 section compensator was tried. From the root locus plot, the following were obtained:

$\Phi_4 = 46^\circ$

$\zeta = 56.35$

$\sqrt[4]{K/G} = .908$

$\cot \Phi_4 = .966$

$\csc \Phi_4 = 1.39$

$\lambda_4 = \cot^{-1} (\cot \Phi_4 - \sqrt[4]{K/G} \csc \Phi_4)$

$= \cot^{-1} (.966 - 1.26) = \cot^{-1} (-.294) = \underline{106^\circ}$

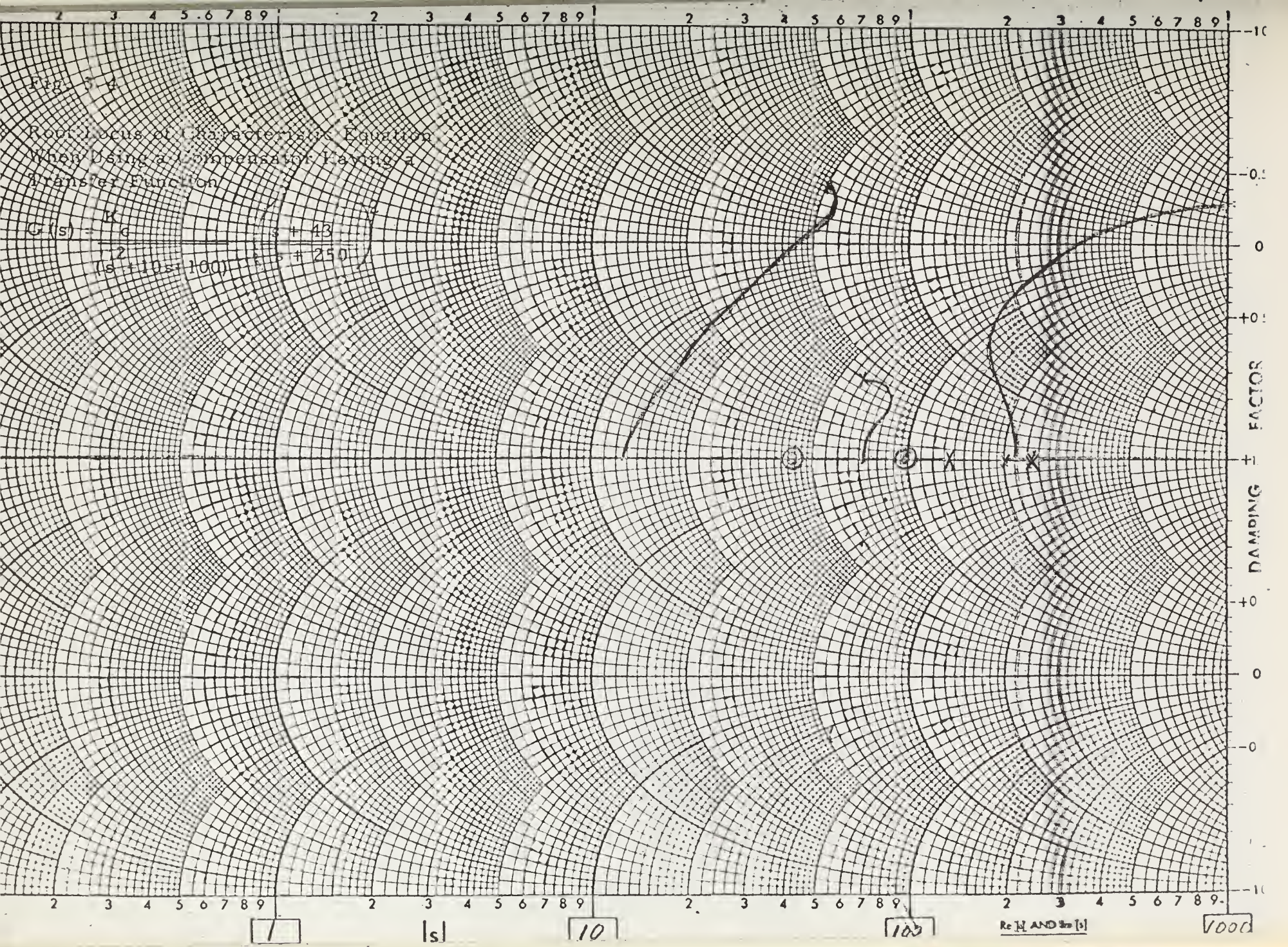
Fig. 5-4
Root Locus of Characteristic Equation When Using a Compensator Having a Transfer Function
$G(s) = \frac{K_c (s + 43)}{(s^2 + 10s + 100)(s + 250)}$
DAMPING FACTOR
|s|
Re N AND Im [s]
1
10
100
1000

$$\Theta_4 = \Pi + \Phi_4 + \zeta - \lambda_4$$

$$= 180 + 46 - 56.35 - 106 = \underline{63.65^\circ}$$

and since $\Theta_4 > \Phi_4$, this compensator is allowable. Hence:

$$z = h \left[\sqrt[4]{K/G} \; \frac{\sin \lambda_4}{\sin \Theta_4} \right] = 18.908 \; \frac{\sin 106}{\sin 63.65}$$

$$= \underline{\underline{17.4}}$$

$$p = \frac{h \sin \lambda_4}{\sin (\Theta_4 - \Phi_4)} = \frac{18 \times .956}{.304}$$

$$= \underline{\underline{56.2}}$$

and the compensated system becomes

$$-1 = \left(\frac{s + 17.4}{s + 56.2} \right)^4 \left[\frac{11,500 \, (s+100)^2 \, s \, (s^2 + 105 + 100)}{(s+200)(s+100)^2 \, s \, (s^2 + 10s + 100) + 18.1 \times 10^{10}} \right]$$

This was tested for stability on the Esiac and the results are shown on Fig. 3.5. From this, it can be seen that the system was unstable (having two roots in the right hand plane).

The next compensator investigated by this method was a 3 section filter. From root locus plot,

$\Phi_3 = 61.3^\circ$ $\qquad$ $\cot \Phi_3 = .547$

$\sqrt[3]{K/G} = .88$ $\qquad$ $\csc \Phi_3 = 1.14$

$h = 18$

$\zeta = 56.35$

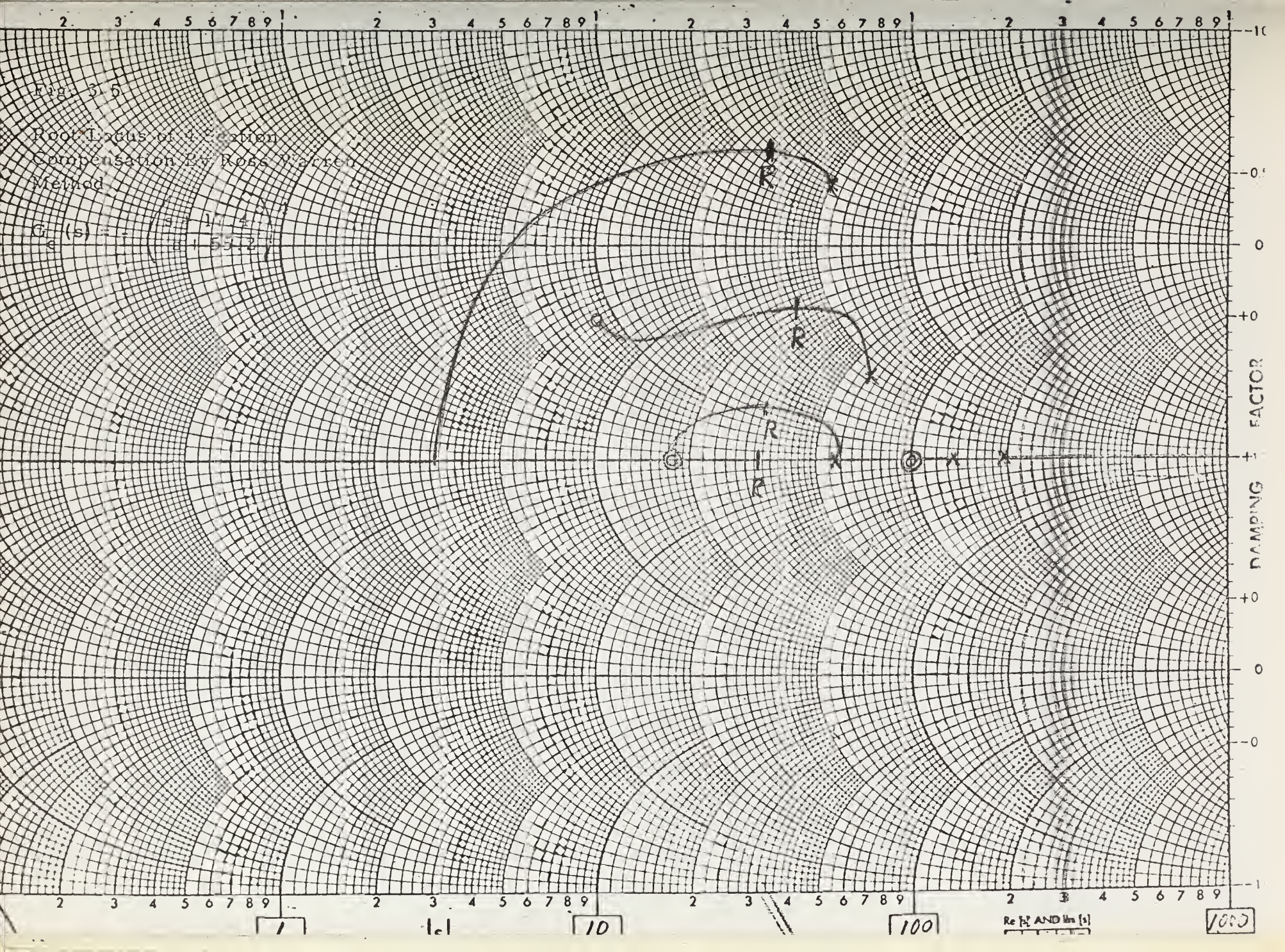
Fig. 3.5
Root Locus of Lead Section Compensation By Ross Warren Method
$G_c(s) = \frac{s+1}{s+55.2}$
R
R
R
R
DAMPING FACTOR
|s|
1
10
100
1000
Re [s] AND Im [s]

$$\lambda_3 = \cot^{-1}(\cot \phi_3 - \sqrt[3]{K/G} \csc \phi_3)$$

$$= \cot^{-1}(.547 - 1.01)$$

$$= \cot^{-1}(-.463) = \underline{114.8^\circ}$$

$$\theta_3 = \pi + \phi_3 - \delta - \lambda_3 = 180 + 61.3 - 56.35 - 114.8$$

$$= \underline{70.15^\circ}$$

and $\theta_3 > \phi_3$ which shows that 3 sections is allowable.

Hence $z = h \sqrt[3]{K/G} \quad \frac{\sin \lambda_3}{\sin \theta_3} = 18 \times .88 \times \frac{.907}{.940} = 15.4$

$$p = \frac{h \sin \lambda_3}{\sin(\theta_3 - \phi_3)} = \frac{18 \times .907}{.154} = 106$$

The resulted in the following:

$$-1 = \left(\frac{s+15.4}{s+106}\right)^3 \frac{11{,}500\,(s+100)^2\, s\,(s^2 + 10s + 100)}{(s+200)\,(s+100)^2\, s\,(s^2+10s+100) + 18.1 \times 10^{10}}$$

This was tested for stability on the Esiac, and the results shown on Fig. 3.6 show that the system is still unstable (having two roots in the right hand plane $s = 26 \pm 36j$).

3.6 Compensator with Zero at the Origin

A compensator having a transfer function

$$G(s) = \frac{K_c\, s}{s + p} \qquad (3\text{-}16)$$


Fig. 3-6
Root Locus of 2-section Compensation by Ross Warren Method
$G_c(s) = \left(\frac{s+1.5}{s+10}\right)^2$
R
X
O
DAMPING FACTOR
+1
0
-0
1
|s|
10
100
1000
Re[s] AND Im[s]
estac FORM 47

was investigated. Substituting Equation 3-16 into Equation 3-2 yields

$$\frac{11{,}500\, s\,(s+100)^2\,(s^2+10s+100)\,K_c s}{(s+197)\,(s+135)\,(s+60+j43)\,(s+60-j43)\,(s-21+j28.5)\,(s-21-j28.5)\,(s+p)} = -1 \qquad (3\text{-}17)$$

and it follows that:

$$\frac{57.5\,K_c\,(0)}{p} \ll 1$$

$$K_c \ll \infty$$

This satisfies the criterion for any finite value of K_c. The effects of varying p were studied by selecting several values of p and plotting the root loci on the Esiac. It was determined that for values of $/p/ \lesssim 4$, root loci from the two right half plane poles of Equation 3-17 came into cancel the zeros at the origin; giving either roots in the right half plane or roots in the left half plane with real parts ≤ 1; neither of which is acceptable.

The Esiac investigation further revealed that an optimum value of p was $p \simeq -3.5$. With this pole location, there could be produced two pairs of complex conjugate roots, the real part of each being $\simeq 3.5$. K_c required to obtain these root was $K_c = 8.96$. The Esiac plot of this is Fig. 3.7.

However, the Esiac is not sensitive enough to determine the actual value of K_c and root locations. Therefore a digital computer program was utilized to determine the exact root location for various

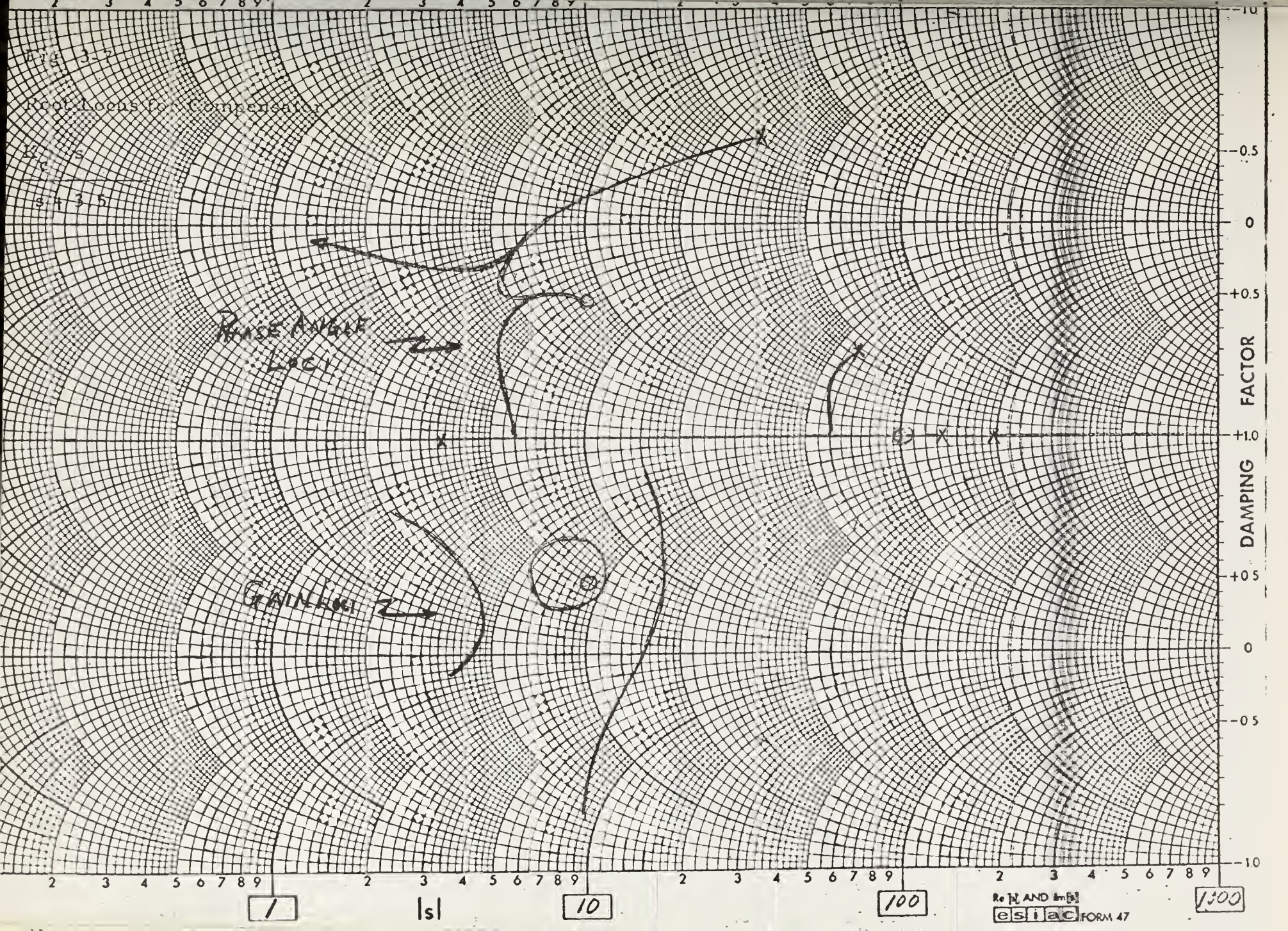
Fig. 3-7
Root Locus for Compensator
K_c = 5
s + 3.5
PHASE ANGLE LOCI
GAIN LOCI
DAMPING FACTOR
+1.0
+0.5
0
-0.5
-1.0
1
|s|
10
100
1000
Re[s] AND Im[s]
esiac FORM 47

values of K_c. It was found that optimum results were obtained with $K_c = 4.35$. This gave roots as follows:

$s = -2.48 \pm j\,4.46$

$s = -2.58 \pm j\,5.925$

$s = -101.904$

$s = -97.978$

$s = -5.02 \times 10^4$

These results satisfy all steady-state and transient specifications except settling time and the response to unit load torque. Checking the response to a unit load torque, the block diagram of the system is given in Fig. 3.8. The characterisitic determinant may be written by inspection. ($G_{c3} = 0$).

$$\Delta = \begin{vmatrix} 1 & 0 & 0 & 0 & 0 & \frac{1}{300s} \\ -50 & 1+\frac{5\times10^4 s}{(s+200)(s+3.5)} & 0 & 0 & 0 & 0 \\ 0 & \frac{-11,500}{s+200} & 1 & 0 & 0 & 0 \\ 0 & 0 & -\frac{10^6}{(s+100)^2} & 1 & \frac{9.43}{s+.246} & 0 \\ 0 & 0 & 0 & -\frac{10.4}{s+10} & 1 & 0 \\ 0 & 0 & 0 & 0 & -\frac{9.09}{s+.246} & 1 \end{vmatrix}$$

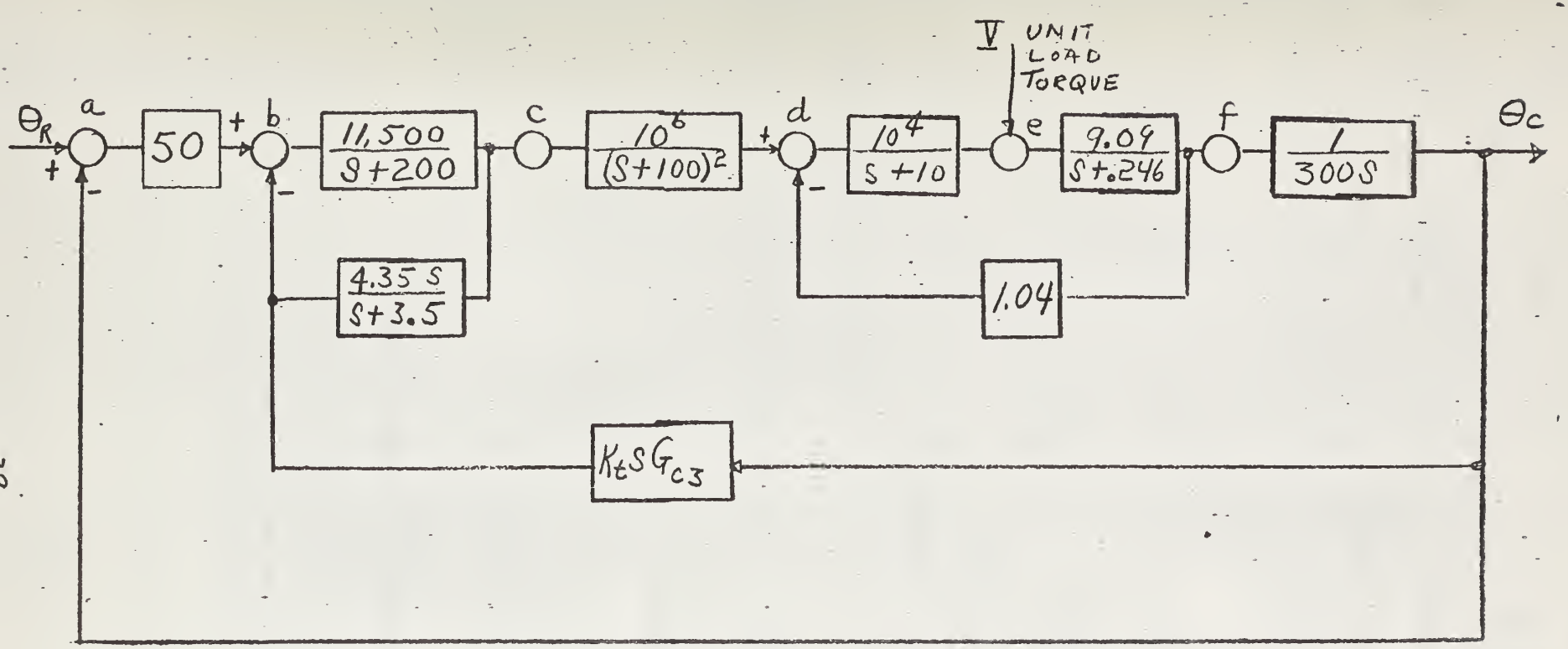
UNIT LOAD TORQUE
θ_R
a
50
b
$\frac{11,500}{S+200}$
c
$\frac{10^6}{(S+100)^2}$
d
$\frac{10^4}{S+10}$
e
$\frac{9.09}{S+.246}$
f
$\frac{1}{300S}$
θ_c
$\frac{4.35\,S}{S+3.5}$
1.04
$K_t S G_{c3}$

FIG 3.8

For the unit load torque input:

$$\Theta c_{ss} = \left[\frac{\Delta_{ef} \; G_{f\Theta c}}{\Delta} \right]_{s \to 0} \qquad (3\text{-}18)$$

Obtaining each term separately:

$$\Delta_{s \to o} = (1 + 7.5s)\, 41 + \frac{36,800}{s}$$

$$G_{f\Theta c}{}_{s \to 0} = \frac{1}{300s}$$

$$\Delta_{ef}{}_{s \to 0} = 36.9 + 2640s$$

Substituting these into Equation 3-18

$$\Theta c_{ss} = \left. \frac{(36.9 + 2640s)\, \frac{1}{300s}}{(1 + 71.5s)\, 41 + \frac{36,800}{s}} \right|_{s \to 0}$$

$$= \frac{36.9}{(300)(36,800)}$$

$$= \frac{1}{300,000} \text{ Radian}$$

And this is

$$\Theta c_{ss} = .0115 \text{ minutes of arc.}$$

3.7 Combining of Amplidyne Path with Tach Path

Prior to attempting any compensation schemes an investigation was made to determine if there were any restrictions on the types

of compensators that could be used in these paths. Assuming an unspecified compensator in each path, the block diagram of Fig. 3.9 is obtained.

From the block diagram of Fig. 3.9, the characteristic determinant may be written down by inspection.

(3-19)

$$\Delta = \begin{vmatrix} 1 & 0 & \dfrac{.315 \times 10^6}{s(s+100)^2(s^2+10s+100)} \\ -50 & 1 + \dfrac{11,500}{s+200} G_{c1} & \dfrac{.315 \times 10^6 K_t G_{c3}}{(s+100)^2(s^2+10s+100)} \\ 0 & -\dfrac{11,500}{s+200} & 1 \end{vmatrix}$$

Now for a step input at Θ_R

$$E_{ss_{step}} = \left[1 - \frac{\Delta_{ac} \; G_c \Theta_c}{\Delta} \right]_{s=0} \qquad (3\text{-}20)$$

Evaluating each term separately:

$$\Delta_{s \to 0} = \begin{vmatrix} 1 & 0 & \dfrac{.315}{s} \\ -50 & 1+57.5G_{c1} & .315K_tG_{c3} \\ 0 & -57.5 & 1 \end{vmatrix}$$

$$\Delta_{s \to 0} = 1 + 57.5\, G_{c1} + 18.1\, K_t\, G_{c3} + \frac{905}{s}$$

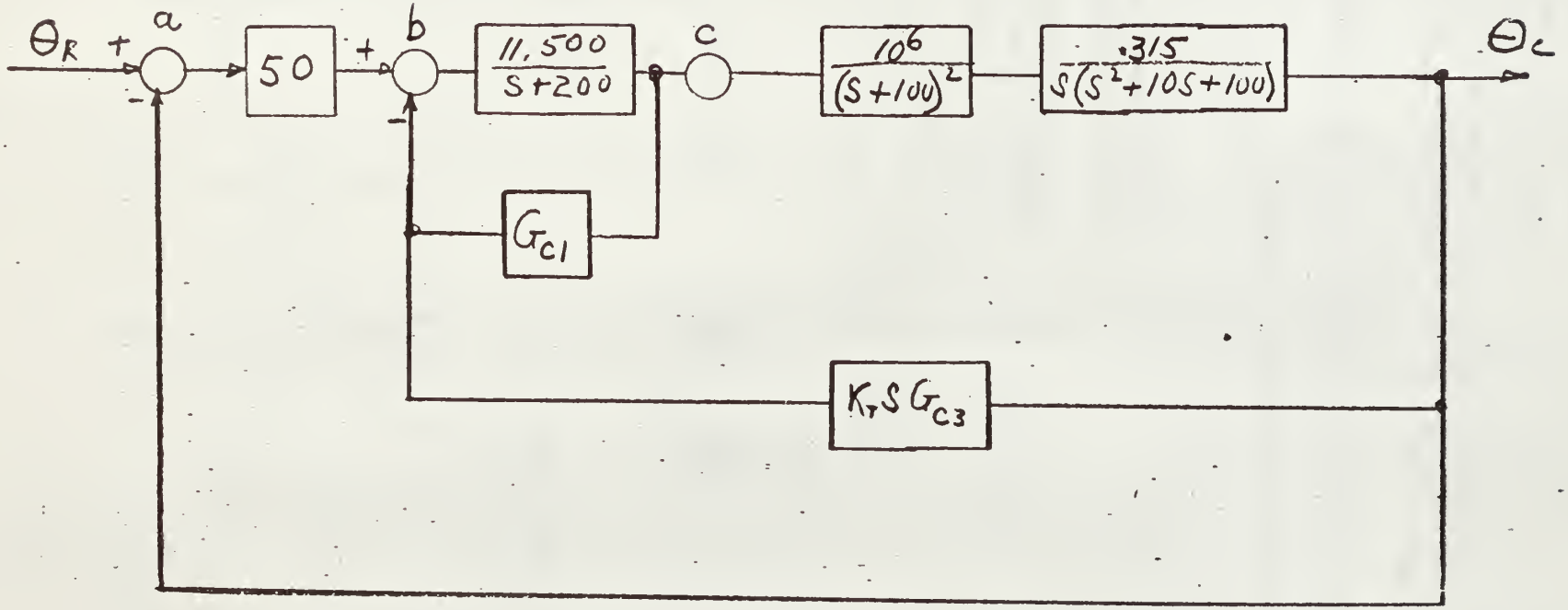

FIG 3.9

$$\Delta_{ac}\Big|_{s\to 0} = 2877$$

$$G_{c\Theta c}\Big|_{s\to 0} = \frac{.315}{s}$$

Substituting into Equation 3-20

$$E_{ss_{step}} = \left[1 - \frac{2877\left(\frac{.315}{s}\right)}{1 + 57.5 G_{c1} + 18.1 K_t G_{c3} + \frac{905}{s}} \right]_{s\to 0}$$

$$E_{ss_{step}} = \left[1 - \frac{905}{57.5 G_{c1} s + 18.1 K_t G_{c3} s + 905} \right]_{s\to 0}$$

By inspection, it is seen that if it is desired that $E_{ss_{step}}$ be zero, then G_{c1} and G_{c3} can contain no terms of the form $\frac{1}{s^N}$. If however, N=1 and the feedbacks be of opposite sign such that

$$57.5 G_{c1} = -18.11 K_t G_{c3}$$

$$-3.18 G_{c1} = K_t G_{c3}$$

Then the desired zero error will be attained.

Now,

$$E_{ss_{RAMP}} = \frac{1}{s} \left[1 - \frac{\Delta_{ac} G_{c\Theta c}}{\Delta} \right]_{s\to 0} \qquad (3\text{-}21)$$

Substituting the already obtained values into this equation

$$E_{ss_{RAMP}} = \frac{1}{s}\left[1 - \frac{905/s}{1 + 57.5\,G_{c1} + 18.1\,K_t G_{c3} + 905/s}\right]_{s\to 0}$$

$$= \frac{1}{s}\left[\frac{1 + 57.5\,G_{c1} + 18.1\,K_t G_{c3}}{1 + 57.5\,G_{c1} + 18.1\,K_t G_{c3} + 905/s}\right]_{s\to 0}$$

$$= \left.\frac{1 + 57.5\,G_{c1} + 18.1\,K_t G_{c3}}{57.5\,G_{c1}s + 18.1\,K_t G_{c3}s + 905}\right|_{s\to 0}$$

From this equation, it can be seen that G_{c1} and G_{c3} cannot contain terms of the form $\frac{1}{s^N}$ where $N \geq 1$ because this would cause the numerator to go to ∞. This then negates this possibility of a solution using positive feedback in one path and negative in the other while using a term $\frac{1}{s}$ as suggested from the equations for $E_{ss_{step}}$.

It is further seen from this equation that since the required

$$E_{ss_{RAMP}} \leq \frac{1}{905}$$

That the $\text{Lim}_{s\to 0}\ G_{c1} = \text{Lim}_{s\to 0}\ G_{c3} \equiv 0$

Considering now the possibility that the response to a unit load torque may place additional restrictions on the type of compensator adopted, use the block diagram of Fig. 3.8 with $\frac{4.35\,s}{s + 3.5}$ being replaced by a general compensator G_{c1}.

$$\Theta c_{ss\ u.l.t.} = \left[\frac{\Delta_{ef}\ G_{f\Theta c}}{\Delta} \right]_{s \to 0} \qquad (3\text{-}22)$$

Writing down Δ_{s-0} by inspection of Fig. 3.8 with $\frac{4.35\ s}{s + 3.5} \triangleq G_{cl}$

$$\Delta_{s-0} = \begin{vmatrix} 1 & 0 & 0 & 0 & 0 & \frac{1}{300s} \\ -50 & 1+57.5G_1 & 0 & 0 & 0 & \frac{K_t\ G_{c3}}{300} \\ 0 & -57.5 & 1 & 0 & 0 & 0 \\ 0 & 0 & -100 & 1 & 38.3 & 0 \\ 0 & 0 & 0 & -1.04 & 1 & 0 \\ 0 & 0 & 0 & 0 & -36.9 & 1 \end{vmatrix}$$

$$= 1 + 57.5\ G_{cl} + 18.1\ K_t\ G_{c3} + \frac{905}{s}$$

$$\Delta_{ef\ s \to 0} = 36.9 + 2064\ G_{cl}$$

$$G_{f\Theta c\ s-0} = \frac{1}{300s}$$

Substituting these equations into Equation 3-22,

$$\Theta c_{ss\ u.l.t.} = \left. \frac{1/300s \left[36.9 + 2064\ G_c \right]}{1 + 57.5\ G_{cl} + 18.1\ K_t G_{c3} + \frac{905}{s}} \right|_{s \to 0}$$

$$= \frac{36.9 + 2064\ G_{cl}}{300s\ (\ 1 + 57.5\ G_{cl} + 18.1\ K_t\ G_{c3}\ ) + 271{,}500}$$

Now it can be seen that if the previously derived restrictions are observed; i.e. $\lim_{s\to 0} G_{c1} \quad G_{c1} = \lim_{s\to 0} G_{c3} = 0$

then $\Theta c_{ss_{ult}} = \frac{36.9}{271,500} = \frac{1}{7530}$ radian $= .468$ minutes.

Now that restrictions on the type of compensation have been determined, it is useful to put the equations of Δ into a convenient form for working with G_{c1} and G_{c3} simultaneously. It is impossible to obtain a form of the characteristic equation in which G_{c1} and G_{c3} appear simultaneously as cascade compensators. It is possible however to obtain an equation of a root locus which will be of the form

$$-1 = \frac{K_1 \prod_{i=1}^{n} (s + z_i)\ G_{c3}}{1 + \dfrac{K_2 \prod_{j=1}^{n} (s + z_j)\ G_{c1}}{s^m \prod_{k=1}^{n} (s + p_k)}}$$

or conversely:

$$-1 = \frac{K_3 \prod_{i.1}^{n} (s + z_i) n G_{c1}}{1 + \dfrac{K_4 \prod_{j.1}^{n} (s + z_j)\ G_{c3}}{s^m \prod_{k.1}^{n} (s + p_j)}}$$

Now clearing the denominator:

$$\Delta = 1 + \frac{18.1\times10^{10}(s+100)^2(s^2+10s+100)\,G_{c1} + 36.2\times10^8 K_t s G_{c3}}{s^6+410^5+5.41\times10^4 s^4+2.54\times10^6 s^3+2.5\times10^7 s^2+2\times10^8 s+18.1\times10^{10}}$$

Letting this 6th order equation $\triangleq D_\Delta$

$$\Delta = 1 + \frac{18.1\times10^{10}(s+100)^2(s^2+10s+100)}{D_\Delta}\;\frac{K_{c1}N_{c1}}{D_{c1}} +$$

$$\frac{36.2\times10^8 K_t s\, N_{c3}}{D_\Delta \quad D_{c3}}$$

where

$$G_{c1} \triangleq \frac{K_{c1}\;N_{c1}}{D_{c1}} \quad ; \quad G_{c3} \triangleq \frac{N_{c3}}{D_{c3}}$$

Now Δ may be put into one of the two previously mentioned forms.

The first form is :

$$\Delta = 1 + \frac{\dfrac{36.2\times10^8\;K_t s N_{c3}}{D_\Delta \quad D_{c3}}}{1 + \dfrac{s(s+100)(s^2+10s+100)N_{c1}\;K_{c1}}{D_\Delta \qquad\qquad D_{c1}}}$$

Clearing the denominator

$$\Delta_1 = 1 + \frac{36.2\times10^8 K_t s N_{c3} D_{c1}}{\left[D_\Delta D_{c1} + s(s+100)^2(s^2+10s+100) K_{c1} N_{c1}\right] D_{c3}} \qquad (3\text{-}23)$$

The bracketed term in the denominator may now be used to form the root locus equation

$$\Delta_A = 1 + \frac{s(s+100)^2(s^2+10s+100) K_{c1} N_{c1}}{D_\Delta \qquad D_{c1}} \qquad (3\text{-}24)$$

Thus it is seen that the effect of the compensator G_{c1} is to supply zeros in Equation 3-23 for each pole of G_{c1} and also to provide the poles of Equation 3-23 in the form of the roots of Equation 3-24.

The alternate form of the equation, by the principle of similarity is:

$$\Delta_2 = 1 + \frac{18.1\times10^{10} (s+100)^2(s^2+10s+100) D_{c3} N_{c1} K_{c1}}{\Delta_D \; D_{c3} + 36.2\times10^8 K_t s N_{c3}) D_{c1}}$$

Of which the denominator bracketed term may be taken to form the root locus equation

$$\Delta_B = \frac{36.2\times10^8 K_t s N_{c3}}{\Delta_D \qquad D_{c3}}$$

Assuming a compensator $G_{c1} = \frac{4.35\ s}{s + 3.5}$,

This function for G_{c1} is the compensator which almost met specifications previously. It is therefore taken as a starting point to find a G_{c3} which will actually meet specifications.

Substituting this equation for G_{c1} into Equation 3-23:

$$\Delta_1 = 1 + \frac{36.2 \times 10^2 K_t\ s\ (s+3.5)\ G_{c3}}{\text{Roots obtained in Section VII (e)}}$$

It is seen that the pole zero array of Fig. 3.10 will result. Now G_{c3} must be a compensator containing a term (s) in the numerator. This will result in a double zero at the origin of Fig. 3.10. Obviously, a root locus will always appear in the region between one pair of the complex poles at s =-2.5 and the origin. Since this will always give a set of roots with their real parts $\geq$ -2.5, this compensator will not produce satisfactory results in terms of transent response settling time specifications.

It can be seen that to achieve satisfactory compensation with the assumed G_{c1}, it will probably be necessary for G_{c3} to cancel all four complex poles at s = - 2.5. If the compensator G_{c3} must be this complicated, it would be just as well to use a complicated compensator for G_{c1} and achieve compensation by use of the mag amp path alone.

Fig. 3-10

Pole-Zero Array for

$$-1 = \frac{36.2 \times 10^{8} K_t 3 (s + 3.5)}{\text{Roots of Section VII(e)}} G_{c3}$$

Note: Poles & Zeros of G_{c3} Not plotted.

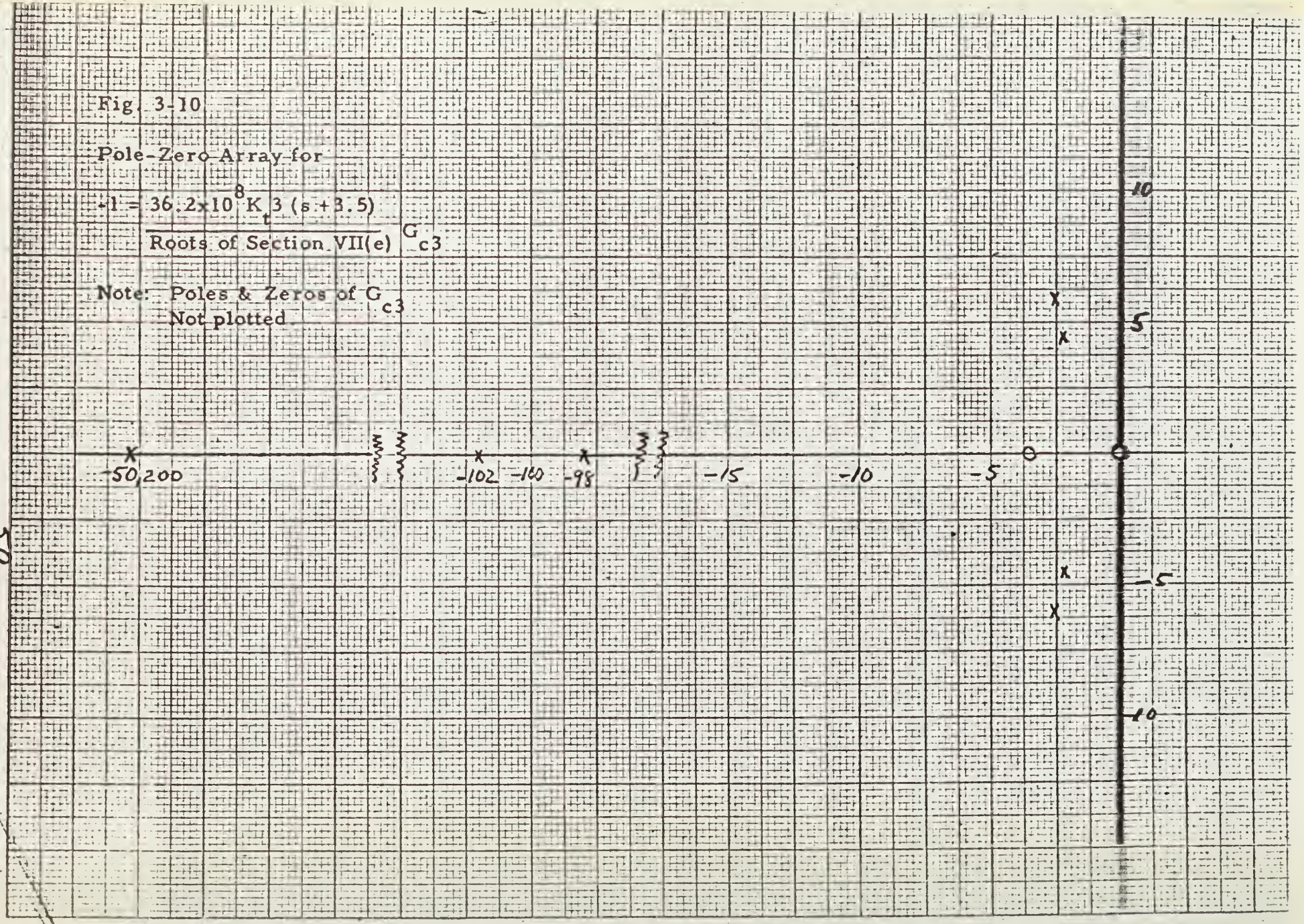

It may be seen further from the sketch of Fig. 3.11, the root locus of

$$\Delta_A = 1 + \frac{11,500s(s+100)^2(s^2+10s+100)}{\Delta_D} G_{c1} \qquad (3\text{-}26)$$

where it is required that G_{c1} contain a term (s) in the numerator that there will always be at least two roots of Equation 3-26 in the area between s=20 and s = - 5; since the root locus from the right half plane poles will always go to either the zeros at the origin or at s = - 5± j 8.6. These roots would then become poles of the equation

$$\Delta_B = \frac{36.2 \times 10^8 K_t \, s \, D_{c1}}{\prod_{i=1}^{n} (s+pi)} G_{c3}$$

and since as mentioned previously G_{c3} must contain a term s in the numerator there would in all probability be root locus between the poles under discussion and the double zero at the origin; unless of course, G_{c3} produced zeros to cancel those poles. Since it is necessary to retain the zeros at the origin, the obvious alternative is to cancel the zeros at s = - 5 ± j8.6 with an active compensator for G_{c1}. If this be done, all specifications can be met using the mag amp path only and no additional advantages accrue from also compensating with the tach path.

Fig. 3-11

Pole-Zero Sketch of Eg. 3-26

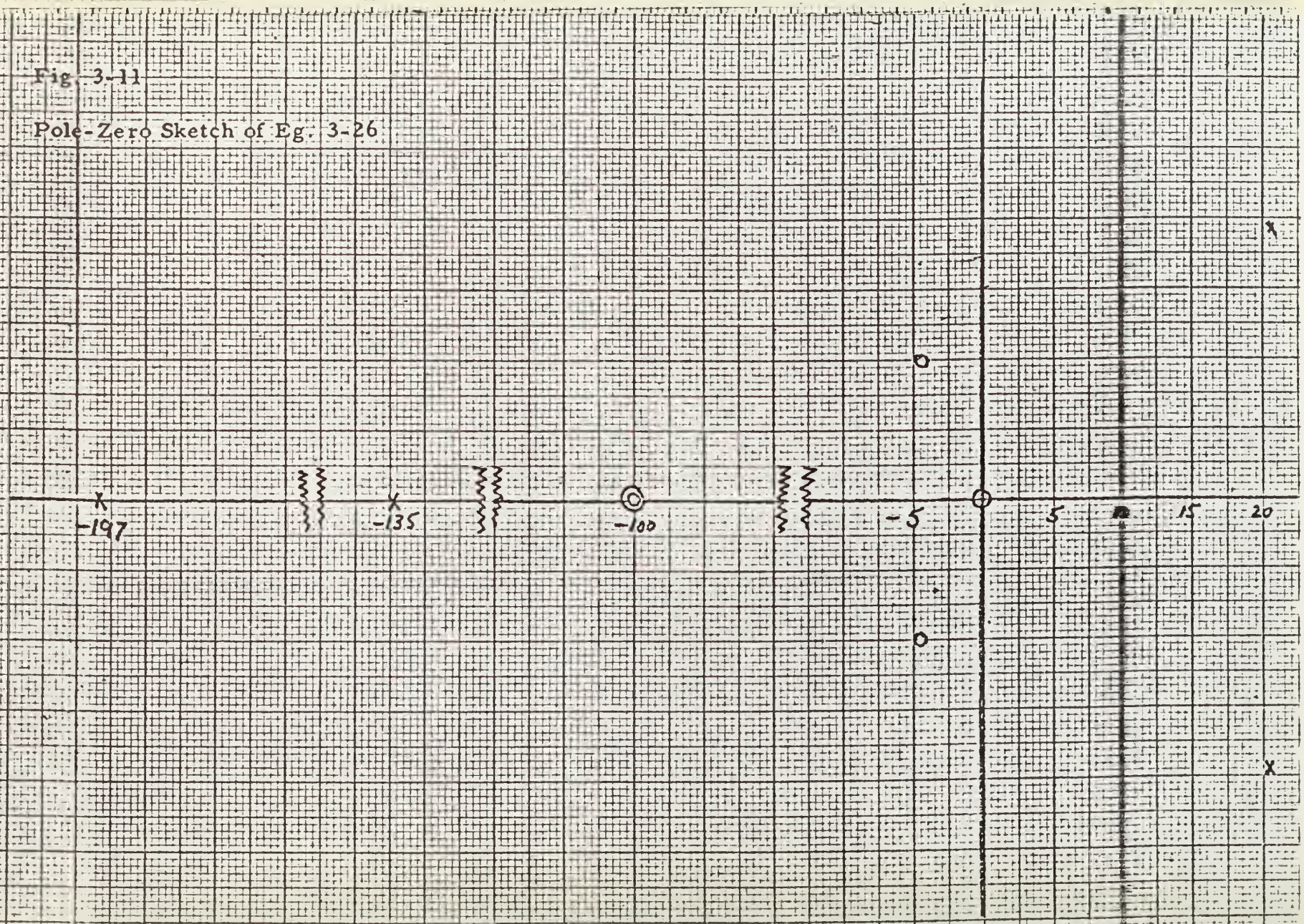

The denominator of each of these root locus equations is another root locus. The denominator root locus is a function of only one compensator thus one compensator may be used to determine the poles which the other compensator will work with. In many cases, this may be a useful tool. Obtaining these forms for the two compensation paths now under consideration:

Expanding the determinant of Equation 3-19:

$$\Delta = 1 + \frac{18.1 \times 10^{10}}{s(s+100)^2(s+200)(s^2+10s+100)} + \frac{11,500}{s+200} G_{c1} + \frac{36.2 \times 10^8 K_t G_{c3}}{(s+100)^2(s+200)(s^2+10s+100)}$$

$$= 1 + \frac{\frac{11,500}{s+200} G_{c1}}{1 + \frac{18.1 \times 10^{10}}{s(s+100)^2(s+200)(s^2+10s+100)}} + \frac{\frac{36.2 \times 10^8 K_t G_{c3}}{(s+100)^2(s+200)(s^2+10s+100)}}{1 + \frac{18.1 \times 10^{10}}{s(s+100)^2(s+200)(s^2+10s+100)}}$$

When using an active compensator in the mag amp path to cancel the zeros at $s = -5 \pm j8.6$, as a first consideration this compensator must be cascaded with a compensator of the form $\frac{s}{s+p}$. An active compensator may be used to produce poles at $s = -5 \pm j8.6$. There will be two real zeros which come as an integral part of this compensator, which may be placed as desired. The farther out on the real axis these zeros are placed, the lower the root locus gain will become to place roots in the desired locations. This presents no real problem since a voltage divider network may be made part of the compensator and only a part of the mag amp output feedback as compensation.

Therefore, for simplicity, let the two real zeros cancel the poles at $s = -197$ and $s = -135$. This gives the equation

$$\Delta = \frac{11{,}500s(s+100)^2(s^2+10s+100)K_{c1}s\ (s+135)(s+197)}{\Delta_D \qquad\qquad (s+p)\ (s^2+10s+100)} + 1$$

$$= \frac{11{,}500\ K_{c1}\ s^2\ (s+100)^2}{(s-21+j28.5)(s-21j28.5)(s+60+j43)(s+60-j43)(s+p)} + 1$$

It was determined from Esiac investigation that p = - 3 would produce a root locus through the desired ζ range. (See Fig. 3.12) The root locus gain to produce roots with real part $\doteq$ 7.5 was 102. The compensator then becomes

$$G_{cl} = \frac{\frac{102}{11,500}(s + 135)(s+197)\,s}{(s^2 + 10s + 100)\qquad (s+3)}$$

Substituting this into Equation 3-26 and setting $\Delta_A = 0$, the characterisitic equation polynomial becomes:

$$0 = s^5 + 181.68s^4 + 22,035.85s^3 + 1,095,320.975^2 + 8,506,777.62s + 25,070,121$$

Solving this equation on the digital computer gave the following roots:

$$s = - 4.47 \pm 2.88j$$

$$s = - 53.28 \pm 103j$$

$$s = - 66.18$$

Investigation of these roots showed that the required specifications were not met. Several values of gain were used until satisfactory roots were obtained to meet specifications. The value of K used was 39.0 giving the following roots:

$$s = - 42.6 \pm 60j$$

$$s = - 11.2 \pm 20j$$

$$s = - 16.0$$

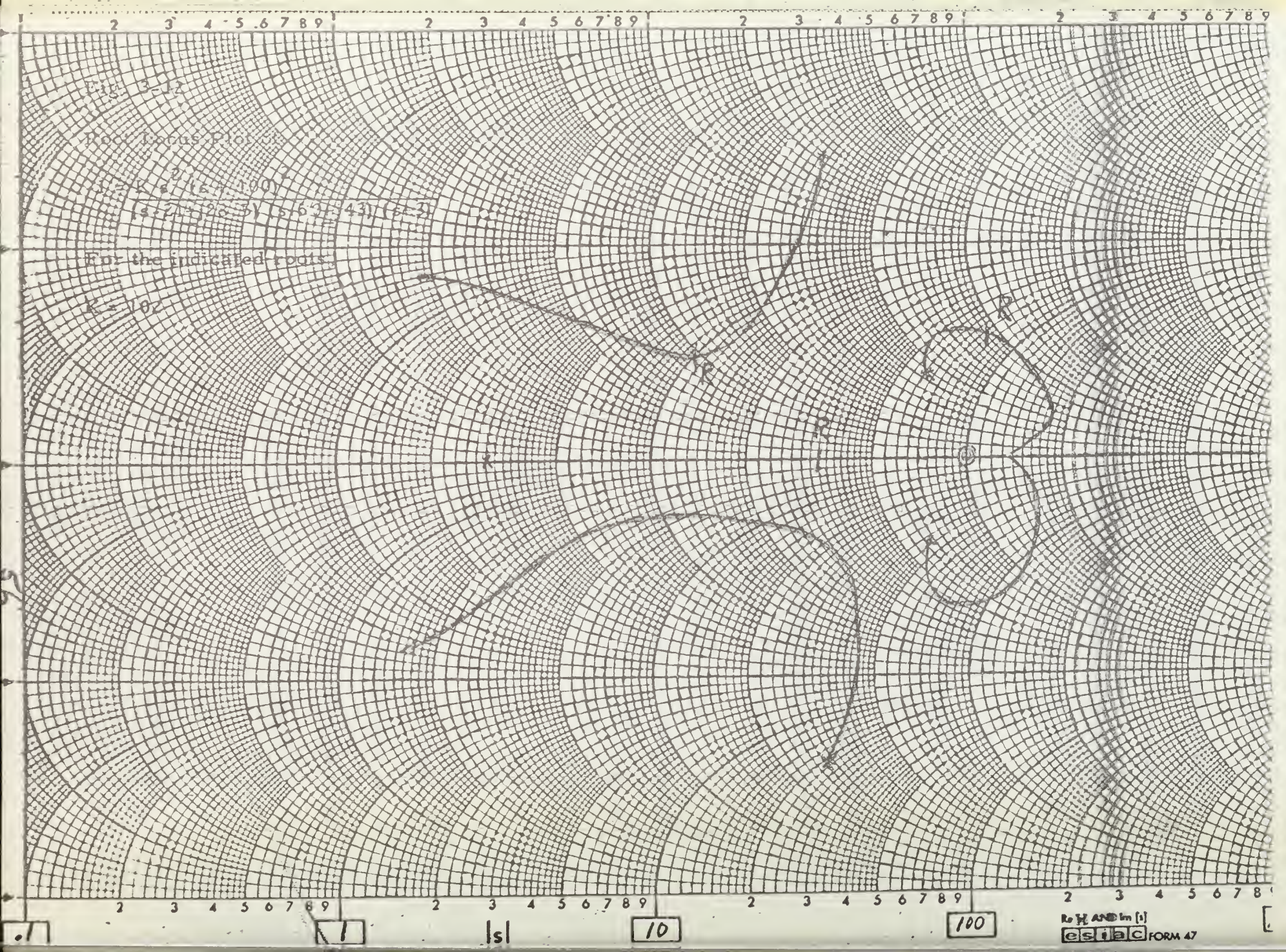
Fig. 3-12
Root Locus Plot of
$G(s) = \frac{K(s+100)}{(s+2)(s+5)(s^2+4s+13)}$
For the indicated roots,
K = 102
R
R
R
R
K
|s|
.1
1
10
100
Re s AND Im [s]
esiac FORM 47

These roots were obtained from the root locus plot shown in Fig. 3.13. Since the compensator satisfies the steady state criteria and these roots satisfy the transient specifications, this compensator was selected. From Fig. 3.13, it can be seen that the dominant ($s \equiv 16.0$) root is far enough away from the origin to give a settling time within the required specifications. A damping coefficient of $\zeta = .485$ resulted from the above roots. Since the inclusion of the tach path offered no advantages in simplification of the compensator required, it was not investigated further. Analyzing the transient response gives:

$$\frac{\Theta_c}{\Theta_R} = \frac{10.1 \times 10^{10} s\,(s+8)\,(s^2+10s+100)}{(s+16)\,(s+11.2 \pm 20j)\,(s+42.6 \pm 60j)}$$

From this, it can be seen that the settling time is $4 \times \frac{1}{11.2} = .357$ seconds which is well within the required specifications.

This detailed illustration is intended to show some of the uses of the determinant-block diagram relation. The solution obtained is not a complete one, nor does the problem itself have any bearing on the self-adaptive problem other than as an illustration of manipulative methods.

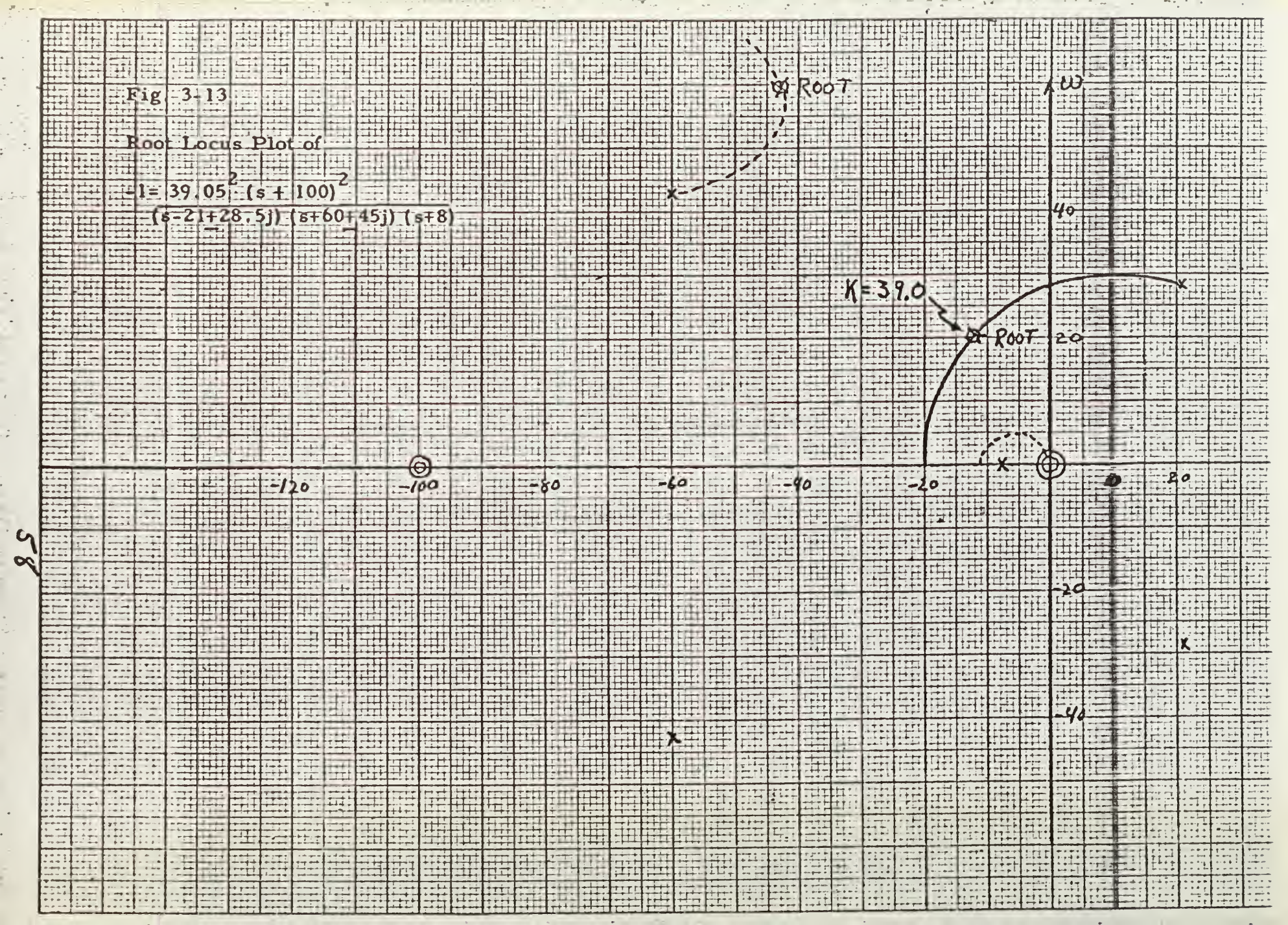
Fig 3-13
Root Locus Plot of
$-1 = \frac{39.05^2 (s+100)^2}{(s-21+28.5j)(s+60+45j)(s+8)}$
ROOT
ROOT
K=39.0
jω
40
20
-20
-40
-120
-100
-80
-60
-40
-20
0
20
σ

4. DEFINITION OF SYMBOLS USED IN FOLLOWING SECTIONS

$U \triangleq$ x component of velocity (scalar)

$V \triangleq$ y component of velocity (scalar)

$W \triangleq$ z component of velocity (scalar)

$A \triangleq$ Moment of inertia about x axis, slug-ft^2 (whole mass)

$B \triangleq$ moment of inertia about y axis, slug-ft^2 (whole mass)

$C \triangleq$ moment of inertia about z axis, slug-ft^2 (whole mass)

$D \triangleq$ product of inertia, $\int yz\, dm$, slug-ft^2

$E \triangleq$ product of inertia, $\int xz\, dm$, slug-ft^2

$F \triangleq$ product of inertia, $\int xy\, dm$, slug-ft^2

$P \triangleq$ angular component of rotation about x-axis (scalar) radian/sec

$Q \triangleq$ angular component of rotation about y-axis (scalar) radian/sec

$R \triangleq$ angular component of rotation about z-axis (scalar) radian/sec

$K_1 \triangleq$ relative angular velocity of rotor term on x-axis (scalar)

$K_2 \triangleq$ relative angular velocity of rotor term on y-axis (scalar)

$K_3 \triangleq$ relative angular velocity of rotor term on z-axis (scalar)

$a \triangleq$ moment of inertia of rotor along x-axis

$b \triangleq$ moment of inertia of rotor along y-axis

$c \triangleq$ moment of inertia of rotor along z-axis

$a_c \triangleq$ acceleration of airframe at its mass center ft/sec^2

$m \triangleq$ mass of control surface

$e \triangleq$ eccentricity of control surface between hinge and the control mass center

$\phi \triangleq$ angular displacement about the reference (x_*) axis

$\dot{\phi}$ $\triangleq$ Angular velocity about the reference (x_*) axis

θ $\triangleq$ angular displacement about the reference (y_*) axis

$\dot{\theta}$ $\triangleq$ angular velocity about the reference (y_*) axis

ψ $\triangleq$ angular displacement about the reference (z_*) axis

$\dot{\psi}$ $\triangleq$ angular velocity about the reference (z_*) axis

$12p \triangleq \frac{\rho Uo\ SrCr^2}{4ir} C_{h_{rp}}$

$12r \triangleq \frac{\rho Uo\ SrCr^2}{4ir} C_{h_{r_r}}$

$12\zeta \triangleq \frac{\rho Uo^2 SrCr}{2ir} C_{h_{r\zeta}}$

$12\dot{\zeta} \triangleq \frac{\rho Uo\ SrCr^2}{4ir} C_{h_{r\dot{\zeta}}}$

η $\triangleq$ the elevator position angle (radians)

ξ $\triangleq$ the sileron position angle (radians)

ζ $\triangleq$ the rudder position angle (radians)

Fx $\triangleq$ force in the direction of the x axis (scalar)

Fy $\triangleq$ force in the direction of the y axis (scalar)

Fz $\triangleq$ force in the direction of the z axis (scalar)

L $\triangleq$ moment about the x axis (scalar)

M $\triangleq$ moment about the y axis (scalar)

N $\triangleq$ moment about the z axis (scalar)

$$X_u \triangleq \frac{\rho S U_o}{2m} \left[(2C_{T_o} + C_{T_U}) \cos \Theta_T - (2C_{D_o} + C_{D_u}) \right]$$

$$X_w \triangleq \frac{\rho S U_o}{2m} (C_L - C_D \alpha)$$

$$X_{\dot{w}} \cong 0$$

$$X_q \cong 0$$

$$Z_u \triangleq \frac{\rho S U_o}{2m} \left[(2C_{T_o} + C_{T_u}) \sin \Theta_T - (2C_{L_D} + C_{L_u}) \right]$$

$$Z_w \triangleq - \frac{\rho S U_o}{2m} (C_L \alpha + C_{D_o})$$

$$Z_{\dot{w}} \triangleq \frac{\rho S C C_L \dot{\alpha}}{4m}$$

$$Z_q \triangleq - \frac{\rho S U_{oc}}{4m} C_{L_q}$$

$$Z\eta \triangleq \frac{\rho U^2 S}{2m} C_{L\eta}$$

$$Mu \triangleq \frac{\rho S U_{oC}}{2B} \left[(C_{m_u} + 2C_{m_o}) + z_m (2C_{T_o} + C_{T_u}) \right]$$

$$Mw \triangleq \frac{\rho S U_{oC}}{2B} C_{m\alpha}$$

$$M\dot{w} \triangleq \frac{\rho S c^2 C_{m_{\dot{\alpha}}}}{4B}$$

$$Mq \triangleq \frac{\rho U_o S c^2}{4B} C_{m_q}$$

$$M\eta \triangleq \frac{\rho S U_o^2 oc}{2B} C_{m_\eta}$$

$$M\dot{\eta} \triangleq \frac{\rho S U^2 oc}{4B} C_{m_{\dot{\eta}}}$$

$$10u \triangleq \frac{\rho S U_o c_e}{2\, ie} C_{h_{e_u}}$$

$$10w \triangleq \frac{\rho S U_o c_e}{2\, ie} C_{h_{c\alpha}}$$

$$10\dot{w} \triangleq \frac{\rho S U_o^2 c_e}{2\, ie} C_{h_{e\dot{\alpha}}}$$

$$10q \triangleq \frac{\rho S U_o^2 c_e}{2\, ie} C_{h_{e_q}}$$

$$10\eta \triangleq \frac{\rho U^2 o S_{ece}}{2\, ie} C_{h_{e\eta}}$$

$$10\dot{\eta} \triangleq \frac{\rho U\, o S_{c\dot{e}}^2}{4\, ie} C_{h_{e\dot{\eta}}}$$

$$Y_u \triangleq \frac{\rho U_o S_{cy} \beta}{2m}$$

$$Y_p \triangleq \frac{\rho U_o S b C_{y_p}}{4m}$$

$$Y_r \triangleq \frac{\rho U_o SbC_{yr}}{4m}$$

$$Y_\zeta \triangleq \frac{1}{2m}\rho SU_o^2 C_{y_\zeta}$$

$$L_v \triangleq \frac{\rho SU_{ob} C_{l_\beta}}{2A}$$

$$Lp \triangleq \frac{\rho SU_o b^2 C_p}{4A}$$

$$L_r \triangleq \frac{\rho SU_o b^2 C_{l_r}}{4A}$$

$$L_\xi \triangleq \frac{\rho SUo^2 b}{2A} C_{l_\xi}$$

$$L_{\dot{\xi}} \triangleq \frac{\rho SUo\, b^2}{4A} C_{l_{\dot{\xi}}}$$

$$L_\zeta \triangleq \frac{\rho SUo^2 b}{2A} C_{l_\zeta}$$

$$N_V \triangleq \frac{\rho SUob}{2C} C_{n_\beta}, \quad N_\beta = Uol_V$$

$$Np \triangleq \frac{\rho SUob^2}{4C} C_{Np}$$

$$Nr \triangleq \frac{\rho SUob^2}{4C} C_{N_r}$$

$$N\zeta \triangleq \frac{\rho SUob}{2C} C_{n\zeta}$$

$$N\dot{\zeta} \triangleq \frac{\rho SUob^2}{4C} C_{\eta\dot{\zeta}}$$

$$11p \triangleq \frac{\rho Uo\ SaCa^2}{ia} C_{h_a p}$$

$$11r \triangleq \frac{\rho Uo\ SaCa^2}{ia} C_{h_{a_r}}$$

$$11\zeta \triangleq \frac{\rho Uo^2 SaCa}{2ia} C_{h_a \zeta}$$

$$11\dot{\zeta} \triangleq \frac{\rho Uo\ SaCa^2}{4ia} C_{h_a \dot{\zeta}}$$

$$12\beta \triangleq \frac{\rho Uo^2 SrCr}{2\ ir} C_{h_r \beta}$$

5. DERIVATION OF THE STANDARD BLOCK DIAGRAM FOR THE AIRFRAME.

5.1 Introduction

The types of motion that result from a disturbance in some equilibrium flight condition and the transient motion of the aircraft in response to control movements are analyzed in the study of the dynamic characteristics of an airplane. Over the course of years the effects of dynamic stability in aircraft have been known to designers. The mathematical computations were discussed by early aeronautics pioneers which included Lanchester, Bryant and Glauert. In spite of the fact that dynamic stability effects were known, most people paid little concern to this field. As design groups solved other problems of aircraft design, the dynamic stability effects were automatically solved as a secondary result. However, since World War II, aircraft development has pushed into the field of very high performance aircraft. In many cases the dynamic stability problem doesn't solve itself as happened previously. Furthermore, the fire control problem has entered the scene which has generated a control problem of no small magnitude.

This work will consider the aircraft in six degrees of freedom and explore paths of compensation and solution. It is the prime intention to explore the work of Chu (1) in multi loop servo systems and determine the value of it as applied to the aircraft stability.

The first section will set down a general definition of terms and the basic equations of motion as related to aircraft. It will further set down the basic assumptions upon which the equations are formed.

The equations motion for the airframe which are completely derived in Appendix I are:

$$F_x = (U + QW - RV)\, m = X - mg \sin \Theta \tag{5-1}$$

$$F_y = (V + RU - PW)\, m = Y + mg \cos \Theta \sin \Psi \tag{5-2}$$

$$F_z = (W + PV - QU)\, m = Z + mg \cos \Theta \cos \Psi \tag{5-3}$$

$$L = A\dot{P} + a\dot{K}_1 + (C - B)\, QR + D\,(Q^2 - R^2) - E\,(\dot{P}Q + R) + FPR + cK_3Q - bK_2R \tag{5-4}$$

$$M = B\dot{Q} + b\dot{K}_2 + (A - C)\, PQ + E\,(P^2 - R^2) - FQR + DPQ + aK_1R - cK_3R \tag{5-5}$$

$$N = C\dot{R} + c\dot{K}_3 + (B - A)\, PQ + F\,(Q^2 - P^2) + E\,(QR - \dot{P}) - DPQ + bK_2P - aK_1Q \tag{5-6}$$

$$H_e + F_e = I_e \ddot{\eta} = m_e l_e a_{cz} = P_{ex}\,(RP - Q) \tag{5-7}$$

$$H_r + F_r = I_r \ddot{\xi} = m_r l_r a_{cy} - (R + PQ)\, P_{rx} - (RQ - P)\, r_z \tag{5-8}$$

$$2H_a + F_a = I_a \ddot{\xi} + 2P_{ay}\,(RQ + P) \tag{5-9}$$

The angular and linear velocity of a free body in space are:

$$P = \dot{\Phi} - \dot{\Psi} \sin \Theta \tag{5-10}$$

$$Q = \dot{\Theta} \cos \Phi + \dot{\Psi} \sin \Phi \cos \Theta \tag{5-11}$$

$$R = \dot{\Psi} \cos \Phi \cos \Theta - \dot{\Theta} \sin \Phi \tag{5-12}$$

$$\frac{dx^*}{dt} = U \cos \Theta \cos \Psi + V (\sin \Phi \sin \Theta \cos \Psi - \cos \Phi \sin \Psi)$$

$$+ W (\cos \Phi \sin \Theta \cos \Psi + \sin \Phi \sin \Psi) \tag{5-13}$$

$$\frac{dy^*}{dt} = U \cos \Theta \sin \Psi + V (\sin \Phi \sin \Theta \sin \Psi + \cos \Phi \cos \Psi)$$

$$+ W (\cos \Phi \sin \Theta \sin \Psi - \sin \Phi \cos \Psi) \tag{5-14}$$

$$\frac{dz^*}{dt} = - U \sin \Theta + V \sin \Phi \cos \Theta + W \cos \Phi \cos \Theta \tag{5-15}$$

Consideration of the aerodynamic forces must be resolved into the effects they produce on various parts of the body in some flight conditions and also the resultant moment effects they produce.

The first or necessary condition is to establish a reference condition and proceed from there. A reference condition is some flight condition where equilibrium exists in all equations and the summation of forces is zero. This is a steady state condition.

The set of axis upon which this rigid body is oriented is commonly called the Eulerian Axis system. General aerodynamics usage modifies the z axis so the positive direction points downward.

The first rotation moves about the Z axis in a direction ψ and is known as yaw. The next is the movement about the Y axis which is term Θ and known as pitch. The third motion about an axis is roll about the X axis and is maneuvered in terms of Φ. Caution must be used in determining these positions because the order in using this system is not commutative.

The derivation for the yaw rate R, the roll rate P and the pitch rate Q are shown in detail in Appendix Two. They are:

$$P = \dot{\Phi} - \dot{\Psi} \sin \Theta \tag{5-16}$$

$$Q = \dot{\Theta} \cos \Phi + \dot{\Psi} \sin \Phi \cos \Theta \tag{5-17}$$

$$R = \dot{\Psi} \cos \Phi \cos \Theta - \dot{\Theta} \sin \Phi \tag{5-18}$$

and where small angles are involved

$$P \cong \dot{\Phi} \tag{5-19}$$

$$Q \cong \dot{\Theta} \tag{5-20}$$

$$R \cong \dot{\Psi} \tag{5-21}$$

Similarly, Etkin shows:

$$\dot{\Theta} = Q \cos \Phi - R \sin \Phi \tag{5-22}$$

$$\dot{\Phi} = P + Q \sin \Phi \tan \Theta + R \cos \Phi \tan \Theta \tag{5-23}$$

$$\dot{\Psi} = (Q \sin \Phi + R \cos \Phi) \sec \Theta \tag{5-24}$$

The general equations of motion have to be applied to the aircraft motion. The effects of axis movement upon the weight force of the aircraft will be shown as well as the reference state condition. It must be remembered that the gravity force is always oriented toward the center of the earth. The reference body axis may or may not be oriented in this direction.

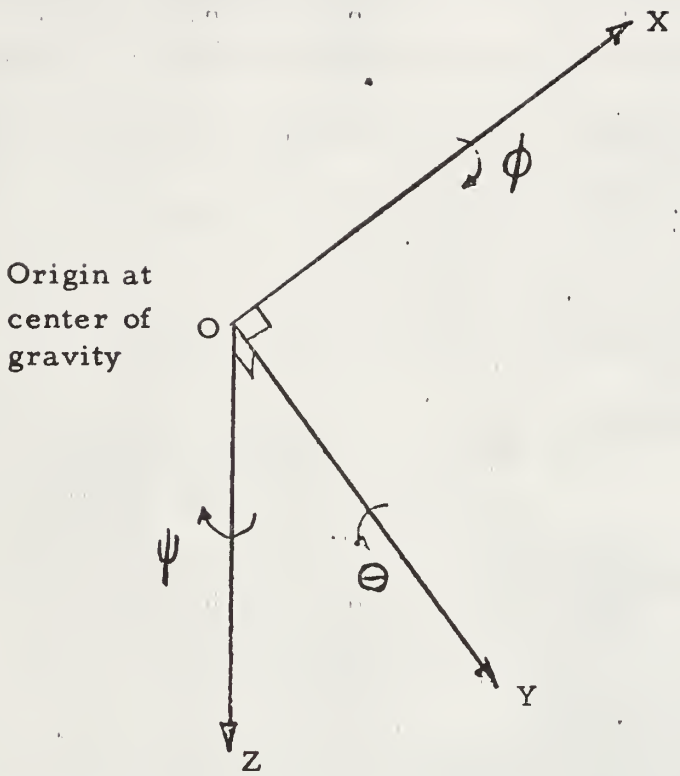

NORMAL AIRFRAME AXIS ORIENTATION

From the discussion of the Eulerian angle concept, it is determined that a reasonable reference condition would be

$$F_x = 0 = X_o - mg \sin \Theta_o \tag{5-25}$$

$$Fy = Y_o - W \cos \Theta_o \sin \Phi_o \tag{5-26}$$

$$F_z = 0 = Z_o \cos \Theta_o \cos \Phi_o \tag{5-27}$$

This allows for a steady state condition where the aircraft is not accelerating but neither is it necessarily in straight and level flight. From the previous illustration of Eulerian angles coupled with the derivations in Appendix II, the gravity forces can be determined as shown below.

$$\begin{bmatrix} \cos\Theta\cos\Psi & \cos\Theta\sin\Psi & -\sin\Theta \\ \cos\Psi\,\Theta\sin\Phi & \cos\Psi\cos\Phi & \cos\Theta\sin\Phi \\ -\sin\Psi\cos\Phi & +\sin\Psi\sin\Theta\sin\Phi & \\ \cos\Psi\sin\Theta\cos\Phi & \sin\Psi\sin\Theta\cos\Phi & \cos\Theta\cos\Phi \\ -\sin\Psi\sin\Phi & -\cos\Psi\sin\Phi & \end{bmatrix} \text{xmg} = \begin{bmatrix} my_x \\ my_y \\ \\ my_z \\ \end{bmatrix}$$

Discussion and derivation of this general cosine matrix are found in several sources (2, 3). The overall result of the equations of motion is shown below.

$$m(\dot{U} + QW - RV) = X - (mg \sin \Theta_o)(\cos \Theta \cos \Psi) + mg(\cos \Theta_o \sin \Phi_o)$$
$$(\cos \Theta \sin \Psi) - mg(\cos \Theta_o \cos \Phi_o)(\cos \Theta \sin \Phi) \quad (5\text{-}28)$$

$$m(\dot{V} + RU - PW) = Y - mg(\sin \Theta_o)(\cos \Psi \sin \Theta \sin \Phi - \sin \Psi \cos \Phi)$$
$$+mg(\cos \Theta_o \sin \Phi_o)(\cos \Psi \cos \Phi + \sin \Psi \sin \Theta \sin \Phi)$$
$$+mg(\cos \Theta_o \cos \Phi_o)(\cos \Theta \sin \Phi) \quad (5\text{-}29)$$

$$m(\dot{W} + PV - QU) = Z - mg(\sin \Theta_o)(\cos \Psi \sin \Theta \cos \Phi - \sin \Psi \sin \Phi)$$
$$+ mg(\cos \Theta_o \sin \Phi_o)(\sin \Psi \sin \Theta \cos \Phi - \cos \Psi \sin \Phi)$$
$$+ mg(\cos \Theta_o \cos \Phi_o)(\cos \Theta \cos \Phi) \quad (5\text{-}30)$$

$$L = A\dot{P} + a\dot{K}_1 + QR(C-B) - E(PQ + \dot{R}) + cK_3Q - bK_2R \quad (5\text{-}31)$$

$$M = B\dot{Q} + b\dot{K}_2 + PQ(A-C) + E(P^2 - R^2) + aK_1R - cK_3P \quad (5\text{-}32)$$

$$N = C\dot{R} + c\dot{K}_3 + PQ(B-A) + E(QR - \dot{P}) + bK_2P - aK_1Q \quad (5\text{-}33)$$

The above equations are complete except for the external forces X, Y, and Z and the external moments L, M, and N. These forces and moments are composed of aerodynamic and propulsion effects and the moments due to control surfaces. These equations are very general in nature and contain the following assumptions for simplification from the most general and complex case. These assumptions are:

1. The earth is assumed to be fixed in space and the Earth's atmosphere is assumed to be fixed with respect to the earth.
2. The airframe is assumed to be a rigid body.

3. The mass of the body is assumed constant during the time of the problem.

4. For an aircraft or missile, the XZ plane is assumed to have mirror symmetry.

The above equations then cover the six degrees of freedom found in an aircraft or missile. Coupled with the other auxiliary equations covering roll, pitch and yaw effects along with control motions, solution is probably possible. To date, this has been accomplished either by a machine using specific coefficients for various terms or several simplifications. Discussion of this will be conducted in succeeding sections.

5.2 Consideration of External Forces and Moments on a Body in Motion

In the previous section the equations of motion were discussed. The aerodynamic thrust and control effects were simply grouped in X, Y, Z, L, M and N. It is the aim of this chapter to discuss these in detail with respect to the effect on the dynamic control stability problem.

Consider the term X when the aircraft is in a disturbed condition. The reference condition is X_o and thus $X = X_o + \Delta X$ for some disturbed condition. The question is then to determine the ΔX components.

The force and moment variables can be expressed in a Taylor's Series[6].

$$F = Fo + \left(\frac{\partial F}{\partial \alpha}\right)\alpha + \left(\frac{\partial^2 F}{\partial \alpha^2}\right)\frac{\alpha^2}{2!} \text{ ---} + \left(\frac{\partial F}{\partial \beta}\right)\beta + \frac{\partial^2 F}{\partial \beta^2}\frac{\beta^2}{2!} \qquad (5\text{-}34)$$

For practical reasons the effects of second and higher order terms are omitted from further considerations as will be discussed later. Considering the motion of the aircraft itself the X forces would be (5-35)

$$X = Xo + \left(\frac{\partial X}{\partial u}\right)u + \left(\frac{\partial X}{\partial \dot{u}}\right)\dot{u} + \left(\frac{\partial X}{\partial w}\right)w + \left(\frac{\partial X}{\partial \dot{w}}\right)\dot{w} + \left(\frac{\partial X}{\partial q}\right)q + \left(\frac{\partial X}{\partial \dot{q}}\right)\dot{q}$$
$$+ \left(\frac{\partial X}{\partial v}\right)v + \left(\frac{\partial X}{\partial \dot{v}}\right)\dot{v} + \left(\frac{\partial X}{\partial p}\right)p + \left(\frac{\partial X}{\partial \dot{p}}\right)\dot{p} + \left(\frac{\partial X}{\partial r}\right)r + \left(\frac{\partial X}{\partial \dot{r}}\right)\dot{r}$$

Similarly, (5-36)

$$Y = Yo + \left(\frac{\partial Y}{\partial u}\right)u + \left(\frac{\partial Y}{\partial \dot{u}}\right)\dot{u} + \left(\frac{\partial Y}{\partial w}\right)w + \left(\frac{\partial Y}{\partial \dot{w}}\right)w + \left(\frac{\partial Y}{\partial q}\right)q + \left(\frac{\partial Y}{\partial \dot{q}}\right)\dot{q}$$

For convenience all terms will be expressed in letter subscript form. It can readily be seen then that considering X, Y, Z, L, M and N and

the effects of U, V, W, P, Q, and R plus the acceleration terms U, V, W, P, Q, and R there are 72 derivative terms required. This does not include the control effects which can add another 36 derivatives. Needless to say, considerable effort has been expended in justifying simplifying assumptions. In addition to this, obtaining reliable coefficients for various derivative terms is not always possible.

It is not the intention of this work to cover the computational methods for these various derivatives. The scope is too large. A search of all authoritative books [3, 4, 5, 6,] on the subject yields a table of terms which can be reasonably determined. This appears as Table 1. These considerations are mentioned to bring out the awareness of the different causes and effects of external forces. There are considerable gaps in the table. Determination of these to complete the table would be a topic of a complete study in itself. Much work remains to be done in this field.

Furthermore, some of the methods of computing the known stability derivatives are questionable. Some computations from theory prove quite accurate. Others are very poor and empirical methods or model testing are used. Even these fail at times and "educated guesses" from previous airplanes are used as a basis of determining stability derivatives for a new design. Tail effects are the most notable in this last category.

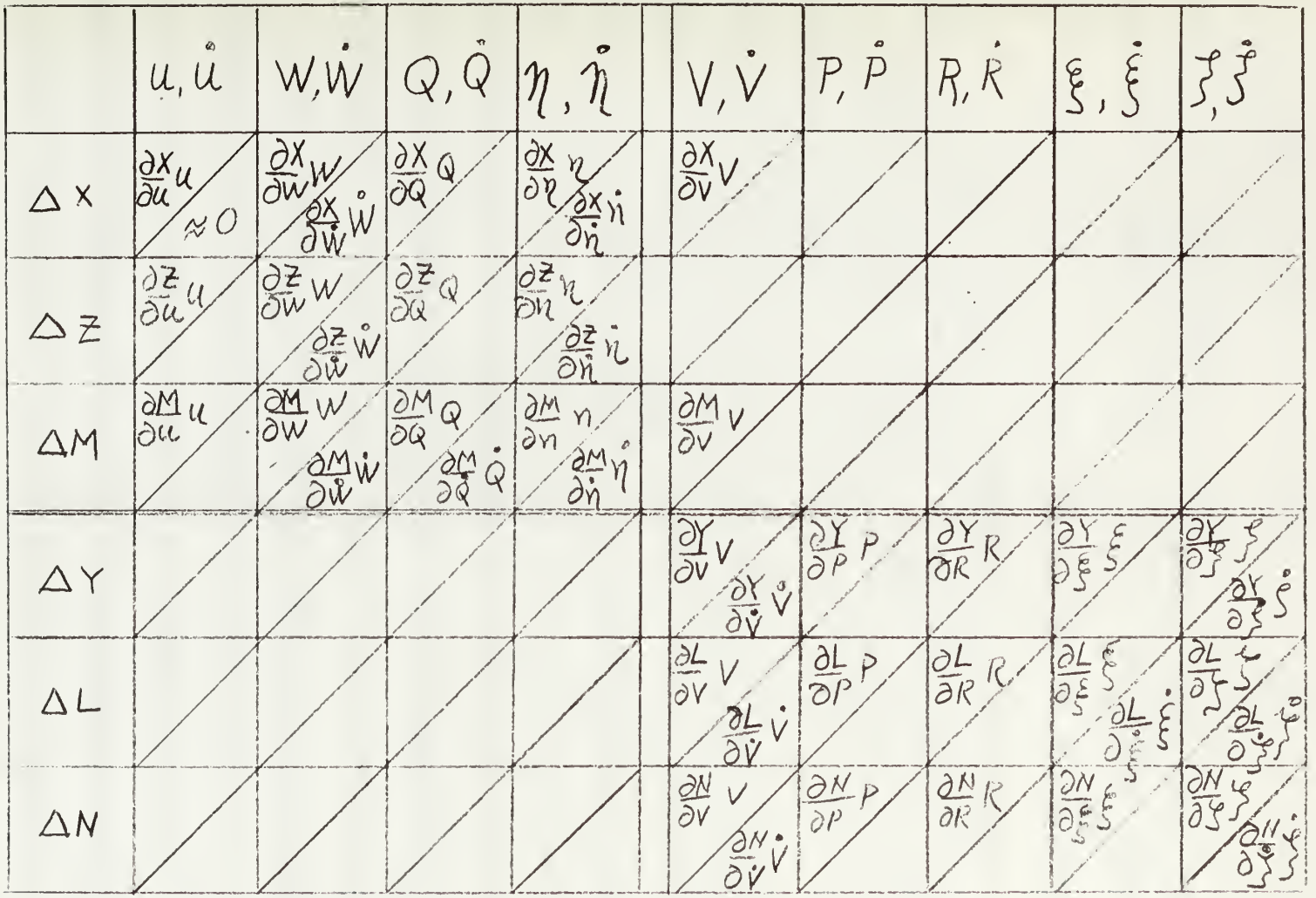

TABLE 5-1 KNOWN AERODYNAMIC STABILITY DERIVATIVES

Blanks indicate derivatives for which no estimate can be found.

In all aerodynamics problems, considerable effort is made to non-dimensionalize the equations. The advantages of doing this are of considerable merit. For the most part, it is rather simply done. It has been found in both theory and actual practice that

$$F = 1/2\ \rho V^2 S C_F \tag{5-37}$$

Where S is a reference area, usually the wing area, V is the absolute reference velocity and C_F is some non-dimensional coefficient. C_F varies with Mach Number and Reynolds Number depending on the force considered. (lift, drag, etc.) ρ is the density of the fluid through which the body is passing. Thus a term such as Zw has the following relationship:

$$Zw' = \frac{\partial Z}{\partial w} = 1/2\ \rho U_o^2 S \left(\frac{\partial C_Z}{\partial w}\right) = 1/2\ \rho U_o' S C_{Z_w} = 1/2 \rho S U_o C_{Z_w} \tag{5-38}$$

Here again V and S are the velocity and wing area terms respectively. The same concept applies to the moment terms except that a moment arm term must also appear in the equation. A generalized example is:

$$M = \rho U_o^2 S l C_m \tag{5-39}$$

In this example M is some moment and C_M is a needed dimensionless coefficient to satisfy the equation. ρ, U_o and S are the same as mentioned above while ℓ is the moment arm.

Likewise in a stability moment the derivative can be of the following form:

$$M_h = SU_o^2 l \left(\frac{\partial M}{\partial h}\right) h = U'_o S l C_{m_h} \qquad (5\text{-}40)$$

Another external force to be considered is that of thrust. This becomes an important factor in most flight conditions. The location of the thrust axis is seldom coincident with any reference axis in the body.

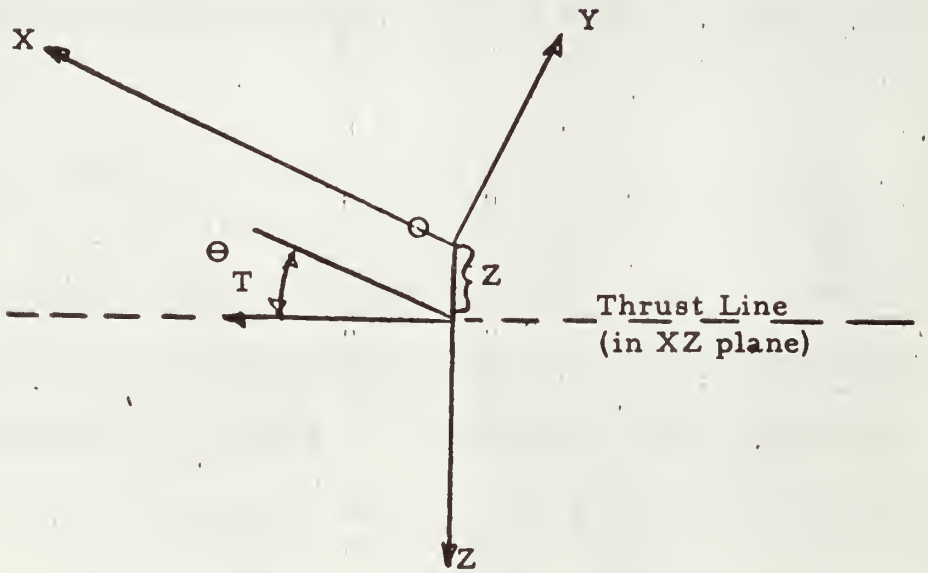

FIGURE 5-2

AXIS SYSTEM FOR LOCATING THRUST IN AN AIRFRAME

Assuming the thrust line lies in the xz plane, then the thrust forces can be resolved in this generalized manner.

$$X_T = T \cos \Theta_T \tag{5-41}$$

$$Z_T = T \sin \Theta_T \tag{5-42}$$

$$M_T = T_z \tag{5-43}$$

For a steady state condition the equations become

$$X_{o_T} = To \cos \Theta_T \tag{5-44}$$

$$Z_{o_T} = To \sin OT \tag{5-45}$$

$$M_{o_T} = T_{oz} \tag{5-46}$$

while in a disturbed condition where the body axis remains fixed in the mass,

$$X_T = T_1 \cos \Theta_T \tag{5-47}$$

$$Z_T = T_1 \sin \Theta_T \tag{5-48}$$

$$M_T = T_{1z} \tag{5-49}$$

and $$T_1 = To + \Delta T \tag{5-50}$$

Assuming the air density remains constant so the engine thrust will not be affected

$$T = \left(\frac{\partial T}{\partial u}\right) u + \left(\frac{\partial T}{\partial \delta_{RPM}}\right) \delta_{RPM} \tag{5-51}$$

or

$$T = T_u u + T_{\delta_{RPM}} \delta_{RPM}$$

These are the considerations for the external forces on a body in motion. While the dimensionless coefficient has been used extensively by the aeronautical engineering field, it will not be used further in this work. The primary mission of this work is to investigate the control response and paths for possible compensation.

The generalized equations of motion then appear:

(5-52)

$$m(\dot{U} + QW - RV) + mg \sin \Theta_o (\cos \Theta \cos \Psi) - mg (\cos \Theta_o \sin \Phi_o)$$
$$(\cos \Theta \sin \Psi) + mg (\cos \Theta_o \cos \Phi_o) (\sin \Theta) = X_o + X'_u u + X'_w w +$$
$$X'_{\dot{w}} \dot{w} + X'_q q + X'_\eta \eta + X'_{\dot{\eta}} \dot{\eta} + X'_v v + T_o \cos \Theta_T + T_u \cos \Theta_T u +$$
$$T_{\delta_{rpm}} \cos \Theta_1 \delta_{rpm}$$

(5-53)

$$m(\dot{V} + RU - PW) + mg \sin \Theta_o (\cos \Psi \sin \Theta \sin \Phi - \sin \Psi \cos \Phi) - mg$$
$$(\cos \Theta_o \sin \Phi_o) (\cos \Psi \cos \Phi + \sin \Psi \sin \Theta \sin \Phi) - mg (\cos \Theta_o \cos \Phi_o)$$
$$(\cos \Theta \sin \Phi) = Y_o + Y'_v v + Y'_{\dot{v}} \dot{v} + Y'_p p + Y'_r r + Y'_\xi \xi + Y'_\zeta \zeta + Y'_{\dot{\zeta}} \dot{\zeta}$$

(5-54)

$$m(\dot{W} + PV - QU) + mg \sin \Theta_o (\cos \Psi \sin \Theta \cos \Phi + \sin \Psi \sin \Phi)$$
$$- mg (\cos \Theta_o \sin \Phi_o) (\sin \Psi \sin \Theta \cos \Phi - \cos \Psi \sin \Phi) - mg$$
$$(\cos \Theta_o \cos \Phi_o) (\cos \Theta \cos \Phi) = Z_o + Z'_u u + Z'_w w + Z'_{\dot{w}} \dot{w} + Z'_q q +$$
$$Z'_\eta \eta + Z'_{\dot{\eta}} \dot{\eta} - T_o \sin \Theta_T - T_u \sin \Theta_T u - T_{\delta_{RPM}} \sin \Theta_T \delta_{RPM}$$

(5-55)

$$A\dot{P} + a\dot{K}_1 + QR (C-B) - E (PQ + \dot{R}) + cK_3 Q - bK_2 R = L_o + L'_v v +$$
$$L'_{\dot{v}} \dot{v} + L'_p p + L'_r r + L'_\xi \xi + L'_{\dot{\xi}} \dot{\xi} + L'_\zeta \zeta + L'_{\dot{\zeta}} \dot{\zeta}$$

(5-56)

$$B\dot{Q} + b\dot{K}_2 + PQ(A-C) + E(P^2 - R^2) + aK_1R = cK_3P = M_o + M'_u u + M'_w w + M'_{\dot{w}} \dot{w} + M'_q q + M'_{\dot{q}} \dot{q} + M'_{\eta} \eta + M'_{\dot{\eta}} \dot{\eta} + T_o z + T_u u + T_{\delta_{rpm}} \delta_{rpm}$$

(5-57)

$$C\dot{R} + c\dot{K}_3 PQ(B-A) + E(QR-\dot{P}) + bK_2P = aK_1Q = N_o + N'_v v + N'_p p + N'_r r + N'_{\xi} \xi + N'_{\zeta} \zeta + N'_{\dot{\zeta}} \dot{\zeta}$$

Thus, it has been shown that the equations of motion have the above external forces which will affect the rigid mass in motion. The assumptions made are:

1. The earth is assumed to be fixed in space and the Earth's atmosphere is assumed to be fixed with respect to the Earth.
2. The mass is a rigid body.
3. The mass of the body is assumed constant during the time of the problem.
4. For an aircraft or missile, the xz plane is assumed to have mirror symmetry.

These assumptions were made in the first section. In addition the following assumptions and simplifications are made in considering the aerodynamic forces:

1. The flow is assumed to be quasi-steady.
2. The effects of auxiliary aerodynamic equipment such as flaps, speed brakes, slats and spoilers are neglected.
3. The thrust can be affected only by change of speed and/or revolutions per minute. No change is considered for change in fuel mixture, manifold pressure, side slip or propeller fin effect.

These assumptions were made for several reasons. In the first and third cases, absence of adequate information on many of the coefficients makes ignoring or setting them equal to zero mandatory. In all probability these coefficients are very small. Assumption two covers special cases. While these items may have considerable effect when used, they are eliminated from the general case at this time because an aircraft probably uses them less than two percent of its flying time. For the special cases, these effects may be quickly added.

The work in these first two sections is developed primarily for background purposes. There is nothing new or startling in this. For further examination of this subject, the reader is referred to the works in Ref. 7 and 8 which closely parallel the development in this work.

The aerodynamic force and moment terms carry a primed notation for ease in publication. In later sections these terms will be divided by mass or moment of inertia. These terms after division will not carry the prime(') notation. There are far more of the latter terms used. Thus, it is for ease of publication only and does not affect theory in any way.

5.3 The Airframe Equations in a Standard Form

This section will take the general equations developed in the previous chapters and simplify them. The simplification will extend to an aircraft in straight and level flight and subject to small perturbations. This is the standard method of dealing with the problem as found in present day texts. However, these equations will be used in block diagram form and in determinantal arrays as developed in Chu's work. (1) The results will be compared with present day classical methods to determine validity of this determinantal concept.

The first simplification is the concept of the lateral system being independent of the longitudinal system. Therefore, the six equations of motion are divided into the two groups. The longitudinal group includes the directional motion in the X and Z directions and rotary motion about Y axis. The lateral group consists of directional motion along the Y axis and rotary motion about the X and Z axis. The axis system referred to here is the body axis system of the airplane.

Secondly, the aircraft is initially in a steady state condition. This is the reference state as mentioned previously. When the disturbance terms are all zero Equation 5-52 reduces to:

$$m (U_o + Q_o W_o - R_o V_o) + mg \sin \Theta_o = X_o + T_o \cos \Theta_T \qquad (5\text{-}58)$$

However, it was stated that this situation was restricted to longitudinal or lateral systems. Thus for motion along the X body axis, a yaw motion Ro and a side motion Vo would be zero. Further it was

stated that the aircraft was in a steady state reference condition. Therefore $\dot{u}$ would be zero. Thus Equation 5-58 reduces to

$$m (Qo\ Wo) + mg \sin \Theta_o = X'o + To \cos \Theta\ T \qquad (5\text{-}59)$$

Similarly, it may be observed that Equation 5-53 for the steady state reduces to

$$Y'o = 0 \qquad (5\text{-}60)$$

Likewise Equation 5-54 reduces to

$$m (Qo\ Vo) - Z'_o + mg \cos \Theta_o + To \sin \Theta\ T = 0 \qquad (5\text{-}61)$$

The moment equations all reduce to zero provided the rotor effects are neglected or considered zero.

$$Lo = Mo = No = 0 \qquad (5\text{-}62)$$

Recalling that only small disturbances were to be considered and these disturbances were to be in only the symmetrical or longitudinal system for the longitudinal group the derivative due to assymmetric variables of V, P, R, ξ and ζ are zero. In a similar manner, when the asymmetric system effects are considered the symmetric disturbances are ignored. This leaves the variables V, W, Q, and η out of the asymmetric equations. Finally, because of the small disturbances, the change angle Θ will be small so the approximation $\cos \Theta \cong 1$ and $\sin \Theta \cong \Theta$ is valid.

The result of the previous discussion is subtracting Equations 5-59 and 5-52, eliminating the asymmetric changes and supplying

the small disturbance considerations. The result is:

$$m(\dot{u}+) + mg\,\Theta \cos\Theta_o = X_u'U + X_w'W + X_{\dot{w}}'\dot{W} + X_q'Q \qquad (5\text{-}63)$$

$$+X_\eta'\eta + X_{\dot{\eta}}'\dot{\eta} + Tu' \cos\Theta_T U + T_{\delta}'_{RPM} \cos\Theta_T' \delta RPM$$

For the z direction taking 5-61 from 5-54 and using the same assumptions:

$$m(w-) + mg\,\Theta \sin\Theta_o = Z_u'U + Z_w'W + Z_{\dot{w}}'\dot{W} + Z_q'Q + \qquad (5\text{-}64)$$

$$Z_\eta'\eta + Z_{\dot{\eta}}'\dot{\eta} - TuU \sin\Theta_T - T_{\delta RPM}\,\delta RPM \sin\Theta T$$

For the moment in the y axis, the following applies:

$$B\dot{Q} = M_u'U + M_{\dot{w}}'\dot{W} + M_{\dot{w}}'\dot{W} + M_q'Q + M_{\dot{q}}'\dot{Q} + M_\eta'\eta + M_{\dot{\eta}}'\dot{\eta} + \qquad (5\text{-}65)$$

$$T_u'U_{z1} + T_{\delta RPM}\,\delta RPMz$$

To complete the case for the symmetrical group, the action of the elevators must be included. From appendix I the elevator hinge moment effects are reduced to:

$$Ie\,\ddot{\eta} = H_e'_\eta\eta + H_e'_{\dot{\eta}}\dot{\eta} + He_{\dot{w}}'\dot{W} + He_{\dot{w}}'\dot{W} + He_u'U + He_q'Q + \Delta Fe \qquad (5\text{-}66)$$

In most cases where moment of inertia terms are handled it is usually expedient to use an axis system which is the principal inertia axis. This means that the product of inertia terms are zero. For aerodynamic motion problems, this applies for some cases.(8) This case is not one of them. What is gained in simplification of the rotary motion equations by use of principal axis is lost in attempting to handle the force equations with the wind velocity considerations in sine and cosine terms. By orienting the X axis

into the reference wind velocity the result is:

$$V_c^2 = U^2 + v^2 + w^2 \qquad (5\text{-}67)$$

where $U = U_o + u$.

Therefore, in the steady state reference condition $V_c = U_o$ and $V_o = W_o = 0$. With the assumption that u, v and w were very small, their products and squares can be neglected.

$$V_c \cong \sqrt{U_o^2 + 2U_o u}$$

and since U_o^2 is much greater than $2 U_o u$, then $V_c \cong U_o \cong U$ and these terms are interchangeable in this section.

As previously stated, the reference situation is a steady state motion and includes first order effects only. The orientation of the axis U_o is a finite value while $V_o = W_o = 0$. Furthermore, the author is hard pressed to visualize an aircraft or missile tumbling along with a Q_o motion although P_o exists in spinning missiles and bullets. Furthe: $X_w = X_q = Z_{\dot{w}} = X_\eta = X_{\dot{\eta}} = T_{\delta_{RPM}} = 0$ as an assumption. These terms are usually very small.

The "standard" determinant form as stated in Chapter 3 of Chu[1] is:

$$\begin{vmatrix} 1 + PF_1 & PF_{11} & PF_2 & PF_{21} & PF_3 & PF_{31} \\ -PF_1 & & 1 + PF_2 & PF_{22} & PF_3 & PF_{32} \\ -PF_{13} & & -PF_2 & & 1 + PF_3 & PF_{33} \end{vmatrix}$$

where the PF* indicates a performance function. The system may have n nodes. This example contains only three nodes. The "standard" block diagram for this form is:

*In sections 2 and 3 the symbol G was used to designate the transfer function of a component, and the component itself was normally a distinct piece of hardware. The performance function PF is also a transfer function, but as used with regard to the airframe it designates a relationship between two variables which are not visualized as the input and output of a piece of hardware. The use of PF notation from here on is therefore a deliberate choice to emphasize this distinction.

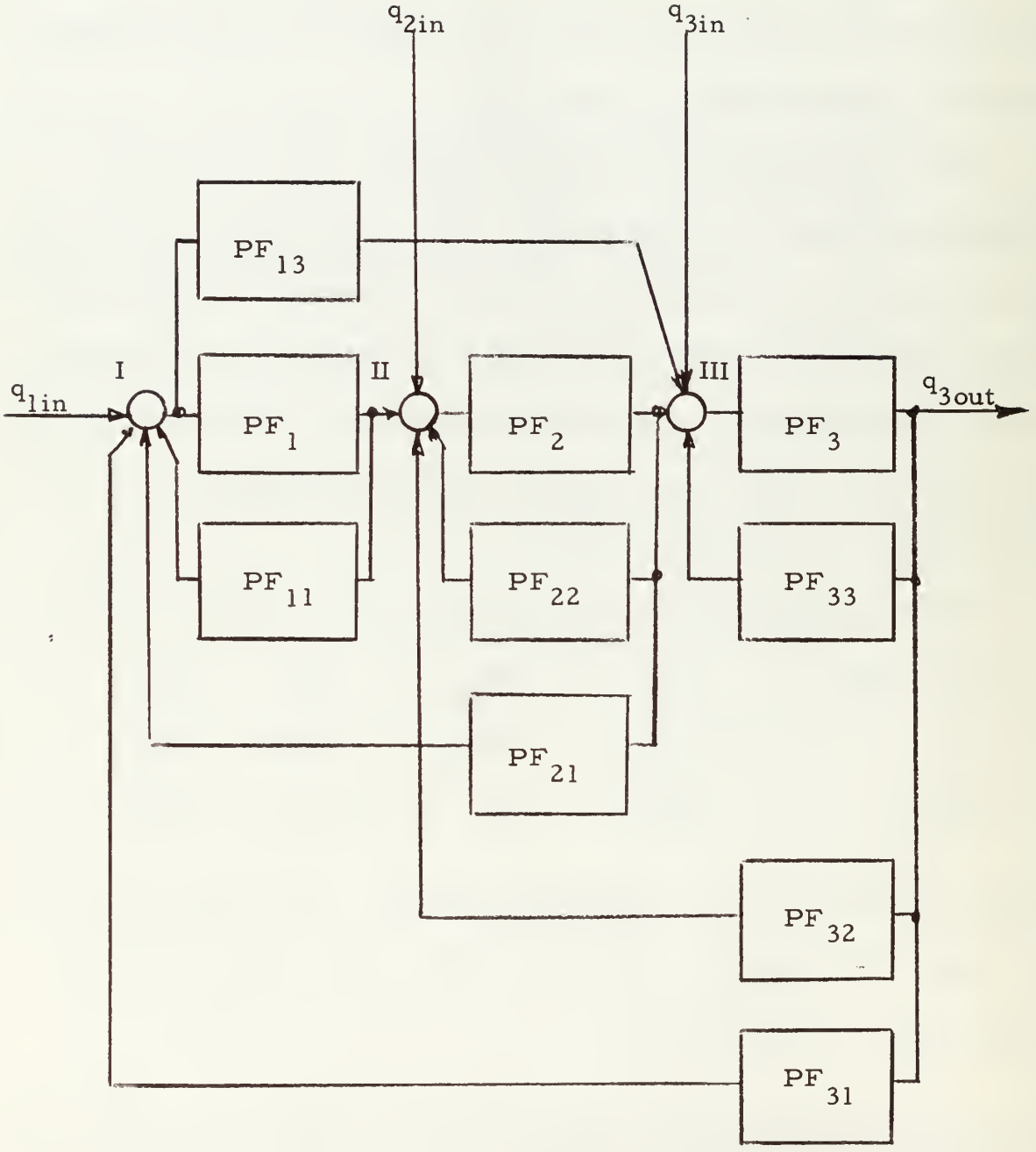

FIGURE 5.3 STANDARD BLOCK DIAGRAM DRAWN FROM 3 x 3 DETERMINANT.

The nodes are labeled in Roman Numerals. The basic rules of nodal signals allow several inputs, but only one output. This output from the node goes directly to a performance function with a single subscript number. Signals may be picked off from the node output and fed forward to another node. An example of this is contained in the signal going through PF_{13}. In this case the signal is also multiplied by the function PF_{13} and then fed to node III. Feedback takes place in a similar manner. The signal output from the first system PF_1 is picked off and fed through PF_{11} back to node I. Similarly the other nodes function in the same manner.

For feedback blocks, the first subscript number denotes the output signal source for the feed back and the second subscript number the input node to which the feedback signal is going. The notable points about the determinant are:

1. The main diagonal always has terms of one plus the direct path performance function times the self-loop feedback performance function.

   $(1 + PF_1 PF_{11})$

2. All terms above and to the right of the main diagonal are feedback terms.

3. All terms below and to the left of the main diagonal of the "standard" determinant form are of a feed forward nature. All of these feed forward terms are negative. The term immediately below the main diagonal term is the

direct path performance function. Thus, where the second column main diagonal spot has $1 + PF_2\, PF_{22}$, the direct path term PF_2 will appear in the location immediately below as $-PF_2$.

These rules are strictly mechanical. For a rigorous derivation of this system the reader is referred directly to Chu's work.

In Chapter 9 of Etkin (4), there exists a two degree of freedom situation where Θ and W vary and the speed in the forward direction is constant. This is the short period approximation. The equations using the LaPlace transforms and nondimensional coefficients are:

$$(2\mu s - G_{Z\alpha})\bar{\alpha} - (2\mu + G_{Zq})\, s\,\bar{\theta} - Gz_{\eta}\eta = 0 \qquad (5\text{-}68)$$

$$-G_{m\alpha}\bar{\alpha} + (i_{\beta} s^2 = G_{mqs})\,\bar{\theta} - Gm_{\eta}\eta = 0 \qquad (5\text{-}69)$$

$$-G_{h\alpha}\bar{\alpha} - G_{hq_s}\,\theta + (i_e s^2 - G_{h\eta})\,\eta = \Delta C_{f_e} \qquad (5\text{-}70)$$

This author also grouped his acceleration terms such that $G_{h_{\eta}}$ included $C_{h_{\eta}}$ and $C_{h_{\dot{\eta}}}$. Similar situations exist for $G_{h\alpha}$, $G_{m\alpha}$. and $G_{m_{\eta}}$. Note that $r \cong \dot{\psi}$ and $P \cong \phi$ for this consideration. From these equations a block diagram is evolved.

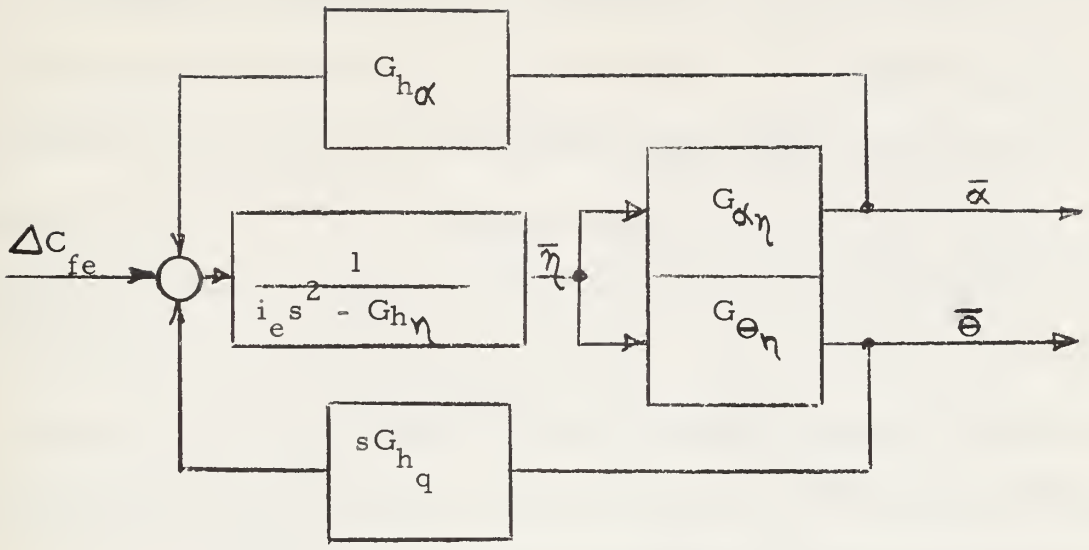

FIGURE 5.4 BLOCK DIAGRAM OF TWO DEGREES OF FREEDOM IN THE LONGITUDINAL SYSTEM SHOWN BY ETKIN[4]

Further, Etkin derives:

$$G_{\theta\eta} = \frac{\bar{\theta}}{\eta} = \frac{G_{m\eta}(2\mu s - G_{Z\alpha}) + G_{Z\eta} m_\alpha}{(2\mu s - G_{Z\alpha})(i_\beta s^2 - G_{mq_s}) - G_m(2\mu + G_{Zq}) s} \quad (5\text{-}71)$$

$$G_{\alpha\eta} = \frac{\Delta\alpha}{\eta} = \frac{G_{Z\eta}(i_\beta s^2 - C_{mq_s}) + G_m(2\mu + G_{Zq}) s}{(2\mu s - G_{Z\alpha})(i_\beta s^2 - G_{mq_s}) - G_{m\alpha}(2\mu + G_{Zq}) s} \quad (5\text{-}72)$$

Now it is intended to use Chu's work involving the use of "standard" block diagrams and "standard" determinant form to prove that the "standard" system applies for the airframe as well as a multiloop servo system.

The Z, M and η equations of motion with the applied assumptions and $\Theta_o = 0$ are:

$$\dot{w} - U_o q - Z_w W - Z_q Q - Z_\eta \eta - Z_{\dot{\eta}} \dot{\eta} = 0 \qquad (5\text{-}73)$$

$$\dot{\theta} - M_w W - M_{\dot{w}} \dot{W} - M_q Q - M_\eta \eta - M_{\dot{\eta}} \dot{\eta} = 0 \qquad (5\text{-}74)$$

$$\ddot{\eta} - 10_\eta \eta - 10_{\dot{\eta}} \dot{\eta} - 10_w W - 10_{\dot{w}} \dot{W} - 10_q q = \Delta Fe \qquad (5\text{-}75)$$

Recalling that $\omega = Uo \tan \Delta\alpha$ and for small angles

$$\omega \cong U_o \Delta\alpha \text{ and } \dot{\theta} \cong q.$$

The equations in LaPlace notation then become:

$$(s^2 - s10_{\dot{\eta}} + 10_\eta)\eta - (s10_{\dot{w}} + 10_w) U_o \Delta\alpha - (s10_q)\Theta = \Delta Fe \qquad (5\text{-}76)$$

$$(s^2 - sM_q)\Theta - (sM_{\dot{\eta}} + M_\eta)\eta - (sM_{\dot{\alpha}} + M_\alpha) Uo \Delta K = 0 \qquad (5\text{-}77)$$

$$(s - Z_w) U_o \Delta\alpha - (sU_o + sZ_q)\Theta - n(sZ_{\dot{\eta}} + Z_\eta)\eta = 0 \qquad (5\text{-}78)$$

These equations in standard determinant form now become:

η	$\Delta\alpha$	Θ
$1 - \frac{(s10_{\dot{\eta}} + 10_\eta)}{s^2}$	$-\frac{(s10_{\dot{\alpha}} + 10_\alpha)}{s^2}$	$-\frac{s10_q}{s^2}$
$-\frac{(sZ_{\dot{\eta}} + Z_\eta)}{s}$	$1 - \frac{Z_\alpha}{s}$	$-\frac{s(Uo + Z_q)}{s}$
$-\frac{(sM_{\dot{\eta}} + M_\eta)}{s^2}$	$-\frac{(sM_{\dot{\alpha}} + M_\alpha)}{s^2}$	$1 - \frac{sM_q}{s^2}$

Ordinarily, it is not necessary to divide by s or s^2. However, it is done here to demonstrate more closely the standard form.

To take the differential equations and arrange them by rows and columns to see the actual physical system is to no avail. The arrangement does not exist in the above form. It will be shown how to achieve this form later.

Consider the "standard form" array as set forth above. The block diagram for this in Chu's "standard form" is:

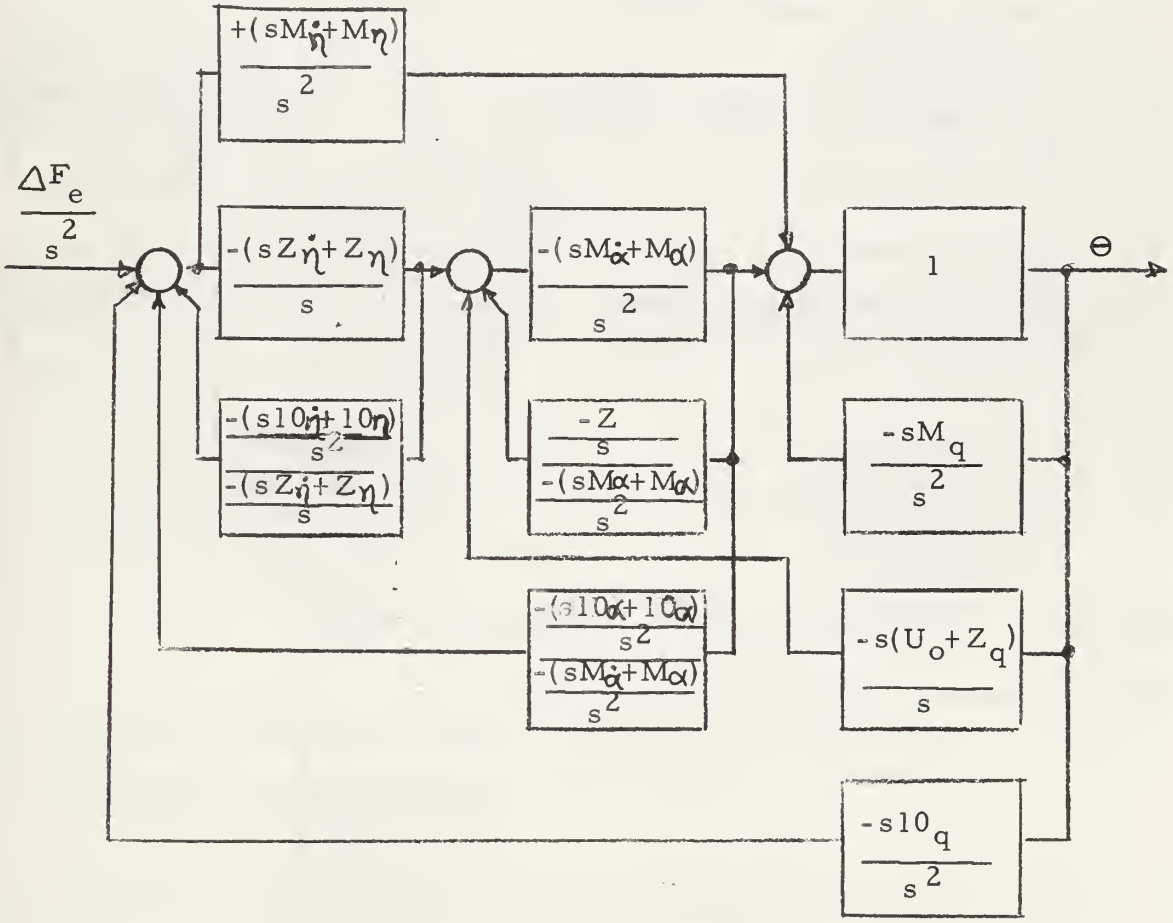

FIGURE 5.5 RESULT OF BLOCK DIAGRAMING EQUATIONS 5-76, 5-77, and 5-78.

The above block diagram then is a three node system but the outputs from the first and second main path blocks are nothing that is readily recognized in an airframe. Because of the fact that the main block following the third node is 1, the output here is Θ.

A few simple block diagram manipulations clears the situation and shows true signal outputs that are physically realized in the airframe. Block diagram manipulations allow the changing of a pick off point provided the transfer function is corrected. Further, two blocks can be combined into one equivalent transfer function.

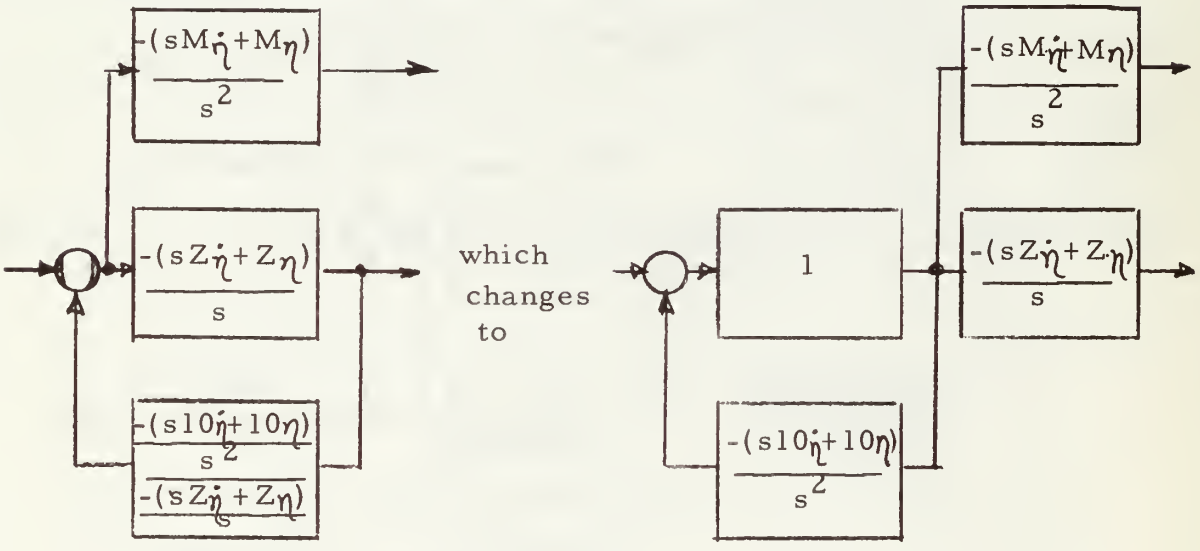

Figure 5.6 EQUIVALENT BLOCK DIAGRAM TERMS

Adding a dummy node this now changes to:

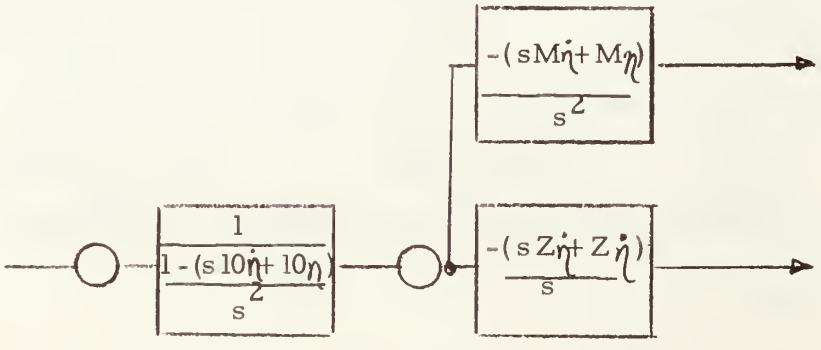

Figure 5.7 FURTHER BLOCK DIAGRAM COMBINATIONS

The result of using these two maneuvers rearranges the block diagram to the following:

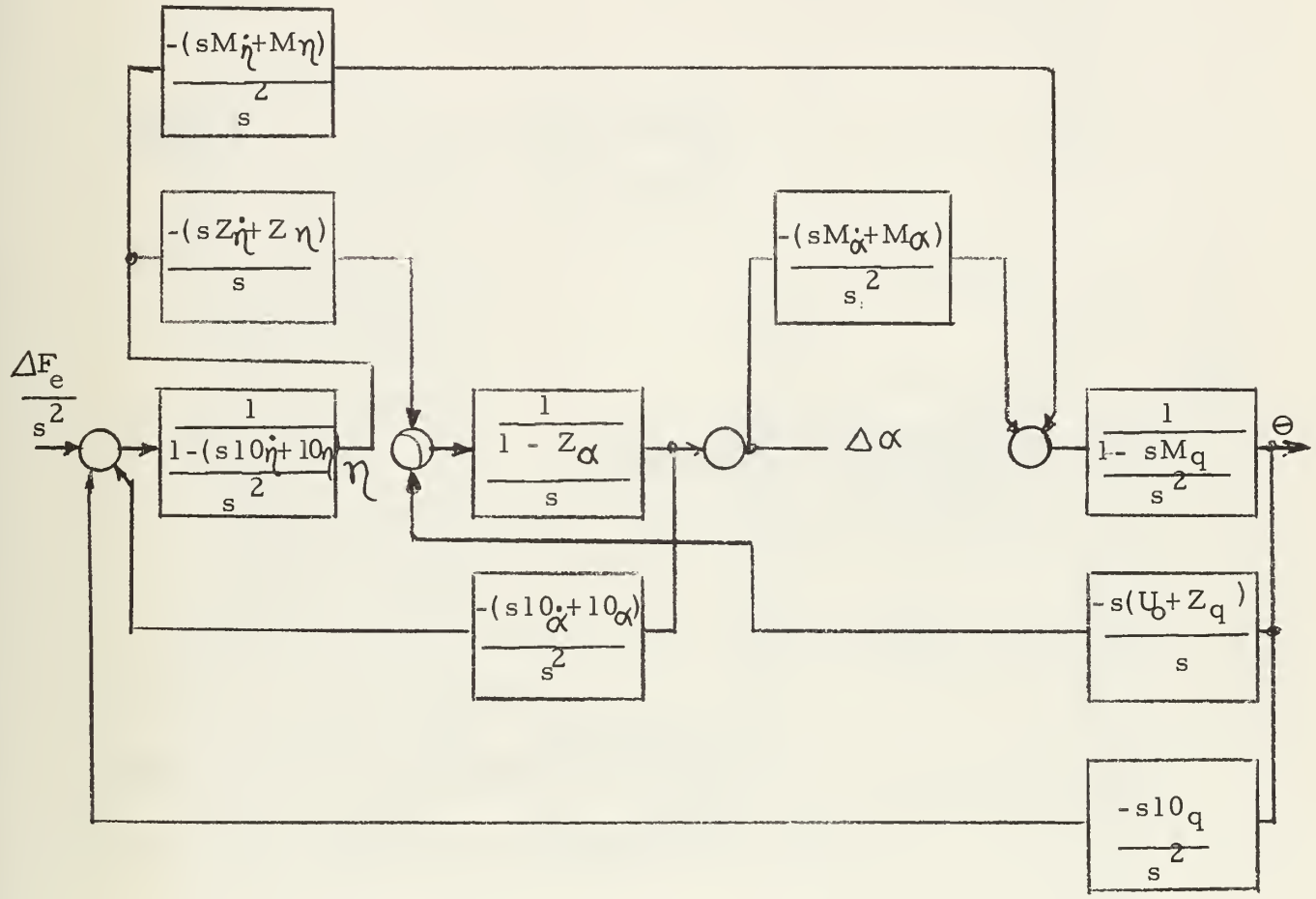

Figure 5.8 REARRANGED BLOCK DIAGRAM OF FIGURE 5.5, USING MANIPULATIONS OF FIGURES 5.6 and 5.7.

Maneuvering the above diagram location, the block diagram takes the form of Fig. 5.9, which coincides with Fig. 5.4.

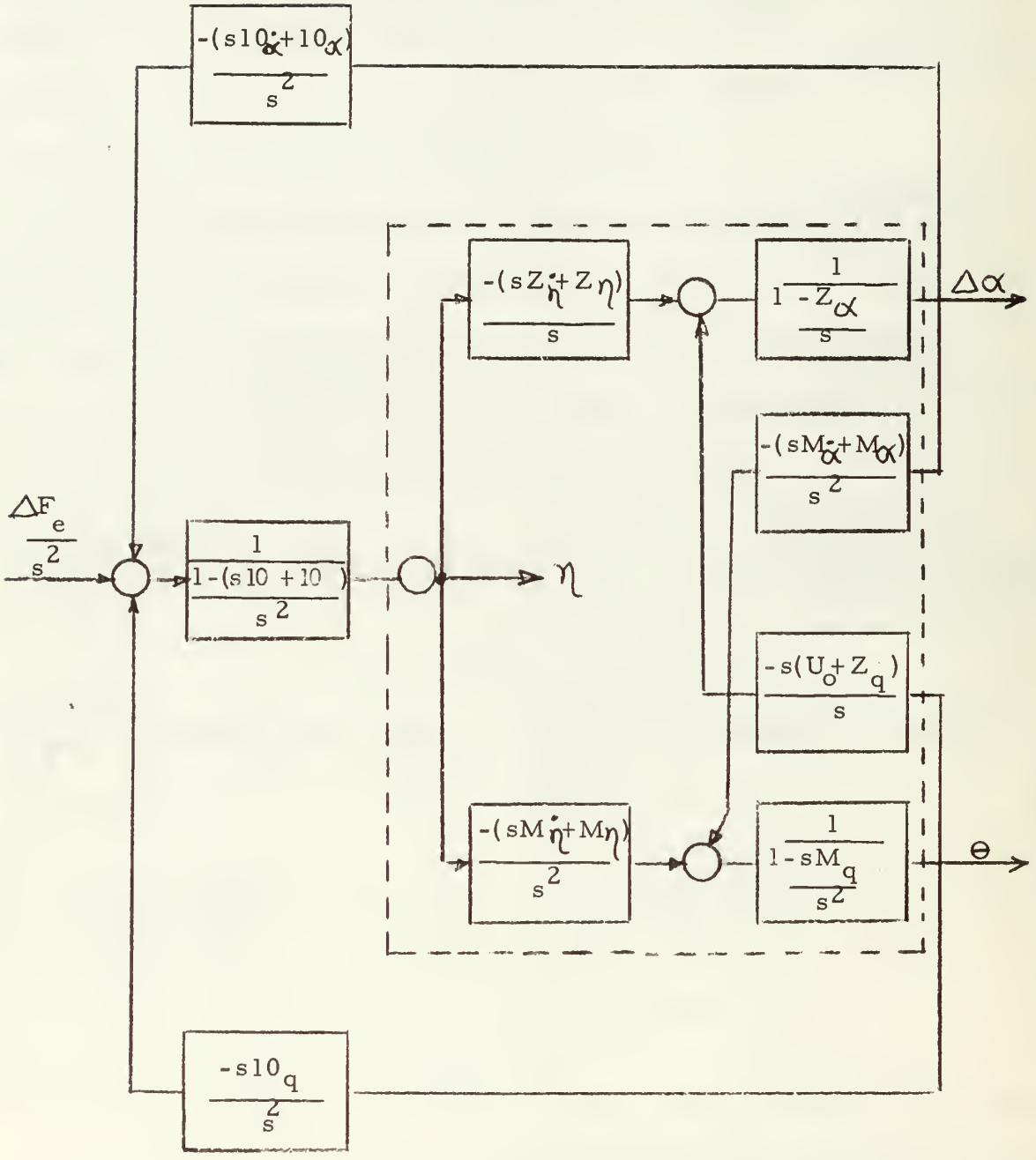

Figure 5.9 TWO DEGREES OF FREEDOM IN AN AIRFRAME LONGITUDINAL SYSTEM.

(rearranged diagram of Fig. 5.8 to compare with Fig. 5.4)

It is noted that this block diagram approaches the form set down in Etkin except for nondimensionalizing the terms. The dashed area in the diagram is what Etkin labels $G_{\theta\eta}$ and $G_{\alpha\eta}$.

The determinant from the above dashed portion of the block diagram is:

$$\begin{vmatrix} 1 & 0 & 0 & 0 & 0 \\ -\frac{(sZ\dot{\eta} + Z\eta)}{s} & 1 - \frac{Z\alpha}{s} & 0 & \frac{-s(Uo + Z_q)}{s} & 0 \\ 0 & -1 & 1 & 0 & 0 \\ \frac{-(sM\dot{\eta} + M\eta)}{s^2} & 0 & \frac{-(sM\dot{\alpha} + M\alpha)}{s^2} & 1 - \frac{sM_q}{s^2} & 0 \\ 0 & 0 & 0 & -1 & 1 \end{vmatrix}$$

Evaluating for the transfer functions $\frac{\theta}{\eta}$ and $\frac{\Delta\alpha}{\eta}$, the results will be in the form $\frac{G_{jk}\Delta_{iy}}{\Delta}$

This form is the type expressed by Chu (1) and Thaler (12). The Δ term, which is the whole determinant, reduces to:

$$\Delta = \begin{vmatrix} 1 - \frac{Z\alpha}{s} & 0 & \frac{-s(U_o + Z_q)}{s} \\ -1 & 1 & 0 \\ 0 & \frac{-(sM\dot{\alpha} + M\alpha)}{s^2} & 1 - \frac{sM_q}{s^2} \end{vmatrix}$$

which is $\Delta = \left(1 - \frac{Z\alpha}{s}\right)\left(1 - \frac{sM_q}{s^2}\right) - s\left(\frac{U_o + Z_q}{s}\right)\left(\frac{sM\dot{\alpha} + M\alpha}{s^2}\right)$ (5-79)

or $\Delta = \frac{1}{s^3}(s - Z\alpha)(s^2 - sM_q) - s(Uo + Z_q)(sM\dot{\alpha} + M\alpha)$

To consider the $\frac{\Delta\alpha}{\eta}$ term the cofactor Δiy of this determinant is obtained by crossing through the first row and the second column.

$$-\Delta_{12} = \begin{vmatrix} -\frac{(sZ\dot{\eta} + Z_n)}{s} & 0 & \frac{-s(U_o + Z_q)}{s} \\ 0 & 1 & 0 \\ -\frac{(sM\dot{\eta} + M\eta)}{s^2} & -\frac{(sM\dot{\alpha} + M\alpha)}{s^2} & 1 - \frac{sM_q}{s^2} \end{vmatrix}$$

$$\Delta_{12} = \frac{+1}{s^3}\left[+(sZ\dot{\eta} + Z\eta)(s^2 - sM_q) + s(U_o + Z_q)(sM\dot{\eta} + M\eta)\right]$$

The main feed forward transfer function between the input signal from node 2 to the output is +1 in this case. This is also true of node 4 input to output. Hence $G_{2\Delta\alpha} = +1$.

The transfer function

$$G_{\Delta\alpha\eta} = \frac{\Delta\alpha}{\eta} = \frac{G_2 \Delta\alpha \Delta_{12}}{\Delta}$$

(5-81)

$$G_{\Delta\alpha\eta} = \frac{(sZ\dot{\eta} + Z\eta)(s^2 - sM_q) + s(Uo + Z_q)(sM\dot{\eta} + M\eta)}{(s - Z\alpha)(s^2 - sM_q) - s(U_o + Z_q)(sM\dot{\alpha} + M\alpha)}$$

It can be noted that this equation 5-80 is the same equation as 5-72 given by Etkin save the non-dimensionalizing terms.

To evaluate the transfer function Θ l η, the same method is used.

$$G_{4\Theta} = -1$$

$$\Delta_{14} = \begin{vmatrix} -\frac{(sZ\dot{\eta} + Z\eta)}{s} & 1 - \frac{Z\alpha}{s} & 0 & 0 \\ 0 & -1 & 1 & 0 \\ -\frac{(sM\dot{\eta} + M\eta)}{s^2} & 0 & -\frac{(sM\dot{\alpha} + M\alpha)}{s^2} & 0 \\ 0 & 0 & 0 & 1 \end{vmatrix}$$

$$\Delta_{14} = \begin{vmatrix} -\frac{(sZ\dot{\eta} + Z\eta)}{s} & 1 - \frac{Z\alpha}{s} & 0 \\ 0 & -1 & 1 \\ -\frac{(sM\dot{\eta} + M\eta)}{s^2} & 0 & -\frac{(sM\dot{\alpha} + M\alpha)}{s^2} \end{vmatrix}$$

$$\Delta_{14} = \frac{1}{s^3} (sM\dot{\eta} + M\eta)(s - Z\alpha) + (sM\dot{\alpha} + M\alpha)(sZ\dot{\eta} + Z\eta) \qquad (5\text{-}82)$$

Therefore:

$$G_{\Theta\eta} = \frac{\Theta}{\eta} = \frac{G_{4\Theta}\ \Delta_{14}}{\Delta}$$

$$G_{\Theta\eta} = \frac{(sM\dot{\eta} + M\eta)(s - Z\alpha) + (sM\dot{\alpha} + M\alpha)(sZ\dot{\eta} + Z\eta)}{(s - Z\alpha)(s^2 - sM_q) - s(U_o + Z_q)(sM\dot{\alpha} + M\alpha)} \qquad (5\text{-}83)$$

Here again, excepting the non-dimensionalzing, the result is the same. Equation 5-83 is equal to equation 5-71 as given by Etkin.

The system of "standard" forms then works for the airframe differential equations after some manipulation. It can be noted that there is a method of making up this standard form without the necessity of the manipulation which will yield physically realizable output signals. When the block diagram of Fig. 5.8 is converted into a determinant for solution of the transfer function, there appears a series of alternating rows where the equation -1 + 1 = 0 appears. It also appears that these simple equations occur in a sequence where the plus one term is placed in the 2n ! row and column. n is the number of differential equations in the problem. The minus one term is placed in the 2n ! rows and (2n !-1) columns. All feedforward terms (those below and to the left of the main diagonal) are moved one column to the right and remain in the same row. This doubles the size of the determinant. However, there are several zero terms introduced and the actual work involved in evaluation of the determinant is not markedly increased.

The next item is to look at the lateral motion problem. It is slightly more complex because there are five differential equations of motion instead of four.

Equation 5-35 with simplifications becomes:

$$(\dot{v} + Uor) - \emptyset\, mg \cos \Theta_o - YvV - Yp - Y_R R - Y_S \zeta = 0 \qquad (5\text{-}84)$$

$$(\dot{\beta} + r) - \frac{\phi\, g \cos\Theta_o}{U_o} - Y_\beta \beta - \frac{Y_p p}{U_o} - \frac{Y_r r}{U_o} - \frac{Y_\zeta \zeta}{U_o} = 0 \qquad (5\text{-}85)$$

The moment equation 5-55 becomes

$$\dot{P} - \frac{E}{A}\dot{R} - L_\beta \beta - L_p p - L_r r - L_\xi \xi - L_\zeta \zeta = 0 \qquad (5\text{-}86)$$

and equation 5-57 becomes

$$\dot{R} + \frac{E\dot{P}}{C} - N_\beta \beta - N_p P - N_r R - N_\xi \xi - N_\zeta \zeta - N_{\dot{\zeta}} \dot{\zeta} = 0 \qquad (5\text{-}87)$$

The aileron hinge motion equations from Appendix I are

$$\ddot{\zeta} - 11_p p - 11_r r - 11_\xi \xi - 11_\zeta \zeta = \Delta Fa \qquad (5\text{-}88)$$

And also from Appendix I, the rudder hinge motion is

$$\ddot{\zeta} - 12_\beta \beta - 12_p p - 12_r r - 12_\zeta \zeta - 12_{\dot{\zeta}} \dot{\zeta} = \Delta Fr \qquad (5\text{-}89)$$

From these terms a determinantal array can be made. It should be noted that this time a set of equations of -1 + 1 = 0 will be inserted in the system. This permits direct drawing of the block diagram and omitting the need of manipulation. Table 5-2 then presents this array. From this Fig. 5.10 is drawn directly.

	ζ		ψ		β		ϕ		ξ
$\frac{1-(s12_{\dot{\zeta}}+12_{\zeta})}{s^2}$	0	$\frac{-s12_r}{s^2}$	0	$\frac{12_\beta}{s^2}$	0	$\frac{-12_p s}{s^2}$	0	0	0
-1	1	0	0	0	0	0	0	0	0
0	$\frac{-(sN_{\dot{\zeta}}+N_\zeta)}{s^2}$	$\frac{1-sN_r}{s^2}$	0	$\frac{-N_\beta}{s^2}$	0	$\frac{s(s\frac{E}{C}-N_p)}{s^2}$	0	$\frac{-sN_\xi}{s^2}$	0
0	0	-1	1	0	0	0	0	0	0
0	$\frac{-Y_\zeta}{s}$	0	$\frac{+s(1-Y_r)}{s}$	$1-\frac{Y_\beta}{s}$	0	$\frac{-(g+sY_p)}{s}$	0	0	0
0	0	0	0	-1	1	0	0	0	0
0	$\frac{-L_\zeta}{s^2}$	0	$\frac{-s(s\frac{E}{A}+L_r)}{s^2}$	0	$\frac{-L_\beta}{s}$	$\frac{-1-sL_p}{s^2}$	0	$\frac{-L_\xi}{s^2}$	0
0	0	0	0	0	0	-1	1	0	0
0	0	0	$\frac{-sl1_r}{s^2}$	0	0	0	$\frac{-sl1_p}{s^2}$	$-\frac{(sl1_{\dot{\zeta}}+l1_\zeta)}{s^2}$	0
0	0	0	0	0	0	0	0	-1	1

TABLE 3-1 DETERMINANT ARRAY OF LATERAL SYSTEM EQUATIONS FOR SMALL DISTURBANCES

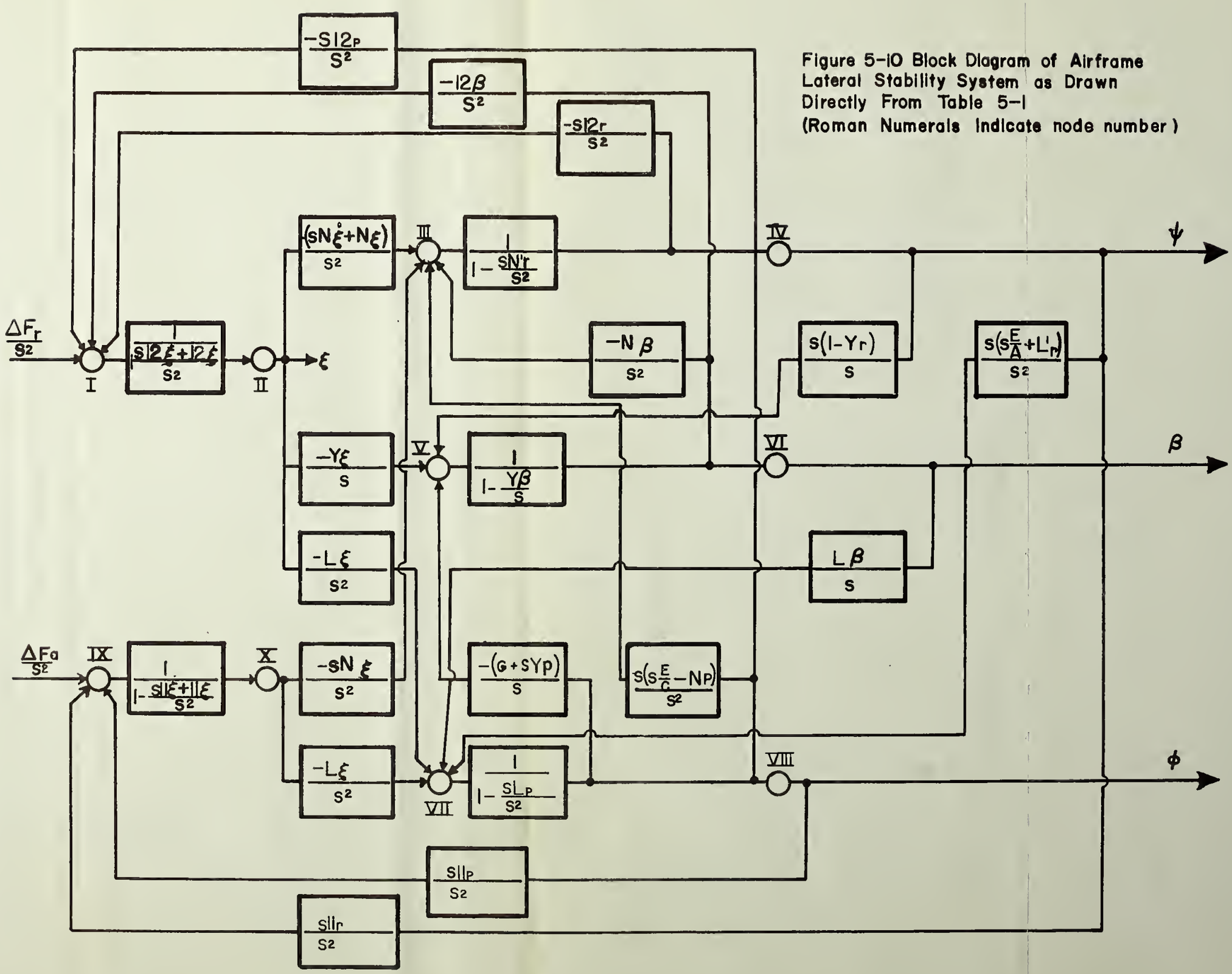

Figure 5-10 Block Diagram of Airframe Lateral Stability System as Drawn Directly From Table 5-1 (Roman Numerals Indicate node number)

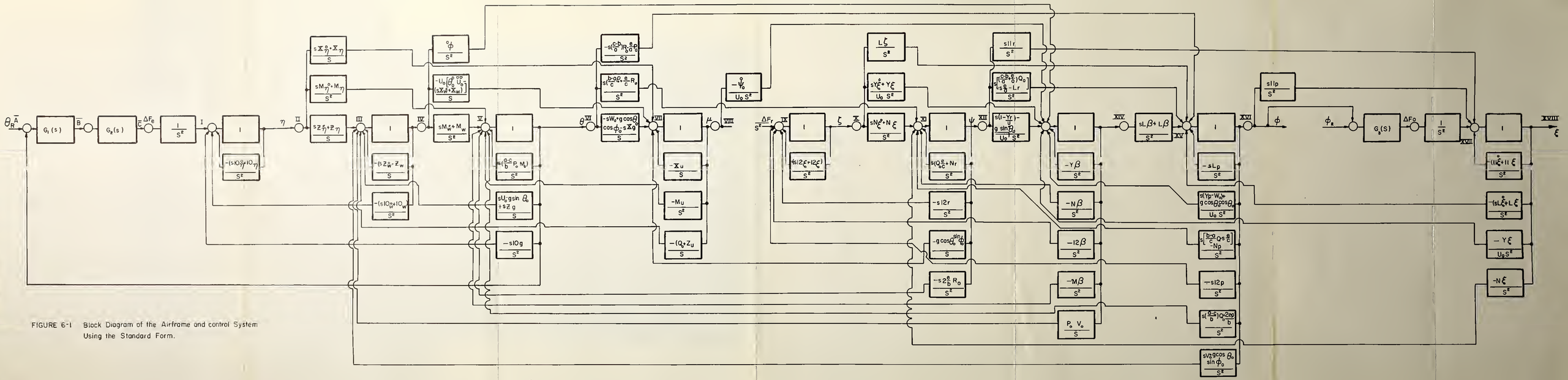

FIGURE 6-1 Block Diagram of the Airframe and control System Using the Standard Form.

The resulting block diagram very clearly parallels that of the eral system shown by Etkin in Chapter 9 (4). The "standard" form achieve this block diagram differs.

There is, then, the question of why does this differ from the iginal "standard" form set forth by Chu.

Chapter Two of Chu (1) discusses at some length the idea of rangment of varying performance functions into a "standard" block agram. The individual pieces of hardware are at hand with known dividual performance functions. The orderly arrangement of these rmit the construction of a "standard" determinant for the whole system. om this, a multiloop servo system can be handled in generalized sults. In the case of the airframe, the determinant formed by the fferential equations was known and the block diagram had to be rmed. Admittedly a block diagram (Fig. 5.5) was made up but the tput signals are not the physically realizable type that are generally own to pilots and engineers. The same performance function results om the system. Both are mathematically correct.

The difference lies in the fact that Chu is taking individual pieces hardware where the functions are known. The blocks are made up nd then the "standard" determinant form is made. In the case of the rplane, the equations of motion are known and a determinant is mmediately formed. Each column contains the performance functions

multiplied by the direct function signal output term. Chu's standard form dictates that all terms above the main diagonal are multiplied by the node output or input to the direct function. Steps must be taken then to change this in the differential equations. The addition of the alternating -1 + 1 = 0 equations solves this very nicely and in no way alters the value of the equation.

A series of evaluations of determinant forms is given in Appendix III. The results show that the addition of these terms in no way changes the final value of a determinant or a cofactor value.

Referring to Fig. 5.8 there are other block forms that may change the values within the blocks, but will not alter the final outcome. Consider the first node in Fig. 5.8 as an example. The four forms expressed in Fig. 5.11 are equivalent. The original form is shown in Fig. 5.11a. The self-loop feedback path is combined with the direct path in Fig. 5.11b. The s^2 term is eliminated and the performance functions are then in the form shown in Fig. 5.11c. A further change can be made by dividing the nodal input terms by the denominator of the direct path feed-forward function. The result is then in the form shown in Fig. 5.11d. The performance functions in each block differ somewhat, but the final result remains the same. These manipulations allow the user more freedom in the forms of the performance functions. It allows changes in form to fit the needs of the particular problem.

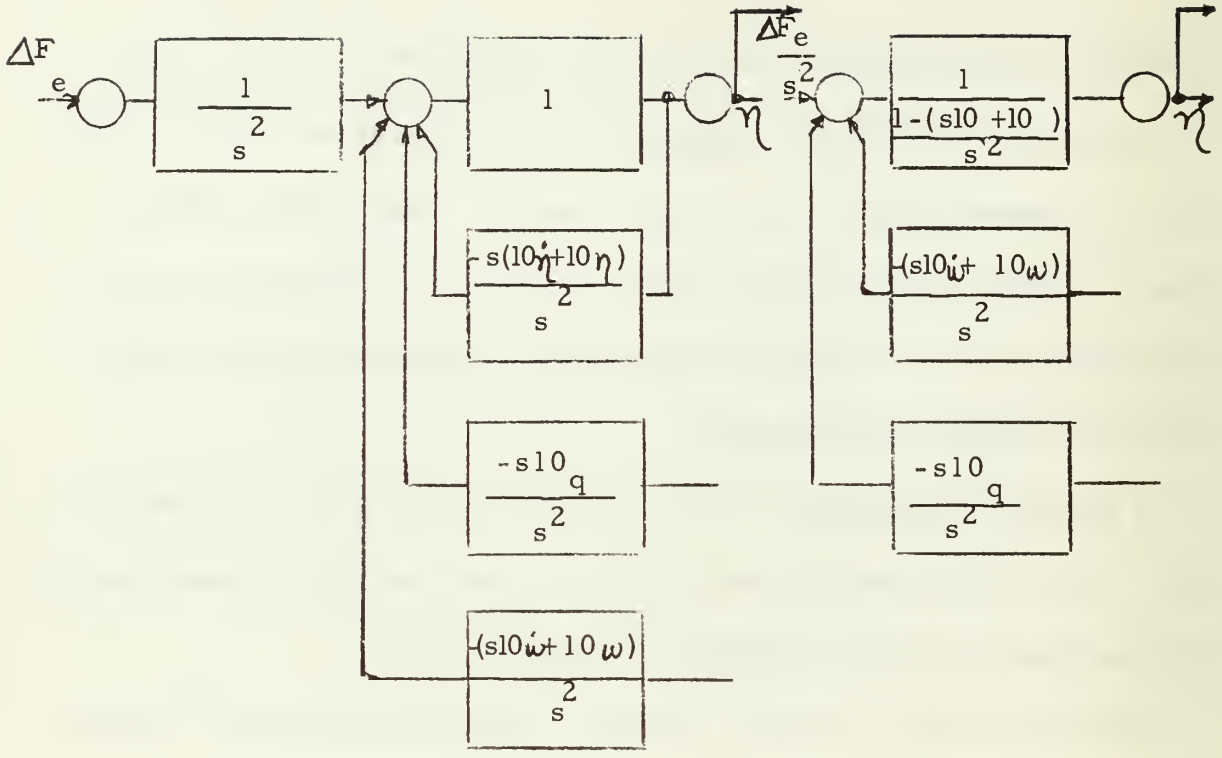

Figure 5.11 (a)

Figure 5.11 (b)

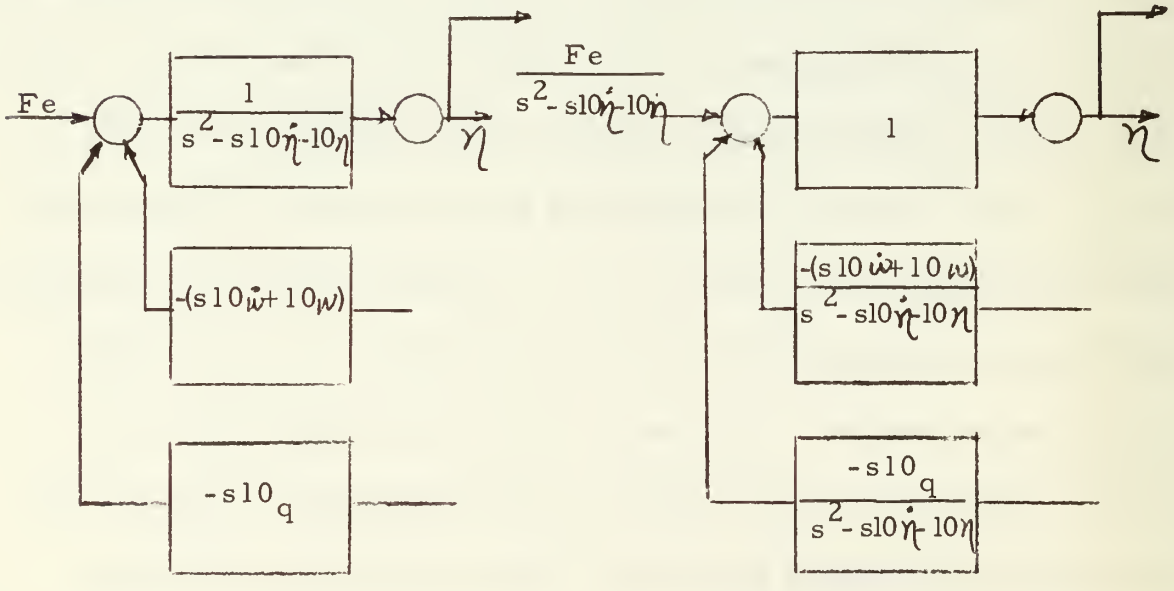

Figure 5.11 (c)

Figure 5.11 (d)

FIGURE 5.11 PERMISSIBLE BLOCK VALUE VARIATIONS AT A NODE.

The pick-off point for the feed forward terms does differ in requirements. It is seen in Figs. 5.11a and (d) that the pick-off can be either off the output signal of node I or II. The final result will not change. However, this is not the case in Figs. 5.11b and (c). The pick-off point must be off the output signal of node II. The final result will differ if the output of node I was tapped in the latter case.

For converting a set of linear differential equations into the standard block diagram form, the following rules can be applied.

1. Between each differential equation, an equation $-1 + 1 = 0$ shall be inserted. An additional equation $-1 + 1 = 0$ shall be added at the bottom of the set so the number of additional equations shall equal the number of differential equations originally in the problem.
2. The arrangement of the values of these added equations in the determinant shall be such that the positive one value is always in the main diagonal block. The minus one term shall always be placed in the block immediately to the left of the main diagonal term.
3. All other blocks in the rows of these added equations shall be of zero value.
4. All finite performance functions of the original differential equations which are located below the main diagonal shall be moved one place to the right. The vacated blocks shall be replaced with a zero value. This last rule is optional

to the user. It does save the possibility of error which could appear because of cases shown in Fig. 5.11b and (d).

With the simplified rules of making a standard block diagram from the standard determinant, a valuable tool is developed for many purposes. It can provide a student with a means to draw and visualize a complex feedback system such as an airframe from a group of differential equations. For the research groups, it makes analog computer programming a simplified matter with respect to amplifier usage. In this latter case, pitfalls do exist. The airframe is no simple matter. The reader is referred to Howe (8) for an excellent coverage of the airframe problem for analog computers. Most important, though, is the fact that this standard form of Chu's is valid for any multi-loop linear feedback system whether it is electrical, mechanical or a combination of the two. This then puts a regular form to the multi-loop control system from which design or synthesis can proceed in an orderly manner.

6. Expansion of the Standard Form for Greater Disturbances

The system developed by Chu was for linear functions. It is the purpose of this section to explore the equations of motion and determine whether the equations of motion can be used for larger disturbances than considered in Section V. If so, then to what degree can this system be used.

For all practical purposes, the small angle approximation holds quite well up to one-tenth radian. Therefore, $\Theta \approx \sin \Theta$ and $\cos \Theta \approx 1$. With this simplification in mind, Equation 5-52 is then rewritten.

$$m(\dot{U} + QW - RV) + mg \sin \Theta_o - \Psi mg(\cos \Theta_o \sin \Phi_o) + \Theta mg(\cos \Theta_o \cos \Phi_o) = X_o + X'_u U + X'_w W + X'_{\dot{w}} \dot{W} + X'_q Q + X'_\eta \eta + X'_{\dot{\eta}} \dot{\eta} + X'_v V + T_o \cos \Theta_T + T_u \cos \Theta_T U + T_{\delta RPM} \delta RPM \cos \Theta_T \tag{6-1}$$

The thrust forces are combined into the forward velocity motion u and a steady state reference condition of

$$m(Q_o W_o - R_o V_o) + mg \sin \Theta_o = X_o + T_o \cos \Theta_T \tag{6-2}$$

is assumed.

Subtracting 6-2 from 6-1 the following equation results

$$m(\dot{u} + Q_{ow} + W_{oq} + qw - R_{ov} - V_o r - vr) - \Psi mg(\cos \Theta_o \sin \Phi_o) + \Theta mg(\cos \Theta_o \cos \Phi_o) - X'_u - X'_w - X'_{\dot{w}} \dot{W} - X'_q Q - X'_\eta \eta - X'_{\dot{\eta}} \dot{\eta} - X'_v V = 0 \tag{6-3}$$

The product term qw is dropped as a small value product situation. The same applies to the vr term.

Converting to La Place notation and dividing by the mass the following equation will result

$$su + \Theta_o U_o \Delta\alpha + sW_o\Theta - \Psi_o U_o \beta - \Psi g \cos\Theta_o \sin\Phi_o$$

$$+ \Theta g \cos\Theta_o \cos\Phi_o - X_u U - (sX_{\dot{w}} + X_w)\Delta\alpha - sXq\,\Theta$$

$$- (sX_{\dot{\eta}} + X_\eta)\eta - X_\beta\beta = 0 \qquad (6\text{-}4)$$

The y and z direction force equations will form up in the same manner.

$$sU_o\beta + \dot{\Psi}_o u + U_o\dot{\Psi} - \dot{\Phi}_o U_o \Delta\alpha - W_o\dot{\Phi} - \Psi g \sin\Theta_o$$

$$- g(\cos\Theta_o \sin\Phi_o) - g\Phi\cos\Theta_o \cos\Phi_o + Y_\beta\beta \qquad (6\text{-}5)$$

$$- sY_p\Phi - sY_r\Psi - (Y_\xi)\xi - (sY_{\dot{\zeta}} + Y_\zeta)\zeta = 0$$

$$sU_o\Delta\alpha + P_o U_o\beta + V_{os}\Phi - Q_{ou} - V_{os}\Theta + g\sin\Theta_o\Theta$$

$$+ g\cos\Theta_o \sin\Phi_o\Phi - g\cos\Theta_o\cos\Phi_o - Z_u U$$

$$- (sZ_{\dot{w}} + Z_w)U_o\Delta\alpha - sZ_q\Theta - (sZ_{\dot{\eta}} + Z_\eta)\eta = 0 \qquad (6\text{-}6)$$

The moment equations can be formed in much the same manner. From Section Five, Equation 5-55 would convert to this equation:

$$s^2 \phi + \left(\frac{C-B}{A}\right)(sQ_o \psi + sR_o \theta) - \frac{E}{A}(sP_o \theta - sQ_o \psi) - \frac{E}{A} s^2 \psi$$

$$- (sL_{\dot{\beta}} + L_{\beta})\beta - L_{ps} \phi - (sL_r \psi) - (sL_{\dot{\xi}} + L_{\xi})\xi + L_{\zeta}\zeta \qquad (6-7)$$

In a similar manner Equations 5-56 and 5-57 can be brought to a similar maximum linear condition. They are shown in the following equations:

$$s^2 \theta + \left(\frac{A-C}{B}\right)(sP_o \theta + sQ_o \phi) + \frac{2E}{\beta}(sP_o \phi - sRo\ \psi)$$

$$- M_u u - (sM\dot{w} + M_w) U_o \Delta\alpha - s(sM_{\dot{q}} + M_q)\theta - (sM_{\dot{\eta}} +$$

$$M_{\eta})\eta = 0 \qquad (6-8)$$

$$s^2 \psi + \left(\frac{B-A}{C}\right)(sP_o \theta + sQ_o \phi) + \frac{E}{C}(sQ_o \psi + sR_o \theta - s^2 \phi)$$

$$- N_{\beta}\beta - sN_p \phi - sN_R \psi - N_{\xi}\xi - (sN_{\dot{\zeta}} + N_{\zeta})\zeta \qquad (6-9)$$

Also the control hinge moment Equations 5-66, 5-88, and 5-89 are recalled in their same form.

These nine equations represent the linear equations of motion of the airframe and include all cross-coupling effects. These equations still retain the requirement of a linear approximation. The equations with the author's modification of adding the equations -1 + 1 = 0 make up Table 6-1. This is an 18 x 18 determinant. From this table the block diagram of Fig. 6.1 can be drawn.

	η		ω		θ		μ		ζ		ψ		β		ϕ		ξ
$1-\frac{s10\mathring{\eta}+10\eta}{s^2}$	0	$\frac{-(s10\mathring{\omega}+10\omega)}{s^2}$	0	$\frac{-s10q}{s^2}$	0	0	0	0	0	0	0	0	0	0	0	0	0
-1	1	0	0	0	0	0	0	0	0	0	0	0	0	0	0	0	0
0	$\frac{-(sz\mathring{\eta}+z\eta)}{s}$	$1-\frac{(sz\mathring{\omega}+z\omega)}{s}$	0	$\frac{-\left[\begin{matrix}sV_0-g\sin\theta_0\\+szg\end{matrix}\right]}{s}$	0	$\frac{-(Q_0+z\mu)}{s}$	0	0	◑	0	0	$\frac{P_0V_0}{s}$	0	$\frac{sV_0+q\cos\theta_0\sin\phi_0}{s}$	0	0	0
0	0	-1	1	0	0	0	0	◑	0	0	◑	0	0	◑	0	0	0
0	$\frac{-(sM\mathring{\eta}+M\eta)}{s^2}$	0	$\frac{-(sM\mathring{\omega}+M\omega)}{s^2}$	$1+\frac{s\left(\frac{A-C}{\beta}P_0-M_0\right)}{s^2}$	0	$\frac{-M\mu}{s^2}$	0	◐	0	$\frac{-s\frac{2E}{\beta}R_0}{s^2}$	0	$\frac{-M\beta}{s^2}$	0	$\frac{s\frac{A-C}{\beta}Q_0+\frac{2E}{\beta}P_0}{s^2}$	◐	0	0
0	0	◑	◑	-1	1	0	0	0	0	0	0	0	0	0	◐	0	0
0	$\frac{-(sX\mathring{\eta}+X\eta)}{s}$	◑	$\frac{\theta_0(sX\mathring{\omega}+X\omega)}{s}$	0	$\frac{sW_0+g\cos\theta_0\cos\phi_0-sXq}{s}$	$1-\frac{X\mu}{s}$	0	0	0	$\frac{-g\cos\theta_0\sin\phi_0}{s}$	0	$\frac{-(\psi\mu_0+X\beta)}{s}$	0	0	◐	◑	0
0	0	0	0	0	0	-1	1	0	0	0	0	0	0	0	0	0	0
0	0	0	0	0	◐	0	0	$1-\frac{(s12\mathring{\xi}+12\xi)}{s^2}$	0	$\frac{-s12r}{s^2}$	◑	$\frac{-12\beta}{s^2}$	◑	$\frac{-12p}{s^2}$	0	0	◑
0	0	0	0	0	0	0	0	-1	1	0	0	0	0	0	0	0	0
0	◑	0	◑	0	$\frac{s\left(\frac{B-A}{C}P_0+\frac{E}{C}R_0\right)}{s^2}$	0	0	◑	$\frac{-(sN\mathring{\xi}+N\xi)}{s^2}$	$1+\frac{s(Q_0\frac{E}{C}-Nr)}{s^2}$	◑	$\frac{-N\beta}{s^2}$	0	$\frac{s\left(\frac{B-A}{C}Q_0-S\frac{E}{C}-Np\right)}{s^2}$	0	$\frac{-N\xi}{s^2}$	0
0	0	0	0	0	0	0	0	0	0	-1	1	0	0	0	0	0	0
0	0	0	$\frac{-\mathring{\phi}_0}{U_0s^2}$	0	0	0	$\frac{\mathring{\psi}_0}{U_0s^2}$	0	$\frac{-(sY\xi+Y\mathring{\xi})}{U_0s^2}$	◑	$\frac{s(U-Yr)-g\sin\theta_0}{U_0s^2}$	$1-\frac{Y\beta}{s^2}$	0	$\frac{s(Yp-W_0)+g\cos\theta_0\cos\phi_0}{U_0s^2}$	0	$\frac{-Y\xi}{U_0s^2}$	◑
0	0	0	0	0	0	0	0	0	0	0	0	-1	1	0	0	0	0
0	0	0	0	0		0	0	0	$\frac{-L\xi}{s^2}$	0	$-s\frac{\left[\begin{matrix}\frac{c-b}{a}+\frac{e}{a}Q_0\\-\frac{se}{a}-L_r\end{matrix}\right]}{s^2}$	0	$\frac{-(sL\mathring{\beta}-L\beta)}{s^2}$	$1-\frac{sLp}{s^2}$	0	$\frac{-(sL\mathring{\xi}+L\xi)}{s^2}$	0
0	0	0	0	0	0	0	0	0	0	0	0	0	0	-1	1	0	0
0	0	0	0	0	0	0	0	0	0	◐	$\frac{-s11r}{s^2}$	0	0	0	$\frac{-s11p}{s^2}$	$1-\frac{(s11\mathring{\xi}+11\xi}{s^2}$	0
0	0	0	0	0	0	0	0	0	0	0	0	0	0	0	0	-1	1

TABLE 6-1 Determinant Array of Airframe with Linear Approximations for Six Degrees of Freedom.

This block diagram then represents the complete airframe response maintaining linear approximations. Even then this system has limitations. As an example, consider some airplane flying with a steady state wing angle of attack of 15 degrees. (assume a "convention" wing and the reference axis is the zero lift line) Any pilot will quickly testify that an increase of 5 degrees angle of attack at that point will probably result in a rather wildly oscillating maneuver popularly known as a spin. This condition is generally outside of the range of the aerodynamic forces and moments usually computed. Some aerodynamic coefficients such as lift (C_L) are decidedly non-linear in this region. Therefore, the restrictions imposed on this derivation of terms must include a restriction that the airframe is not operating at the very edge of its flight envelope.

The system has been diagrammed directly from Table 6-1. The terms in Column One are all connected at node I of Fig. 6.1. Likewise, the terms in Column Two of Table 6-1 are all connected to node II. Extra nodes appear in the beginning and end of the block diagram. These are inserted as provisions for control functions. These control nodes are lettered alphabetically. The block diagram contains the required loops for aileron and elevator control. The rudder control loop can be easily inserted when desired.

Examination of Fig. 6.1 reveals many interesting points heretofore known but sometimes only by intuitive reasoning. The concept

of separate systems for the symmetric axis and asymmetric axis systems is very well shown. The level flight steady state conditions used in Section Three stated that

$$Po = Qo = Ro = Vo = Wo = 0 \qquad (6\text{-}10)$$

Examining the paths between nodes VIII and IX reveal that all of the performance functions are zero under these specified conditions of steady state flight. There is no direct, feedforward or feedback paths between nodes VIII and IX. Thus the restricted case of steady state level flight conditions with small perturbation is clearly divided into the two systems. The longitudinal system includes the forward velocity, vertical velocity, pitching motion and elevator position. The block diagram for the system can be further restricted to two degrees of freedom by holding the X velocity change, u, at zero. This allows change in vertical motion and pitch. This would then be Figs. 5-8 and 5-9 of Section 5.

The so-called lateral airframe response system comprises the nodes from IX to XVIII. The rudder and aileron motion, sideslip, yaw and roll comprise the motion for this system. With the steady state level flight conditions previously mentioned, the block diagram is identical to Fig. 5-10 of Section 5.

An interesting note of these separate systems is the cross coupling terms that begin to arise with larger disturbances. An

important one is the pitch due to sideslip. The effects are labeled M_β in the diagram. Several aircraft are subject to this. Usually, this is a tucking or nose down motion that appears as sideslip angle (β) increases. In the simplified systems this effect was neglected. It is of negligible value for very small disturbances, but can become noticeable by the time the sideslip angle (β) reaches five degrees. The effect exists and is shown by this expanded system.

Excellent methods of analysis are available for these standard forms brought forth in this work. Methods of analyzing outputs in response to one or more inputs are available. Work by Thaler (10) contains a very useable system.

Where $N \triangleq$ the output signal at the n th node

$\Delta \triangleq$ characteristic determinant

$\Delta_{a_n} \triangleq$ the cofactor of the determinant with "a" the node location receiving the input and "n" the node location of the output signal.

$G_{1a} \triangleq$ the performance function on the input signal prior to entering the input node.

$I \triangleq$ the input signal

$G_{nN} \triangleq$ the direct path performance function between the output node and the output signal.

Thus a single input signal would yield an output signal

$$N_I = \frac{G_{nN}}{\Delta} \left[\Delta_{a_n} \; G_{1_a} \; I \right] \tag{6-11}$$

For two or more input signals additional subscripts would be used and the functions are additive. The rules of superposition of linear outputs justify this method.

$$N = \frac{G_{nN}}{\Delta}\left[\Delta_{a_n} G_{1_a} \; I + \Delta_{b_n} G_{2_b} \; II + \Delta_{c_n} G_{3_c} \; III + \text{----}\right] \quad (6\text{-}12)$$

This equation would give the resulting ouput of one or more inputs at various nodes in the system.

The degrees of freedom can be restricted also. In the block diagram, (Fig. 6-2) consider a cut made in the path at point "s".

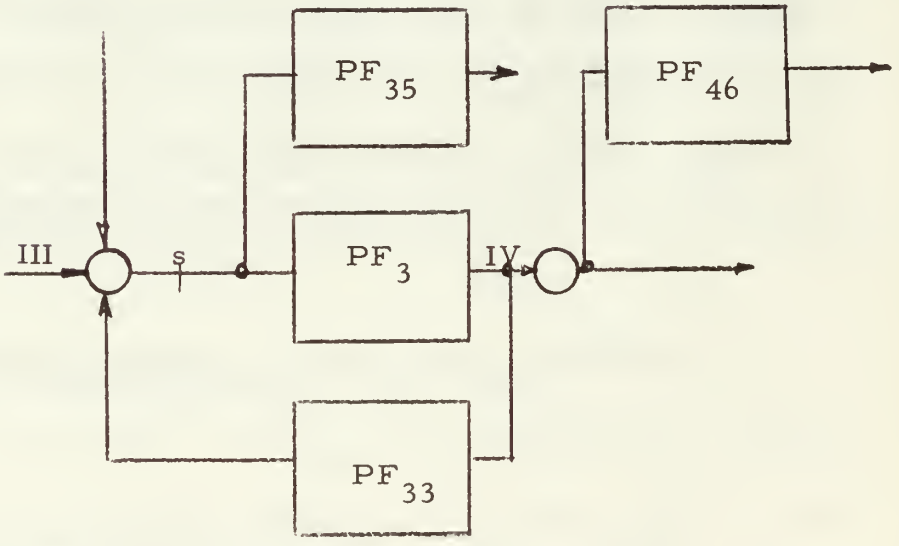

FIGURE 6-2 ILLUSTRATION OF RESTRICTING FREEDOM OF MOVEMENT IN A SYSTEM BY CUTTING A NODE OUTPUT IN THE BLOCK DIAGRAM.

This opening in the path now eliminates the signal to the direct path, the feedback and the feedforward path. The result of this in the determinant is the insertion of zeros in all the performance functions in the column. It leaves only the constant, one, in the main diagonal block. The reader will recall that the main diagonal has the term $1 + PF_3PF_{33}$. This is shown below as opening the output path from a third node.

$$\begin{matrix} x & x & 0 & x & x & x \\ x & x & 0 & x & x & x \\ x & x & 1 & x & x & x \\ x & x & 0 & x & x & x \\ x & x & 0 & x & x & x \\ x & x & 0 & x & x & x \end{matrix}$$

The output path from node three is opened at point s and the determinant is changed in this manner.

A special case occurs for the diagram illustrated in Fig. 6-2. The second node has only one input signal. Because the path was cut at point "s", the output from the second node will also be zero. Thus,

all feedforward values from this node will be zero. The direct and feedback paths of the second node are non-existant to being with and remain so. The determinant form would appear as now shown.

$$\begin{matrix} x & x & 0 & 0 & x & x \\ x & x & 0 & 0 & x & x \\ x & x & 1 & 0 & x & x \\ x & x & 0 & 1 & x & x \\ x & x & 0 & 0 & x & x \\ x & x & 0 & 0 & x & x \end{matrix}$$

Simple manipulation now reduces the six by six determinant to a four by four determinant. Therefore, when it is desired to consider a problem with one or more degrees of freedom held at zero, the simple method of opening the output signal path from the node and placing a zero for all the performance functions in the column leaving only the constant value one in the main diagonal point accomplishes this.

Referring to Section 5, the reader can observe the general equations of motion for mass particles and examine one such as Equation 5-55 which is repeated below.

$$\dot{AP} + a_1\dot{K}_1 + QR\,(C-B) - E\,(PQ + \dot{R}) + cK_3Q - bK_2R =$$

$$L_o + L'_v v + L'_{\dot{v}}\dot{v} + L'_p p + L'_r r + L'_\xi \xi + L'_{\dot{\xi}}\dot{\xi} \qquad (6\text{-}13)$$

$$+ L'_\zeta \zeta + L'_{\dot{\zeta}}\dot{\zeta} - 0$$

Note the third term QR is a product of $(Q_o + q)(R_o + r)$. The product when multiplied is $Q_o R_o + Q_o r + R_o q + qr$. From the equations of Section 5:

$$Q = \dot{\Theta} \cos \Phi + \dot{\Psi} \sin \Phi \cos \Theta \tag{6-14}$$

$$R = \dot{\Psi} \cos \Phi \cos \Theta - \dot{\Theta} \sin \Phi \tag{6-15}$$

When the small angle approximation is no longer valid, the handling of this product term becomes rather involved. Furthermore, the aerodynamic coefficients of the L'_v, L'_p, L'_r etc terms lose their linear approximations over large changes in flight conditions. Most aerodynamic coefficients are of a decidedly non-linear nature over the full span of an aircraft's maneuvering capability. The coefficients are definitely non-linear with Mach number when the velocity range covers the subsonic, transonic and supersonic spectrum. The reader can observe the general equations of motion in Section 5. Considering the complexities of incorporating equations 6-14 and 6-15 for large movements and the non linearities of the aerodynamic coefficients, it is not long before one realizes that the non linearities are numerous and cover all the equations. The prospect of block diagramming for the purpose of placing all non linearities in one block to be handled by a describing function scheme is hopeless.

The possibility of doing the problem with an analog computer and using no approximations is fair. Undoubtedly the task, if attempted.

will be of considerable magnitude.

Thus, it is seen that this system of standard determinant arrays and standard block diagrams can be used to handle the airframeproblem as long as a linear approximation is maintained. The system is flexible and can carry varied conditions of multiple inputs. It can also be noted that for the six degrees of freedom problem over a large variation, it is of limited value except for diagramming a computer problem.

7. APPLICATION OF THE DETERMINANTAL APPROACH TO A SIMPLIFIED AIRFRAME CONTROL PROBLEMS.

The system to be considered is a surface to air homing missile using proportional navigation. A sketch of the missile shape is shown in Fig. 7.1, which also defines the coordinate system. A guidance computer provides command signals for the yaw and pitch autopilots, which have the same form because of the symmetry of the missile. The missile is to be considered a rigid body, and gravity forces are considered to be trimmed out in steady flight. The missile is also to be considered in steady state operation such that the speed (Mach) is constant and the pitch angle of attack is constant at α_o. Assuming that $\beta \leq 5^\circ$; $\cos\beta = 1.0$, $\sin\beta = \beta$, assuming that the mass and moments of inertia are constant, the linearized equations of motion of the missile can be derived and are:

Yaw force equation

$$\dot{\beta} - \phi \sin\alpha_o + \dot{\psi}\cos\alpha_o - Y_\beta\beta - Y_\zeta\zeta - Y_\xi\xi = 0 \qquad (7\text{-}1)$$

Yaw moment equation

$$\ddot{\psi} \quad -N_\beta\beta \quad -N_\zeta\zeta \quad -N_\xi\xi \quad = 0 \qquad (7\text{-}2)$$

Roll moment equation

$$\ddot{\phi} - Lp\,\phi - L_\beta\beta - L_\xi\xi - L_\zeta\zeta = 0 \qquad (7\text{-}3)$$

Where the coefficients are as defined in Section 4.

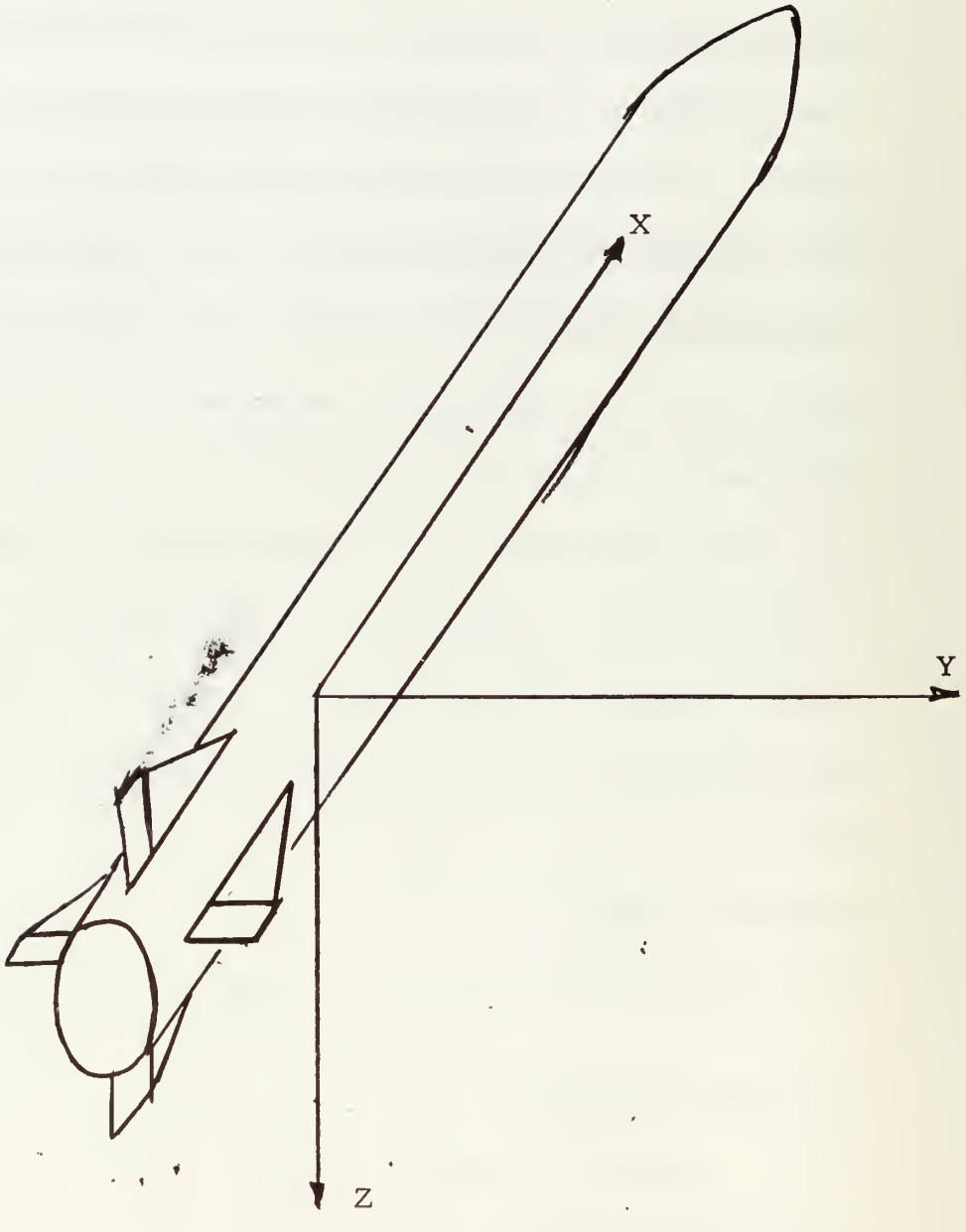

Fig. 7-1 SKETCH OF MISSILE SHAPE

Since pitch is constant, the equations for the roll and yaw control systems are needed. The measuring devices used are accelerometers which measure acceleration in the y and z direction or, within a scale factor

$Y_{\beta}\beta + Y_{\zeta}\zeta + \xi\, Y_{\beta}\alpha$ and $Y_{\beta}\alpha + Y_{\zeta}\zeta + Y_{\xi}\xi$

Other measuring devices are rate gyros which measure ϕ, $\dot{\psi}$ and $\dot{\theta}$. The relationships existing in the controlled missile are defined by the functional block diagram of Fig. 7.2.

If the sensors are considered perfect $G_1 = G_2 = G_3 = G_4 = G_5 = 1.0$, and the control equations may be written:

$$s\zeta = \left[K_1 Y_{\beta}\beta + K_1 Y_{\varphi}\varphi + K_1 Y_{\xi}\xi \right] + K_2 \dot{\psi} + K_3 \dot{\psi} \qquad (7\text{-}4)$$

$$s\xi = (-) \left[K_4 \phi + K_5 \dot{\phi} + K_6 \ddot{\phi} \right] \qquad (7\text{-}5)$$

The coefficients of these equations may be arranged in a determinantal array as shown on Table 7-1.

A block diagram may be constructed directly from this Δ, then manipulated using the methods indicated in Section 5, or some preliminary algebraic manipulations may be used to define transfer functions. Using the latter scheme, each row is divided by the entry in the main diagonal of that row, providing a new determinantal array (Equation 7-7) shown as Table 7-2 and 7-2a.

The standard block diagram may be drawn from Equation 7-7, and inspection of the diagram indicates that a rearrangement of

FIGURE 7-2

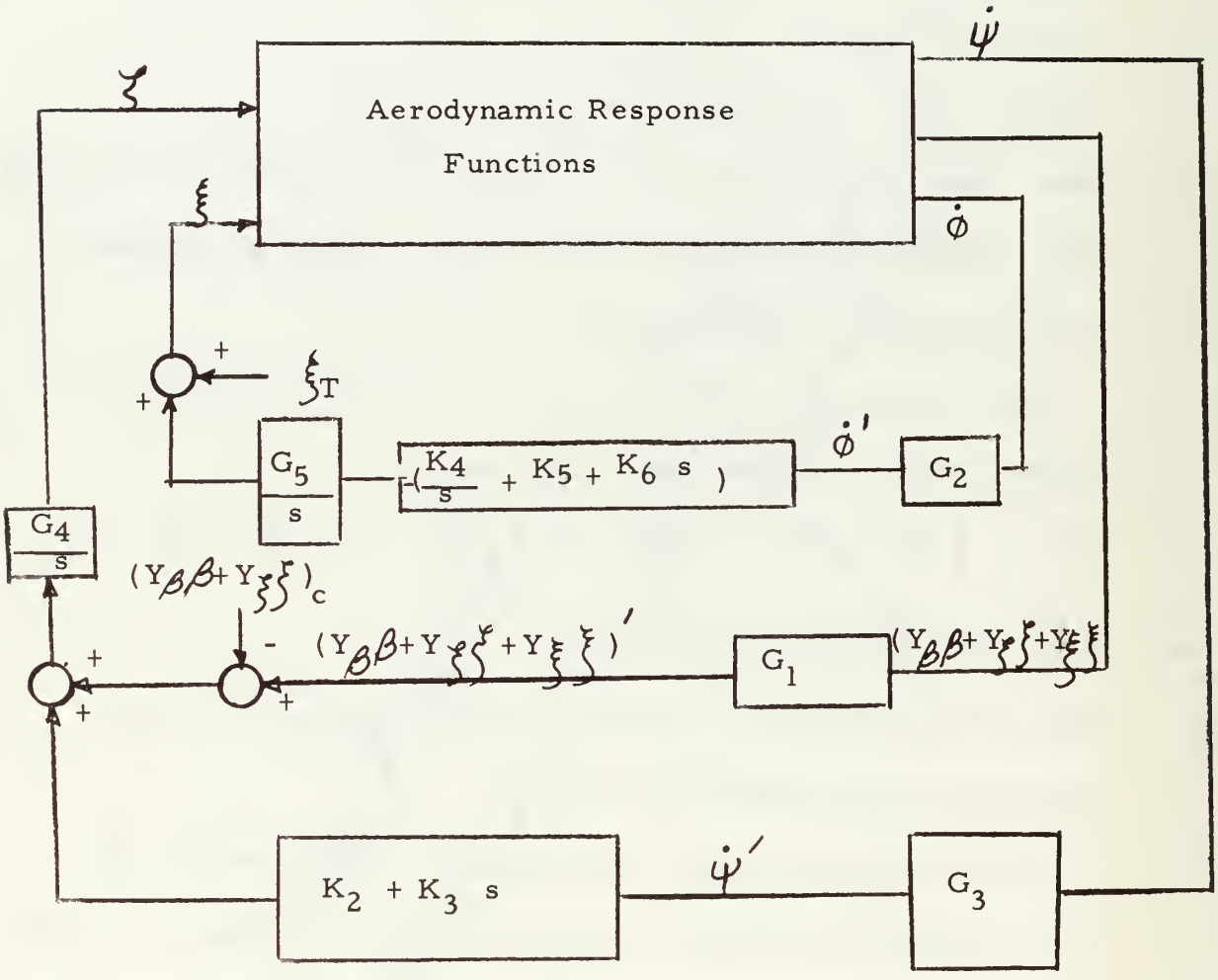

Where i K_2, K_3, K_4, K_5, K_6 = gain constants G_1, G_2, G_3, G_4, G_5, = transfer function of the form

$$G_n = \frac{W_n^2}{s^2 + 2\zeta W_n s + W_n^2}$$

TABLE 7-1

$\Delta =$

β	$\dot{\psi}$	$\dot{\phi}$	ζ	ξ
$s - Y_\beta$	$\cos \alpha_o$	$- \sin \alpha_o$	$- Y_\zeta$	$- Y_\xi$
$- N_\beta$	s	0	$- N_\zeta$	$- N_\xi$
$- L_\beta$	0	$s - L_p$	$- L_\zeta$	$- L_\xi$
0	0	$\dfrac{(Ko\, s^2 + K_5\, s + Ky)}{s^2}$	0	1
$- K_1 Y_\beta$	$- (K_3 s + K_2)$	0	$s - K_1 Y_\zeta$	$- K_1 Y_\xi$

Equation (7-6)

ζ		$\dot{\psi}$		β		ϕ		ξ	
1	0	$\frac{-(K_3 s + K_2)}{(s - K_1 Y_\zeta)}$	0	$-\frac{(K_1 Y_\beta)}{(s - K_1 Y_\zeta)}$	0	0	0	$\frac{-(K_1 Y_\xi)}{(s - K_1 Y_\zeta)}$	0
-1	1	0	0	0	0	0	0	0	0
0	$-\frac{N_\zeta}{s}$	1	0	$\frac{-N_\beta}{s}$	0	0	0	$\frac{-N_\xi}{s}$	0
0	0	-1	1	0	0	0	0	0	0
0	$\frac{-Y_\zeta}{(s - Y_\beta)}$	0	$\frac{+\cos\alpha_o}{(s - Y_\beta)}$	1	0	$\frac{-\sin\alpha_o}{(s - Y_\beta)}$	0	$\frac{-Y_\xi}{(s - Y_\beta)}$	0
0	0	0	0	-1	1	0	0	0	0
0	$\frac{-L_\zeta}{s - L_p}$	0	-0	0	$\frac{-L_\beta}{s - L_p}$	1	0	$\frac{-L_\xi}{s - L_p}$	0
0	0	0	0	0	0	-1	1	0	0
0	0	0	0	0	0	0	$+\frac{(K_6 s^2 + K_5 s + K_4)}{s^2}$	1	0
0	0	0	0	0	0	0	0	-1	1

TABLE 7-2 Equation (7-7)

Where the performance functions of Section 5 are defined as:

$$\frac{\zeta}{\dot{\psi}} = \frac{(K_3 s + K_2)}{(s - K_1 Y_\zeta)} \qquad \frac{\beta}{\zeta} = \frac{Y_\zeta}{(s - Y_\beta)} \qquad \frac{\dot{\phi}}{\xi} = \frac{L_\xi}{(s - Lp)}$$

$$\frac{\zeta}{\beta} = \frac{K_1 Y_\beta}{(s - K_1 Y_\zeta)} \qquad \frac{\beta}{\dot{\psi}} = \frac{-\cos \alpha_o}{(s - Y_\beta)} \frac{\xi}{\phi} \qquad \frac{(-K_6 s^2 + K_5 s K_4)}{s^2}$$

$$\frac{\zeta}{\xi} \qquad \frac{K_1 Y_\xi}{(s - K_1 Y_\zeta)} \qquad \frac{\beta}{\phi} = \frac{\sin \alpha_o}{(s - Y_\beta)}$$

$$\frac{\dot{\psi}}{\zeta} = \frac{N_\zeta}{s} \qquad \frac{\beta}{\xi} = \frac{Y \dot{\xi}}{(s - Y_\beta)}$$

$$\frac{\dot{\psi}}{\beta} = \frac{N_\beta}{s} \qquad \frac{\dot{\phi}}{\zeta} = \frac{L_\zeta}{(s - Lp)}$$

$$\frac{\dot{\psi}}{\xi} = \frac{N_\xi}{s} \qquad \frac{\dot{\phi}}{\beta} = \frac{L_\beta}{(s - Lp)}$$

TABLE 7-2a

nodes and blocks can produce a separation of the roll and yaw subsystems. If this is done the block diagram takes the standard form shown in Fig. 7.3. Note that the yaw and roll subsystems are clearly separated, and that specific blocks are obviously representative of cross-coupling effects. A load disturbance ξ_T is indicated, and a command input is also shown as $(Y_\beta \beta + Y_\xi \xi)c$. The input block PFa is defined as

$$\frac{\xi}{(Y_\beta \beta + Y_\xi \xi)c} = \frac{-K_1}{s - K_1 Y_\xi} \triangleq PFa$$

It can be noted for a simple missile, various cross coupling terms are zero at zero angle of attack in the asymmetric system

$$\frac{K_1 Y_\xi}{(s - K_1 Y_\xi)} = \frac{N_\xi}{s} = \frac{Y_\xi}{(s - Y_\beta)} = \frac{L_\zeta}{(s - Lp)} = 0 \qquad (7\text{-}8)$$

and since $\alpha_o = 0$, then $\sin \alpha_o = 0$

$$\frac{\sin \alpha_o}{(s - Y_\beta)} = 0$$

Examining Fig. 7-3, and noting the zero blocks resulting from Equation 7-8, the standard determinant can be formed as shown in Equation 7-9. (Table 7-3)

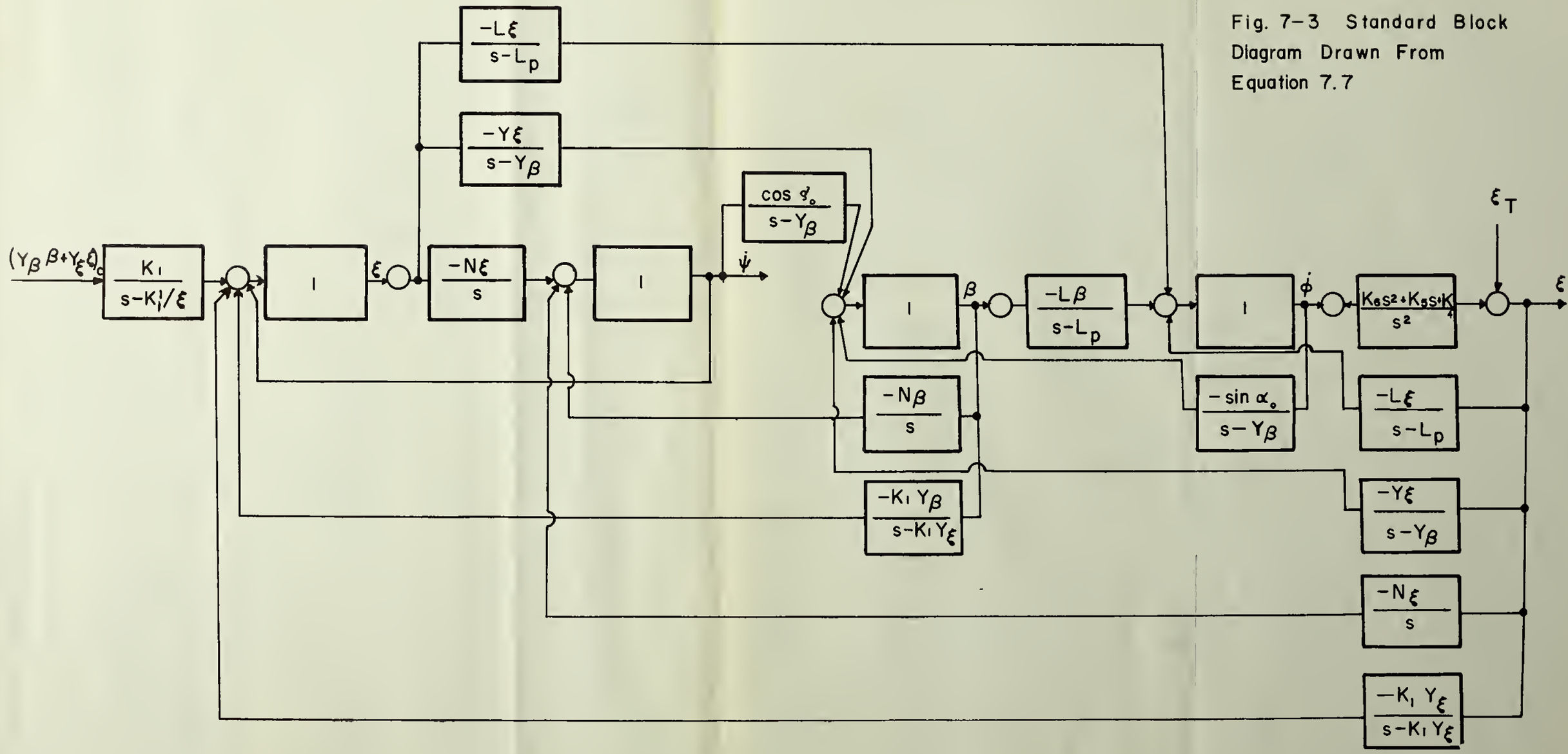

Fig. 7-3 Standard Block Diagram Drawn From Equation 7.7

Yaw Subsystem			Roll to yaw couplings	
1	$\frac{-K_3 s+K_2}{(s-K_1 Y_\zeta)}$	$\frac{-K_1 Y_\beta}{(s-K_1 Y_\zeta)}$	0	0
$\frac{-N_\zeta}{s}$	1	$\frac{-N_\beta}{s}$	0	0
$\frac{-Y_\zeta}{(s-Y_\beta)}$	$\frac{1}{(s-Y_\beta)}$	1	0	0
0	0	0	1	$\frac{-L_\zeta}{(s-Lp)}$
0	0	0	$\frac{K_6 s^2+K_5 s+K_4}{s^2}$	1
Yaw to roll couplings			Roll subsystem	

TABLE 7-3 Equation 7-9

Therefore, the selection of input nodes in the order of $\zeta, \dot{\psi}, \beta, \dot{\phi}$ and ξ has allowed the formation of a yaw and roll subsystem. The array clearly shows the two subsystems and the two attendant cross coupling areas.

Specifications for dynamic response of simple missiles is often most rigid at the zero angle of attack condition. It can be noted from Equation 7-9 that compensation can be made separately in the two subsystems. After these specifications for zero angle of attack are met, the cross coupling consideration may be brought into the problem to check design requirement at other angles of attack.

It is evident that this resultant block diagram is in a form which conveys a maximum amount of information to the designer. With proper manipulations the design of a well controlled aircraft or missile becomes a much simpler problem.

No attempt is made here to apply the results just obtained. The purpose of this section was to indicate how the block diagram, determinant technique can be applied to the simplification of complex airframe control problems. It is felt that the preceding considerations have accomplished this.

8. THE GENERATION OF COMPLEX ZEROS

8.1 Introduction

Any closed loop system which can be represented by a block diagram has a characteristic equation which may always be manipulated into the form

$$\frac{K \prod_{i=1}^{n} (s + Z_i)}{s^m \prod_{j=1}^{n} (s + p_j)} G_c = -1 \qquad (8\text{-}1)$$

Where, $0 < K < \infty$, $-\infty < m < \infty$, and the z_i and p_j may be real and/or complex. K is assumed to represent a variable gain element of the system. G_c represents the transfer function of a compensator which may be in any single feed forward or feedback path, or may be cascaded in the main transmission channel. G_c is of the form

$$G_c = \frac{K_c \prod_{i=1}^{n} (s + Z_i)}{s^m \prod_{j=1}^{n} (s + p_j)} \qquad (8\text{-}2)$$

The definitions of the terms in Equation 8-2 are the same as Equation 8-1. The total gain of Equation 8.1 is then

$$K_{RL} = KK_c \qquad (8\text{-}3)$$

The selection of a transfer function for G_c, besides being based upon physical realizability is guided by the desire to force the roots of the characteristic equation to lie in such locations on the s-plane that the

transient response of the system to be compensated will meet specifications without affecting steady state accuracy. Steady state accuracy specifications are normally met before compensation by setting system gain to obtain an acceptable steady state error coefficient. However, it is conceivable that compensation could be required to meet steady state specifications.

It is common practice to select two complex conjugate root locations and then to choose G_c so that the two selected locations will be roots of the characteristic equation. Generally, it is hoped that the selected roots will prove to be dominant, but a certain amount of experience and foresight is required in order to ensure that this end will be attained. Even with experience, some trial and error is frequently involved. In any case, only calculation of the transient response will determine whether or not a particular solution is acceptable. The concept of dominance states that if the residues at certain roots of the characteristic equation are large compared to the residues at all other roots, and if the real parts of those certain roots are several times smaller than the real parts of any other roots, then those certain roots are dominant. A transient response calculated using only the dominant roots will be sufficiently accurate for engineering purposes. All roots must be included however when calculating the phase angle of the transient response. Note that this concept may significantly reduce the labor involved in calculating the transient response of higher order systems.

The common use of passive networks to effect compensation is with G_c containing only negative real poles and zeros, and usually with $K_c < 1$. It is possible to generate complex poles or zeros with passive networks, but it is difficult to use these networks practically due to large attenuation in the compensator and extreme sensitivity of the complex pole or zero location to variations of components within the network. In some cases an additional amplifier is required to correct for the attenuation of a passive compensator, so the compensator could have been designed as an active compensator from the start.

The terms "active network" and "active compensator" are interchangeable and refer to networks which contain passive components, a summer, and one or two amplifiers.

Frequently, complex poles and/or complex zeros are present in a system before compensation is attempted. Having networks available to use as compensators which will produce complex poles or zeros will in some instance make the compensation problem easier. The active networks investigated in this report are flexible in that the complex poles or zeros resulting from them may be relocated on the s-plane by varying either an amplifier gain or the magnitude of one or more of the passive elements in the network.

The passive networks, which are essential to active compensators, may be either RC or RL networks. However, RL networks pose some problems due to difficulties in determining and allowing for the resistance of the inductive elements.

Active compensation is not envisioned as replacing passive compensation, but rather as supplementing it by providing solutions to compensation problems not easily attainable with passive compensators alone. In some instances it may prove desirable to combine active and passive compensators to achieve desired results.

Two major disadvantages of active compensators are cost and complexity. Both of these factors arise from the fact that amplifiers and summers are required as parts of the compensator.

The passive networks, their transfer functions, and s-plane pole-zero arrays which will be used as basic components in the active networks are depicted in Fig. 8.1. They are held to simple configurations primarily to provide attainable goals for this investigation. In addition, all compensation problems attempted could be solved using compensators which required only these simple networks. The transfer function of Fig. 8.1 are defined on Table 8-1 for algebraic manipulation.

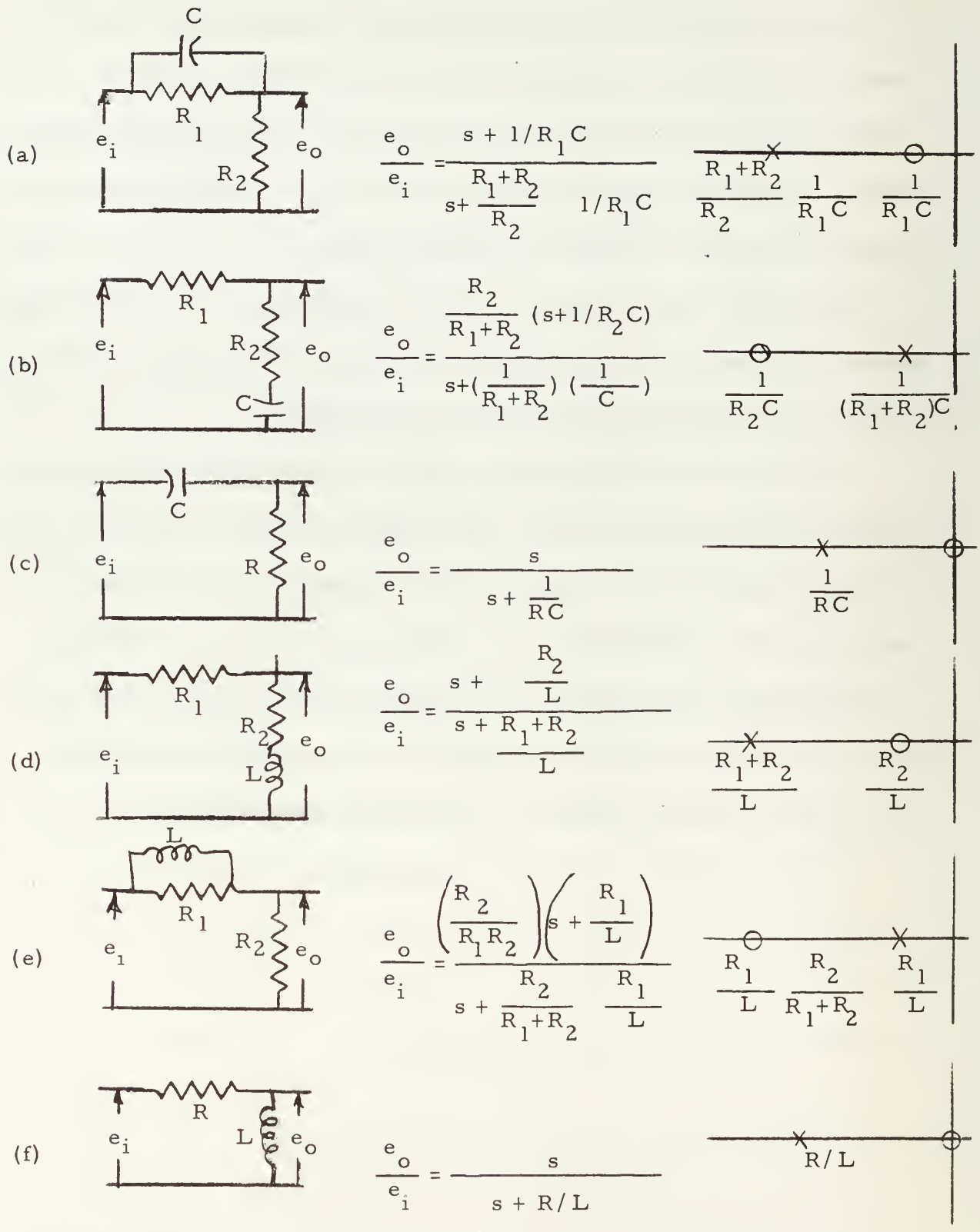

Fig. 8.1 Networks, transfer functions, and s-planes of passive networks used. The network of Fig. 8.1 (c) cannot ordinarily be used in the main transmission path unless there exists a parallel forward path through which dc components may pass.

TABLE 8-1

$\dfrac{s + \dfrac{1}{R_1 C}}{s + \dfrac{R_1+R_2}{R_2}\ \dfrac{1}{R_1 C}}$	$\triangleq$	$\dfrac{s + Z_d}{s + p_d}$
$\dfrac{\dfrac{R_2}{R_1+R_2}\left(s + \dfrac{1}{R_2 C}\right)}{s + \dfrac{1}{(R_1+R_2)\,C}}$	$\triangleq$	$\dfrac{\alpha(s + Z_g)}{(s + p_g)}$
$\dfrac{s}{1 + \dfrac{1}{RC}}$	$\triangleq$	$\dfrac{s}{s + Z_d}$
$\dfrac{s + \dfrac{R_2}{L}}{s + \dfrac{R_1 + R_2}{L}}$	$\triangleq$	$\dfrac{s + Z_d}{s + p_d}$
$\dfrac{\dfrac{R_2}{R_1+R_2}\left(s + \dfrac{R_1}{L}\right)}{s + \dfrac{R_2}{R_1+R_2}\ \dfrac{R_1}{L}}$	$\triangleq$	$\dfrac{\alpha(s + Z_g)}{(s + p_g)}$
$\dfrac{s}{s + R/L}$	$\triangleq$	$\dfrac{s}{s + p_d}$

Definitions of the transfer functions of Fig. 8-1 for algebraic manipulation. The subscript d refers to poles or zeros resulting from a lead network. The subscript g refers to poles or zeros resulting from a lag network.

8.2 Investigation of Some Active Networks

Not all active networks will yield complex poles or zeros. It is therefore necessary to investigate several combinations of amplifiers, summers, and passive networks to determine some of the configurations which will produce the desired complex poles and zeros.

Two basic network configurations, one a parallel feed forward and the other a feedback, were selected for investigation. Solutions were obtained by placing a lag or a lead transfer function and amplifier in each path available. The overall transfer function of the network was then determined and investigated for the existence of complex poles or zeros.

Fifteen different networks were investigated using this plan. Some were unsuccessful in that they did not yield the desired complex poles and zeros. Only those producing the desired result are treated here. There are, undoubtedly other simple active networks which will produce complex poles and zeros.

Lead-lead feed forward difference compensator

Fig. 8.2 is the block diagram of this compensator. The transfer function of Fig. 8.2 is

$$\frac{V_o}{V_i} = \frac{A_1 (s + z_{d1}) (s + p_{d2}) - A_2 (s + z_{d2}) (s + p_{d1})}{(s + p_{d1}) (s + p_{d2})} \qquad (8\text{-}4)$$

For factoring by root locus, the numerator of Equation 8-4 may be

manipulated into the form

$$\frac{A_1 (s + z_{d1}) (s + p_{d2})}{A_2 (s + z_{d2}) (s + p_{d1})} = 1 \qquad (8\text{-}5)$$

Note that Equation 8-5 is a zero degree root locus. The possible root loci arising from Equation 8-5 are Figs. 8.3, 8.4, 8.5, and 8.6. It can be seen from Figs. 8.5 and 8.6 that complex roots of Equation 8-5 will obtain for certain values of $\frac{A_1}{A_2}$. These complex roots will become complex zeros in Equation 8-4 and result in Equation 8-4 having the form

$$\frac{V_o}{V_i} = \frac{(A_1 - A_2) (s + \sigma + j\omega) (s + \sigma - j\omega)}{(s + p_{d1}) (s + p_{d2})} \qquad (8\text{-}6)$$

This transfer function is of further interest because p_{d1} and p_{d2}, the real poles, may be placed far out in the left half plane if desired.

There can be no complex root resulting from the root loci of Figs. 8.5 or 8.6. Therefore they are of no further interest in this investigation.

Lead-lead negative feedback compensator.

Fig 8.7 is the block diagram of this compensator. The transfer function of Fig. 8.7 is

$$\frac{V_o}{V_i} = \frac{(s + z_{d1}) (s + p_{d2})}{(s + p_{d1}) (s + p_{d2}) + A_1 (s + z_{d1}) (s + z_{d2})} \qquad (8\text{-}7)$$

For factoring by root locus, the denominator of Equation 8-7 may be manipulated into the form

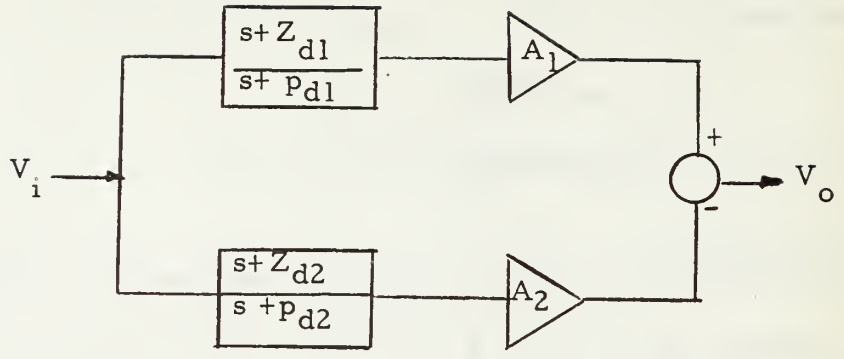

Fig. 8.2 Block diagram of the lead-lead feed forward difference compensator.

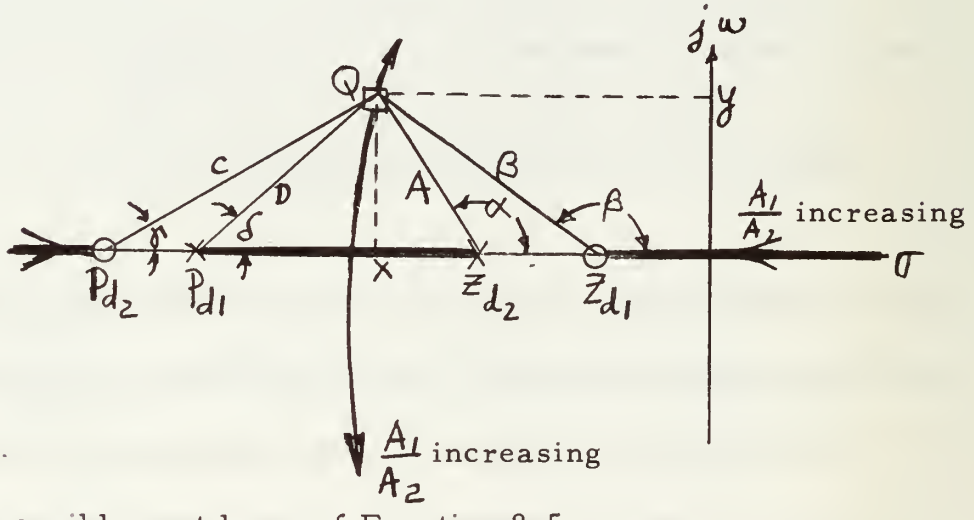

Fig. 8.3 A possible root locus of Equation 8-5.

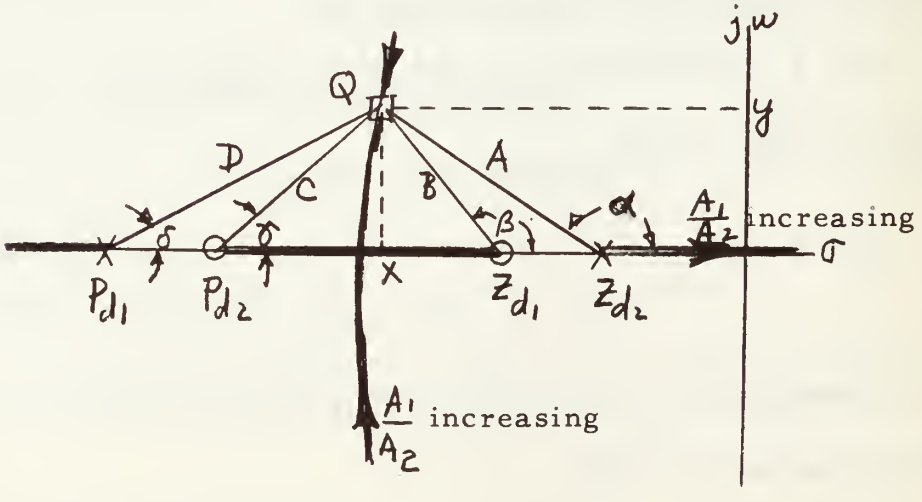

Fig. 8.4 A possible root locus of Equation 8-5.

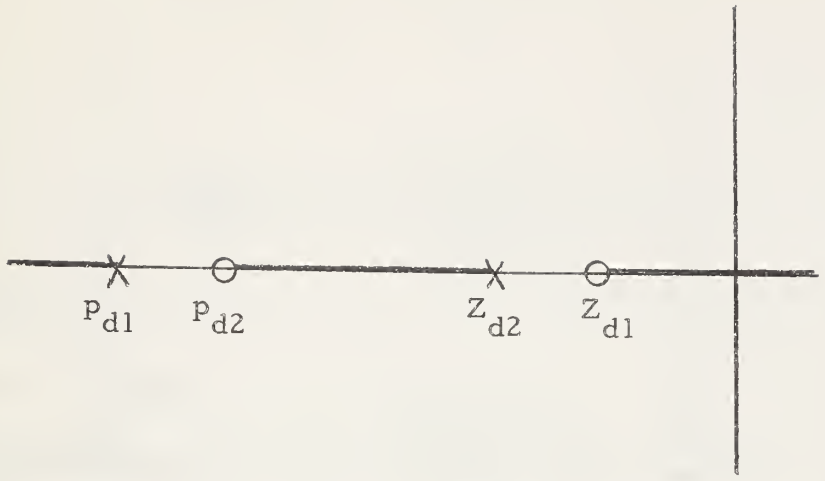

Fig. 8.5 A possible root locus of Equation 8-5.

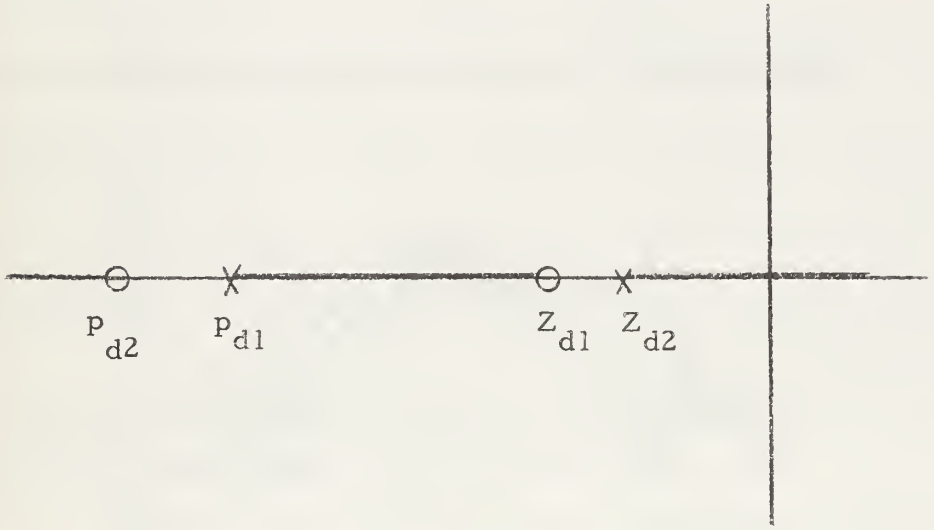

Fig. 8.6 A possible root locus of Equation 8-5.

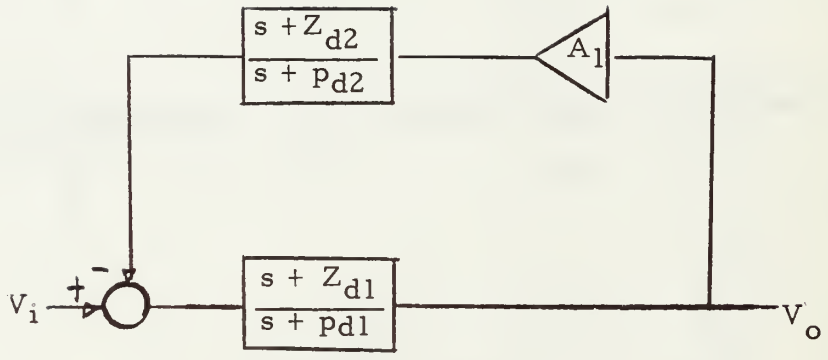

Fig. 8.7 Block diagram of the lead-lead negative feedback compensator.

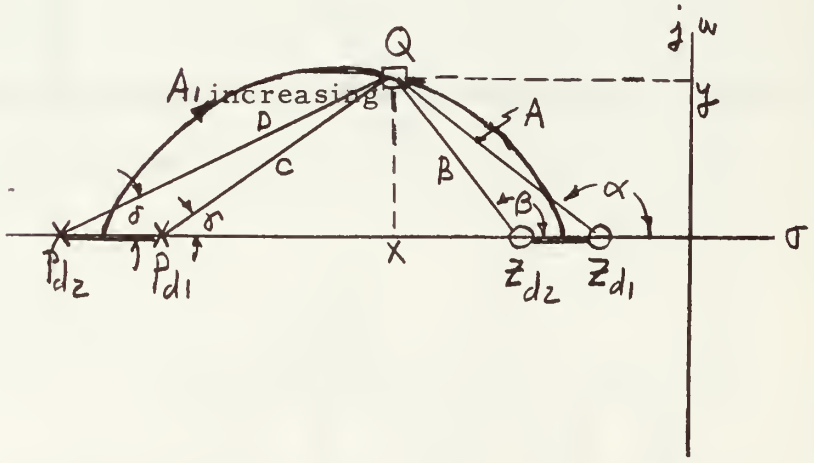

Fig. 8.8 A possible root locus of Equation 8-8.

$$\frac{A_1 (s + z_{d1}) (s + z_{d2})}{(s + p_{d1}) (s + p_{d2})} = - 1 \qquad (8\text{-}8)$$

Fig. 8.8 is the root locus of Equation 8-8. Any locations of p_{d1}, p_{d2}, z_{d1}, or z_{d2} will produce the locus of Fig. 8.8 unless $|z_{d2}| > |p_{d1}|$ or $|z_{d1}| > |p_{d2}|$. The complex roots which obtain for certain values of A_1 will become complex poles in Equation 8-7 and result in that equation having the form

$$\frac{V_o}{V_i} = \frac{(s + z_{d1}) (s + p_{d2})}{(A_1 + 1) (s + \sigma + j\omega) (s + \sigma - j\omega)} \qquad (8\text{-}9)$$

This transfer function is of further interest because one of the real zeros of Equation 8-9 may be placed close to the origin while the other may be placed as far out in the left half plane as desired. Note from Fig. 8.8 that the complex poles will always be in the left half s-plane.

Lag-lag feed forward difference compensator.

Fig. 8.9 is the block diagram of this compensator. The transfer function of Fig. 8.9 is

$$\frac{V_o}{V_i} = \frac{A_1 \alpha_1 (s + Z_{g1}) (s + p_{g2}) - A_2 \alpha_2 (s + Z_{g2}) (s + p_{g1})}{(s + p_g) (s + p_{g2})} \qquad (8\text{-}10)$$

For factoring by root locus, the numerator of Equation 8-10 may be manipulated into the form

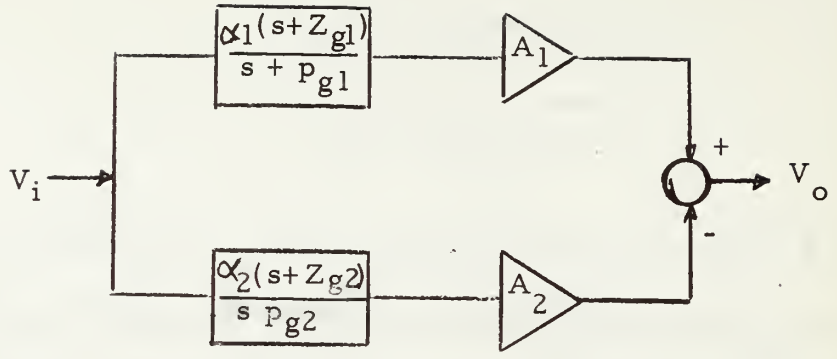

Fig. 8.9 Block diagram of the lag-lag feed forward difference compensator.

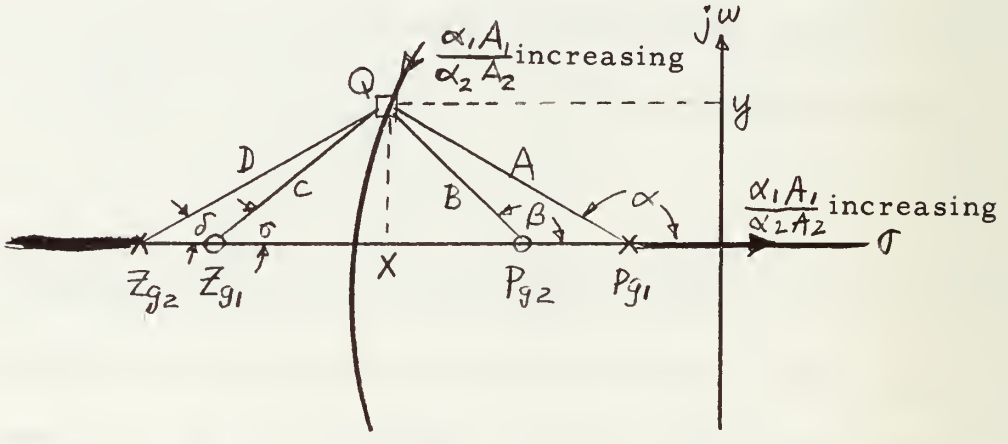

Fig. 8.10 A possible root locus of Equation 8-11.

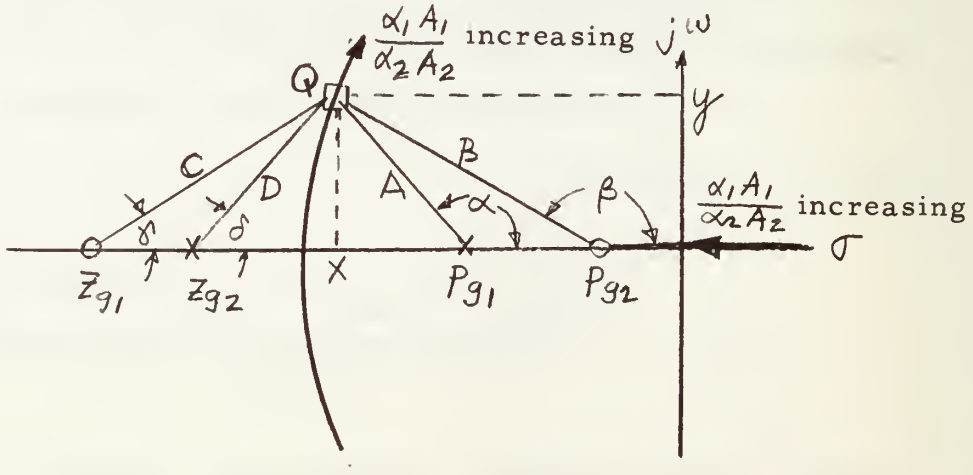

Fig. 8.11 A possible root locus of Equation 8-11.

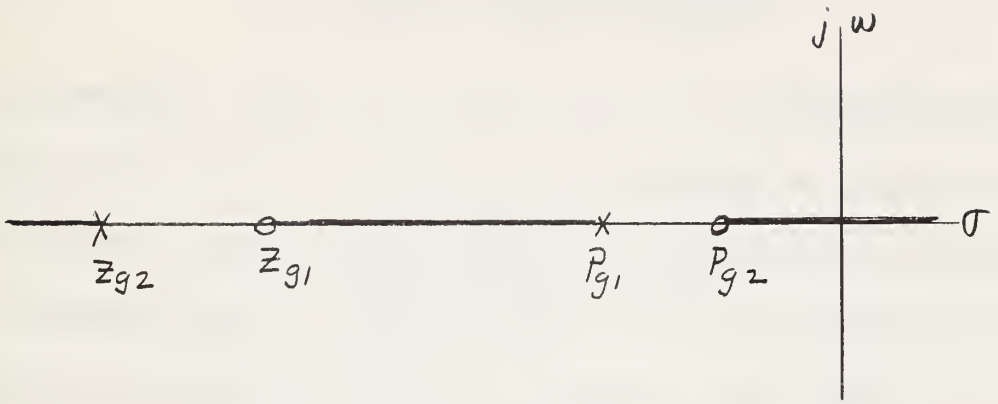

Fig. 8.12 A possible root locus of Equation 8-11.

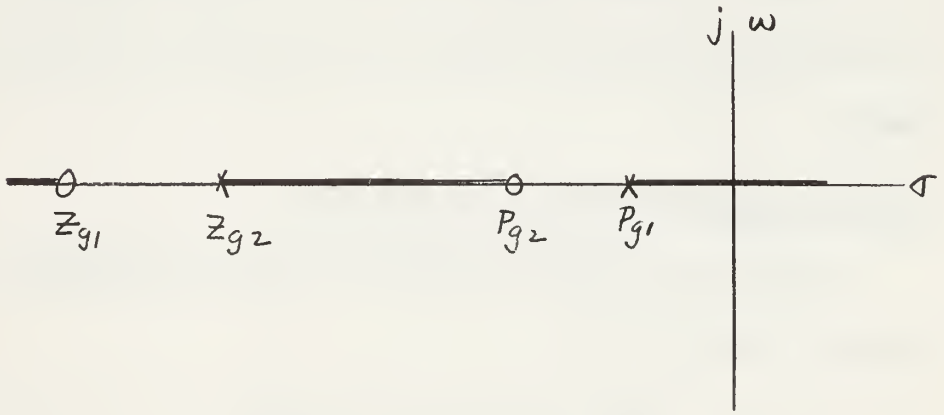

Fig. 8.13 A possible root locus of Equation 8-11.

$$\frac{A_1 \alpha_1 (s + z_{g1})(s + p_{g2})}{A_2 \alpha_2 (s + z_{g2})(s + p_{g1})} = 1 \qquad (8\text{-}11)$$

Note that Equation 8-11 is a zero degree root locus. The possible root loci arising from Equation 8-11 are Figs. 8.10, 8.11, 8.12, and 8.13. It can be seen from Figs. 8.10 and 8.11 that complex roots of Equation 8-11 will obtain for certain values of $\frac{A_1 \alpha_1}{A_2 \alpha_2}$. These complex roots will become complex zeros in Equation 8-10 and will result in the equation having the form

$$\frac{V_o}{V_i} = \frac{(A_1 \alpha_1 - A_2 \alpha_2)(s + \sigma + j\omega)(s + \sigma - j\omega)}{(s + p_{g1})(s + p_{g2})} \qquad (8\text{-}12)$$

This transfer function is of further interest because p_{g1}, and p_{g2}, the real poles of Equation 8-12, may be placed fairly close to the origin in the left hand s-plane.

There can be no complex roots resulting from the root loci of Figs. 8.12 and 8.13. Therefore they are of no further interest in this investigation.

Lag-lag negative feedback compensator.

Fig. 8.14 is the block diagram of this compensator. The transfer function of Fig. 8.14 is

$$\frac{V_o}{V_i} = \frac{\alpha_1 (s + z_{g1})(s + p_{g2})}{(s + p_{g1})(s + p_{g2}) + A_1 \alpha_1 \alpha_2 (s + z_{g1})(s + z_{g2})} \qquad (8\text{-}13)$$

For factoring by root locus, the denominator of Equation 8-13 may be manipulated into the form

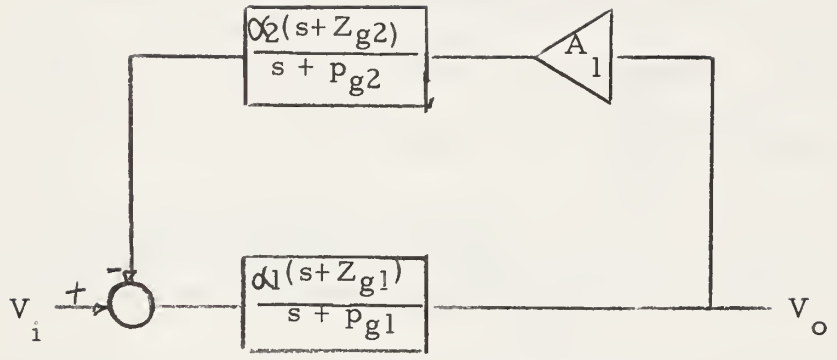

Fig. 8.14 Block diagram of the lag-lag negative feedback compensator.

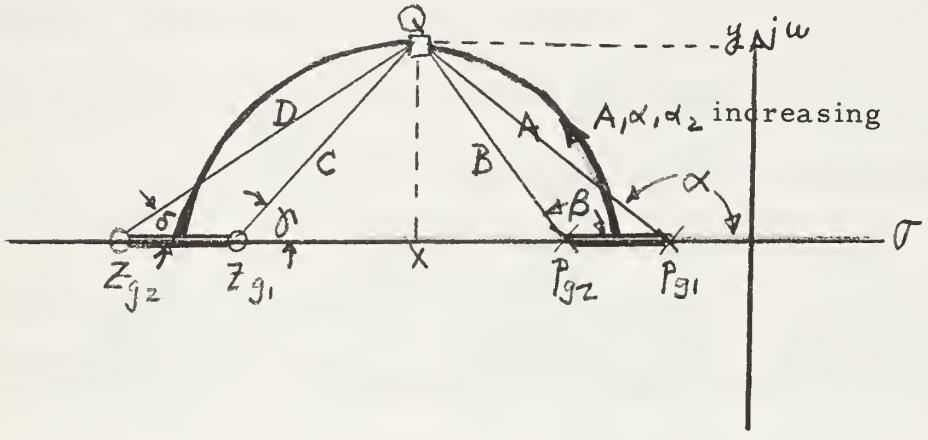

Fig. 8.15 A possible root locus of Equation 8-14.

$$\frac{A_1 \alpha_1 \alpha_2 (s + z_{g1}) (s + z_{g2})}{(s + p_{g1}) (s + p_{g2})} = - 1 \qquad (8\text{-}14)$$

The root locus of Equation 8-14 is Fig. 8.15. It can be seen from Fig. 8.15 that complex roots of Equation 8-14 will obtain for certain values of $A_1 \alpha_1 \alpha_2$. These complex roots will become complex poles in Equation 8-13 and will result in that equation having the form

$$\frac{V_o}{V_i} = \frac{\alpha_1 (s + z_{g1}) (s + p_{g2})}{A_1 \alpha_1 \alpha_2 + 1) (s + \sigma + j\omega) (s + \sigma - j\omega)} \qquad (8\text{-}15)$$

This transfer function is of further interest because one of the real zeros of Equation 8-15 may be placed near the origin while the other may be as far out in the left hand s-plane as desired. The complex poles will always be in the left hand s-plane.

Note that Fig. 8.15 will be the root locus of Equation 8-14 unless $|p_{g2}| > |z_{g1}|$ or $|p_{g1}| > |z_{g2}|$. In neither of these cases could complex roots be obtained from Equation 8-14. They are therefore of no interest in this investigation.

Lag-lead feed forward summing compensator.

The block diagram of this compensator is Fig. 8.16. The transfer function of Fig. 8.16 is

$$\frac{V_o}{V_i} = \frac{A_1 \alpha (s + z_g) (s + p_d) + A_2 (s + z_d) (s + p_g)}{(s + p_d) (s + p_g)} \qquad (8\text{-}16)$$

For factoring by root locus, the numerator of Equation 8-16 may be manipulated into the form

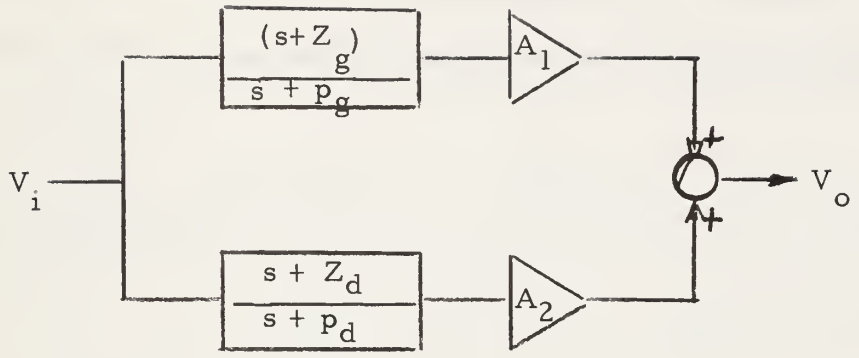

Fig. 8.16 Block diagram of lag-lead feed forward summing compensator.

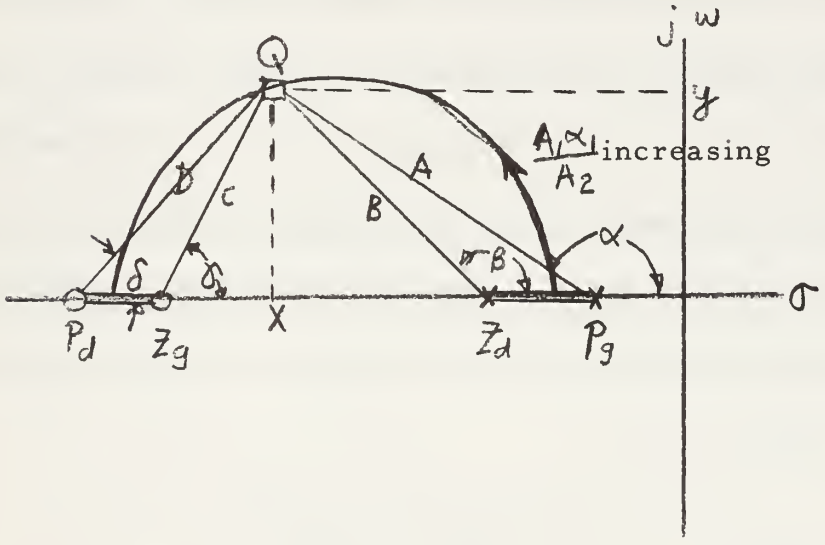

Fig. 8.17 A possible root locus of Equation 8-17.

$$\frac{A_1 \alpha (s + z_g)(s + p_d)}{A_2 (s + z_d)(s + p_g)} = -1 \qquad (8\text{-}17)$$

Fig. 8.17 is the root locus of Equation 8-17. It can be seen by inspection of Fig. 8.17 that complex roots will obtain for certain values of $\frac{A_1 \alpha}{A_2}$ so long as $|z_g| > |z_d|$ and $|p_d| > |p_g|$. These complex roots will become complex zeros in Equation 8-16 resulting in that equation having the form

$$\frac{V_o}{V_i} \qquad \frac{A_1 \alpha + A_2)(s + \sigma + j\omega)(s + \sigma - j\omega)}{(s + p_g)(s + p_d)} \qquad (8\text{-}18)$$

This transfer function is of further interest because one of the real poles of Equation 8-18 may be placed close to the origin in the left hand s-plane while the other may be placed as far out on the negative real axis as desired. The complex zeros will always be in the left hand s-plane.

Lag-lead positive feedback compensator; lag in the feedback path.

The block diagram of this compensator is Fig. 8.18. The transfer function of Fig. 8.18 is

$$\frac{V_o}{V_i} = \frac{(s + z_d)(s + p_g)}{(s + p_g)(s + p_d) - A_1 \alpha (s - z_g)(s + z_d)} \qquad (8\text{-}19)$$

For factoring by root locus, the denominator of Equation 8-19 can be manipulated into the form

$$\frac{A_1 \alpha (s + z_g)(s + z_d)}{(s + p_g)(s + p_d)} = 1 \qquad (8\text{-}20)$$

Note that Equation 8-20 is a zero degree root locus. Possible root loci resulting from Equation 8-20 are Figs. 8.19, 8.20, 8.21, and 8.22. It can be seen by inspection of Figs. 8.21 and 8.22 that complex roots of Equation 8-20 will obtain for certain values of $A_1 \alpha$. These complex roots will become complex poles in Equation 8-19 and result in that equation having the form

$$\frac{V_o}{V_i} = \frac{(s + z_d)(s + p_g)}{(1 - A_1\alpha)(s + \sigma + j\omega)(s + \sigma - j\omega)} \qquad (8\text{-}21)$$

This transfer function is of further interest because z_d and p_g, the real zeros of Equation 8-21 may be placed as close to the origin of the s-plane as desired. There can be no complex roots resulting from the root loci of Figs. 8.19 and 8.20. Therefore, they are of no further interest in this investigation.

Lag-lead positive feedback compensator; lead in the feedback path.

Fig. 8.23 is the block diagram of this compensator. The transfer function of Fig. 8.23 is

$$\frac{V_o}{V_i} = \frac{(s + z_g)(s + p_d)}{(s + p_g)(s + p_d) - A_1\alpha(s + z_d)(s + z_g)} \qquad (8\text{-}22)$$

For factoring by root locus, the denominator of Equation 8-22 may be manipulated into the form

$$\frac{A_1\alpha(s + z_d)(s + z_g)}{(s + p_d)(s + p_g)} = 1 \qquad (8\text{-}23)$$

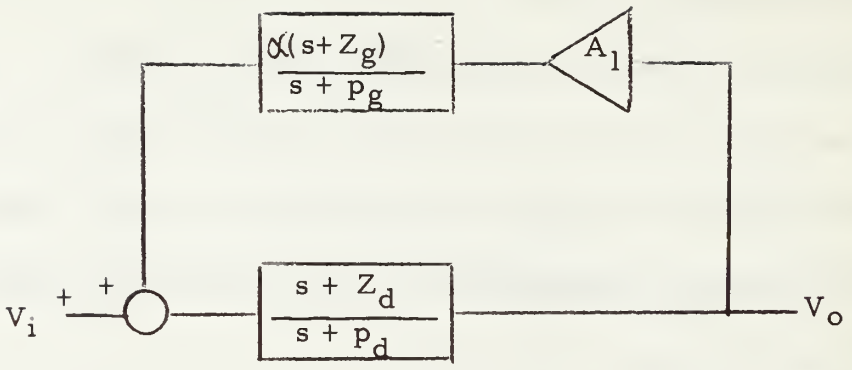

Fig. 8.18 Block diagram of the lag-lead positive feedback compensator. Lag in the feedback path.

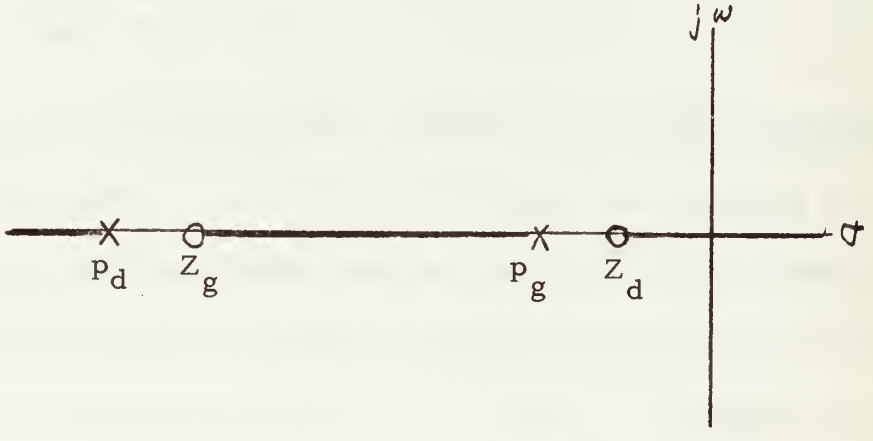

Fig. 8.19 A possible root locus of Equation 8-20.

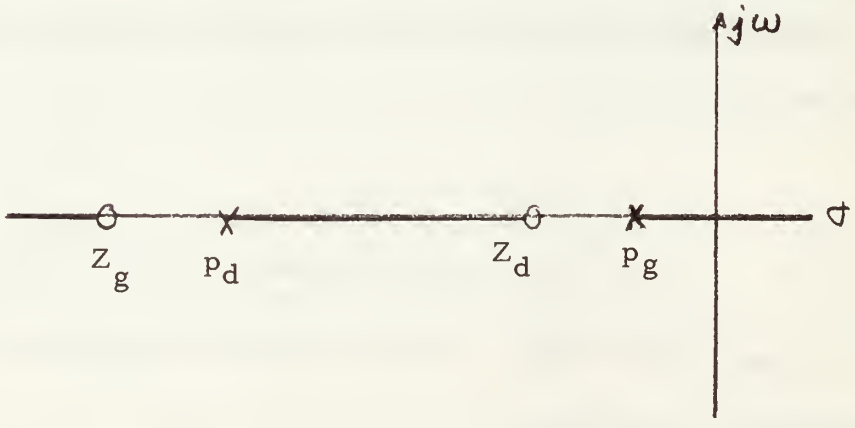

Fig. 8.20 A possible root locus of Equation 8-20.

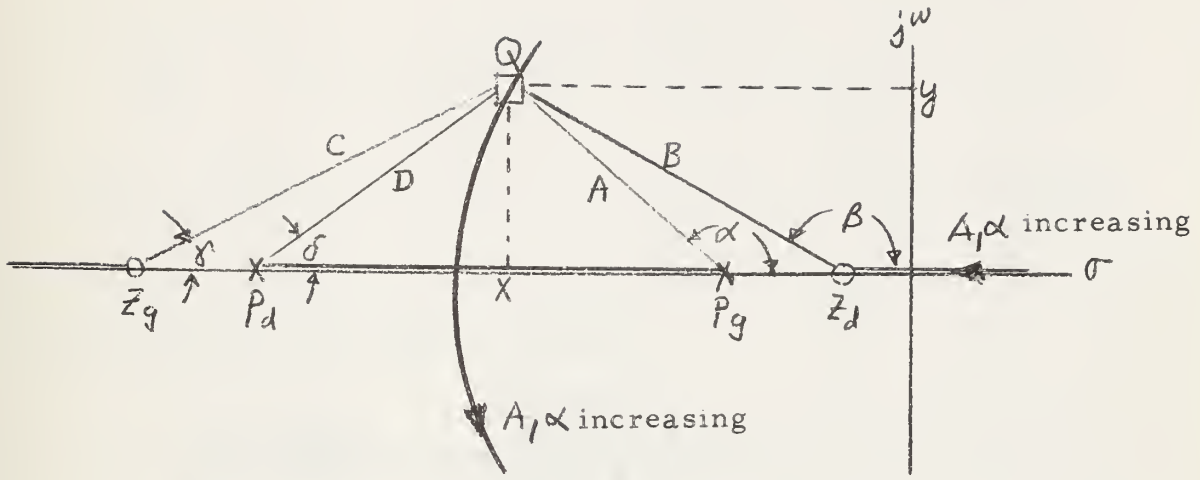

Fig. 8.21 A possible root locus of Equation 8-20.

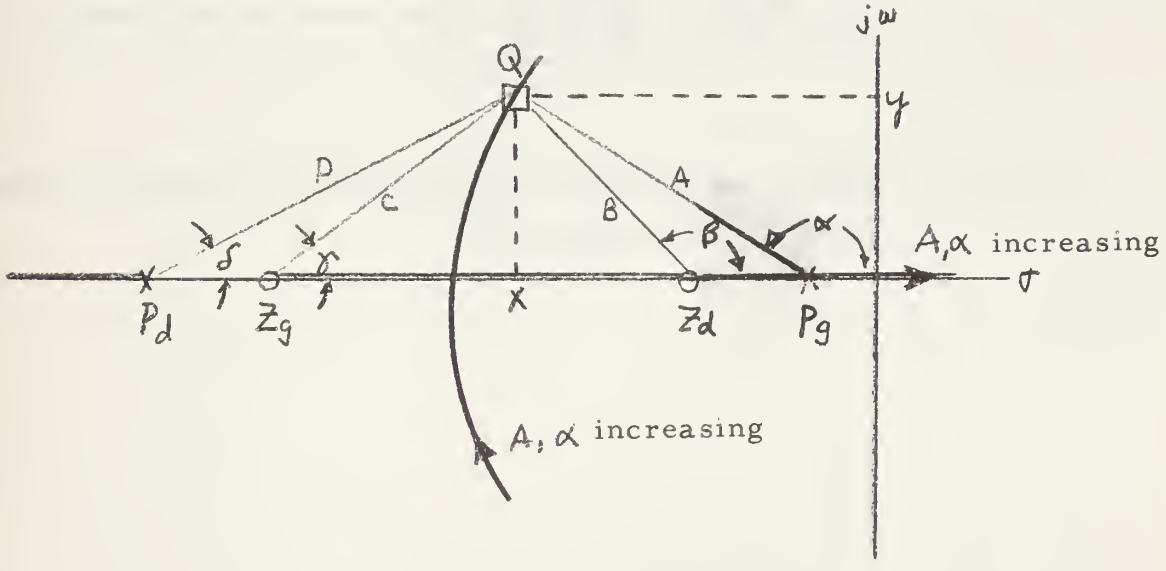

Fig. 8.22 A possible root locus of Equation 8-20.

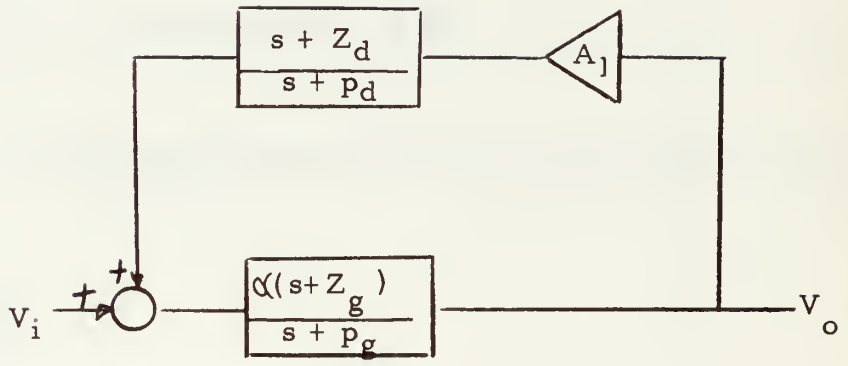

Fig. 8.23 Block diagram of the lag-lead positive feedback compensator. Lead in the feedback path.

Equation 8-23 is identical to Equation 8-20. Therefore the root loci of Equation 8-23 will be those of Figs. 8.19, 8.20, 8.21, and 8.22. Thus, Equation 8-22 will be of the form

$$\frac{V_o}{V_i} = \frac{(s + z_g)(s + p_d)}{(1 - A\alpha)(s + \sigma + j\omega)(s + \sigma - j\omega)} \qquad (8\text{-}24)$$

The same comments may be made for Equation 8-24 as for Equation 8-21 except that z_g and p_d, the real zeros of Equation 8-24 be placed far out in the left hand s-plane if desired.

8.3 Algebraic Equations for the Loci

The complex zeros generated by the active compensators all lie on circles. For some purposes the equations of these circles are of interest. The derivations are simple and are not given here. The results fall naturally into two sets of algebraically similar equations, which are listed in Tables 8-2 and 8-3.

COMPENSATOR	EQUATION OF THE ROOT LOCUS OF COMPLEX ZEROS
Lead-lead feed forward difference compensator	$\left[X+\frac{p_{d2}z_{d1}-p_{d1}z_{d2}}{z_{d2}-z_{d1}+p_{d1}-p_{d2}}\right]^2+y^2=\frac{p_{d1}p_{d2}(z_{d1}-z_{d2})+z_{d1}z_{d2}(p_{d2}-p_{d1})}{z_{d2}-z_{d1}+p_{d1}-p_{d2}}+\left[\frac{p_{d2}z_{d1}-p_{d1}z_{d2}}{z_{d2}-z_{d1}+p_{d1}-p_{d2}}\right]^2$
Lag-lag feed forward difference compensator	$\left[X+\frac{p_{g2}z_{g1}-p_{g1}z_{g2}}{z_{g2}-z_{g1}+p_{g1}-p_{g2}}\right]^2+y^2=\frac{p_{g1}p_{g2}(z_{g1}-z_{g2})+z_{g1}z_{g2}(p_{g2}-p_{g1}}{z_{g2}-z_{g1}+p_{g1}-p_{g2}}+\left[\frac{p_{g2}z_{g1}-p_{g1}z_{g2}}{z_{g2}-z_{g1}+p_{g1}-p_{g2}}\right]^2$
Lag-lead feed forward summing compensator	$\left[X+\frac{p_d z_g-p_g z_d}{-z_g+z_d+p_g-p_d}\right]^2+y^2=\frac{p_d p_g(z_g-z_d)+z_d z_g(p_d-p_g)}{z_d-z_g+p_g-p_d}+\left[\frac{p_d z_g-p_g z_d}{z_d-z_g+p_g-p_d}\right]^2$

TABLE 8-2

COMPENSATOR	EQUATION OF THE ROOT LOCUS OF COMPLEX POLES
Lead-lead negative feedback compensator	$\left[\sigma + \frac{p_{d1}\,p_{d2} - z_{d1}\,z_{d2}}{z_{d1} + z_{d2} - p_{d1} - p_{d2}}\right]^2 + y^2 = \frac{p_{d1}\,p_{d2}(z_{d1} + z_{d2}) - z_{d1}\,z_{d2}(p_{d1} + p_{d2})}{z_{d1} + z_{d2} - p_{d1} - p_{d2}} + \left[\frac{p_{d1}\,p_{d2} - z_{d1}\,z_{d2}}{z_{d1} + z_{d2} - p_{d1} - p_{d2}}\right]^2$
Lag-lag negative feedback compensator	$\left[\sigma + \frac{p_{g1}\,p_{g2} - z_{g1}\,z_{g2}}{z_{g1} + z_{g2} - p_{g1} - p_{g2}}\right]^2 + y^2 = \frac{p_{g1}\,p_{g2}(z_{g1} + z_{g2}) - z_{g1}\,z_{g2}(p_{g1} + p_{g2})}{z_{g1} + z_{g2} - p_{g1} - p_{g2}} + \left[\frac{p_{g1}\,p_{g2} - z_{g1}\,z_{g2}}{z_{g1} + z_{g2} - p_{g1} - p_{g2}}\right]^2$
Lag-lead positive feedback compensator	$\left[\sigma + \frac{p_d\,p_g - z_d\,z_g}{z_d + z_g - p_d - p_g}\right]^2 + y^2 = \frac{p_g\,p_d(z_d + z_g) - z_d\,z_g(p_d + p_g)}{z_d + z_g - p_d - p_g} + \left[\frac{p_d\,p_g - z_d\,z_g}{z_d + z_g - p_d - p_g}\right]^2$

TABLE 8-3

9. MANIPULATIONS AND DESIGN

9.1 Introduction

The equations of the root locus circles, while of definite interest, are not suitable to work with when designing active compensators. A convenient form may be obtained by manipulation of the equations of Table 8-2 and 8-3. For complex zeros the relationship of Table 8-2 may be manipulated into the form:

$$(Z_1 - Z_2 + p_2 - p_1)(x^2 + y^2) + 2x(Z_1 p_2 - Z_2 p_1) + p_1 p_2 (Z_1 - Z_2) + Z_1 Z_2 (p_2 - p_1) = 0 \tag{9-1}$$

for use in design. Table 9.1 gives the particular form of Equation 9-1 applicable to each of the complex zero producing compensators. It will be shown that four of the six variables in Equation 9-1 may be chosen to meet the needs of a specific problem. Equation 9-1 will then reduce to an equation in two unknowns which may be chosen so as to satisfy that equation and the requirement of physical realizability.

A significant simplification of Equation 9-1 occurs if:

$$\begin{aligned} Z_1 / p_1 &= Z_2 / p_2 \\ Z_1 p_2 &= Z_2 p_1 \triangleq K_1 \end{aligned} \tag{9-2}$$

Substituting Equation 9-2 into Equation 9-1 and simplifying yields

$$x^2 + y^2 = K_1 \tag{9-3}$$

Note that due to restrictions imposed by Equation 9-2, Equation 9-3 can be used only in those active compensators which contain two lag or two lead networks.

COMPENSATOR	WORKING EQUATION	NUMERATOR ROOT LOCUS EQUATION	REAL POLES	K_c
Lead-lead feed forward difference compensator	$(z_{d2} - z_{d1} + p_{d1} - p_{d2})(x^2 + y^2) + 2x(p_{d2} z_{d1} - p_{d1} z_{d2}) = p_{d1} p_{d2} (z_{d1} - z_{d2}) + z_{d1} z_{d2} (p_{d2} - p_{d1})$	$\frac{A_1(s + z_{d1})(s + p_{d2})}{A_2(s + z_{d2})(s + p_{d1})} = 1$	p_{d1}, p_{d2}	$(A_1 - A_2)$
Lag-lag feed forward difference compensator	$(z_{g2} - z_{g1} + p_{g1} - p_{g2})(x^2 + y^2) + 2x(p_{g2} z_{g1} - p_{g1} z_{g2}) = p_{g1} p_{g2} (z_{g1} - z_{g2}) + z_{g1} z_{g2} (p_{g2} - p_{g1})$	$\frac{A_1 \alpha_1 (s + z_{g1})(s + p_{g2})}{A_2 \alpha_2 (s + z_{g2})(s + p_{g1})} = 1$	p_{g1}, p_{g2}	$(A_1 \alpha_1 - A_2 \alpha_2)$
Lag-lead feed forward summing compensator	$(z_d - z_g + p_g - p_d)(x^2 + y^2) + 2x(p_d z_g - p_g z_d) = z_d z_g (p_d - p_g) + p_d p_g (z_g - z_d)$	$\frac{A_1 \alpha (s + z_g)(s + p_d)}{A_2 (s + z_d)(s + p_g)} = -1$	p_d, p_g	$(A_1 \alpha + A_2)$

TABLE 9.1

For complex poles, the equations of Table 8-2 may be manipulated into the form

$$(z_1 + z_2 - p_1 - p_2)(x^2 + y^2) + 2x(p_1 p_2 - z_1 z_2) +$$

$$z_1 z_2 (p_1 + p_2) - p_1 p_2 (z_1 + z_2) = 0$$

for use in design. Table 9-2 gives the particular form of Equation 9-4 applicable to each of the complex pole producing compensators. It will be shown that four of the six variables in Equation 9-4 may be chosen to meet the needs of a specific problem. Equation 9-4 will then reduce to an equation in two unknowns which may be chosen so as to satisfy that equation and the requirement of physical realizability.

A significant simplification of Equation 9-4 occurs if

$$z_1 z_2 = p_1 p_2 \triangleq K_2 \tag{9-5}$$

Substituting Equation 9-5 into Equation 9-4 and simplifying yields

$$x^2 + y^2 = K_2 \tag{9-6}$$

Note that due to restrictions imposed by Equation 9-5, Equation 9-6 can be used only in those active compensators which contain a lag and a lead network.

COMPENSATOR	WORKING EQUATION	DENOMINATOR ROOT LOCUS EQUATION	REAL ZEROS	K_c
Lead-lead negative feedback compensator	$(z_{d1} + z_{d2} - p_{d1} - p_{d2})(x^2 + y^2) + 2x(p_{d1} p_{d2} - z_{d1} z_{d2} = p_{d1} p_{d2}(z_{d1} + z_{d2}) - z_{d1} z_{d2}(p_{d1} + p_{d2})$	$\frac{A_1 (s+z_{d1})(s+z_{d2})}{(s+p_{d1})(s+p_{d2})} = -1$	z_{d1}, p_{d2}	$\frac{1}{1 + A_1}$
Lag-lag negative feedback compensator	$(z_{g1} + z_{g2} - p_{g1} - p_{g2})(x^2 + y^2) + 2x(p_{g1} p_{g2} - z_{g1} z_{g2}) = p_{g1} p_{g2}(z_{g1} + z_{g2}) - z_{g1} z_{g2}(p_{g1} + p_{g2})$	$\frac{A_1 \alpha_1 \alpha_2 (s+z_{g1})(s+z_{g2})}{(s+p_{g1})(s+p_{g2})} = -1$	z_{g1}, p_{g2}	$\frac{1}{1 + A_1 \alpha_1 \alpha_2}$
Lag-lead positive feedback compensator, lag in feedback path	$(z_g + z_d - p_g - p_d)(x^2 + y^2) + 2x(p_g p_d - z_g z_d) = p_g p_d (z_d + z_g) - z_g z_d (p_g + p_d)$	$\frac{A_1 \alpha (s+z_g)(s+z_d)}{(s+p_g)(s+p_d)} = 1$	z_g, p_d	$\frac{1}{1 - A_1 \alpha}$
Lag-lead positive feedback compensator, lead in feedback path	$(z_g + z_d - p_g - p_d)(x^2 + y^2) + 2x(p_g p_d - z_g z_d) = p_g p_d (z_d + z_g) - z_g z_d (p_d + p_g)$	$\frac{A_1 \alpha (s+z_g)(s+z_d)}{(s+p_g)(s+p_d)} = 1$	p_g, z_d	$\frac{1}{1 - A_1 \alpha}$

TABLE 4.2

9.2 Construction of the Locus of Complex Poles or Complex Zeros Producing a Constant Phase Angle at a Point in the S-plane.

It has been shown by Carpenter (19) that if the angle at a point in the s-plane due to an array of poles and zeros be known, it is possible to construct the locus of complex conjugate poles or complex conjugate zeros which will cause this point to be on a root locus. This locus of complex poles or zeros proves to be an arc of a circle. Carpenter's derivation is as follows:

Figure 9.1 shows the necessary construction in proving the locus of complex conjugate poles or zeros, R and R', producing a constant phase at a point p, in the s-plane, is an arc of a circle passing through that point. The center of the circle lies on the real axis.

From the figure:

$$a = 90^{\circ} + \alpha + \beta$$

$$b = 90^{\circ} + \alpha$$

$$a + b = \beta + 2\alpha + 180 = M = \text{angle contributed by} \qquad (9\text{-}6)$$

complex pair at point p.

But $\beta + 2\alpha + \gamma' = 180^{\circ}$ (9-7)

Subtracting 9.7 from 9.6

$360 - M = \gamma' =$ a constant

The vertex of γ', therefore, lies on an arc pp', of a circle whose center is on the real axis, by a fundamental theorem of plane geometry.

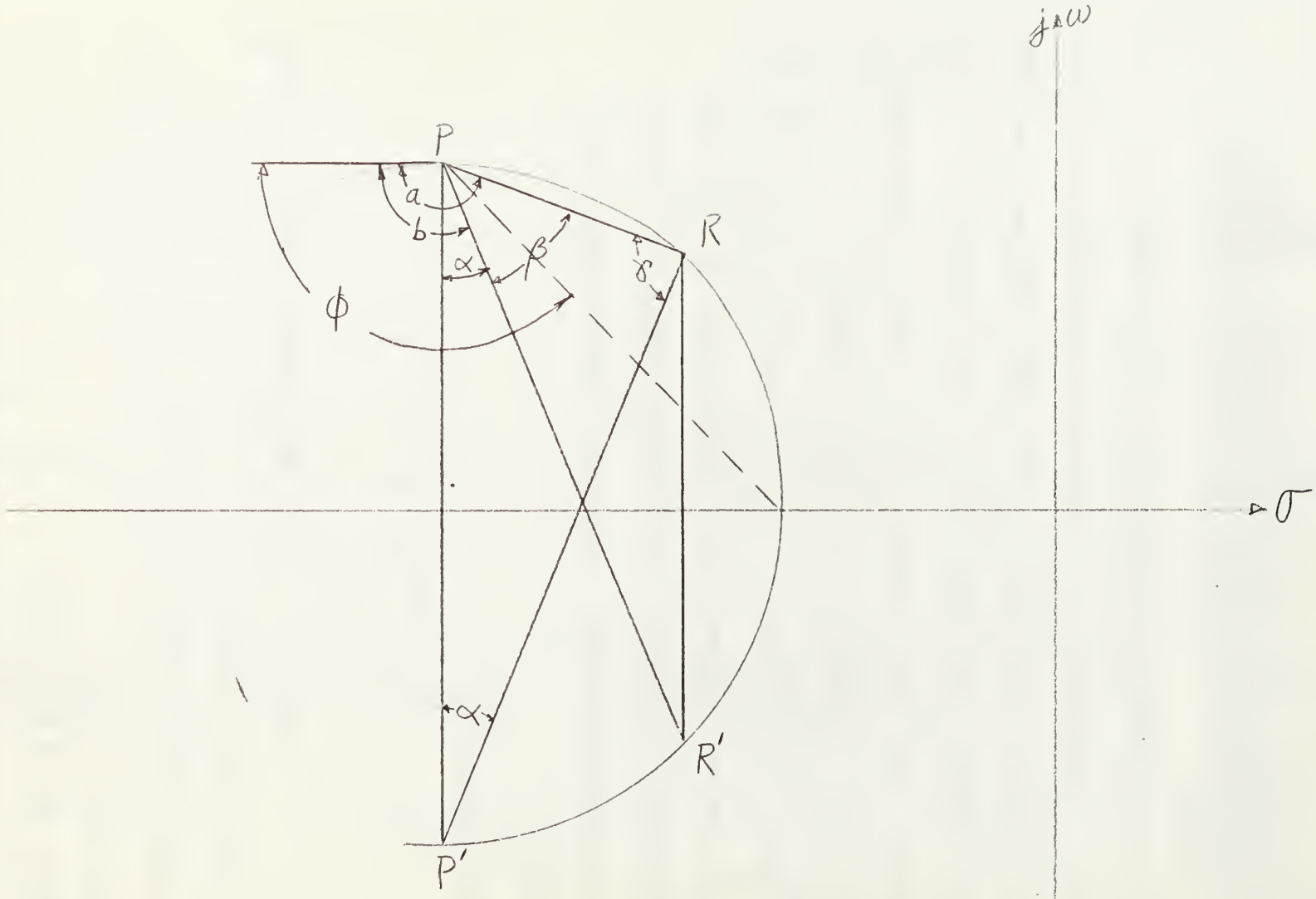

Fig. 9-1 CONSTRUCTION NECESSARY IN PROVING CARPENTER'S WORK

Since the arc always intersects the real axis, the arc may be quickly constructed by first locating that intersection. The intersection is found by constructing the angle,

$$\phi = M/2 \tag{9-8}$$

at the point P.

It can also be shown that the construction angle at the point P which locates the center of the circular arc on the real axis is

$$\Gamma = M \tag{9-9}$$

The necessary construction to show this is Fig. 9-2. F is the intersection of the circular arc with the real axis defined by the angle ϕ. HG is the perpendicular bisector of PF. Since the center of the circular arc is on the real axis, the intersection G must be the center of the circular arc, by plane geometry. From Fig. 9-2;

$$\phi + g = 90^{\circ} \tag{9-10}$$

$$2\phi + 2g = 180^{\circ} \tag{9-11}$$

$$2g = h \tag{9-12}$$

Subtracting Equation 9.5 from 9.4 obtains

$$2\phi = 180^{\circ} - h \tag{9-13}$$

$$h + \Gamma = 180^{\circ} \tag{9-14}$$

$$\Gamma = 180^{\circ} - h \tag{9-15}$$

Subtracting Equation 9-15 from 9-13

$$2\phi = \Gamma = M$$

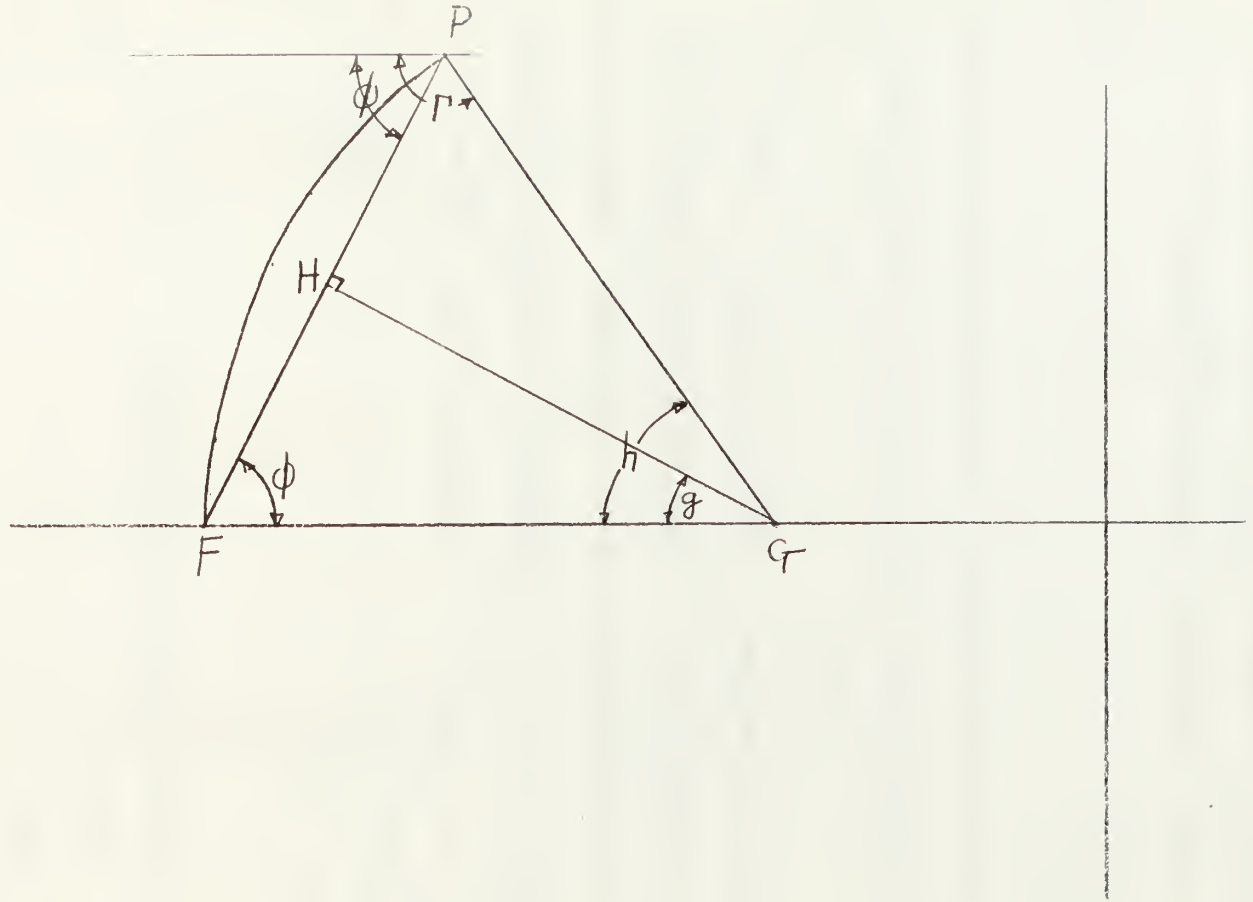

Fig. 9-2 CONSTRUCTION NECESSARY IN LOCATING THE CENTER OF THE CIRCULAR ARC

from Equation 9.9, thus proving the statement.

With the center of the circular arc and its point of intersection with the real axis known from ϕ and K, the arc may be easily constructed.

This construction provides a simple means of finding where on the s-plane complex poles or zeros may be placed in order to force a selected point to be on a root locus. This technique will not always be needed. For example when it is desired to cancel existing complex poles with complex zeros, the desired location of the complex zeros is specified by the location of the complex poles. However, in the more general cases, this construction becomes a powerful tool in problem solution.

Note that the circular arcs resulting from this construction will tell the designer where complex compensating poles or zeros should be placed in order to cause a desired point to be on a root locus. The circular equations for the active compensators of Section 9.1 then allows one to place complex zeros at the required locations.

9.3 A Technique for Compensation Using Active Networks

Relocation of the root loci of the characteristic equation so that they pass through a specified point is not in itself any great problem. Simultaneously meeting the requirements of dominance, steady state accuracy, and transient response is, however, quite another matter. A considerable number of techniques exist for the simultaneous solution of the steady state accuracy and root location problems. See for example 20, 21 . These techniques apply only to compensation with negative real poles and zeros and do not easily extend to the use of complex poles and zeros. The technique presented here requires some intuition and trial and error as thus far no more straight forward approach has been found. For the trial and error phases, the Electro-measurements, Inc., ESIAC algebraic Computer, Model 10 was a valuable tool.

The techniques of solution, whether for complex poles or complex zeros, are practically identical. Therefore they will be presented separately to avoid any possibility of confusion.

(A). Solutions requiring complex zeros.

a. Select the compensation path. Then determine the open loop transfer function and manipulate the characteristic equation into the form:

$$\frac{K \prod_{i=1}^{n} (s + Z_i)}{s^m \prod_{j=1}^{n} (s + p_j)} \quad G_c = -1 \qquad (9\text{-}17)$$

b. Plot the z_i, p_j, and s^m on the s-plane.

c. Select the real poles of G_c so as to be most convenient. Convenience will be determined by the particular problem. Plot these poles on the s-plane. This will usually determine which of the complex zero producing active networks is to be used.

d. Select the desired locations, P and P', of two complex conjugate closed loop roots. Plot P and P' on the s-plane. As mentioned previously, it is hoped that these roots will prove dominant, but there is no way of ensuring this.

e. Calculate the phase angle at P or P' due to z_i, p_j, s^m, and the real poles of G_c. Then construct the locus of complex zeros in the manner described in Section 9.2, which will result in P and P' being on a 180 degree locus.

f. Choose two complex conjugate points, Q and Q', on this constructed locus. These will be the complex zeros of G_c.

g. Determine the root locus gain, K_{RL} which will cause roots to be at P and P' with the z_i, p_j, s^m, and the chosen real poles and complex zeros of G_c.

h. Substitute K_{RL} and the real poles and complex zeros of G_c into the open loop transfer function to determine if steady state accuracy specifications are met. If not, choose two new locations of the complex zeros of G_c and repeat steps f and g.

i. Determine x and y from the chosen locations of the complex zeros of G_c.

j. Substitute x and y and the selected real poles of G_c into the appropriate equation of Table 9-1 to determine the algebraic relationship between the real zeros of the compensator passive networks.

k. Construct a graph of this equation or evaluate it for several values of one variable and select any convenient, physically realizable values for the zeros of the passive networks. The z/p ratios of lead networks should be $\zeta \geq 0.1$.

l. Substitute the real poles and zeros of the passive networks into the numerator root locus equation of Table 9-1 corresponding to the active network chosen. Plot this equation and the selected complex compensator zeros on another s-plane.

m. Determine the value of A_1/A_2 which will cause the roots of the numerator of G_c to lie at the selected locations for the complex zeros.

n. Using the results of steps g and m A_1 and A_2 may be calculated and the compensator design is completed.

o. The transient response must be computed and compliance with specifications determined.

(B). Solutions requiring complex poles.

a. Select the compensation path. Then determine the open loop transfer function and manipulate the characteristic equation into the form:

$$\frac{K \prod_{i=1}^{n} (s + z_i)}{s^m \prod_{i=1}^{n} (s + p_j)} G_c = -1 \qquad (9\text{-}18)$$

b. Plot the z_i, p_j, and s^m on the s-plane.

c. Select the real zeros of G_c so as to be most convenient. Convenience will be determined by the particular problem. Plot these zeros on the s-plane. This selection will determine the particular active network to be used.

d. Select the desired locations, P and P', of two complex conjugate closed loop roots. Plot P and P' on the s-plane. As mentioned previously, it is hoped that these roots will be dominant, but there is no way of ensuring this.

e. Calculate the phase angle at P or P' due to z_i, p_j, s^m, and the real zeros of G_c. Then construct the locus of complex poles in the manner described in Section 9.2, which will result in P and P' being on a 180 degree locus.

f. Choose two complex conjugate points on this constructed locus. These will be the complex poles of G_c.

g. Determine the root locus gain, K_{RL}, which will cause roots to be at P and P' with the z_i, p_j, s^m, and the chosen complex poles and real zeros of G_c.

h. Substitute K_{RL} and the complex poles and real zeros of G_c into the open loop transfer function of the system to determine if steady state accuracy specifications are met. If not, choose new locations for the complex poles of G_c and repeat steps f and g.

i. Determine x and y from the chosen locations of the complex poles of G_c.

j. Substitute x and y and the selected real zeros of G_c into the appropriate equation of Table 9-2 to find the algebraic relationship between the real poles of the passive networks.

k. Construct a graph of this equation or evaluate it for several values of one variable and select any convenient, physically realizable values of the passive network poles. The z/p ratio for lead networks should be $\zeta \geq 0.1$.

l. Substitute the values of the poles and zeros of the passive networks into the denominator root locus equation of Table 9-2 corresponding to the active network chosen. Plot this equation and the selected complex compensating poles on another s-plane.

m. Determine the value of A_1 which will cause the roots of the denominator of G_c to lie at the selected locations of the complex compensating poles. This completes the design of the compensator.

n. The transient response must now be computed and compliance with specifications determined.

9.4 Numerical Examples

This section applies the techniques of solution to further clarify their use. The examples presented herein are straightforward so as to illustrate the use of active networks as compensators without becoming unnecessarily involved in other considerations. It is assumed that active compensation was necessary in these examples due to unspecified conditions. The subsections of each numerical example correspond to the steps in the applicable technique of solution.

Example 1

Given:

The feedback control system of Fig. 9.3 $K_v = 5.0$.

Requirements:

Use cascade compensation. Desired root location to be such that $0.5 \leq \zeta \leq 0.7$, settling time = 1.0 seconds. K_v not to be reduced.

Solution:

a. The compensated open loop transfer function of Fig. 9.3 is

$$F_o = \frac{K}{s(s^2 + 5s + 100)} = G_c \qquad (9\text{-}19)$$

The characteristic equation of the compensated system is

$$1 + \frac{K}{s(s^2 + 5s + 100)} = 0 \qquad (9\text{-}20)$$

b. The z_i, p_j, and s^m of Equation 9.19 are plotted on Fig. 9.4.

c. Select $p_{d1} = -25$, $p_{d2} = -30$, so as not to add any more poles in the region near the origin. p_{d1} and p_{d2} are also plotted on Fig. 9.4.

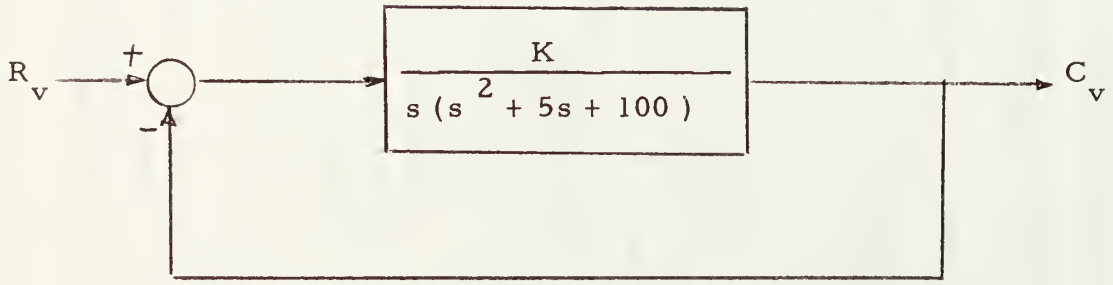

Fig. 9.3 BLOCK DIAGRAM OF THE FEEDBACK CONTROL SYSTEM FOR EXAMPLE 1.

Fig. 9.4

S-plane constructions for solving Example 1.

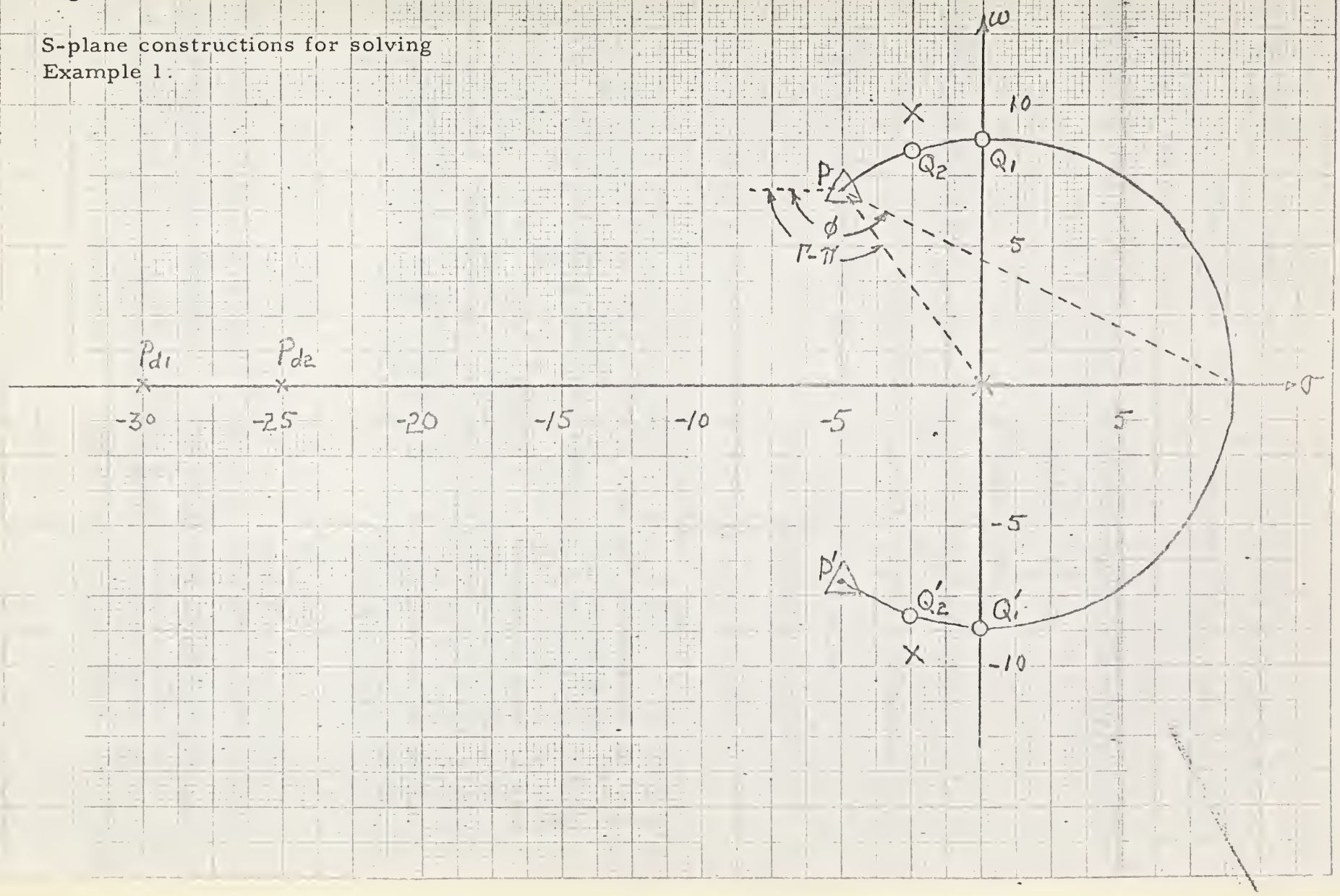

d. Select the points $s = -5 \pm j\ 7$ to be P and P', the roots of the characteristic equation which will meet the requirements.

e. From Fig. 9-4, the lead angle required at P is 307.3 degrees. The construction angles at P are

$$\emptyset = 153.65 \text{ degrees}$$

$$\Gamma = 307.3 \text{ degrees}$$

The arc of the circle on which complex compensating zeros can be located was constructed on Fig. 9-4 using these angles.

f. On Fig. 9-4, choose $s = \pm j\ 8.8$ to be Q_1 and Q'_1, the locations of the complex compensator zeros.

g. The root locus gain at P using all poles and zeros is

$$K_{RL} = 3,250$$

h. Substituting this value of gain and the chosen compensator poles and zeros into the open loop transfer function obtains $K_v = 3.51$. This does not meet requirements. Therefore, choose two new complex compensator zeros a little closer to the desired root locations. Let these new locations be $s = -2.5 \pm j\ 8.4$, Q_2 and Q'_2. With these new zeros, the root locus gain at P is

$$K_{RL} = 6,578$$

Substituting this root locus gain and the new complex zeros into the open loop transfer function yields $K_v = 6.72$. This meets the requirements.

i. From the chosen locations of the complex zeros,

$$x = -2.5$$

$$y = \pm 8.4$$

j. Substituting these values of x and y, p_{d1} and p_{d2} into the working equation of the lead-lead feed forward difference compensator of Table 9-1 yields

$$\not{z}_{d1} = 140.34 \left[\frac{\not{z}_{d2} + .5446}{135.34 - \not{z}_{d2}} \right] \qquad (9\text{-}21)$$

The algebraic relationship between z_{d1} and z_{d2} .

k. Several values of z_{d2} were substituted into this equation and $z_{d1} = -2.5$, $z_{d2} = -3.0$ were selected as the zeros of the lead networks.

l. Substituting the chosen z_{d1}, z_{d2}, p_{d1}, and p_{d2} into the numerator root locus equation of the lead-lead feed forward difference compensator of Table 9-1 yields

$$\frac{A_1 (s + 2.5)(s + 30)}{A_2 (s + 3)(s + 25)} = 1 \qquad (9\text{-}22)$$

Equation 9-22 and the chosen complex compensator zeros are plotted on Fig. 9.5.

m. From Fig. 9.5, $A_1/A_2 = 0.8368$ will cause the numerator zeros to be at the chosen complex conjugate locations.

n. The values of A_1 and A_2 may now be computed from the equations

$$\begin{aligned} A_1/A_2 &= 0.8368 \\ K(A_1 - A_2) &= K_{RL} = 6578 \end{aligned} \qquad (9\text{-}23)$$

Since K is a variable gain element, any values of K, A_1, and A_2, which satisfy Equations 9-23 will yield satisfactory results.

Fig. 9.5

S-plane pole zero array of
Equation 9-22.

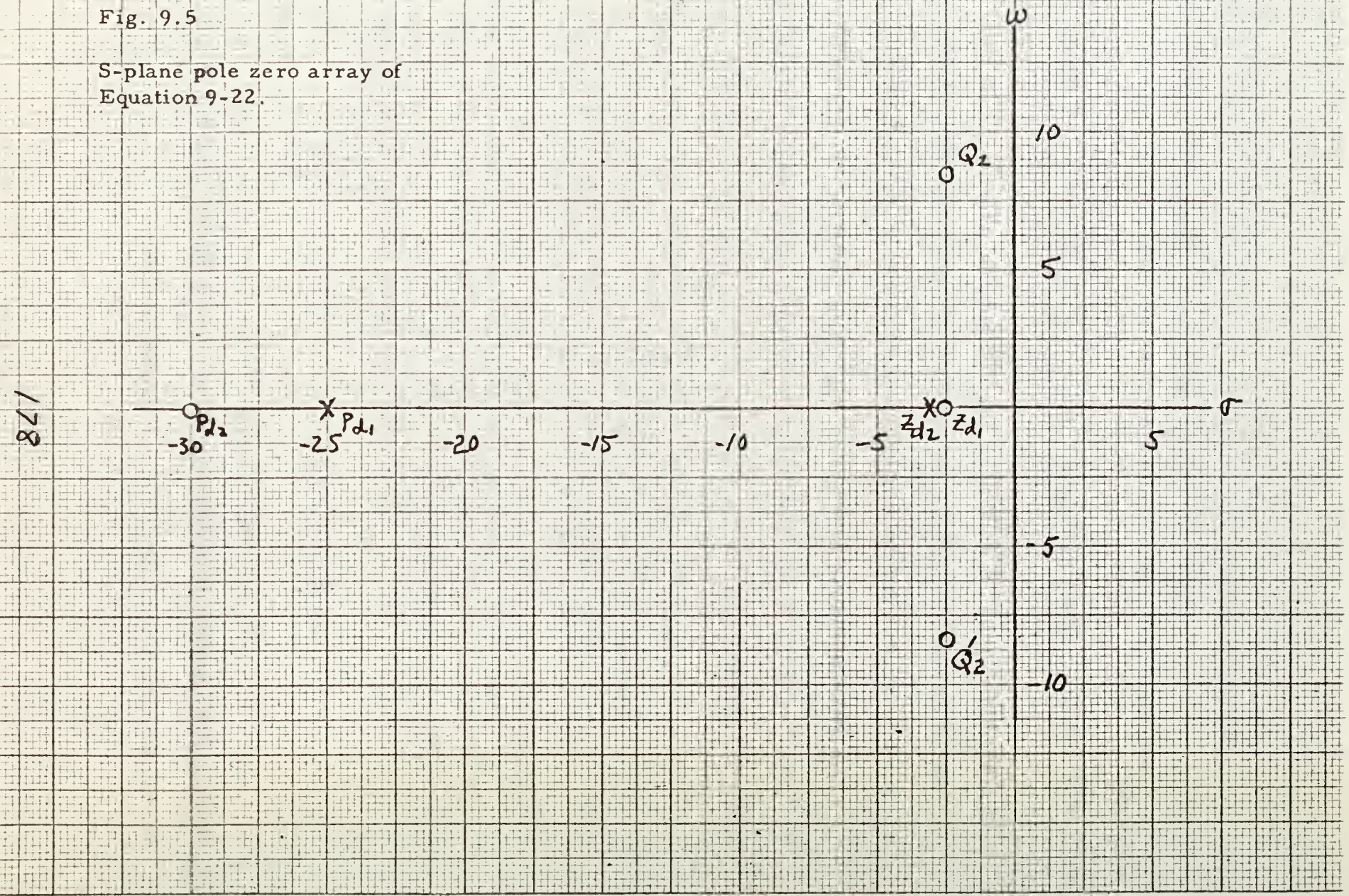

o. The characteristic equation of the compensated system may now be written as

$$\frac{6578\,(s + 2.5 + j\,8.4)\,(s + 2.5 - j\,8.4)}{s\,(s^2 + 10s + 100)\,(s + 25)\,(s + 30)} = -1 \qquad (9\text{-}24)$$

The roots of this equation were obtained by calculation on the Control Data Corporation 1604 digital computer as

$$s = -5.11 + j\ 7.26$$
$$s = -5.11 - j\ 7.26$$
$$s = -4.69 + j\ 11.69$$
$$s = -4.69 - j\ 11.69$$
$$s = -40.4$$

The roots as $s = -5.11 + j\,7.26$ and $s = -5.11 - j\,7.26$ correspond to those selected early in the solution. There is some error due to the graphical techniques required in the solution, however the agreement is close enough for engineering work. The transient response may now be calculated and final agreement with requirements determined.

Example 2.

Given:

The feedback control system of Fig. 9.6. $K_v = 100$

Requirements:

Use cascade compensation. Desired root location such that $0.5 \leq \beta \leq 0.7$, settling time = 1.0 seconds. K_v not to be reduced.

Solution:

a. The compensated open loop transfer function of Fig. 9-6 is

$$F_o = \frac{K}{s\,(s + 1)^2}\,G_c \qquad (9\text{-}25)$$

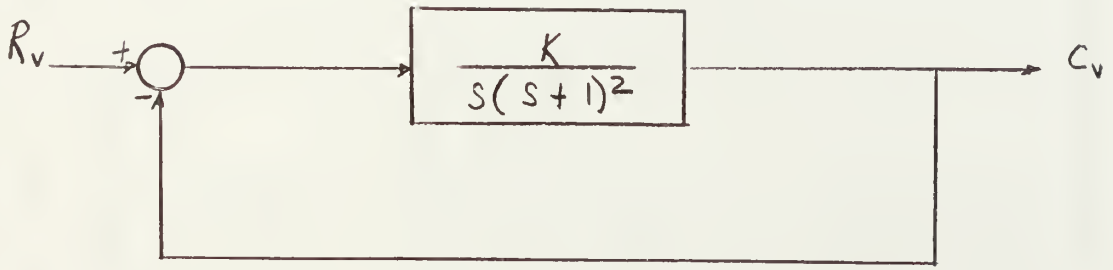

FIG 9.6 BLOCK DIAGRAM FOR EXAMPLE 2

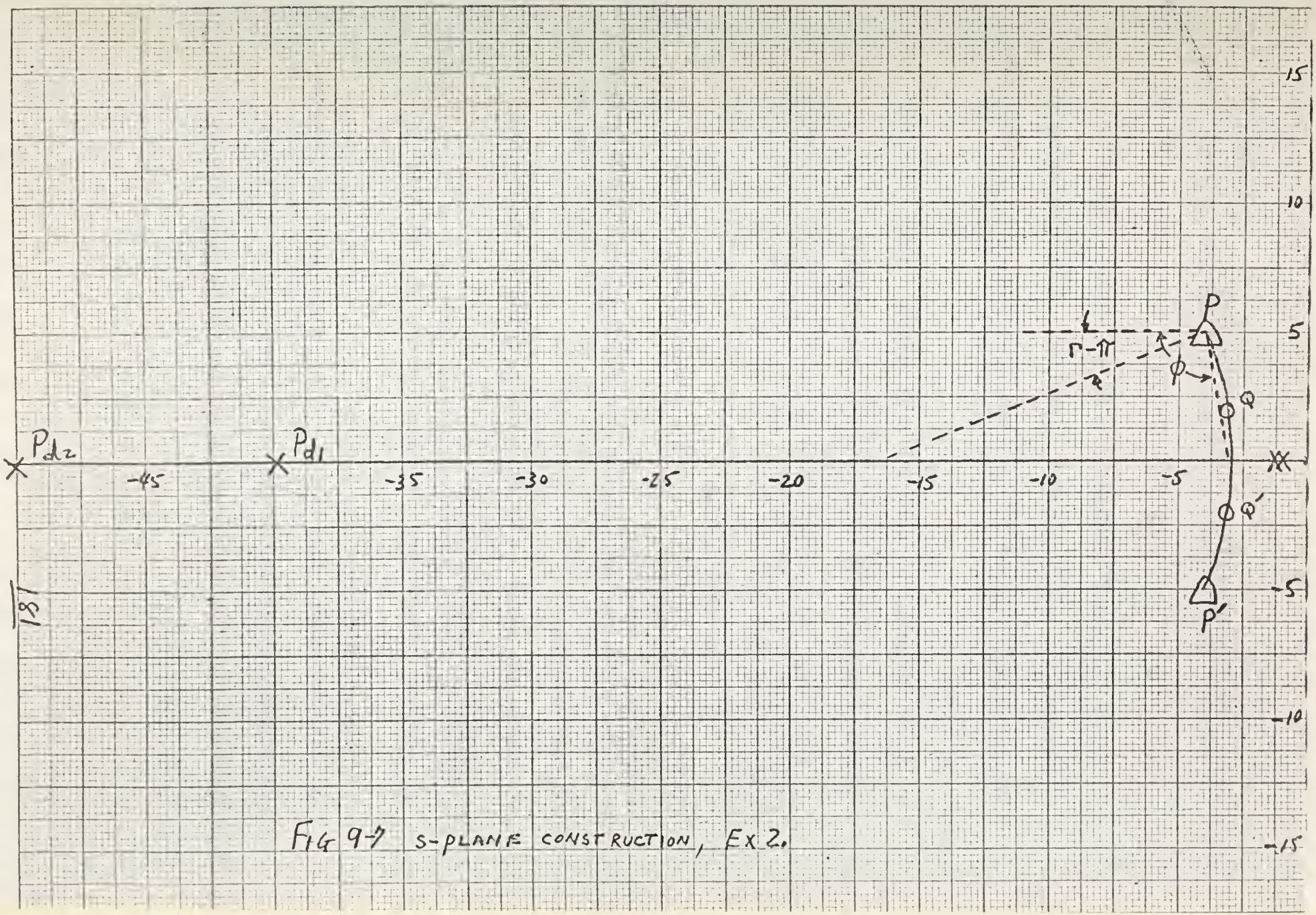

FIG 9-7 S-PLANE CONSTRUCTION, EX 2.

The characteristic equation of the compensated system is

$$1 + \frac{K}{s(s+1)^2} G_c = 0 \qquad (9\text{-}26)$$

b. The z_i, p_j, and s^m of Equation 9-26 are plotted on Fig. 9.7.

c. Select $p_{d1} = -40$, $p_{d2} = -50$ so any root loci from these poles will not affect the region where the desired root will be located. p_{d1} and p_{d2} are also plotted on Fig. 9.7.

d. Select the points $s = -4 \pm j5$ to be P and P', the roots of the characteristic equation which will satisfy the requirements.

e. From Fig. 9.7, the lead angle required at P is 203.8 degrees. The construction angles at P are

$$\phi = 101.9 \text{ degrees}$$

$$\Gamma = 201.8 \text{ degrees}$$

The arc of the circle on which complex compensating zeros can be located was constructed on Fig. 9.7 from these angles.

f. Choose the points $s = -3.2 \pm j2$ to be Q and Q', the locations of the complex compensator zeros.

g. The root locus gain at P and P' using all poles and zeros is

$$K_{RL} = 15,316$$

h. Substituting this value of gain and the chosen poles and complex zeros of the compensator into the open loop transfer function obtains $K_v = 108.8$.

This meets requirements.

i. From the chosen locations of the complex compensating zeros:

$$x = -3.2$$

$$y = \pm 2.0$$

j. Substituting these values of x and y, p_{d1} and p_{d2} into the working equation of the lead-lead feed forward difference compensator from Table 9-1 yields

$$Z_{d2} = 169.424 \left[\begin{array}{l} Z_{d1} - .08405 \\ Z_{d1} + 175.824 \end{array} \right]$$

the algebraic relationship between z_{d1} and z_{d2}.

k. Several values of z_{d1} were substituted into this equation and $z_{d1} = -30$, $z_{d2} = -34.95$ were selected as the zeros of the lead networks.

l. Substituting the chosen z_{d1}, z_{d2}, p_{d1}, and p_{d2} into the numerator root locus equation of the lead-lead feed forward difference compensator on Table 9-1 yields

$$\frac{A_1 (s + 30)(s + 50)}{A_2 (s + 34.95)(s + 40)} = 1 \qquad (9\text{-}27)$$

Equation 9-27 and the chosen complex compensator zeros are plotted on Fig. 9.8.

m. From Fig. 9.8 $A_1/A_2 = 0.9314$ will cause the numerator zeros to be at the chosen complex conjugate locations.

n. The values of A_1 and A_2 may now be computed from the equations

$$\begin{aligned} A_1/A_2 &= 0.9314 \\ K(A_1 - A_2) &= K_{RL} = 15,316 \end{aligned} \qquad (9\text{-}28)$$

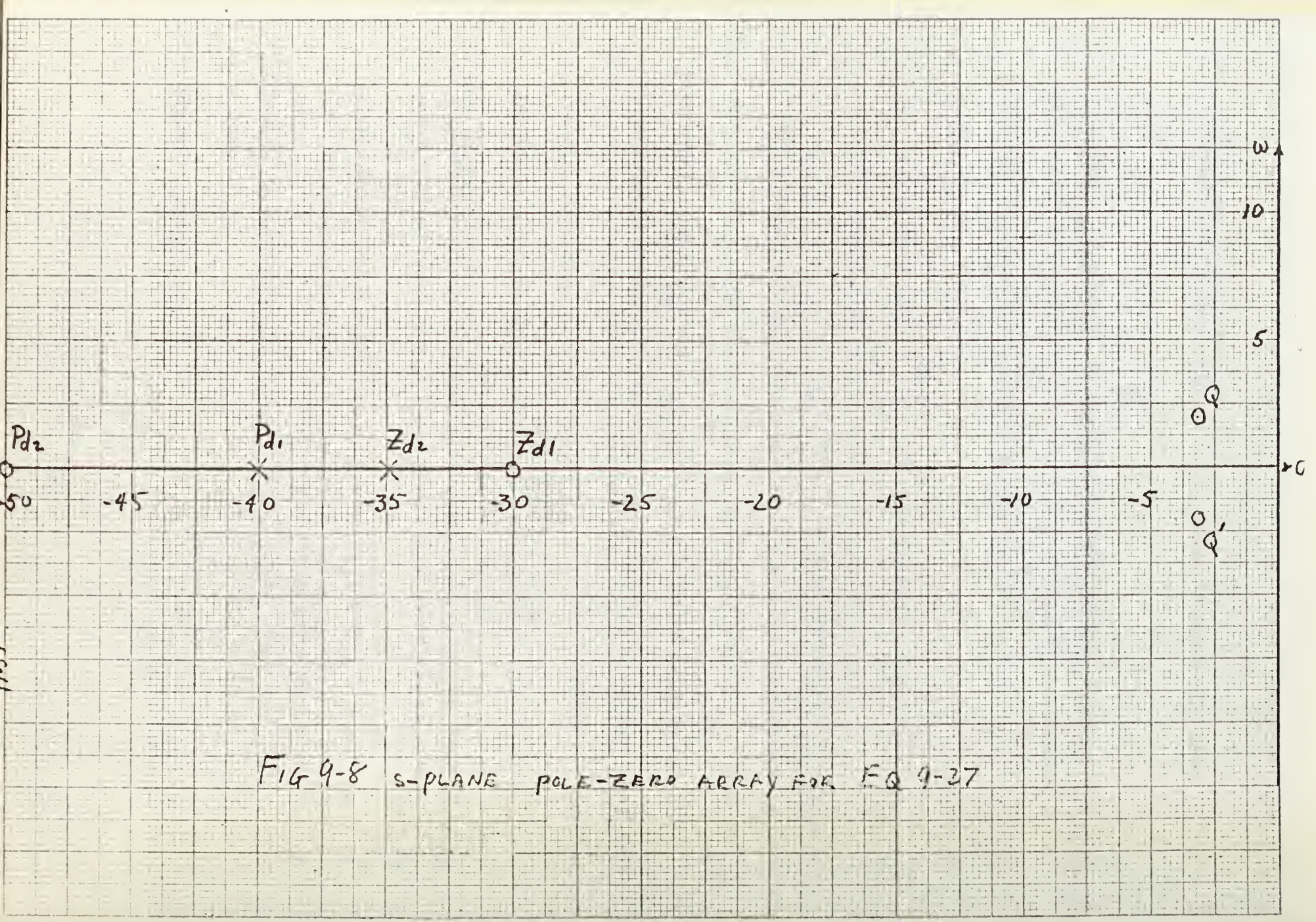

FIG 9-8 S-PLANE POLE-ZERO ARRAY FOR EQ 9-27

Since K is a variable gain element, any values of K, A_1, and A_2, which satisfy Equations 9-28 will yield satisfactory results.

o. The characteristic equation of the compensated system may now be written as

$$\frac{15.316\,(s + 3.2 + j\,2)\,(s + 3.2 - j\,2)}{s\,(s + 1)^2\,(s + 40)\,(s + 50)} = -1 \qquad (9\text{-}29)$$

The roots of this equation were obtained by calculation on the Control Data Corporation 1604 digital computer as

$s = -3.39 + j\,5.4$
$s = -3.39 - j\,5.4$
$s = -4.33$
$s = -19.73$
$s = -61.06$

The roots as $s = -3.39 + j\,5.4$ and $s = -3.39 - j\,5.4$ correspond to those selected early in the solution. There is some error due to the graphical techniques required in the solution, however the agreement is close enough for engineering work. The transient response may now be calculated and final agreement with the requirements determined.

9.5 Summary

For both the examples chosen, the lead-lead feed forward difference compensator proved to be the most practical for solution. However, the use of the other active networks follows exactly the same procedure as demonstrated.

It was found that there are some regions on the circular loci of the active networks at which the gain ratio A_1/A_2 is extremely critical; i.e., a small variation in the gain ratio results in a large movement of the complex zeros of the active network. This sensitivity may be overcome to some extent by a trial and error method of varying the real poles and zeros of the passive networks so that the critical area of the circular locus is moved away from the desired location of the complex zeros.

The active networks presented afford a simple method of generating complex poles and zeros. The locations of these complex poles and zeros may be accurately predicted and are easily varied by adjusting an amplifier gain or one or more of the passive elements of the networks. The varying of an amplifier gain is the more attractive of these two methods as it results in the complex poles or zeros moving along a circle which is precisely defined by the passive circuit elements.

Since the location of the complex poles and zeros is a function of amplifier gain, a requirement for a very stable amplifier is generated. This requirement may be relaxed somewhat if the compensated system is not too sensitive to the compensator pole and zero locations.

The lag-lead feed forward summing compensator has characteristics which merit special attention. Since the K_c of this compensator is $A_1 + A_2$ the possibility presents itself of using this compensator as the main transmission path amplifier. The complex zeros resulting from the network could be adjusted to best suit the needs of a specific system while the overall gain remained independent.

10. APPLICATION TO A JET AIRPLANE

In any discussion, the argument is strengthened by an analysis of a practical problem, feasibility permitting. The agreement of calculated values and test responses of the actual vehicle is proof for the skeptic. This section will use the arrays presented in previous sections and substitute the aerodynamic stability derivatives of the North American Aviation Inc. Jet Trainer (Navy designation T2J-1). This particular vehicle was selected as a model because of the wealth of flight test and aerodynamic data immediately available to the authors.

The discussion will be limited to the longitudinal system where the aircraft is originally in equilibrium at a level flight attitude. An additional comparison will show the differences between a two degree and three degree of freedom calculated estimate.

Considering first, the following condition of flight:

$h = 30{,}000$ feet, $\rho = 8892.7 \times 10^{-7} \frac{\text{slug}}{\text{ft}^3}$, $M = .6$, $V_o = 597$ ft/sec

$W = 9660$ pounds, $m = 300$ slugs, $B = 13157.7$ slug-ft^2

The aerodynamic stability effects were calculated and the following values found:

$Xu = -.01264$ $\qquad$ $Xw = .0384$

$zu = -.0924$ $\qquad$ $Mw = -.0288$

$Mu = .0004$ $\quad M\dot{w} = -.00134$

$Mq = -1.603$

$zw = -1.092$ $\quad M\eta = -24.771$

$zq = -4.00$ $\quad 10\eta = -1.400$

$z\eta = -142.0$ $\quad 10\dot{\eta} = -172.00$

$X\dot{w} = Xq = z\dot{w} = M\dot{\eta} = 10u = 10w = 10\dot{w} = 10q = 0$

Placing these numerical values in a determinant, the following form results as shown in Table 10-1.

Evaluating the Δ of this determinant, the result is $\Delta = (s^2+172s+1.4)(s^4+3,5056s^3+18.99122s^2+.2535s+.0998)$ (10-1)

This results in the following set of roots,

$s = -.01$
$s = -171.99$ } elevator motion

$s = -.006205 \pm j.07232$ (phugoid motion)

$s = -1.7466 \pm j\ 3.9864$ (short period)

If only a short period estimate is required, then the determinant of Table 10-2 is used. This assumed no speed change (u) during the short period and the X force equation is eliminated.

Evaluating the Δ of the determinant, the results are:

$s = -.01$
(elevator response)
$s = -171.99$

$s = -1.745 \pm j\ 3.985$ (short period)

TABLE 10-1 Longitudinal System at h=30,000 ft M=.6

Δ Fe	η		W		Θ		U
$\frac{s^2+172s+1.4}{s^2}$	O	O	O	O	O	O	O
- 1	1	O	O	O	O	O	O
O	$\frac{142.0}{s}$	$\frac{s+1.092}{s}$	O	$\frac{-597s}{s}$	O	$\frac{.094}{s}$	O
O	O	-1	1	O	O	O	O
O	$\frac{24.771}{s^2}$	$\frac{.00134s+.0288}{s^2}$		$\frac{s^2+1.603s}{s^2}$	O	$\frac{-.0004}{s^2}$	O
O	O	O	O	- 1	1	O	O
O	$\frac{O}{s}$	O	$\frac{-.0348}{s}$	O	$\frac{32.2}{s}$	$\frac{s+.01264}{s}$	O
O	O	O	O	O	O	- 1	1

TABLE 10-2 Two Degree of Freedom System for T2V-1

	η		$U_o \quad \Delta\alpha$		Θ
$\frac{s^2+172s+1.4}{s^2}$	0	0	0	0	0
-1	1	0	0	0	0
0	$\frac{142.0}{s}$	$\frac{s+1.092}{s}$	0	$\frac{-597\,s}{s}$	0
0	0	-1	1	0	0
0	$\frac{24.771}{s^2}$	0	$\frac{.00134s+.0288}{s^2}$	$\frac{s^2+1.063s}{s^2}$	0
0	0	0	0	-1	1

h=30,000 ft
M=.6

The short period response using the results of Δ in Equation 10-1 is

$$T = \frac{2\pi}{3.9864} = 1.575 \text{ seconds per cycle}$$

and the damping to 1/2 amplitude is

$$t_{1/2} = \frac{.69}{1.7466} = .395 \text{ seconds}$$

From the North American Aviation flight report NA-594-282, the flight test results for the T2J at conditions similar to the above calculated flight conditions were T=1.6 seconds cycle.

$$t_{1/2} = .4725 \text{ seconds}$$

There is very good agreement between calculated and flight test results.

There was insufficient information available in the North American report with respect to the long period longitudinal oscillation. Therefore, a second set of level flight condition derivativeswas computed using the same aircraft model.

The conditions specified are:

h = 20,000 feet, $\rho = 12664 \times 10^{-7}$ slugs/ft^3 $\dot{M}$=.463 U_o=480ft/sec

W =9660 pounds m=300 slugs B=13157.7 slug-ft^2

For these conditions the following stability derivatives were found:

$xu = -.01382$	$zq = -4.60$
$zw = -1.425$	$Mq = -1.87$
$Mw = 8.59 \times 10^{-4}$	$z\eta = -130.0$
$Xw = .0222$	$M\eta = -24.45$
$zw = -1.265$	$10\dot{\eta} = -2.02$
$Mw = -.03365$	$10\ddot{\eta} = -179.0$
$z\dot{w} \cong 0$	$10u = 10w = 10w10q = X\dot{w} = Xq \cong 0$
$Mw = -.00193$	$M\dot{\eta} = z\ddot{\eta} = X\eta = X\dot{\eta} = 0$

Thus a determinant can be formed as shown in Table 10-3. Evaluating the resultant Δ, it is found that the following roots exist

$s = -.0125$
$s = -178.9875$
} elevator motion

$s = -.006698 \pm j.10129$ (phugoid motion)

$s = -2.0257 \pm j\ 3.7756$ (short period motion)

Using the results from Table 10-3, the period of phugoid motions is $T = \frac{2\pi}{.10129} = 62.0$ seconds per cycle.

The time to dampen to 1/2 amplitude is $t_{1/2} = \frac{.69}{.00670} = 103.0$ seconds. If a two degree of freedom estimate is desired, it can be determined from the above table. For the phugoid motion, the estimate can be made by considering angle of attack constant

TABLE 10-3 T2V-1 Longitudinal System at 20,000 feet Three Degrees of Freedom

Δ Fe	η		W		Θ		U
$\frac{s^2+179s+2.02}{s^2}$	O	O	O	O	O	O	O
- 1	1	O	O	O	O	O	O
O	$\frac{130.0}{s}$	$\frac{s+1.265}{s}$	O	$\frac{-475.4s}{s}$	O	$\frac{.1425}{s}$	
O	O	- 1	1	O	O	O	O
O	$\frac{24.45}{s^2}$	O	$\frac{.00193s+.0033}{s^2}$	$\frac{s^2+1.87s}{s^2}$	O	$\frac{.000859}{s^2}$	O
O	O	O	O	- 1	1	O	O
O	O	O	$\frac{-.0222}{s}$	O	$\frac{32.2}{s}$	$\frac{s+.01382}{s}$	O
O	O	O	O	O	O	- 1	1

TABLE 10-5 Formation of a Δ_{15} Determinant

	η		w			u
-1	1	0	0	0	0	0
0	$\frac{-(sZ_{\dot{n}}+Z_n)}{s}$	$1-\frac{(sZ_{\dot{w}}+Z_w)}{s}$	0	0	$\frac{-(Q_o+Z_u)}{s}$	0
0	0	-1	1	0	0	0
0	$\frac{-(sM_{\dot{n}}+M_n)}{s^2}$	0	$\frac{-(sM_{\dot{w}}+M_w)}{s^2}$	0	$\frac{-M_u}{s^2}$	0
0	0	0	0	1	0	0
0	$\frac{-(sX_{\dot{n}}+X_n)}{s}$	0	$\frac{\left[\dot{\theta}_o U_o-(sX_{\dot{w}}+X_w)\right]}{s}$	$\frac{sw_o+g\cos\Theta_o\cos\phi_o-sZ_q}{s}$	$\frac{s-X_u}{s}$	0
0	0	0	0	0	-1	1

TABLE 10-4 T2V-1 Restricted to Two Degrees of Freedom at 20,000 Feet and M=.463

Δ Fe	η		Θ		U
$\frac{s^2+179s+2.02}{s^2}$	O	O	O	O	O
- 1	1	O	O	O	O
O	$\frac{130.0}{s}$	$\frac{-475.4s}{s}$	O	$\frac{.1425}{s}$	O
O	O	- 1	1	O	O
O	O	O	$\frac{32.2}{s}$	$\frac{s+.01382}{s}$	O
O	O	O	O	- 1	1

and the moment equation equal to zero in all nodes. Thus Table 10-4 can be made from Table 10-3. The roots from this determinant are:

$$\Delta = (s+178.9575)\,(s+.0125)\,(s+.0069+j.0979)\,(s+.0069-j.0979) \tag{10-2}$$

The flight test information for the phugoid was determined by the authors. On 5 January 1961, a T2J-1 (Navy 148204), piloted by McCamey and Borthwick yielded the following results for h=20,000 feet, M=.463:

T = 64 seconds per cycle

$t_{1/2}$ = 103 seconds

These results show excellent agreement with the calculated estimates and prove the system to be very valid one for both long and short period. It reaffirms the previous knowledge that:

1. Given reasonably accurate aerodynamic stability derivative, an accurate estimate of dynamic response can be made.

2. For conventional subsonic aircraft, a two degree of freedom approximation is quite close to the three degrees of freedom result and should be sufficiently accurate for preliminary design estimates. Furthermore, factoring a second order polynomial is far simpler than a fourth order polynomial.

As mentioned in previous sections the performance function is stated thus

$$PF = \frac{G_j K \Delta_{1j}}{\Delta} \tag{10-3}$$

It is noted that the Δ values have already been found in solving the natural periods of the airframe. A simple additional step yields the performance function desired.

For example, if the output $\frac{\Theta}{\Delta Fe}$ is desired the Δ_{ij} determinant is formed by cancelling the first row and 5th column of Table 6-1 the results form in Table 10-5 is shown.

The result of this determinant in algebraic form where the zero value terms are omitted is:

$$\Delta_{15} = s^2 \left[M\eta (Z\dot{w} - 1) - Z\eta\, M\dot{w} \right] + s \left[M\eta (Zw - Xu \left[Z\dot{w} - 1 \right]) - Xw \left[Zw \right] + Z \left(M\dot{w}\, Xu - Mw \right) \right] + \left[M\eta \left(XwZu - XuZw \right) + Z\eta \left(MuXw - MwXu \right) \right] \qquad (10\text{-}4)$$

Substituting in the appropriate values for the T2J-1 at h=20,000 feet, the following quadratic equation results

$$\frac{\Delta}{15} = s^2 \ (24.20) + s \ (26.900) + (.535038) \qquad (10\text{-}5)$$

Recalling that the direct path function for all cases in this system is one (1), then $G_{56} = 1$.

Therefore

$$\frac{\Theta}{\Delta Fe} = \frac{G_{56}\, \Delta_{15}}{\Delta} \quad \text{or}$$

(10-6)

$$\frac{\Theta}{\Delta Fe} = \frac{24.20\,(s+.0203)\,(s+1.0907)}{(s+.0125)(s+178.9875)(s+.006698 \pm j\,0.10129)(s+2.0257 \pm j3.7756)}$$

Thus the performance function for the pitch output with relation to elevator force is known. The block diagram of the internal sensing and activating equipment can be added as additional parts to control this multiloop system. Such an example is shown in Fig. 10-1.

The functions G1 constitutes an error sensing and signal amplification device such as an autopilot. G2 is the internal control power such as an electric or hydraulic servo mechansim. G3 is the performance function $\Theta/\Delta Fe$.

Assume for the moment that two input signals are desired in the system. For example, the aircraft may also encounter turbulence in the form of vertical gusts (w) as well as changes in elevator force (ΔFe). The equation for consideration of double inputs in general form is

$$q \text{ out} = \sum_{(k)} \frac{1}{\Delta} G_j k \left\{ \Delta_{1j} \; q_{1m} + \Delta_{2j} \; q_{2m} \right\} \qquad (10\text{-}7)$$

This last equation representing multiple inputs is shown only to point out the ability to use this system for such purposes. It will not be used with numerical coefficients at this time, however.

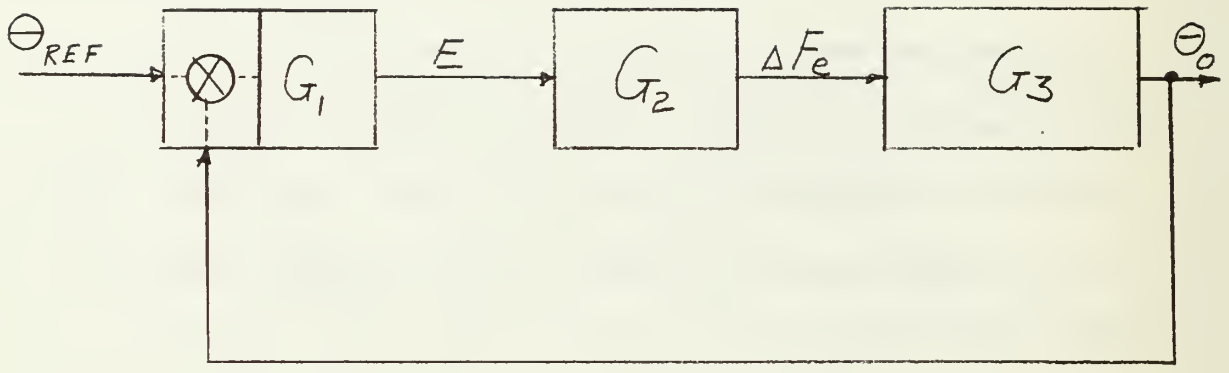

FIGURE 10-1 SIMPLE BLOCK DIAGRAM OF PITCH REFERENCE IN AN AIRPLANE.

This section has demonstrated the practical use of the discussion of previous sections. It has shown the agreement of calculated values and actual test.

This particular airframe is stable, but more often supersonic vehicles are not. While these calculations were limited to the longitudinal system, the use for the lateral system involving the yaw and roll channel is equally valid for the appropriate equations of motion. The system as developed in prior sections shows an orderly process whereby electrical and for mechanical processes can be combined into one multiloop block diagram. From this system, with the various criteria set forth, further research in multiloop compensation theory can be attempted. The airframe problem shows one practical use for this. There are many others.

REFERENCES AND BIBLIOGRAPHY

1. Chu, Yaohan; "A Generalized Theory of Linear Multi-loop Automatic Control Systems" , Ph. D. Thesis, MIT, May 1953.

2. Doolin, B. F.; "The Application of Matrix Methods to Coordinate Transforms Occuring in Systems Studies Involving Large Motions on Aircraft", NACA Technical Note 3968, May 1957.

3. "Dynamics of the Airframe", BuAer Report AE-61-4II prepared by the Servomechanisms Section and Aerodynamics Section, Northrop Aircraft, Inc., 1952.

4. Etkin, Bernard; Dynamics of Flight, Stability and Control, John Wiley and Sons Inc., New York, 1958.

5. Perkins, C. D. and Hage, R. E.; Airplane Performance, Stability, and Control, John Wiley and Sons Inc., New York, 1949.

6. Duncan, W. J.; The Principles of the Control and Stability of Aircraft, Cambridge at the University Press, 1952.

7. Charters, A. C.; "The Linearized Equations of Motion Underlying the Dynamic Stability of Aircraft, Spinning Projectiles, and Symmetrical Missiles", NACA Technical Note 3350, January 1955.

8. Howe, R. M.; "Coordinate Systems for Solving the Three Dimensional Flight Equations", WADC TN 55-747, June 1956.

9. "Dynamics of the Airframe" op cit

10. Thaler, G. J.; "Linear and Non'Linear Compensation Theory", Prepared Notes for Course EE 676, U. S. Naval Postgraduate School, Monterey, California 1961, p 19-21.

11. Anderson, R. W. and Roane, D. P.; "An Investigation of the Roll-Yaw Couplings in a Surface -To-Air Guided Missile", Master's Thesis, MIT, May 1960.

12. Etkin, Bernard; "Aerodynamic Transfer Functions: An Improvement on Stability Derivatives for Unsteady Flight", UTIA Report No. 42, Toronto, Canada, October 1956.

13. Smith, F. and Hicks W.D.T.; "The R.A.E. Electronic Simulator for Flutter Investigations in Six Degrees of Freedom or Less", Aeronautical Research Council, Great Britain, R. and M. 3101. September 1953.

14. Vedrov, V. A. and others; "The Airplane as an Object of Control", (Translation from Russian), NASA Technical Translation F-5, Washington, D. C., October 1959.

15. Lanchester, F. W.; Aerodonetics, D. Van Nostrand Company, New York 1909.

16. Durand, W. F. and Jones, B. M.; Aerodynamic Theory, Volume 5, "Dynamics of the Airframe", Durand Reprinting Committee, California Institute of Technology, 1943.

17. Abzug, M. J.; "Kinematics and Dynamics of Fully-Maneuvering Airplanes", Douglas Aircraft Company (El Segundo), Santa Monica, California, June 1952.

18. Wykes, J. H. and others: "An Analytical Study of the Dynamics of Spinning Aircraft", Part One, North American Aviation Inc., December 1958.

19. W. E. Carpenter, Synthesis of Feedback Systems with Specified Open-loop and Closed-loop Poles and Zeros, Space Technology Laboratories paper, GM-TM-0165-00355, 1958.

20. E. R. Ross and T. C. Warren, An Exact Method of Servomechanism Compensation Developed from a Study of Phase Angle and Gain Loci, Master's Thesis, United States Naval Postgraduate School, Monterey, California, 1959.

21. Charles D. Pollak, An Exact Method of Servomechanism Compensation Using S-plane Concepts, and an Analysis of the Effect of Passive Networks upon Steady State Performance, Master's Thesis, United States Naval Postgraduate School, Monterey, California, 1960.

APPENDIX I

BASIC EQUATIONS OF MOTION

The basic concepts of mass in motion and the equations of motion can be derived in vector notation. This is done using mass particles in motion and determining their effects in two separate axis systems. The basic reference system shown in Fig. AI-I is the starred axis. This is the non-rotating reference system and is also known as the Galilean Axis. The axis system is fixed in the rigid mass but may rotate about the fixed space axis system. It is the relative system. A special set of notation is used here in this appendix which differs from the body of this work.

The definition of the special terms in this appendix is as follows:

$\vec{i} \triangleq$ the vertorial unit along the X axis

$\vec{j} \triangleq$ the vertorial unit along the Y axis

$\vec{k} \triangleq$ the vectorial unit along the Z axis

$\vec{i}^{*} \triangleq$ the vectorial unit along the X^{*} axis

$\vec{j}^{*} \triangleq$ the vectorial unit along the Y^{*} axis

$\vec{k}^{*} \triangleq$ the vectorial unit along the Z^{*} axis

$0 \triangleq$ the origin of the relative axis system

$0^{*} \triangleq$ the origin of the space axis system

$\vec{R} \triangleq$ the vectorial distance from the space axis origin to the relative axis origin

$\vec{r} \triangleq$ the vectorial distance from the space axis origin to a mass particle in space

$\vec{\rho} \triangleq$ the vectorial distance from the relative axis origin to the mass particle

$dm \triangleq$ the mass particle

$\rho_c \triangleq$ the vectorial distance from the mass center to the origin of the relative axis system

$\Omega \triangleq$ rotational velocity vector of the relative axis system about the space axis; an absolute velocity vector

$\vec{\omega} \triangleq$ absolute rotational velocity vector of a rotor whose axis is attached to XYZ axis system

$\vec{L} \triangleq$ momentum vector for the entire mass body

$\vec{H} \triangleq$ moment of momentum vector with respect to the space axis

$\vec{G} \triangleq$ moment vector with respect to the relative axis

$\vec{F} \triangleq$ the summation of the external forces on a body

$f \triangleq$ the summation of the internal forces on a body

This appendix will derive the basic equations of motion for any mass moving in space. After the basic equations have been developed, the effects of control actions will be added. The final equations will then be converted to standard aeronautical terminology which is used in the body of the work for aircraft stability considerations.

These equations have no doubt been derived several times in the past one hundred years. However, the author was unable to find any clear derivations in any of the reference material covered. Therefore, the derivations in this appendix are submitted for the reader's interest and for background information

Fig. AI-I MASS BODY IN MOTION

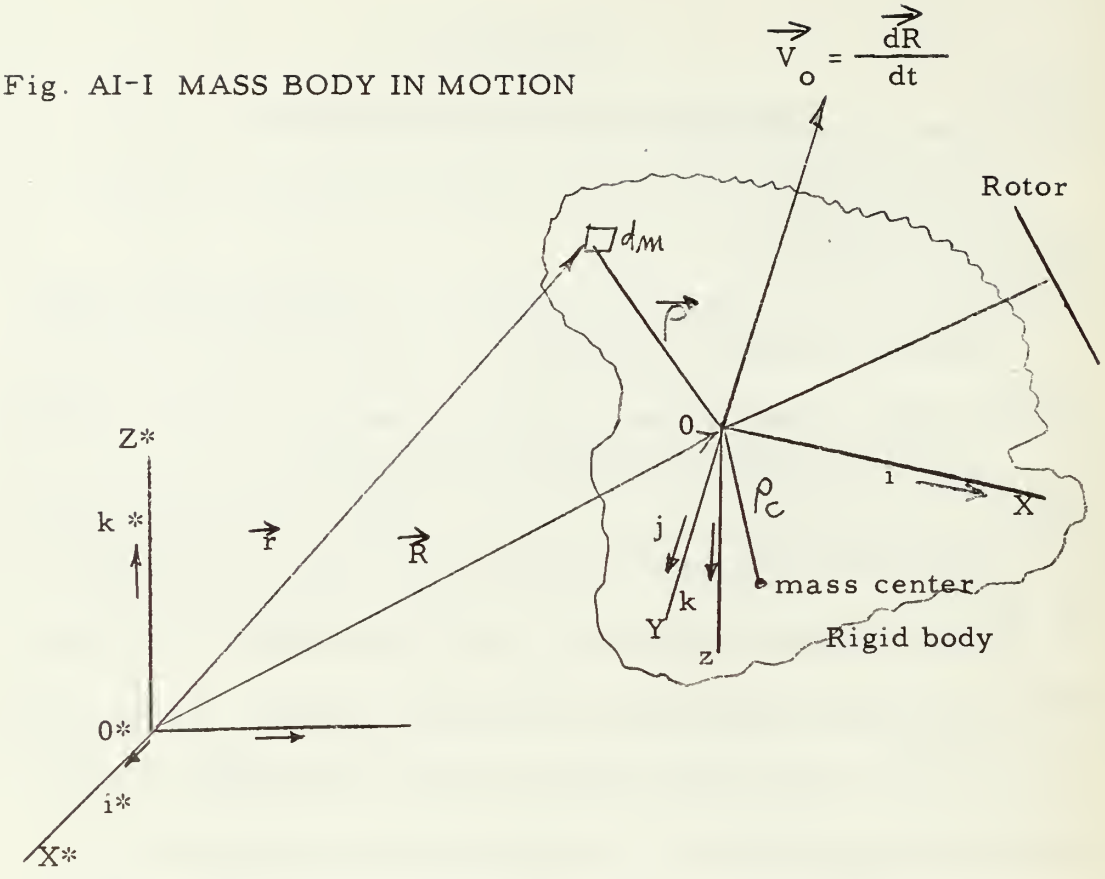

Consider

$$\vec{\rho} = \vec{i}x + \vec{j}y + \vec{k}z$$

$$\vec{\omega} = \vec{\Omega} = i\vec{\omega}_1 + j\vec{\omega}_2 + k\vec{\omega}_3$$

Momentum vector for the whole body $\vec{L} = \int dm \frac{dr}{dt}$

$$\frac{\vec{dr}}{dt} = (\vec{Vo} + (\vec{\omega} \times \vec{\rho}) + \vec{\dot{\rho}} \text{ of rotor})$$

$$\vec{L} = \int dm \frac{\vec{dr}}{dt} = \int dm (\vec{Vo} + (\vec{\omega} \times \vec{\rho}) + \dot{\rho} \text{ rotor})$$

$$\frac{\vec{dL}}{dt} = \int dm \frac{d^2\vec{r}}{dt^2} = f + F \qquad \text{but summation of internal forces equals zero.}$$

Hence

$$\frac{\vec{dL}}{dt} = \int dm \frac{d^2\vec{r}}{dt^2} = \vec{F}$$

For an airframe with a large rotor (i.e. helicopter, STOL aircraft or GEM) consider addition of the rotor to the airframe using the mass center of the aircraft as the origin of the axis system.

$$\frac{d^2\vec{r}}{dt^2} = \frac{d^2\vec{R}}{dt^2} + \dot{\vec{\Omega}} \times \vec{\rho} + \vec{\Omega} \times (\vec{\Omega} \times \vec{\rho}) + \ddot{\vec{\rho}} + 2\vec{\Omega} \times \dot{\vec{\rho}}$$

transport terms; relative acceleration term; coriolis effect

$$\vec{Vo} = \frac{d\vec{R}}{dt}$$

Consider

$$\frac{d^2\vec{r}}{dt^2} = \frac{d\vec{Vo}}{dt} + \dot{\vec{\Omega}} \times \vec{\rho} + \vec{\Omega} \times (\vec{\Omega} \times \vec{\rho}) + \ddot{\vec{\rho}} + 2\vec{\Omega} \times \dot{\vec{\rho}}$$

then

$$\frac{d^2\vec{r}}{dt^2} = \vec{i}^* \dot{Vx} + \vec{j}^* \dot{Vy} + \vec{k}^* \dot{Vz} + \vec{i}^* (\Omega_2 Vz - \Omega_3 Vy) + \vec{j}^* (\Omega_3 Vx - \Omega_1 V_3 + \vec{k}^* (\Omega_1 Vy - \Omega_2 Vx) + 0 + 0 + 0 + 0 \text{ where } \rho = 0$$

Hence $F = m \frac{d^2\vec{r}}{dt^2}$

$$\left.\begin{aligned} \vec{i}^* Fx &= \vec{i}^* (Vx + \Omega_2 Vz - \Omega_3 Vy)\, m \\ \vec{j}^* Fy &= \vec{j}^* (Vy + \Omega_3 Vx - \Omega_1 V_3)\, m \\ \vec{k}^* Fz &= \vec{k}^* (Vz + \Omega_1 Vy - \Omega_2 Vx)\, m \end{aligned}\right\} \text{neglecting rotor effect}$$

Therefore in scalar form

$$\left.\begin{aligned} Fx &= (\dot{Vx} + \Omega_2 Vz - \Omega_3 Vy)m \\ Fy &= (\dot{Vy} + \Omega_3 Vx - \Omega_1 V_3)\, m \\ Fz &= (\dot{Vz} + \Omega_1 Vy - \Omega_2 Vx)\, m \end{aligned}\right\}$$

Concurs with Etkin 4.4.3
Also Duncan Page 64

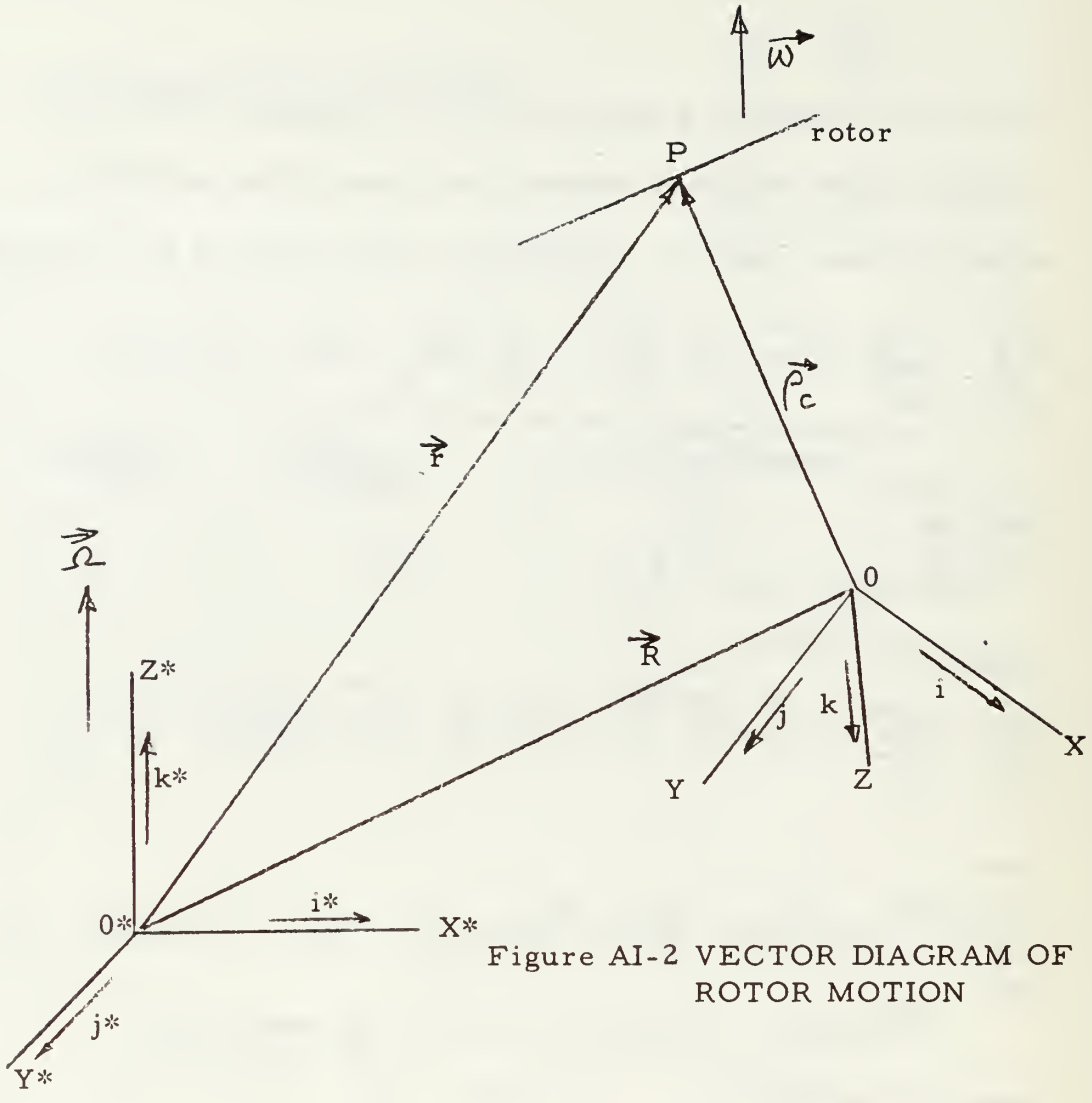

Figure AI-2 VECTOR DIAGRAM OF ROTOR MOTION

ρ_c is fixed in the rigid body. The rotor spins at an absolute angular velocity of but the mass center of the rotor system is at point P. Therefore, $\vec{\dot{\rho}}_c$ and $\vec{\ddot{\rho}}_c = 0$. It is also assumed that $\vec{\Omega}$ = constant. Therefore, the additional term $\Omega \times (\Omega \times \rho_c)$ enters the problem.

$$\vec{\Omega} \times \vec{\rho}_c = \begin{vmatrix} i & j & k \\ \omega_1 & \omega_2 & \omega_3 \\ \rho_{c_x} & \rho_{c_y} & \rho_{c_z} \end{vmatrix}$$

$\vec{A} \times (\vec{B} \times \vec{C}) = (\vec{A} \cdot \vec{C})\vec{B} - (\vec{A} \cdot \vec{B})\vec{C}$ is a basic identity, therefore

$$\vec{\Omega} \times \vec{\Omega} \times \vec{\rho}_c = (\vec{\Omega} \cdot \vec{\rho}_c)\vec{\Omega} - (\vec{\Omega} \cdot \vec{\Omega})\vec{\rho}_c .$$

Note: coordinates $\vec{i}, \vec{j}, \vec{k}$ are those in the body and not the inertial or earth system. The values of Ω are primed for the same reason. It is quite possible that ρ_{cy} will be 0 considering alignment of the rotor on the xz plane.

$F_T = F_1 + F_2 = m_1 a + m_2 a$ F_1 = airframe F_2 = rotor

In resolving this, it must be noted that the mass centers differ from those of the combined masses.

It should be noted that the equations for the acceleration of a particle also contain rotational and relative velocity terms, however, $\ddot{\rho}$ and $\dot{\rho} = 0$ as these particles are in a rigid body. Further, the summation of particles about the mass center makes

$$dm \left[(\dot{\vec{\Omega}} \times \vec{\rho}) + \vec{\Omega} \times (\vec{\Omega} \times \vec{\rho}) \right] \text{ equal to zero.}$$

Moment terms may be considered using Moment of Momentum. $(\vec{H}^*)$

From this the differential may be taken and the moment is then derived. Consider $\vec{H}^*$ to be the moment of momentum of the system with respect to the inertial (non-rotating axis). The derivation will include a rotor spinning on the rigid body.

Figure AI-3 MASS DIAGRAM FOR MOMENT ANALYSIS

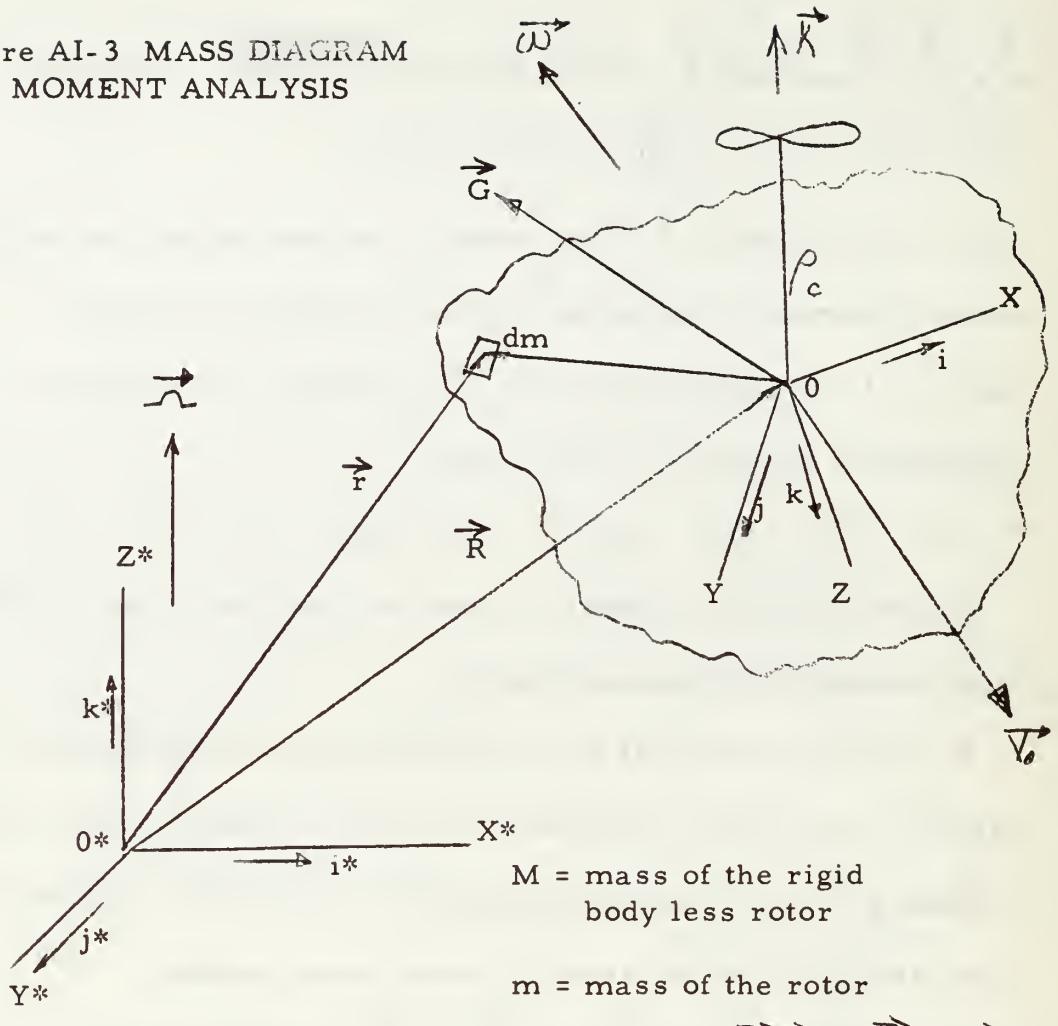

M = mass of the rigid body less rotor

m = mass of the rotor

The absolute angular velocity of the axis OXYZ is $\vec{\Omega} = i\Omega_1 + j\Omega_2 + k\Omega_3$.

The absolute angular velocity of the body is $\vec{\omega} = i\omega_1 + j\omega_2 + k\omega_3$.

The relative angular velocity of the body is $|\vec{\omega} - \Omega| = n$ (scalar)

The angular motion of a rotor in motion, but attached to the body will be

$$\vec{\omega} - \vec{\Omega} = i(\omega_1 - \Omega_1) + j(\omega_2 - \Omega_2) + k(\omega_3 - \Omega_3) .$$

Henceforth this relative term will be noted as $\vec{K}$ (KAPPA).

The equation for H^* is:

$$H^* = \int \vec{r} \times \frac{d\vec{r}}{dt}\, dm \quad \text{where } \vec{r} = R + \vec{\rho}$$

Recalling that the momentum equation was $L = \int dm \frac{d\vec{r}}{dt}$

then

$$\vec{H}^* = \vec{R} \times \vec{L} + \int \vec{\rho} \times \frac{d\vec{r}}{dt} \, dm$$

The term under the integral will be known as $\vec{H}$.

Recalling that $\frac{d\vec{r}}{dt} = \vec{Vo} + \vec{\Omega} \times \vec{\rho} + \dot{\vec{\rho}}$ (rotor) then

$$H = \int \left[\vec{\rho} \times (\vec{Vo} + (\vec{\Omega} \times \vec{\rho}) + \dot{\vec{\rho}} \text{ (rotor)} \right] dm.$$

This can further be resolved into the moment of momentum about its own Oxyz axis;and the velocity moment with respect to the inertial axis.

$$\vec{H} = (M + m) \vec{\rho}_c \times \vec{Vo} + \int (\vec{\rho} \times \vec{\Omega} \times \vec{\rho}) \, dm + \int \rho \times (K \times \rho) \, dm$$

$$\vec{Ho} \triangleq \int \vec{\rho} \times (\vec{\Omega} \times \vec{\rho}) \, dm$$

$$\vec{Ho}_{rel} \triangleq \int \vec{\rho} \times (\vec{K} \times \vec{\rho}) \, dm$$

To derive moments consider recalling $H^* = \int (\vec{r} \times \frac{d\vec{r}}{dt}) \, dm$

$$\frac{d\vec{H}^*}{dt} = \int \left(\frac{dr}{dt} \times \frac{dr}{dt} \right) dm + \int \left[(\vec{R} + \vec{\rho}) \times \frac{d^2\vec{r}}{dt^2} \right] dm$$

$\frac{d\vec{r}}{dt} \times \frac{d\vec{r}}{dt} = 0$ and recalling that $\vec{F} = \frac{d\vec{L}}{dt} = \int \frac{d^2\vec{r}}{dt^2} \, dm$

Then substituting these in,

$$\frac{d\vec{H}^*}{dt} = \vec{R} \times \frac{d\vec{L}}{dt} + \vec{G} \text{ where } \vec{G} \triangleq \int \left[\rho \times \frac{d^2\vec{r}}{dt^2} \right] dm$$

However, we also noted that

$$\vec{H}^* = \vec{R} \times \vec{L} + \int \left(\vec{\rho} \times \frac{d\vec{r}}{dt} \right) dm$$

Therefore:

$$\frac{\vec{dH^*}}{dt} = \frac{\vec{dR}}{dt} \times \vec{L} + \vec{R} \times \frac{\vec{dL}}{dt} + \frac{\vec{dH}}{dt}$$

Equating the two results of $\frac{\vec{dH^*}}{dt}$ it is seen that

$$\vec{R} \times \frac{\vec{dL}}{dt} + \vec{G} = \frac{\vec{dR}}{dt} \times \vec{L} + \vec{R} \times \frac{\vec{dL}}{dt} + \frac{\vec{dH}}{dt}$$

Recall that $\frac{\vec{dR}}{dt} = \vec{Vo}$

and that

$$\vec{L} = (M + m)\,(\vec{Vo} + \vec{\Omega} \times \vec{\rho}_c + \dot{\vec{\rho}}_{c\ \text{rotor}})$$

$$\text{Now } \frac{\vec{dH}}{dt} = \frac{d}{dt}\left[(M + m)\,\vec{\rho}_c \times \vec{Vo} + \vec{Ho} + \vec{Ho}_{rel} \right]$$

$$\frac{dH}{dt} = (m + M)\left[\frac{d\vec{\rho}_c}{dt} \times \vec{Vo} + \vec{\rho}_c \times \frac{\vec{dVo}}{dt} \right] + \frac{d}{dt}\left[\vec{Ho} + \vec{Ho}_{rel} \right]$$

combining

$$\vec{G} = \vec{Vo} \times (\vec{Vo} + \vec{\Omega} \times \vec{\rho}_c)\, M + \vec{Vo} \times (Vo + \vec{\Omega} \times \vec{\rho}_c + \dot{\vec{\rho}}_{c\ \text{rotor}})\, m$$
$$+ (\dot{\vec{\rho}}_c \times \vec{Vo} + (\Omega \times \vec{\rho}_c) \times \vec{Vo})\, m + (\dot{\vec{\rho}}_c \times \vec{Vo} + (\Omega \times \rho_c) \times \vec{Vo})\, M$$
$$+ (M + m)\,\vec{\rho}_c \times \frac{\vec{dVo}}{dt} + \frac{d}{dt}\left[\vec{Ho} + \vec{Ho}_{rel} \right]$$

A further assumption is stated at this point. This is that the point of rotation of the rotor is fixed on the body and remains so. The shaft does not have nutation about some axis but remains fixed on a mount of the rigid body. Therefore, the $\dot{\rho}_c$ of the rotating body is zero. Also, logically, in a rigid body the mass does not shift hence $\dot{\vec{\rho}}_c$ is also zero.

In crossing a vector with itself Vo x Vo the result is zero.

$$\text{Vo x Vo} = \begin{vmatrix} i & j & k \\ V_1 & V_2 & V_3 \\ V_1 & V_2 & V_3 \end{vmatrix} = \vec{i}(V_2V_3 - V_2V_3) + \vec{j}(V_1V_3 - V_1V_3) + \vec{k}(V_1V_2 - V_1V_3) = 0$$

$$\text{Vo x Vo} = 0$$

Furthermore, crossing two dissimilar vectors in opposite order yields opposite signs and equal magnitude

$$\vec{\text{Vo}} \times \vec{\rho}_c = \begin{vmatrix} i & j & k \\ V_1 & V_2 & V_3 \\ \rho_1 & \rho_2 & \rho_3 \end{vmatrix} = \vec{i}(V_2\rho_3 - \rho_2 V_3) + \vec{j}(\rho_1 V_3 - \rho_3 V_1) + \vec{k}(V_1\rho_2 = \rho_1 V_2)$$

$$\vec{\rho}_c \times \vec{\text{Vo}} = \vec{i}(\rho_2 V_3 - \rho_3 V_2) + \vec{j}(\rho_3 V_1 - \rho_1 V_3) + \vec{k}(\rho_1 V_2 - \rho_2 V_1)$$

$$\text{Thus } \vec{\text{Vo}} \times \vec{\rho}_c + \vec{\rho}_c \times \vec{\text{Vo}} = 0$$

Incorporating these two facts, the equation for $\vec{G}$ can be simplified to the following:

$$\vec{G} = \frac{d}{dt}\left[\vec{\text{Ho}} + \vec{\text{Ho}}_{rel}\right] + (M + m)\left(\vec{\rho}_c \times \frac{d\vec{\text{Vo}}}{dt}\right)$$

$\frac{d\vec{\text{Ho}}}{dt} = \vec{\text{Ho}} + \vec{\Omega} \times \vec{\text{Ho}}$ in a general equation.

Thus it is necessary to solve $\frac{d\vec{Ho}}{dt}$ to find $\vec{G}$.

Considering $\vec{Ho} = \int \left[\vec{\rho} \times (\vec{\omega} \times \vec{\rho}) \right]$ which accounts for the absolute velocity.

Recalling an identity of vector algebra:

$\vec{A} \times (\vec{B} \times \vec{C}) = (\vec{A} \cdot \vec{C}) \vec{B} - (\vec{A} \cdot \vec{B}) \vec{C}$ then

$$\vec{\rho} \times (\vec{\omega} \times \rho) = (\vec{\rho} \cdot \vec{\rho}) \vec{\omega} - (\vec{\rho} \cdot \vec{\omega}) \vec{\rho}$$

$$Ho = \int \left[(x^2 + y^2 + z^2) (\vec{i} \omega_1 + \vec{j} \omega_2 + \vec{k} \omega_3) - (x \omega_1 + y \omega_2 + z \omega_3) (\vec{ix} + \vec{jy} + \vec{kz}) \right] dm$$

$$= \left[\vec{i} \left[(y^2 + z^2) \omega_1 - xy \omega_2 - xz \omega_3 \right] + \vec{j} \left[(x^2 + z^2) \omega_2 - yz \omega_3 - xy \omega_1 \right] + \vec{k} \left[(x^2 + y^2) \omega_3 - xz \omega_1 yz \omega_2 \right] \right] dm$$

The above terms can be recognized in part as moment and product of inertia terms.

$Ix \triangleq \int (y^2 + z^2) dm$

$Iy \triangleq \int (x^2 + z^2) dm$

$Iz \triangleq \int (x^2 + y^2) dm$

$Ixy \triangleq \int (xy) dm$

$Iyz \triangleq \int (yz) dm$

$Ixz \triangleq \int (xz) dm$

Therefore:

$$\vec{Ho} = \vec{i}\,(Ix\,\omega_1 - Ixy\,\omega_2 - Ixz\,\omega_3) + \vec{j}\,(-Ixy\,\omega_1 + Iy\,\omega_2 - Iyz\,\omega_3)$$

$$+ \vec{k}\,(Iz\,\omega_3 - Ixz\,\omega_1 - Iyz\,\omega_2)$$

Considering the effects of the aircraft as a rigid body first

$$\frac{d\vec{Ho}}{dt} = \dot{\vec{Ho}} + \vec{\Omega} \times \vec{Ho} \quad \text{and for a rigid body} \quad \vec{\omega} = \vec{\Omega}$$

$$\frac{d\vec{Ho}}{dt} = \vec{i}\,(Ix\,\dot{\Omega}_1 - Ixy\,\dot{\Omega}_2 - Ixz\,\dot{\Omega}_3) + \vec{j}\,(-Ixy\,\dot{\Omega}_1 + Iy\,\dot{\Omega}_2 - Iyz\,\Omega_3)$$

$$+ \vec{k}\,(-Ixy\,\dot{\Omega}_1 - Iyz\,\dot{\Omega}_2 + Iz\,\dot{\Omega}_3) + \begin{vmatrix} i & j & k \\ \Omega_1 & \Omega_2 & \Omega_3 \\ (Ix-Ixy-Ixz) & (Iy-Ixy-Iyz) & (-Ixz-Iyz+Iz) \end{vmatrix}$$

For any ordinary aircraft or missile, the produce of inertia terms Ixy and Iyz can be considered zero because of the mirror symmetry aspect. Ixz may be zero if the principal axis is selected. Thus with no loss in generality, consider Ixy = Ixz = Iyz = 0

$$\frac{d\vec{Ho}}{dt} = \vec{i}\,\left[Ix\,\dot{\Omega}_1 + Iz\,\Omega_2\,\Omega_3 - Iy\,\Omega_2\,\Omega_3\right]$$

$$+ j\,\left[Iy\,\dot{\Omega}_2 + Ix\,\Omega_1\,\Omega_3 - Iz\,\Omega_1\,\Omega_3\right]$$

$$+ k\,\left[Iz\,\dot{\Omega}_3 + Iy\,\Omega_1\,\Omega_2 - Ix\,\Omega_1\,\Omega_2\right]$$

However, including the effects of Ixz, the product of inertia term, which is often not zero:

$$\frac{\vec{dHo}}{dt} = \vec{i}\left[Ix\dot{\Omega}_1 - Ixz\dot{\Omega}_3 - Ixz\Omega_1\Omega_2 + Iz\Omega_2\Omega_3 - Iy\Omega_2\Omega_3 \right] + \vec{j}\left[Iy\dot{\Omega}_2 + Ix\Omega_1\Omega_3 - Ixz\Omega_3^2 + Ixz\Omega_1^2 - Iz\Omega_1\Omega_3 \right] + \vec{k}\left[Iz\dot{\Omega}_3 - Ixz\dot{\Omega}_1 + Iy\Omega_1\Omega_2 - Iy\Omega_1\Omega_2 + Ixz\Omega_2\Omega_3 \right]$$

Using standard aerodynamic terminology, the following items are defined:

$A \triangleq Ix$

$B \triangleq Iy$

$C \triangleq Iz$

$E \triangleq Ixz$

$P \triangleq \Omega_1$

$Q \triangleq \Omega_2$

$R \triangleq \Omega_3$

Thus

$\vec{G} = \frac{\vec{dHo}}{dt}$ where system is chosen such that $\rho_c = 0$

$$\vec{G} = \vec{i}\left[A\dot{P} - E\dot{R} - EPQ + QR(C-B) \right] + \vec{j}\left[B\dot{Q} + PR(A-C) + E(P^2 - R^2) \right] + \vec{k}\left[C\dot{R} - E\dot{P} + PQ(B-C) + EQR \right]$$

These equations concur with Duncan, Page 66, and Etkin, Chapter 4.

To consider the rotor effects it should be remembered that $\vec{\omega} = \vec{\Omega} + K$ where $\vec{K}$ is the relative motion of a rotor on the body. Thus for a rotor there will be a combination of terms considering the absolute angular velocity of the OXYZ system plus the angular velocity of the rotor with respect to the body.

Thus

$$\frac{\vec{dHo}}{dt} = \dot{\vec{Ho}} + \vec{\omega} \times \vec{Ho} \quad \text{where} \quad \vec{\omega} \triangleq \vec{\Omega} + \vec{K}$$

It should be noted, that for a symmetrical rotor or disk the product of inertia terms are zero where the disk is at least a three bladed propeller. The two bladed propeller has a product of inertia dependent on its angular position. This case will not be considered, but the three or more bladed propeller situation will be used in all considerations. Hence with a dynamically and statically balanced rotor $\dot{\rho}_c = 0$ and the product of inertia is zero.

The moment of inertia of the disk must be considered from the axis of the rigid body. Therefore, the moment of inertia must include the md^2 consideration.

$I_{BB} = I_{AA} + md^2$

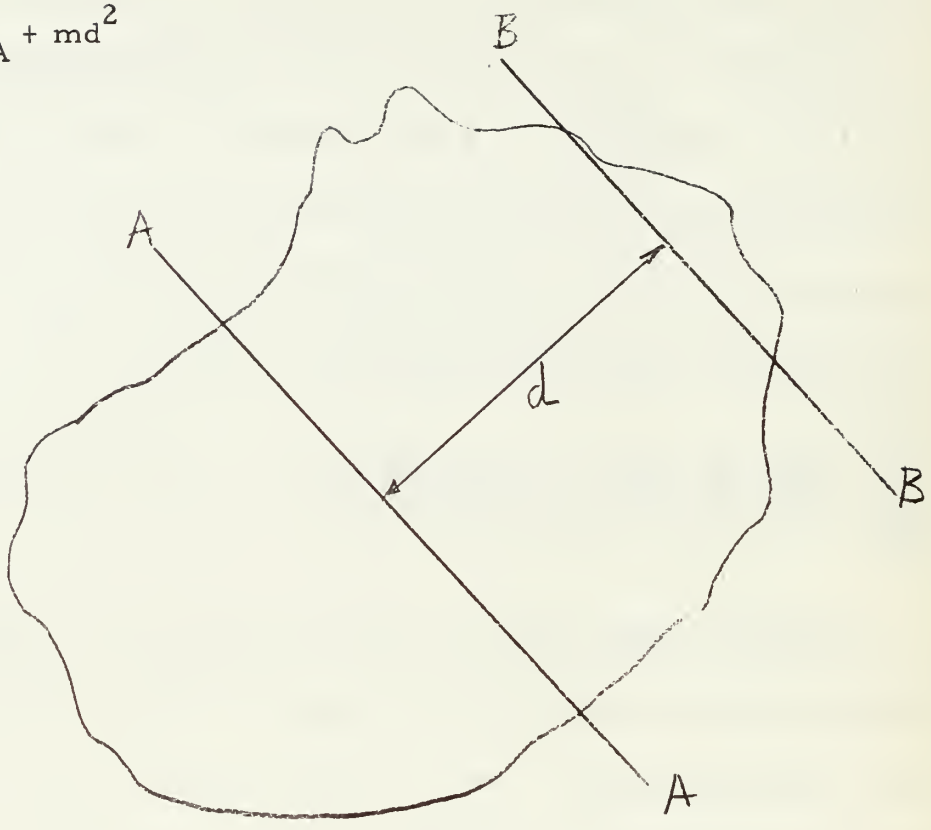

The moment of inertia terms for the rotors will be thus defined in the most general sense

a $\triangleq$ Ix rotor $\triangleq$ Ix + md_1^2 and aligned with the reference axis

b $\triangleq$ Iy rotor $\triangleq$ Iy + md_2^2 and aligned with the reference axis

c $\triangleq$ Iz rotor $\triangleq$ Iz + md_3^2 and aligned with the reference axis

$$\vec{G} = \frac{d\vec{H}}{dt} - \frac{d\vec{H}o}{dt} + \frac{d\vec{H}_{rel}}{dt}$$

Recalling the derivation of moments for the rigid body without the rotor, the same method applies.

$$\frac{\vec{dHo}}{dt} = \vec{i}\, a\dot{\Omega}_1 + \vec{jb}\,\dot{\Omega}_2 + \vec{kc}\,\dot{\Omega}_3 + \vec{\Omega} \times \vec{Ho}$$

$$+ \vec{i}\, a\dot{K}_1 + \vec{jb}\,\dot{K}_2 + \vec{kc}\,\dot{K}_3 + \vec{K} \times \vec{Ho} \qquad \text{for a rotor only}$$

Combining this to a system consisting of a rigid body plus a rotor, the following results occur

$$\vec{G} = \frac{\vec{dH}}{dt} = \vec{i}\left[Ix\,\dot{\Omega}_1 - Ixz\,\dot{\Omega}_3 + Ixz\,\Omega_1\Omega_2 + I_Z\,\Omega_2\Omega_3 - Iy\,\Omega_2\Omega_3\right]$$

$$+ \vec{j}\left[Iy\,\dot{\Omega}_2 + Ix\,\Omega_1\Omega_3 - Ixz\,\Omega_3^2 + Ixz\,\Omega_1^2 - Iz\,\Omega_1\Omega_3\right]$$

$$+ \vec{k}\left[Iz\,\dot{\Omega}_3 - Ixz\,\dot{\Omega}_1 + Iy\,\Omega_1\Omega_2 + Ix\,\Omega_1\Omega_2 + Ixz\,\Omega_2\Omega_3\right]$$

$$+ \vec{i}\, a\dot{K}_1 + \vec{jb}\,\dot{K}_2 + \vec{kc}\,\dot{K}_3 + \begin{vmatrix} \vec{i} & \vec{j} & \vec{k} \\ \Omega 1 & \Omega 2 & \Omega 3 \\ aK_1 & bK_2 & cK_3 \end{vmatrix}$$

Combining and using aerodynamic notation.

$$\vec{G} = \vec{i}\left[A\dot{P} - E\dot{R} + a\dot{K}_1 - EPQ + (C-B)\,QR + ck_3Q - bK_2R\right]$$

$$+ \vec{j}\left[B\dot{Q} + b\dot{K}_2 + (A-C)\,PR + E(P^2 - R^2) + aK_1R - cK_3P\right]$$

$$+ \vec{k}\left[C\dot{R} - E\dot{P} + cK_3 + (B-A)\,PQ + EQR + bK_2P - aK_1Q\right]$$

This result concurs with Etkin, page 116.

Therefore, using a standard aerodynamic notation the moment:

$$\vec{G} = \vec{i}\,L + \vec{j}\,M + \vec{k}N$$

and the scalar quantities are as follows

$$L = A\dot{P} + a\dot{K}_1 - E(PQ + \dot{R}) + QR(C-B) + cK_3Q - bK_2R$$

$$M + B\dot{Q} + b\dot{K}_2 + PR(A-C) + E(P^2 - R^2) + aK_1R - cK_3R$$

$$N = C\dot{R} + c\dot{K}_3 + E(QR - \dot{P}) + PQ(B-A) + bK_2P - aK_1Q$$

Thus, the force and moment equations derived in this appendix are applicable to a rigid body of constant mass where the body is in motion. It also considers the effects of a three bladed or more rotor system which is attached on some fixed point of the rigid body. The rotor effects may be included or discarded depending on the magnitude of rotor inertia and the relative velocity of the rotor.

It should be noted that the derivations are done in a general form, but in the concluding equations, the usual aerodynamic notation is substituted to bring the equations to this specific problem. Furthermore, missile or aircraft shape and density has been considered symmetrical about the xz plane. Thus, the produce of inertia terms Ixy and Iyz have been considered zero. No generality is lost by this and if, for some reason, the body is sufficiently unsymmetrical, the terms can be quickly added in.

The following is taken from Chapter 4 of Etkin (4). The concept of motion on the control surfaces is shown in the following

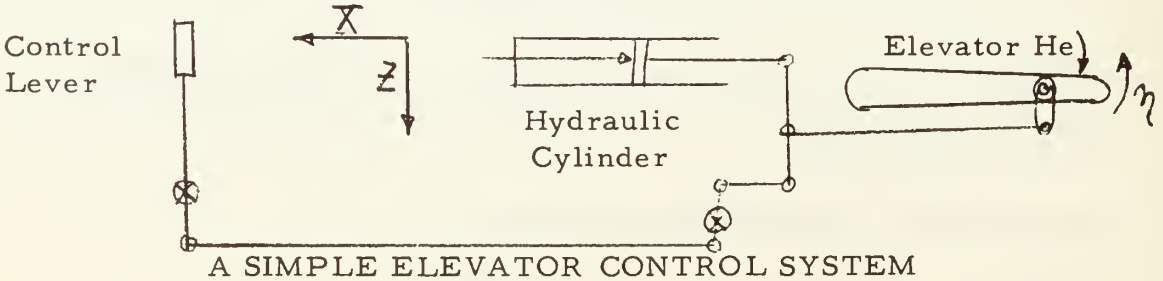

A SIMPLE ELEVATOR CONTROL SYSTEM

The LaGrange equation of motion in a moving reference frame is

$$\frac{d}{dt}\left(\frac{\partial T}{\partial \dot{q}_K}\right) - \frac{\partial T}{\partial q_K} = \mathcal{F}$$

$T \triangleq$ kinetic energy of the system relative to the chosen frame of reference

$\mathcal{F} \triangleq \frac{\partial w}{\partial q_K}$ = generalized force

$W \triangleq$ work done on the system by the external forces which act upon it

q_K = generalized coordinate

H = aerodynamic moments

δ = rotation of control surface in radians

Kinetic energy $T = 1/2\ I\dot{\delta}^2$ and $\frac{\partial T}{\partial q_K} = I\ddot{\delta}$

$$\mathcal{F} = \frac{\partial W}{\partial q_K}$$

For elevator motion

$$\delta W = He\delta(\delta e) + Fe\delta(\delta e) + \delta Wi$$

$Fe \triangleq$ generalized elevator control force

$\delta Wi \triangleq$ work done by inertia forces

Work done by the control forces is

$$Fe\delta(\delta e) = P\delta sp + J\delta sj$$

$$Fe = P\frac{dsp}{d\delta e} + J\frac{dsJ}{d\delta e}$$

$\frac{dsp}{d\delta} \triangleq$ gear rate of pilot's stick to control surface

$\frac{dsJ}{d\delta} \triangleq$ "gear ratio" or advantage of hydraulic cylinder to control surface

Evaluating δ Wi

consider $dFi = \frac{d^2 r}{dt}\, dm$

recalling from previous derivation that

$$\frac{\vec{d^2 r}}{dt} = \frac{\vec{dVo}}{dt} + \vec{\Omega} \times \vec{\rho} + \vec{\Omega} \times \vec{\Omega} \times \vec{\rho} + \vec{\ddot{\rho}} + 2\vec{\Omega} \times \vec{\dot{\rho}}$$

Then

$$dFxi = -\left[\frac{dVo_x}{dt} + 2Q\dot{z} - 2R\dot{y} - x(Q^2 + R^2) + y(PQ - \ddot{R}) + z(PR - \dot{Q})\right] dm$$

dFyi and dFz are similar in form.

Looking at an elevator assembly, it can be seen that assuming a lamina in the xy-plane, the displacement in the C_Z direction is amount $\dot{\delta}$ (δ e).

The work done by the inertia forces is $\delta W_1 = \int \rho_e \delta(\delta e)\, dFzi$

$$\frac{\delta Wi}{\delta(\delta e)} = \int \frac{dVoz}{dt} \rho e\, dm - (PR - \dot{Q}) \int x \rho e\, dm - RQ + \dot{P} \int y \rho\, dm$$

The coriolis terms $2P\dot{y}$ and $-2Q\dot{x}$ are zero as there is no work done in those directions. Furthermore z = 0 because of the assumed lamina.

$acz \triangleq \frac{dVoz}{dt}$ and $acz \int \rho e\, dm = m_e l_e a_{c_z}$

$$(PR - \dot{Q}) \int x \rho e\, dm = P_{e_x} (PR - \dot{Q})$$

$P_{e_x} \triangleq$ product of inertia of the elevator

By symmetry $\int \rho_e y \, dm = 0$

$$\frac{\partial W_i}{\partial(\partial e)} = - m_e l_e a_{c_z} - P_{ex} (PR - \dot{Q})$$

$$I_e \ddot{\partial}_e = \mathcal{F} = m_e l_e a_{c_z} - P_{e_x} (PR - \dot{Q}) + H_e + F_e$$

$$I_e \ddot{\partial}_e + m_e l_e a_{c_z} + P_{ex} (PR - \dot{Q}) = H_e + F_e \qquad \text{(Etkin 4.8, 13)}$$

Similarly for the rudder

$$I_r \ddot{\zeta}_r - a_{cy} m_r l_r - (\dot{R} + PQ) P_{rx} - (RQ - \dot{P}) P_{rz} = H_r + F_a$$

and for the aileron

$$I_a \ddot{\zeta} + 2 P_{ay} (RQ + \dot{P}) = 2 H_a + F_a$$

APPENDIX II

ROLL, YAW AND PITCH

The derivation of the yaw, roll and pitch rates is given here to show the actual motion taking place. Frequently the motion is considered small and small angle approximations are used. These will be noted at the conclusion.

First, consider the Eulerian Axis used in the aeronautical field shown below. The rotation takes place in the order of yaw (ψ), pitch (θ) , and roll (ϕ).

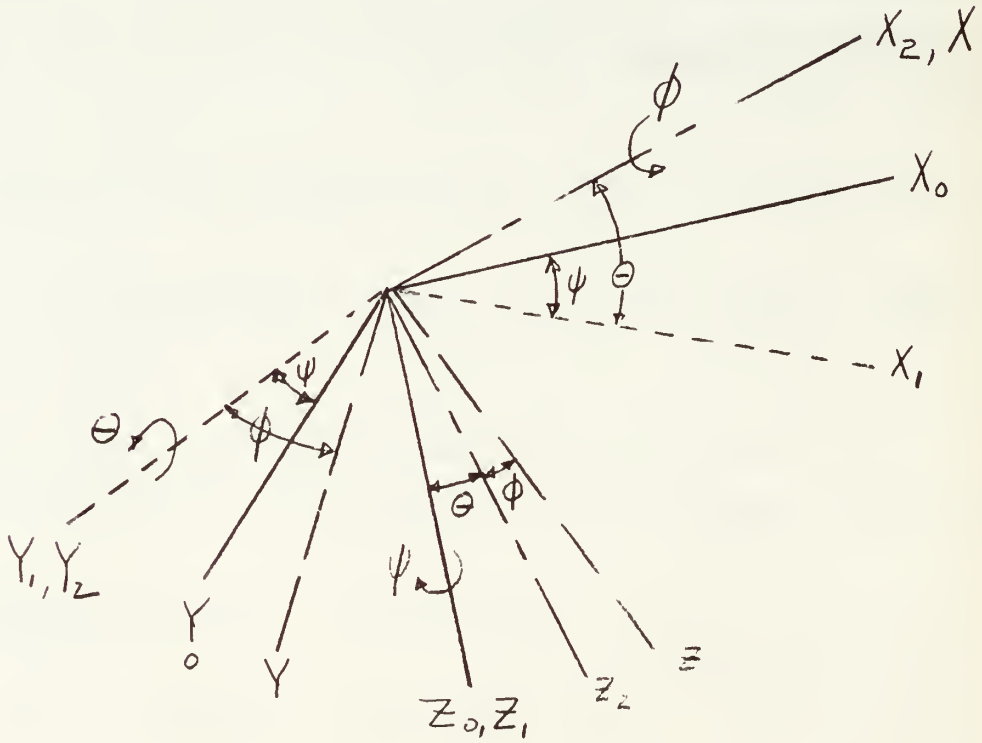

Figure AII-1 EULERIAN AXIS SYSTEM SHOWING ROTATION ABOUT THE Z, Y, AND X AXIS

The initial conditions at X_o, Y_o, and Z_o and the relations of $\dot{\psi}$, $\dot{\Theta}$, and $\dot{\phi}$ can be related to P, Q and R of the body axis at x, y, z. In the above diagram consider the angular velocity P which is about the OX axis. It must be the sum of the velocities about the OZ_o, OY_1, and OX_2 axis respectively.

OZ_o makes an angle $\frac{\pi}{2} + \Theta$ with OX. The rate thus $\dot{\psi} \cos (\frac{\pi}{2} + \Theta) = -\dot{\psi} \sin \Theta$. OY_1 is perpendicular with OX so $\dot{\Theta} \cos \frac{\pi}{2} = 0$ and OX is parallel with OX_2 or the motion $\dot{\phi} \cos \Theta = \dot{\phi}$.

Thus the summation $P = \dot{\phi} - \dot{\psi} \sin \Theta$.

To evaluate Q the angle YOZ_o must be determined. Specifically the value $\dot{\psi} \cos \widehat{YOZ_o}$ is desired.

$$\cos \widehat{YOZ_o} = \cos \widehat{YOZ_2} \cos \widehat{Z_2OZ_o}$$

$$= \cos (\frac{\pi}{2} - \phi) \cos \Theta$$

$$= \sin \phi \cos \Theta$$

Thus the contribution of OZ_o axis motion is $\dot{\psi} \sin \phi \cos \Theta$. The angle between OY and OY_1 is ϕ so the motion here results as $\dot{\Theta} \cos \phi$. OY is perpendicular to OX_2 hence the angular motion $\dot{\phi} \cos \frac{\pi}{2} = 0$.

Thus $Q = \dot{\Theta} \cos \phi + \dot{\psi} \sin \phi \cos \Theta$

In the third angular velocity motion R the yaw motion appears as $\dot{\psi} \cos \phi \cos \Theta$ while the motion of pitch is $\dot{\Theta} \cos (\frac{\pi}{2} + \phi) = -\dot{\Theta} \sin \phi$. The rolling term vanishes $\phi \cos \frac{\pi}{2} = 0$. Thus $R = -\dot{\Theta} \sin \phi + \dot{\psi} \cos \phi \cos \Theta$.

Hence the relationship of the body yaw, pitch and roll rates (P, Q, and R) to the designated reference system angular velocities $\dot{\psi}$, $\dot{\Theta}$ and $\dot{\phi}$ is:

$$P = \dot{\phi} - \dot{\psi} \sin \Theta$$

$$Q = \Theta \cos \phi + \dot{\psi} \sin \phi \cos \Theta$$

$$R = \dot{\psi} \cos \phi \cos \Theta - \dot{\Theta} \sin \phi$$

These results concur with Duncan page 81 and Etkin page 116.

It should be noted that for small angles the approximation below is often used:

$$P \cong \dot{\phi}$$

$$Q \cong \dot{\Theta}$$

$$R \cong \dot{\psi}$$

A second consideration which must be made regarding movement about the reference axis is the velocity or displacement with respect to time. It is desired to obtain the velocity with respect to the fixed frame or inertial axis i* x, j*y, and k*z.

Consider first that in scalar values

$$\frac{dx^*}{dt} = U_1$$

$$\frac{dy^*}{dt} = V_1$$

$$\frac{dz^*}{dt} = W_1$$

It should be noted, however, that in the three position system shown on the previous page that

$$U_3 = U$$

$$V_3 = V \cos \phi - W \sin \phi$$

$$W_3 = V \sin \phi + W \cos \phi$$

and $$W_2 = - U_3 \sin \theta + W_3 \cos \theta$$

$$V_2 = V_3$$

$$U_2 = U_3 \cos \theta + W_3 \sin \theta$$

and $$U_1 = U_2 \cos \psi - V_2 \sin \psi$$

$$V_1 = U_2 \sin \psi + V_2 \cos \psi$$

$$W_1 = W_2$$

Combining the 1, 2 and 3 position terms

$$\frac{dx^*}{dt} = U \cos \theta \cos \psi + V (\sin \phi \sin \theta \cos \psi - \cos \phi \sin \psi)$$

$$+ W (\cos \phi \sin \theta \cos \psi + \sin \phi \sin \psi)$$

$$\frac{dy^*}{dt} = U \cos \theta \sin \psi + V (\sin \phi \sin \theta \sin \psi + \cos \phi \cos \psi)$$

$$+ W (\cos \phi \sin \theta \sin \psi - \sin \phi \cos \psi)$$

$$\frac{dz^*}{dt} = -U \sin \theta + V \sin \phi \cos \theta + W \cos \phi \cos \theta$$

Thus, the velocity or rate of change with respect to the inertial or earth's reference axis in this case is expressed in these terms as derived. These velocity terms are derived in Etkin Page 102 and conincide with the derivation shown.

Therefore, this appendix accounts for the changes in angular and directional displacement of a rigid body with respect to a fixed reference axis system.

APPENDIX III

NOTES ON DETERMINANT MANIPULATION

The body of this project contains several determinant expansions where the order is doubled. These manipulations do not alter the values of the determinant and the resulting values of the performance functions are the same.

The simple determinant

$$\begin{vmatrix} A1 & B1 & C1 \\ A2 & B2 & C2 \\ A3 & B3 & C3 \end{vmatrix} = \Delta$$

evaluated will yield the following result

$$\Delta = \left[\begin{array}{l} A1B2C3 + B1C2A3 + C1A2B3 \\ -C1B2A3 - A1C2B3 - B1A2C3 \end{array} \right] \qquad \text{A3-1}$$

This expansion by the equations -1 + 1 = 0 will result in the following determinant.

$$\begin{vmatrix} A1 & 0 & B1 & 0 & C1 & 0 \\ -1 & 1 & 0 & 0 & 0 & 0 \\ 0 & A2 & B2 & 0 & C2 & 0 \\ 0 & 0 & -1 & 1 & 0 & 0 \\ 0 & A3 & 0 & B3 & C3 & 0 \\ 0 & 0 & 0 & 0 & -1 & 1 \end{vmatrix} =$$

The resulting evaluation will yield the same value as result (A3-1). Furthermore, if the terms below the main diagonal are allowed to remain in their original columns in lieu of shifting one place to the

right as is done in the main body, the resulting Δ is still the same.

The results of evaluating cofactors for particular performance functions remain unchanged. For example it is desired to evaluate the cofactor Δ_{12} of the original determinant. Thus:

$$\Delta_{12} = \begin{vmatrix} A1 & B1 & C1 \\ A2 & B2 & C2 \\ A3 & B3 & C3 \end{vmatrix} = (-1)\left[A2C3 - A3C2\right] \qquad \text{A3-2}$$

In the expanded determinant the equivalent cofactor is Δ_{13}

$$\begin{vmatrix} A1 & 0 & B1 & 0 & C1 & 0 \\ -1 & 1 & 0 & 0 & 0 & 0 \\ 0 & A2 & B2 & 0 & C2 & 0 \\ 0 & 0 & -1 & 1 & 0 & 0 \\ 0 & A3 & B3 & 0 & C3 & 0 \\ 0 & 0 & 0 & 0 & -1 & 1 \end{vmatrix} = \Delta_{13}$$

$$= \begin{vmatrix} -1 & 1 & 0 & 0 \\ 0 & A2 & 0 & C2 \\ 0 & 0 & 1 & 0 \\ 0 & Ae & 0 & C3 \end{vmatrix} = - \begin{vmatrix} A2 & 0 & C2 \\ 0 & 1 & 0 \\ A3 & 0 & C3 \end{vmatrix}$$

$$\Delta_{13} = (-1)\left[A2C3 - AeC2\right] \qquad \text{A3-3}$$

The result of Equation A3-3 equals Equation A3=2. With the values below the main diagonal left in their original columns, the following occurs:

$$\Delta_{13} = \begin{vmatrix} A1 & 0 & B1 & 0 & C1 & 0 \\ -1 & 1 & 0 & 0 & 0 & 0 \\ A2 & 0 & B2 & 0 & C2 & 0 \\ 0 & 0 & -1 & 1 & 0 & 0 \\ A3 & 0 & B3 & 0 & C3 & 0 \\ 0 & 0 & 0 & 0 & -1 & 1 \end{vmatrix}$$

By inspection of columns two and six, two reductions are made to the following:

$$\Delta_{13} = (-1) \begin{vmatrix} A2 & 0 & C2 \\ 0 & 1 & 0 \\ A3 & 0 & C3 \end{vmatrix}$$

$$\Delta_{13} = (-1) \left[A2C3 - A3C2 \right] \qquad \text{A3-4}$$

The resulting equation (A3-4) is the same as equation (A3-2).

A similar examination using a four by four determinant system was made. This was done to insure that the simplified effects of a three by three or lower order system did not cover up an error in a four by four or higher order determinant. The same manipulations can be performed and the resultant value of the determinant is not altered.

Thus, the individual has the option of placing his values in either column. The location of the values is dependent on desired location of the pick-off point on the block diagram. The final result is not altered.

Thaler

Self-adaptive control systems, Part II.

TA7
.U64
no.20 51063

Thaler

Self-adaptive control systems, Part II.